The Institute for Solid State Physics
The University of Tokyo

Activity Report 2014

© 2015 The Institute for Solid State Physics, The University of Tokyo

ISSP

Activity Report 2014

Contents

	Pages
Preface	1
Research Highlights	2 - 29
Highlights of Joint Research	30 - 51
Conferences and Workshops	52 - 59
Subjects of Joint Research	60 - 149
Publications	150 - 182

The Institute for Solid State Physics (ISSP), The University of Tokyo

Address	5-1-5 Kashiwanoha, Kashiwa, Chiba, 277-8581, Japan
Phone	+81-4-7136-3207
Home Page	http://www.u-tokyo.ac.jp

Preface

We are pleased to present the annual ISSP Activity Report for the academic year 2014. ISSP (Institute for Solid State Physics) was established in 1957 as a joint-use research institution attached to the University of Tokyo. Since then both in-house research and collaboration with external users have been essential elements of the activities of ISSP.

The research at ISSP has been pursued along two major directions. Synthesis of new materials and nano-structures in search for novel phenomena and functions using advanced and original techniques is at the core of modern condensed matter science. Such activities are being conducted by relatively small independent groups at ISSP and their collaborators. At the same time, importance of large experimental and computational facilities in materials science has been rapidly increasing in recent years. An important mission of ISSP is active participation in the development and operation of some of those large facilities that are difficult to maintain for typical university faculties. Notable achievements in this direction are summarized below.

(1) ISSP has been operating supercomputers dedicated to materials science. In addition, the Center of Computational Materials Science provides technical supports to facilitate use of massively parallel computational resources such as the K-computer. (2) The International MegaGauss Science Laboratory continues to develop both the destructive ultrahigh magnetic field by electromagnetic compression aimed at 1000 tesla and the non-destructive long-pulse magnetic field by a flywheel generator. (3) ISSP has been providing external users access to advanced spectroscopy that uses quantum beams such as neutron and synchrotron light sources. It is a pity for the neutron scattering society that the JRR-3 reactor at Tokai has been shut down after the earthquake in 2011 but we are expecting reopening in near future. The pulsed neutron spectrometer at J-PARC developed jointly by ISSP and KEK is now in operation. At the Laser and Synchrotron Research Center, we explore frontier of advanced spectroscopy in ultraviolet and soft X-ray region by combining high power laser being developed in Kashiwa and synchrotron beamline installed in Spring-8.

June, 2015

Masashi Takigawa
Director
Institute for Solid State Physics
The University of Tokyo

Research Highlights

Novel Phase Transitions in the Breathing Pyrochlore Lattice: ^{7}Li-NMR on $LiInCr_4O_8$ and $LiGaCr_4O_8$

Takigawa and Hiroi Group

Antiferromagnetically coupled spins on the pyrochlore lattice, a three dimensional network of corner sharing tetrahedra, are expected to show exotic magnetic properties due to strong geometrical frustration. The Cr spinel oxides ACr_2O_4 (A = Mg, Zn, Cd *etc.*) are well-known examples, where Cr^{3+} with spin 3/2 form a pyrochlore lattice. Recently, Okamoto *et al.*[1] studied a new type of Cr oxides $LiInCr_4O_8$ and $LiGaCr_4O_8$, where Li^+ and In^{3+}/Ga^{3+} ions alternately occupy the A site of ACr_2O_4, allowing Cr spins to form a *breathing pyrochlore* lattice with alternation of large and small tetrahedra and two distinct exchange coupling J and J' ($J > J'$) (see Fig. 1). Here we report on novel phase transitions observed by ^{7}Li-NMR in $LiInCr_4O_8$ and $LiGaCr_4O_8$, for which the breathing factor $B_f = J'/J$ is estimated to be 0.1 and 0.6, respectively [2].

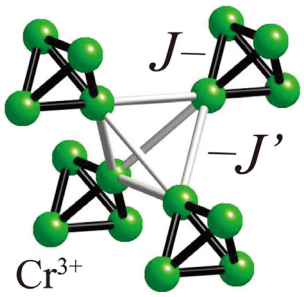

Fig. 1. The structure of the breathing pyrochlore lattice.

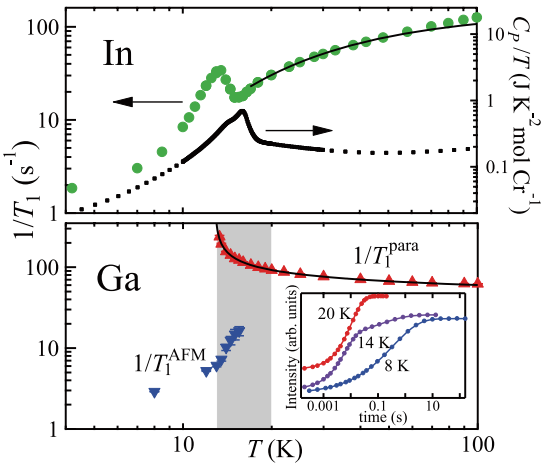

Fig. 2. Upper panel: Temperature dependences of $1/T_1$ (this work) and the specific heat divided by temperature (taken from [1]) in $LiInCr_4O_8$. The line shows an activation law with a spin gap of 31 K. Lower panel: Temperature dependences of $1/T_1$ of the paramagnetic (red) and antiferromagnetic (blue) components in $LiGaCr_4O_8$. The shaded area represents the temperature range, where the NMR spectra in Fig. 3 indicate coexistence of two phases. The solid line shows a fit to a power law divergence towards 13 K. The inset shows the recovery curves at different temperatures. The data at 14 K can be fit to a sum of two components.

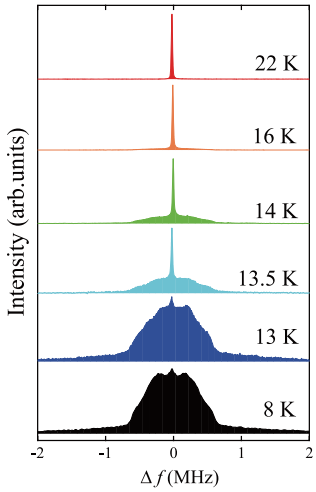

Fig. 3. Temperature dependence of the NMR spectra in $LiGaCr_4O_8$. The vertical scale is normalized by the peak intensity. The origin of the horizontal axis corresponds to the center of gravity.

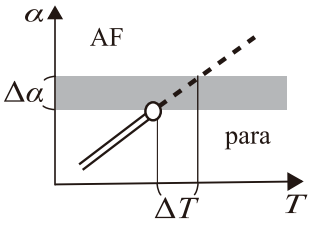

Fig. 4. Schematic phase diagram for $LiGaCr_4O_8$. On the vertical axis, α represents a phenomenological tuning parameter of the Hamiltonian. The region Δα shows the distribution of α in our sample. The dashed and solid double lines indicate first- and second-order transitions, respectively, which are separated by a tricritical point indicated by the open circle.

As shown in the upper panel of Fig. 2, the nuclear spin relaxation rate ($1/T_1$) in $LiInCr_4O_8$ shows activated temperature dependence down to 18 K, indicating a singlet ground state with a spin gap of 31 K. This behavior, however, is disrupted by double phase transitions, one corresponding to the peak at 13 K in $1/T_1$ and another to the peak at 16 K in the specific heat. The former indicates a second order antiferromagnetic (AF) transition with critical slowing down. The AF order is also confirmed by the broadening of NMR spectrum. The latter peak in the specific heat most likely corresponds to a structural transition, which lowers the symmetry of the lattice and thereby relieves the frustration, enabling the AF order at a lower temperature.

The behavior in $LiGaCr_4O_8$ is quite different. As shown in Fig. 3, a broad NMR spectrum develops below 16 K under a sharp peak that persists down to 13.5 K, indicating coexistence of the paramagnetic and AF ordered phases. Furthermore, the width of the broad spectrum does not depend on temperature, meaning that the magnitude of AF moments is constant once the transition has occurred. Therefore, AF transition must be first order. The results of $1/T_1$ in the lower panel of Fig. 2 also support coexistence of two phases. Surprisingly, $1/T_1$ of the paramagnetic component shows divergence toward 13 K as if there were second order AF transition. This transition, however, is not realized because the intensity (volume fraction) of the paramagnetic component vanishes near 13 K. These observations suggest that $LiGaCr_4O_8$ is located near a tricritical point in the phase diagram that separate first- and second-order transition lines as shown in Fig. 4.

The contrasting behavior of the two compounds demonstrates that breathing pyrochlore materials provide unique opportunities to tune the degree of frustration in a controlled manner.

References

[1] Y. Okamoto, G. J. Nilsen, J. P. Attfield, and Z. Hiroi, Phys. Rev. Lett. **110,** 097203 (2013).

[2] Y. Tanaka, M. Yoshida, M. Takigawa, Y. Okamoto, and Z. Hiroi, Phys. Rev. Lett. **113**, 227204 (2014).

Authors

Y. Tanaka, M. Yoshida, M. Takigawa, Y. Okamoto, and Z. Hiroi

Field-Induced Quantum Criticality and Universal Temperature Dependence of the Magnetization of a Spin-1/2 Heisenberg Chain

Sakakibara Group

The spin-1/2 Heisenberg antiferromagnet in one dimension is one of the few exactly solvable models of strongly interacting systems [1]. By now, we have complete understanding of its static properties, and much progress has been made in elucidating its dynamics and excited states. Yet experimental verifications of theoretical predictions on these properties are still limited. There has been a total lack of systematic experiments, in particular, near the magnetic-field-induced quantum critical point, at which the system undergoes a quantum phase transition from a quantum disordered Tomonaga-Luttinger liquid (TLL) to a gapped ferromagnet [1]. We have made precise dc magnetization measurements of $Cu(C_4H_4N_2)(NO_3)_2$, CuPzN, an ideal one-dimensional spin-1/2 Heisenberg antiferromagnet, near the critical field H_s [2]. The power-law dependences of the magnetization on temperature and magnetic field determined by this experiment are in excellent agreement with theory.

Figure 1(a) shows the magnetization M of CuPzN at 0.08 K as a function of the magnetic field up to 14.7 T. $M(H)$ shows a strong upturn as H_s (=13.97 T) is approached, and saturates to the value M_s=1.15 μ_B/Cu. The relation $H_s=J/M_s$ yields the intrachain interaction J=10.8 K. Theory predicts that $M(H)$ close to H_s exhibits a singularity $1-M/M_s = D(1-H/H_s)^{1/\delta}$, where D is a constant (=4/π) and the exponent

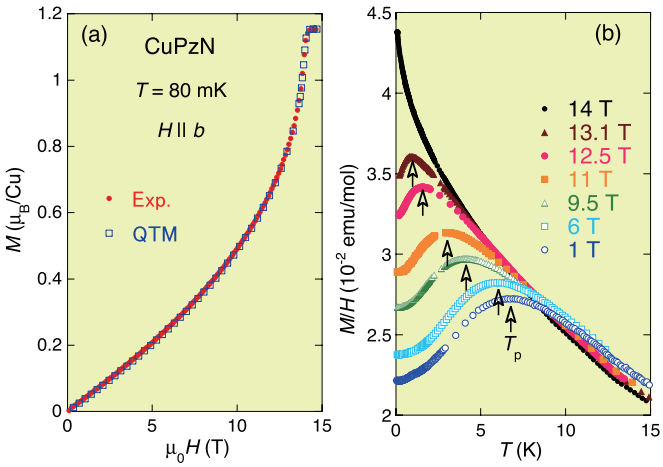

Fig. 1. Field dependence of the magnetization of CuPzN at 0.08 K (dots), along with the result of exact QTM calculations (open squares) for the 1D spin-1/2 Heisenberg antiferromagnet at 0.08 K. Temperature dependence of M/H at various fields.

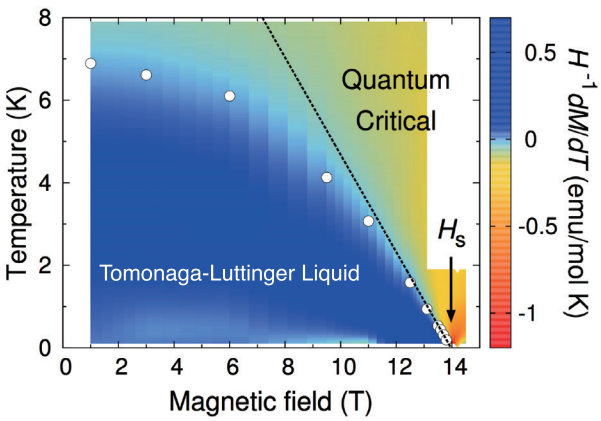

Fig. 2. T vs H phase diagram of CuPzN. Open circles denote the position of T_p. The dotted line is the universal crossover line for the free-fermion limit.

δ=2 [3]. Fitting the expression to the data between 13.6 and 13.9 T yields D=1.24 and δ=1.98, in agreement with the predicted values. Open squares in Fig. 1(a) indicate the exact curve for 0.08 K calculated by the quantum transfer-matrix (QTM) method [4], in close agreement with our experimental data in the whole field range.

The temperature dependence of M/H is shown in Fig. 1(b) for several magnetic fields. In the limit of H→0, M/H is expected to reach a maximum at T_p~0.641J [3]. This relation, combined with the experimental value of T_p=6.89 K at 1 T, yields J=10.8 K, in perfect agreement with the value determined from the $M(H)$ data. As the field increases, T_p gradually decreases, and at 13.9 T the magnetization peak eventually vanishes into a temperature region well below 0.08 K. At $H=H_s$, excitations (magnons) from the ferromagnetic state can be described exactly as free fermions, and $M(T)$ is predicted to exhibit a square-root singularity $M_s-M=bM_s(k_BT/J)^{1/2}$ [5] with the coefficient b=0.48264. This equation can be fitted very well to the 14 T data with b=0.460, in good agreement with theory.

The magnetic phase diagram of CuPzN is presented in Fig. 2 on the basis of $d(M/H)/dT$, with T_p superposed to indicate the crossover to the TLL phase. The free-fermion description gives a parameter-free expression for T_p, $k_BT_p=1.52476M_s(H_s-H)$ [5]. This universal relation, shown as a dotted line with M_s and H_s obtained from the $M(H)$ data, with no fitting parameter, agrees excellently with the data near H_s. As the magnetic field decreases, T_p deviates downward from the straight line, owing to the repulsion between magnons.

The quantum critical behavior of the magnetization of CuPzN withstands quantitative tests against theory [2], demonstrating that the material is a practically perfect one-dimensional spin-1/2 Heisenberg amtiferromagnet.

References

[1] T. Giamarchi, *Quantum Physics in One Dimension* (Oxford University Press, Oxford, England, 2004).

[2] Y. Kono, T. Sakakibara, C. P. Aoyama, C. Hotta, M. M. Turnbull, C. P. Landee, and Y. Takano, Phys. Rev. Lett. **114**, 037202 (2015).

[3] J. C. Bonner and M. E. Fisher, Phys. Rev. **135**, A640 (1964).

[4] A. Klümper, Z. Phys. B **91**, 507 (1993).

[5] Y. Maeda, C. Hotta, and M. Oshikawa, Phys. Rev. Lett. **99**, 057205 (2007).

Authors

Y. Kono, T. Sakakibara, C. P. Aoyama[a], C. Hotta[b], M.M. Turnbull[c], C. P. Landee[c], and Y. Takano[a]

[a] University of Florida

[b] The University of Tokyo

[c] Clark University

Switching of Conductivity and Magnetism by Coupled Deuterium and Electron Transfer in a Purely Organic Conductor κ-D_3(Cat-EDT-TTF)$_2$

Mori Group

A hydrogen bond (H-bond) is one of the most fundamental and important non-covalent interactions in chemistry, biology, physics, and all other molecular sciences. In particular, the dynamics of a proton or a hydrogen atom in the H-bond has attracted increasing attention, because it plays a crucial role for (bio)chemical reactions and some physical properties, such as dielectricity and proton conductivity. Here we report unprecedented H-bond-dynamics-based π-electronic switching of conductivity and magnetism in an H-bonded purely organic conductor crystal, κ-D_3(Cat-EDT-TTF)$_2$ (abbreviated as **κ-D**) [1].

This novel crystal **κ-D,** a deuterated analogue of κ-H_3(Cat-EDT-TTF)$_2$ (abbreviated as **κ-H** [2,3]), is composed only of an H-bonded molecular unit, in which two crystallographically equivalent catechol-fused ethylenedithiotetrathiafulvalene (Cat-EDT-TTF) skeletons with a +0.5 charge are linked by a symmetric anionic $[O\cdots D\cdots O]^{-1}$-type strong H-bond (Fig. 1). The deuterated and parent hydrogen systems, **κ-D** and **κ-H**, are isostructural and paramagnetic semiconductors with a dimer-Mott-type electronic structure in triangular lattice at room temperature. However, the ground states of **κ-D** and **κ-H** are totally different. As shown in Fig. 2(a), ρ of a single crystal of κ-D (blue circles) monotonically increased with decreasing temperature from 300 K to 182 K, showing typical semiconducting behavior similar to that of the parent κ-H (black circles). The room-temperature electrical conductivity σ_{rt} (= $1/\rho_{rt}$) and activation energy E_a of κ-D (6.2 Scm^{-1}, 0.08 eV) are, however, slightly higher and lower than those of κ-H (3.5 Scm^{-1}, 0.11 eV), respectively, probably related to deuterium dynamics. Upon further cooling, κ-D showed a rapid increase in ρ at 182 K, to undergo a semiconductor-insulator-like phase transition, which is in sharp contrast to the continuous monotonic semiconducting behavior in κ-H. Such a remarkable H/D substitution effect is also observed in the temperature dependence of the magnetic susceptibility (χ_p) of **κ-D** and **κ-H** in the polycrystalline state in the temperature range of 2–300 K (Fig. 2(b)). With decreasing temperature, χ_p of **κ-H** (black circles) follows the Heisenberg model of triangular lattice with J/k_B = 80 – 100 K and shows no magnetic order down to 50 mK, indicating quantum spin liquid state [4]. On the other hand, the deuterated analogue **κ-D** (blue circles) exhibits an abrupt drop of χ_p at 185 K after the monotonic increase similar to **κ-H**. After the abrupt drop, χ_p of **κ-D** gradually approaches ~ 0.0 emu mol^{-1} with decreasing temperature. This low-temperature magnetic behavior is reproduced by the singlet-triplet dimer model with an antiferromagnetic coupling of $2J/k_B$ ~ –600 K (orange line in Fig. 2(b)). Therefore, a spin-singlet state is formed in **κ-D** by the magnetic transition from the high-temperature (HT) paramagnetic phase, which leads to a non-magnetic ground state, in sharp contrast to **κ-H** with a quantum spin liquid ground state. Such a surprisingly large increase in T_c by over 180 K, deuterium isotope effect, has not been reported, to our knowledge.

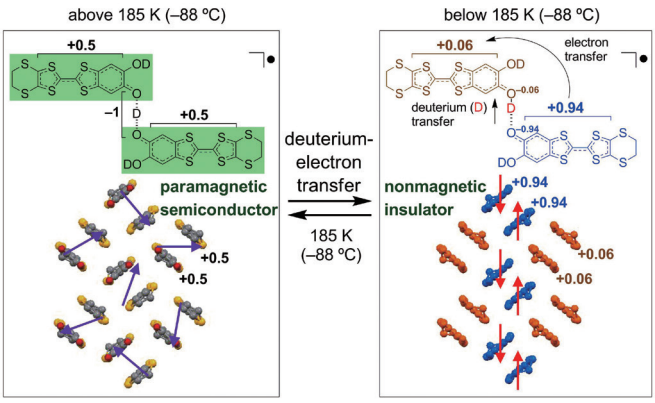

Fig. 1. Schematic drawing of thermal switching of electrical conductivity and magnetism in κ-D_3(Cat-EDT-TTF)$_2$. A purely organic material, κ-D_3(Cat-EDT-TTF)$_2$, is composed of a unit structure where Cat-EDT-TTF molecules (green colored, left) are connected by an [O···D···O] hydrogen bond. At 185 K (–88 °C), the deuterium and electron transfer occurs, to change the electric charge on the two Cat-EDT-TTF molecules [(+0.5 vs +0.5) ↔ (+0.06 vs +0.94)], which results in the switching of electrical conductivity (semiconductor ↔insulator) and magnetism (paramagnetic ↔ nonmagnetic).

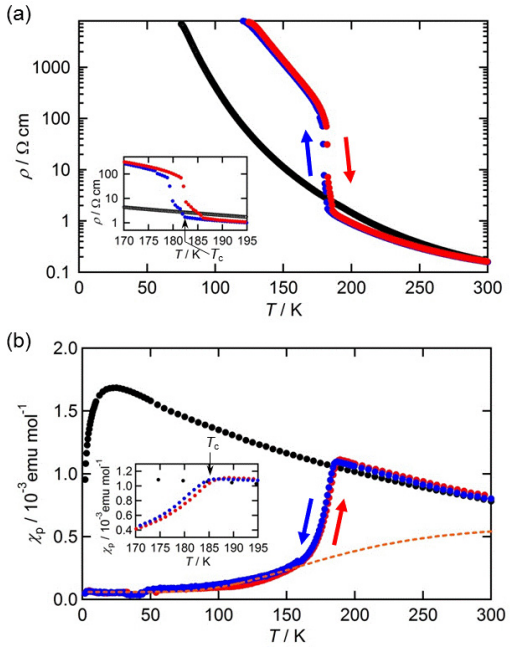

Fig. 2. Temperature dependence of (a) electrical resistivity (on a single crystal) and (b) magnetic susceptibility (of a polycrystalline sample) of κ-D (blue and red circles represent the cooling and heating processes, respectively) and κ-H (black circles in the cooling process). The orange line represents the fitting curve for κ-D by the singlet-triplet dimer model with an antiferromagnetic coupling of $2J/k_B$ ~ –600 K.

In order to gain structural insight into this deuteration-induced phase transition with the electronic switching, we have carried out X-ray diffraction studies on a single crystal of **κ-D** using synchrotron radiation in the temperature range of 50–270 K. The **κ-D** system at 270 K is isostructural to **κ-H** (vide infra). Upon the phase transition, the H-bonded deuterium transfers from the center of the two oxygen atoms towards one oxygen atom, to form an asymmetric $[O–D\cdots O]^{-1}$ H-bond with short O–D (1.02(5) Å) and long O•••D (1.51(5) Å) distances (Fig. 1 right), instead of the two equivalent O•••D distances at 270 K (1.265(7) Å, Fig.1 left). As a result, the two crystallographically equivalent Cat-EDT-TTF$^{+0.5}$ skeletons in the HT phase are also desymmetrized, to give a charge-poor Cat-EDT-TTF$^{+0.06}$ with the short O–D distance and a charge-rich Cat-EDT-TTF$^{+0.94}$ with the long O•••D distance, as estimated from the bond lengths of the TTF skeletons. Due to the intra-unit charge disproportionation through the H-bond, the overall electronic structure of κ-D in the LT phase is intrinsically different from that in the HT phase. Below 180 K, the charge-rich

(blue-colored) and -poor (orange-colored) Cat-EDT-TTF skeletons are separately π-dimerized with their neighboring cofacial Cat-EDT-TTF skeletons having the same valence, to form two kinds of π-dimeric pairs, composed of the charge-rich skeletons or the charge-poor ones. These π-dimers are stacked two-dimensionally with maintaining the κ-type molecular arrangement, which results in a charge-ordered (CO) electronic structure (Fig. 1 right) from a dimer-Mott state in the HT phase (Fig. 1 left). In this CO state, since the charge-rich $TTF^{+0.94}$ skeleton is expected to have nearly one electron spin (S = 1/2), a spin singlet should be formed within each charge-rich π-dimer, which rationalizes the paramagnetic–non-magnetic transition in magnetic susceptibility (Fig. 2(b)) as well as the semiconductor-insulator-like transition in resistivity (Fig. 2(a)).

In summary, we have discovered unprecedented H-bond-dynamics-based π-electronic properties switching in an purely organic conductor crystal: Deuteration of the $[O•••H•••O]^{-1}$ H-bond in a catechol-fused TTF-based purely organic conductor crystal, κ-H_3(Cat-EDT-TTF)$_2$ or **κ-H**, gives rise to a phase transition at 185 K with significant switching of the π-electronic structure (dimer-Mott ↔ charge order), electrical conductivity (semiconducting ↔ insulating), and magnetism (paramagnetic ↔ non-magnetic), due to deuterium transfer or displacement within the H-bond accompanied by electron transfer between the H-bonded Cat-EDT-TTF π-systems. This result clearly demonstrates that the H-bonded deuterium dynamics and the TTF π-electron are cooperatively coupled in the present system. Further systematic tuning of proton and π-electron dynamics in this coupled system will afford novel chemical and physical functionalities beyond the framework of π-electronics so far.

References

[1] A. Ueda, S. Yamada, T. Isono, H. Kamo, A. Nakao, R. Kumai, H. Nakao, Y. Murakami, K. Yamamoto, Y. Nishio, and H. Mori, J. Am. Chem. Soc. **136 (34)**, 12184 (2014).

[2] H. Kamo, A. Ueda, T. Isono, K. Takahashi, and H. Mori, Tetrahedron Lett. **53**, 4385 (2012).

[3] T. Isono, H. Kamo, A. Ueda, K. Takahashi, A. Nakao, R. Kumai, H. Nakao, K. Kobayashi, Y. Murakami, and H. Mori, Nature Commun. **4**, 1344 (2013).

[4] T. Isono, H. Kamo, A. Ueda, K.Takahashi, M. Kimata, H. Tajima, S. Tsuchiya, T. Terashima, S. Uji, and H. Mori, Phys. Rev. Lett. **112**, 177201 (2014).

Authors

A. Ueda, S. Yamada, T. Isono[a], H. Kamo, A. Nakao[b], R. Kumai[c], H. Nakao[c], Y. Murakami[c], K. Yamamoto[d], Y. Nishio[e], and H. Mori

[a] National Institute for Materials Science

[b] Comprehensive Research Organization for Science and Society (CROSS),

[c] CMRC and Photon Factory, Institute of Materials Structure Science, High Energy Accelerator Research Organization (KEK)

[d] Okayama University of Science

[e] Toho University

Field-Induced Quadrupolar Quantum Criticality in PrV_2Al_{20}

Nakatsuji Group

Extensive studies have revealed nontrivial metallic phenomena associated with a magnetic quantum criticality in various correlated electron systems. Whether another type of instability due to orbital degree of freedom may drive novel types of metallic states and unconventional superconductivity has been an active area of research. Since f-electron systems may provide a non-magnetic crystal-electric-field (CEF) ground-state doublet, where orbitals are the only active degree of freedom, we can study the pure orbital contribution. In fact, some Pr ($4f^2$)-based cubic compounds are found to host the Γ_3 non-Kramers ground-state doublet, which has no magnetic moment but carries an electric quadrupole moment. A number of cubic $4f^2\Gamma_3$ systems were studied and various interesting electric phenomena were experimentally reported including a ferro and antiferro quadrupolar ordering. As a competing effect, a non-magnetic form of the Kondo effect has been proposed that quenches the quadrupole moments. Thus, the tuning of these competing effects may lead to quadrupolar quantum criticality.

In fact, strong hybridization effects and quadrupolar quantum criticality have been suggested by recent intensive studies on the new cubic Γ_3 systems PrT_2Al_{20}, where T corresponds to transition metals such as Ti and V [1-5]. Evidence for strong hybridization in PrV_2Al_{20} is further provided by the recent discovery of heavy-fermion superconductivity at T_c = 50 mK in the quadrupolar ordered state below T_Q = 0.6 K [4]. The effective mass of the quasiparticles participating into the superconducting condensate was found to be as large as 140 m_0[4]. This result indicates that PrV_2Al_{20} should be located in the vicinity of a QCP associated only with multipole moments. To realize such quantum criticality due to multipole moments, the magnetic field is one of the useful control parameters. The quantum criticality is expected to be observed near the critical field of the quadrupolar ordered state with T_Q = 0.6 K on the basis of the similarity to the magnetically ordered system. The

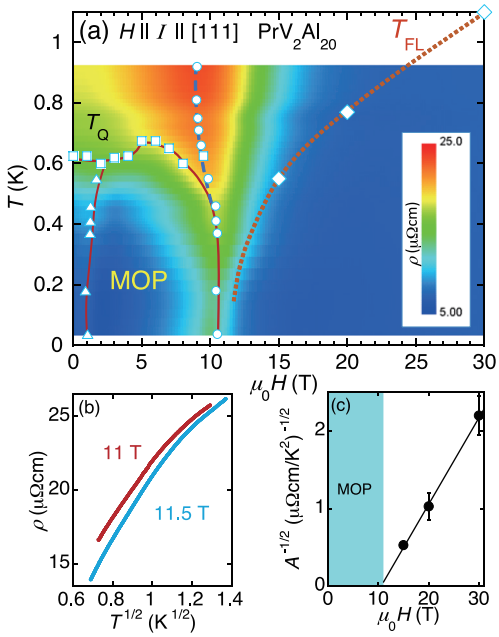

Fig. 1. (a) Magnetic phase diagram of PrV_2Al_{20} with magnetic fields, and current I, parallel to the [111] direction. Color plot indicates the $\rho(H, T)$ values obtained from the field H scans at a constant T. Circles indicate the peak position at H_c = 11 T, separating the low field multipolar ordering phase (MOP) and the paraquadrupolar state at high fields. Triangles represent small peaks observed in $\rho(H)$ for fields below 2 T. The solid line and broken line show the transition temperature/field of the multipole ordered phase and the peak position in $\rho(H)$, respectively. Squares and diamonds respectively indicate T_Q and a characteristic temperature T_{FL} below which $\rho(T)$ follows the Fermi-liquid T^2 law. The dotted line is a guide to the eyes. (b) ρ as a function of $T^{1/2}$ under H = 11 T and 11.5 T. (c) Field dependence of $A^{-1/2}$, where A is the T^2 coefficients in $\rho(T)$. According to the standard Fermi liquid theory, the effective mass m^* is proportional to $A^{1/2}$.

quadrupole ordered state has a nearly H-independent transition temperature under the magnetic field below 9 T, which becomes anisotropic in the higher field [1, 5].

We report the discovery of a field-tuned quantum criticality based solely on the quadrupolar (orbital) degrees of freedom in PrV_2Al_{20} through the magneto-transport measurements up to 35 T by using the high DC magnetic field facilities at the National High Magnetic Field Laboratory [6].

Our study on PrV_2Al_{20} reveals the field-induced quadrupolar quantum criticality at the critical field H_c = 11 T applied along the [111] direction. Near H_c required to suppress the quadrupolar state, we found a marked enhancement of the resistivity $\rho(H, T)$ (Fig. 1 (a)), concomitant non-Fermi liquid (NFL) behavior following $\rho(T) \sim T^n$ with $n < 0.5$ in the vicinity of critical field (Fig. 1 (b)), and a divergent quasiparticle effective mass as a function of the magnetic field toward critical field of 11 T (Fig. 1 (c)). We also observed the Shubnikov-de Haas oscillation above H_c, indicating an effective mass enhancement up to $m^*/m_0 \sim 10$. These reveal the field induced quadrupolar quantum criticality where the competition between the nonmagnetic Kondo effect and the intersite quadrupolar coupling leads to pronounced NFL behaviors in an extensive region of T and H around the quantum critical point.

References

[1] A. Sakai and S. Nakatsuji, J. Phys. Soc. Jpn. **80**, 063701 (2011).
[2] A. Sakai, K. Kuga, and S. Nakatsuji, J. Phys. Soc. Jpn. **81**, 083702 (2012).
[3] K. Matsubayashi, T. Tanaka, A. Sakai, S. Nakatsuji, Y. Kubo, and Y. Uwatoko, Phys. Rev. Lett. **109**, 187004 (2012).
[4] M. Tsujimoto, Y, Matsumoto, T. Tomita, A. Sakai, and S. Nakatsuji, Phys. Rev. Lett. **113**, 267001 (2014).
[5] Y. Shimura, Y. Ohta, T. Sakakibara, A. Sakai and S. Nakatsuji, J. Phys. Soc. Jpn. **82**, 043705 (2013).
[6] Y. Shimura, M. Tsujimoto, B. Zeng, L. Balicas, A. Sakai, and S. Nakatsuji, to be published in Phys. Rev. B (2015).

Authors

Y. Shimura, M. Tsujimoto, B. Zeng[a], L. Balicas[a], A. Sakai[b], and S. Nakatsuji

[a]National High Magnetic Field Laboratory, Florida State University

[b]I. Physikalisches Institut, Georg-August-Universitat

Novel Superconductivity Mediated by Quantum Orbital Fluctuations

Nakatsuji Group

Superconductivity is a quantum macroscopic phenomenon where the electrons in solids form "Cooper pairs" at low temperatures, leading to a zero-resistance state. This has been studied extensively for basic science as well as for industrial applications. In the case of conventional superconductors, lattice vibrations (phonons) provide the "glue" among the electrons to form the Cooper pairs. On the other hand, in the case of magnetic materials such as the cuprate high-temperature superconductors, recent studies have revealed that fluctuations of the microscopic magnets inherent in electrons, namely "spin," causes the formation of the Cooper pairs.

Such superconductivity has been studied extensively especially in the 4f based intermetallics, where a lot of heavy fermion superconductors have been found in the vicinity of magnetic QCPs (Fig. 1(A)). Here, an interesting question is whether novel superconductivity arises at a QCP of orbital

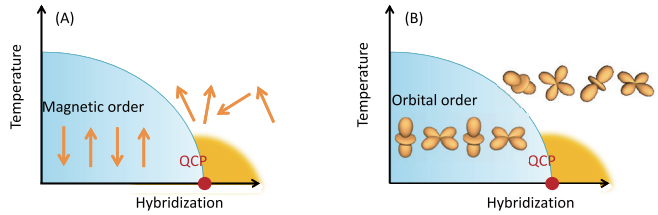

Fig. 1. (A) Schematic image of a quantum critical point that is realized by the suppression of magnetic ordering. There is a quantum phase transition from a magnetic (spin-ordered) state to a paramagnetic (disordered) state at the magnetic quantum critical point (QCP). Unconventional superconductivity mediated by spin fluctuations has been found at the vicinity of the quantum critical point. (B) Image of a quantum critical point realized by the suppression of orbital ordering (Spins in Fig. 1 (A) are changed to orbitals). It is a significant subject to reveal the physical properties in the vicinity of the orbital quantum critical point.

orderings due to orbital fluctuations of the f electrons or not (Fig. 1(B)). In order to study this, the material with purely orbital degrees of freedom is required. Besides, the material should be clean enough and the hybridization should be large. However, there has been no prototypical system that satisfies all these requirements.

On the other hand, recent studies have revealed that PrT_2Al_{20}(T = Ti, V) are the ideal systems to study the quantum criticality arising from orbital degrees of freedom [1]. Both systems have the nonmagnetic cubic Γ_3 crystal electric field doublet. In addition, the hybridization is strong as is evident in many physical properties [1-3]. Significantly, both exhibit heavy fermion superconductivity inside the multipole ordered phases (Fig. 2) [2-4]. In particular, in the case of PrV_2Al_{20}, the effective mass is highly enhanced ($m^*/m_0 \sim 140$) even at ambient pressure, revealing even stronger hybridization in PrV_2Al_{20} than in $PrTi_2Al_{20}$ [4]. Furthermore, the superconductivity emerges from a novel metallic state realized due to the strong fluctuations of the non-magnetic orbital degrees of freedom. This observation indicates the first realization of the novel superconductivity arising from the orbital fluctuations of the f electrons at ambient pressure.

The discovery of the new mechanism for the formation of Cooper pairs may open the new research field of the material science based on orbital degrees of freedom, and may lead to another breakthrough in the superconductivity research.

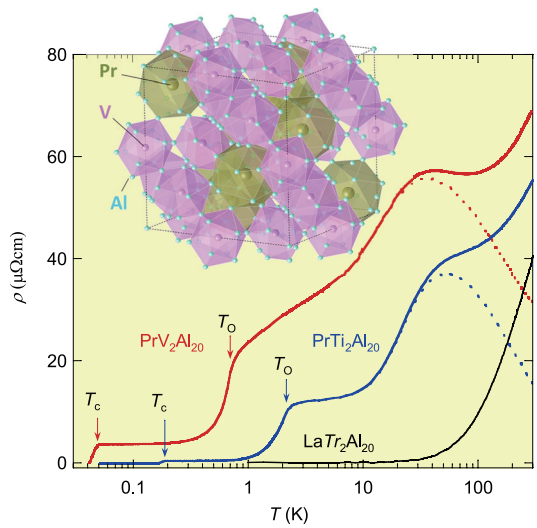

Fig. 2. The resistivity vs. temperature of PrV_2Al_{20} and $PrTi_2Al_{20}$. T_O and T_c represents the multipolar ordering and superconductivity transitions respectively. T_c is 0.05 K for V system and 0.2 K for Ti system. The inset shows the crystal structure of PrV_2Al_{20}.

References
[1] A. Sakai, and S. Nakatsuji, J. Phys. Soc. Jpn. **80**, 063701 (2011).
[2] A. Sakai, K. Kuga, and S. Nakatsuji, J. Phys. Soc. Jpn. **81**, 083702 (2012).
[3] K. Matsubayashi, T. Tanaka, A. Sakai, S. Nakatsuji, Y. Kubo, and Y. Uwatoko, Phys. Rev. Lett. **109**, 187004 (2012).
[4] M. Tsujimoto, Y. Matsumoto, T. Tomita, A. Sakai, and S. Nakatsuji, Phys. Rev. Lett. **113**, 267001 (2014).

Authors
M. Tsujimoto, Y. Matsumoto, and S. Nakatsuji

Field Evolution of Quantum Critical and Heavy Fermi-liquid Components in the Magnetization of the Mixed Valence Compound β-$YbAlB_4$

Nakatsuji, Sakakibara, Tokunaga, and Kindo Group

Formation of novel quantum phases in the vicinity of a quantum critical point (QCP) has been studied extensively in condensed matter physics for a past few decades. In particular, in the heavy fermion intermetallic systems, a number of prototypical examples of novel phenomena, such as unconventional superconductivity and non-Fermi liquid (NFL) behavior, have been discovered in the vicinity of a magnetic QCP where the magnetic ordering temperature is suppressed to zero.

So far, these studies of quantum criticality (QC) have been restricted mostly to the Kondo lattice systems with integer valence. On the other hand, the first Yb-based heavy fermion superconductor β-$YbAlB_4$ provides a unique example of QC in the strongly mixed valence states [1-4]. Furthermore, the QC cannot be described by the standard theory for the spin-density-wave instability. The divergent magnetic susceptibility along the *c* axis exhibits *T*/*B* scaling in the wide temperature (*T*) and magnetic field (*B*) region spanning 3 ~ 4 orders of magnitude. This indicates that the QCP is located just at the zero magnetic field within the experimental resolution of ~ 0.2 mT under ambient pressure [3]. The QC emerging without tuning any control parameter suggests the formation of an anomalous metallic phase.

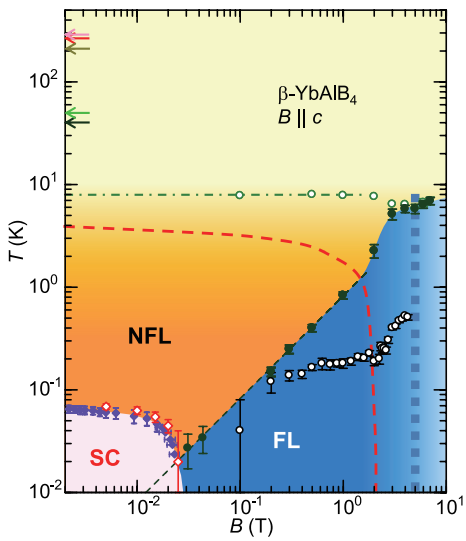

Fig. 1. *T*-*B* phase diagram of β-$YbAlB_4$ for the field applied along the *c* axis. The valence fluctuation scale is shown as pink, red and dark yellow arrows (from top to bottom) at T ~ 200 - 300 K which corresponds to T scale obtained by the X-ray adsorption measurements [7], the coherence peak in $\rho_{ab}{}^{m}$ [1] and the peak temperautre in χ_{ab} at B = 0.1, 7.0 T, respectively. The light and dark green arrows indicate the anomalies in the T derivative of the in-plane resistivity $d\rho_{ab}/dT$ at T ~ 50 K [8] and the peak in the Hall coefficient R_H at ~ 40 K [6], respectively. These temperature scales correspond to the effective Kondo lattice temperature for the low T HF behavior. Green filled circles correspond to the peaks in $-d\chi/dT$, which separates the QC and FL regions. Green open circles correspond to the peak temperature scale T^* in $\Delta(-d\chi/dT)$ obtained after subtracting QC components, which sets the onset of the heavy fermion state. Black open circles correspond to T_{FL} determined by ρ_{ab} [1]. Filled and open diamonds correspond to superconducting phase boundary determined by the SQUID ac susceptibility measurements [9] and the resistivity measurements [2], respectively. Inside the red broken line, the QC scaling is observed. The vertical blue broken line at B ~ 5 T indicates the crossover field above which the HF state is suppressed.

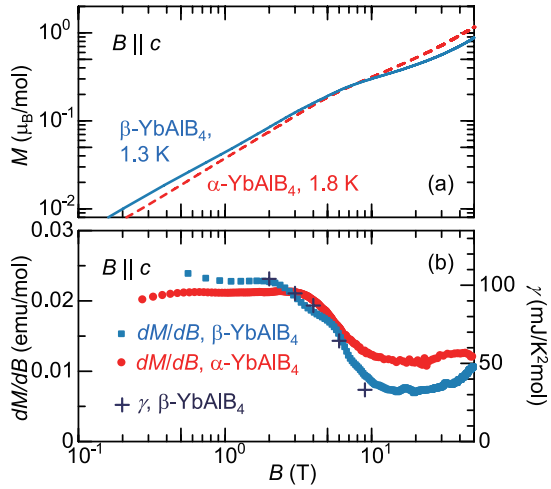

Fig. 2. (a) Magnetization curves of β- and α-$YbAlB_4$ at T = 1.3 and 1.8 K, respectively. (b) dM/dB obtained from the data shown in (a) (the left axis) and the electronic specific heat coefficient γ estimated from the electric specific heat at T = 0.4 K [3] (the right axis).

Here, we discuss the magnetization (*M*) in β-$YbAlB_4$ in the *T* range from 0.02 K to 320 K spanning four orders of magnitude to see how it evolves with magnetic field in detail, providing a *T*-*B* phase diagram to summarize the various *T* and *B* scales for β-$YbAlB_4$ (Fig. 1) [5]. First of all, we examined the possibility of other scaling such as $T/(B-B_c)^{\delta}$ scaling with $B_c \neq 0$ or $\delta \neq 1$, and confirmed that the *T*/*B* scaling reported in our previous work [3] provides the best quality of the fitting [5].

We further estimated the heavy Fermi-liquid component of *M* after subtracting the QC component by using the *T*/*B* scaling. The obtained heavy Fermi-liquid component exhibits the *T* and *B* dependence quite similar to the magnetization of α-$YbAlB_4$, having a peak in $-dM/dT$ at T^* ~ 8 K, which is suppressed above B^* ~ 5 T. Here, α-$YbAlB_4$ is the locally isostructural polymorph of β-$YbAlB_4$ and is also strongly mixed valent ($Yb^{+2.73}$ and $Yb^{+2.75}$ for α- and β-$YbAlB_4$ at 20 K, respectively) [4]. Our observation indicates that the HF behavior in α- and β-$YbAlB_4$ becomes suppressed above B^* ~ 5 T corresponding to the small renormalized Kondo scale. This was also confirmed by the analysis of the field dependence of the electronic specific heat coefficient of β-$YbAlB_4$ and the measurements of the magnetization curve up to ~ 50 T for both α- and β-$YbAlB_4$. This suppression of the HF behavior may be related to the recent observation of the field induced anisotropic NFL behavior in α-$YbAlB_4$. In β-$YbAlB_4$, on the other hand, we found no sign of such field induced NFL behavior.

While the effective *g*-factor estimated from the Zeeman coupling relation $k_BT^* = g\mu_BB^*$ and *T*/*B* scaling suggests the effective moment of ~ 2 μ_B for β-$YbAlB_4$, *M* at the suppression field B^* only reaches a considerably smaller value

~ 0.2 μ_B. This indicates that only a part of the f moments participates in the zero-field QC or HF behavior, as also suggested by the recent Hall effect measurements [6]. The multiple bands and their topological feature should play an important role in the formation of the low temperature heavy fermion state and quantum criticality in the intermediate valence state.

References

[1] S. Nakatsuji, K. Kuga, Y. Machida, T. Tayama, T. Sakakibara, Y. Karaki, H. Ishimoto, S. Yonezawa, Y. Maeno, E. Pearson, G. G. Lonzarich, L. Balicas, H. Lee, and Z. Fisk, Nature Physics **4**, 603 (2008).

[2] K. Kuga, Y. Karaki, Y. Matsumoto, Y. Machida, and S. Nakatsuji, Physical Review Letters **101**, 137004 (2008).

[3] Y. Matsumoto, S. Nakatsuji, K. Kuga, Y. Karaki, N. Horie, Y. Shimura, T. Sakakibara, A. H. Nevidomskyy, and Piers Coleman, Science **331**, 316 (2011).

[4] M. Okawa, M. Matsunami, K. Ishizaka, R. Eguchi, M. Taguchi, A. Chainani, Y. Takata, M. Yabashi, K. Tamasaku, Y. Nishino, T. Ishikawa, K. Kuga, N. Horie, S. Nakatsuji, and S. Shin, Physical Review Letters **104**, 247201 (2010).

[5] Y. Matsumoto, K. Kuga, Y. Karaki, Y. Shimura, T. Sakakibara, M. Tokunaga, K. Kindo, and S. Nakatsuji, Journal of the Physical Society of Japan **84**, 024710 (2015).

[6] E. C. T. O'Farrell, Y. Matsumoto, and S. Nakatsuji, Physical Review Letters **109**, 176405 (2012).

[7] Y. H. Matsuda, T. Nakamura, K. Kuga, S. Nakatsuji, S. Michimura, T. Inami, N. Kawamura, and M. Mizumaki, Journal of the Korean Physical Society **62**, 1778 (2013).

[8] Y. Matsumoto, K. Kuga, T. Tomita, Y. Karaki, and S. Nakatsuji, Phys. Rev. B **84**, 125126 (2011).

[9] Y. Matsumoto, K. Kuga, Y. Karaki, T. Tomita, and S. Nakatsuji, Phys. Status Solidi B **247**, 720 (2010).

Authors

Y. Matsumoto, K. Kuga, Y. Karaki[a], Y. Shimura, T. Sakakibara, M. Tokunaga, K. Kindo, and S. Nakatsuji,

[a]University of the Ryukyus

Magnetic Anomaly due to the Non-Coplanar Antiferromagnetic Spin Structure in NiS_2

Nakatsuji Group

Non-coplanar spin arrangements in frustrated magnets have attracted great interest because the associated spin chirality may induce exotic phenomena such as multiferroicity, topological Hall transport, and chiral spin liquid states. While most non-coplanar magnets are characterized by their ferromagnetic (FM) component, a purely antiferromagnetic (AF) all-in/all-out (AIAO) structure has recently

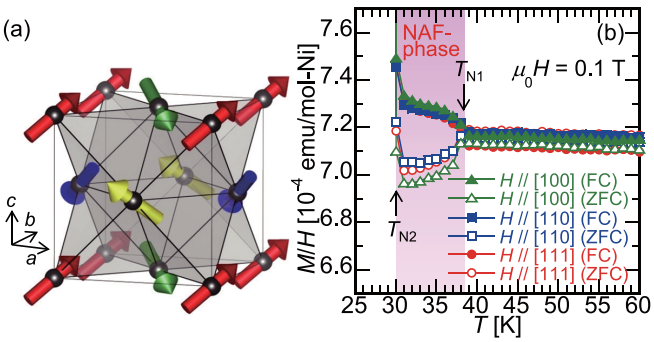

Fig. 1. (a) NAF structure of NiS_2. Arrows indicate the Ni^{2+} magnetic moments [5]. (b) Temperature dependence of the magnetic susceptibility $\chi(T) = M(T)/H$ in the magnetic field of 0.1 T.

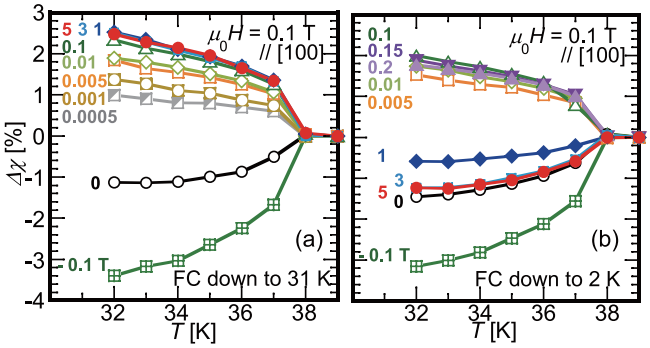

Fig. 2. Temperature dependence of $\Delta\chi(T) = \{\chi(T)-\chi(39\ \mathrm{K})\}/\chi(39\ \mathrm{K})\times100\%$ (the change in $\chi(T)$ from the one at 39 K > T_{N1}) obtained on heating in μ_0H = 0.1 T // [100] after the field cooling (a) down to 31 K and (b) down to 2 K with various magnetic fields for the FC procedure μ_0H_{FC} = -0.1-5 T.

been discovered in several 5d pyrochlore oxide. While this magnetic structure has zero net magnetic moment owing to the cancellation of the moments on the four vertexes of a tetrahedron, it has two types of AF variant, which are connected by the time-reversal operation, and permits a multi-domain state as in the case of FM materials [1]. In this system, it has been theoretically proposed that the magnetic domain wall (DW) induces a net uniform magnetization and hosts a gapless interface state with Fermi arcs [2]. Experimentally, the unconventional weak ferromagnetic (WF) moment and the anomalous magnetoconductivity have been observed in the AIAO-phase of $Eu_2Ir_2O_7$ and $Nd_2Ir_2O_7$, respectively [3]. As the domain physics is inherent to the AIAO structure, similarly interesting physics associated with the DW should generally emerge in other materials that host the non-coplanar AF spin structure. However, to date, there have been almost no reports on studies of domain phenomena related to the non-coplanar AF spin structure.

The antiferromagnet NiS_2 has the pyrite structure. The magnetic ion Ni^{2+} forms an fcc lattice, one of geometrical frustrated lattices. Neutron diffraction measurements have revealed that NiS_2 exhibits a non-coplanar AF spin structure with four spin sublattices (NAF structure), similarly to the AIAO structure [Fig. 1(a)], in the temperature region between T_{N1} = 38 K and T_{N2} = 30 K, and the WF-phase below T_{N2} [4]. We have carried out detailed magnetization measurements using high-quality single crystals of NiS_2 to reveal magnetic properties associated with the NAF structure [5].

A small but distinct hysteresis in the temperature dependence of the susceptibility $\chi(T)$ was observed in the NAF-phase [Fig. 1(b)]. While this type of hysteresis is not observed in a collinear antiferromagnet, a similar behavior has been reported for $Eu_2Ir_2O_7$, suggesting that the behavior is inherent in the non-coplanar AF spin structure. To reveal the origin of the hysteresis, we performed the $\chi(T)$ measurement with the two field cooling (FC) processes, namely, (i) cooling down to 31 K in the NAF-phase, and (ii) cooling down to 2 K in the WF-phase under various FC magnetic fields μ_0H_{FC} between − 0.1 and 5 T. After the FC sequences, we changed the field at the lowest temperatures (31 or 2 K), and measured $\chi(T)$ in μ_0H = 0.1 T.

The results in Fig. 2(a) obtained after the FC process (i), which corresponds to a direct magnetic field control of the NAF structure, show that $\chi(T)$ monotonically increases with increasing μ_0H_{FC} and saturates above 1 T. On the other hand, the results in Fig. 2(b) obtained after the FC process (ii), namely, the indirect magnetic field control of the NAF structure by aligning the WF moment in WF-phase, show the

unusual $\mu_0 H_{FC}$ dependence of $\chi(T)$. While $\chi(T)$ monotonically increases with increasing $\mu_0 H_{FC}$ under $\mu_0 H_{FC} \leqq 0.1$ T, $\chi(T)$ under 0.1 T < $\mu_0 H_{FC} \leqq 3$ T decreases with increasing $\mu_0 H_{FC}$, and $\chi(T)$ under $\mu_0 H_{FC} = 3$ and 5 T exhibits almost the same behavior as the result with $\mu_0 H_{FC} = 0$ T. These observations indicate that the NAF structure can be controlled by using the WF-phase. In addition, the anomalous $\mu_0 H_{FC}$ dependence of the magnetic hysteresis found in the NAF-phase strongly suggests that the small FM moment in the NAF-phase comes from the DWs.

References

[1] T.-h. Arima, J. Phys. Soc. Jpn. **82**, 013705 (2013).
[2] Y. Yamaji and M. Imada, Phys. Rev. X **4**, 021035 (2014).
[3] J. J. Ishikawa, E. C. T. O' Farrell, and S. Nakatsuji, Phys. Rev. B **85**, 245109 (2012); K. Ueda *et al.*, Phys. Rev. B **89**, 075127 (2014).
[4] K. Kikuchi *et al.*, J. Phys. Soc. Jpn. **45**, 444 (1978).
[5] T. Higo and S. Nakatsuji, J. Phys. Soc. Jpn. **84**, 053702 (2015).

Authors
T. Higo and S Nakatsuji

Continuous Mott Transition in the Hubbard Model on the 1/5-Depleted Square Lattice

K. Ueda Group

Metal-insulator (MI) transition is a central problem of the physics of strongly correlated electron systems. In the simplest case of the square lattice Hubbard model, it has been established that the ground state at half-filling is always a Mott insulating state with the antiferromagnetic long range order. Under the assumption of paramagnetic phase it is widely believed that the transition from the paramagnetic metallic phase to the paramagnetic insulating phase takes place through a discontinuous transition. One can ask the question how general is the first order nature of various MI transitions.

In particular, nature of MI transitions in non-Bravais lattices seems to be non-trivial and interesting. We study the MI transition in the one-fifth depleted square lattice Hubbard model. The unit cell contains four lattice sites which form a square. The square plaquettes are connected by dimer bonds. The 1/5-depleted square lattice does not have any effect of the geometrical frustration. However, the Heisenberg model on this lattice shows quantum phase transitions from the dimer singlet phase to the antiferromagnetic ordered phase and then onto the plaquette singlet phase. Since the Heisenberg model is an effective Hamiltonian of the Hubbard model in the strong correlation limit, it is an interesting problem to look at the nature of MI transition of the Hubbard model.

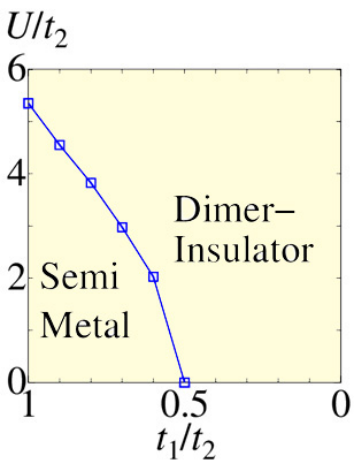

Fig. 1. Phase diagram of the Hubbard model on the 1/5-depleted square lattice. On the dimer side where the intra-dimer hopping, t_2, is bigger than the intra-plaquette hopping, t_1, the MI transition from the semi-metallic phase to the dimer-insulating one is a continuous transition.

In the present study we investigate the MI transition of the Hubbard model on the 1/5-depleted square lattice in the paramagnetic phase by using the cellular dynamical mean field theory. When the intra-plaquette hopping, t_1, is smaller than the intra-dimer hopping, t_2, the MI transition is continuous. This time we use the eight-site cluster to check the finite-size effect of the cellular DMFT. This continuous MI transition is characterized by the Lifshitz transition which is associated with the appearance or annihilation of the pair of electron and hole pockets in different bands. New feature found in this study is that the Lifshitz transition is triggered not only by changing a one-body parameter, t_1/t_2, but also by changing the magnitude of the Coulomb interaction, U. One can see these features clearly by studying the self-energies corresponding to the dimer bonds and the plaquette bonds.

Reference

[1] Y. Yanagi and K. Ueda: Phys. Rev. B**90**, 085113 (2014).

Authors
Y. Yanagi[a], and K. Ueda
[a]Tokyo University of Science

Orbital Angular Momentum and Spectral Flow in Two Dimensional Chiral Superfluids

Oshikawa Group

Fermions can exhibit superfluidity/superconductivity by forming Cooper pairs, which undergo Bose-Einstein Condensation (BEC). In the most conventional metallic superconductors, the Cooper pair is formed with zero relative angular momentum ("*s*-wave pairing"). However, the Cooper pair can be also formed with a non-vanishing relative angular momentum. When the angular momentum of each Cooper pair is aligned, the superfluid as a whole breaks the time-reversal symmetry and is called "chiral superfluid". One of the superfluid phases of ^{3}He called "superfluid A-phase", indeed is such a chiral superfluid, in which each Cooper pair has a relative angular momentum 1 ("*p*+*ip*-wave pairing"). There is also much evidence that Sr_2RuO_4 is a chiral *p*+*ip*-wave superconductor. We can also consider more general chiral superfluids/superconductors, in which each Cooper pair carries the angular momentum ν (ν=1 for *p*+*ip*, ν=2 for *d*+*id*, etc.).

We can then ask a simple question: what is the total orbital angular momentum of the chiral superfluid which consists of N fermions? On one hand, the answer seems obvious: since there would be $N/2$ Cooper pairs, it must be $\nu N/2$. On the other hand, since the pairing energy Δ is usually much smaller than the Fermi energy E_F in Bardeen-Cooper-Schrieffer (BCS) type superfluids, we may also think that only the fermions near the Fermi surface are affected by the pairing. In this picture, we rather expect the total orbital

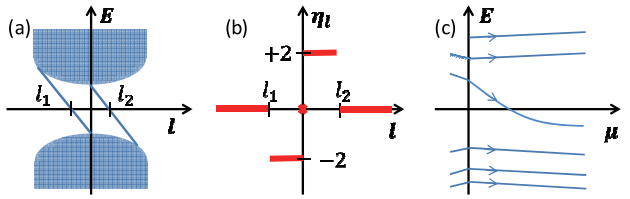

Fig. 1. The total orbital angular momentum of a *d+id*-wave (ν=2) chiral superfluid and spectral flow. (a) The energy spectrum in the weak-pairing (BCS) phase, as a function of the angular momentum l. Two gapless edge modes can be seen within the pairing gap. (b) The contribution η_l in each sector with angular momentum l to the quantum number Q, in the weak-pairing (BCS) phase. Non-vanishing contributions are present in the region between the "Fermi angular momenta" where the gapless edge modes cross the zero energy. They make Q non-vanishing, suppressing the total orbital angular momentum from the "ideal" value $\nu N/2$. (c) The energy spectrum at a fixed angular momentum l, which lies between the Fermi angular momenta inside the weak-pairing (BCS) phase, as a function of the chemical potential μ. When μ is changed from negative (strong-pairing, BEC phase) to positive (weak-pairing, BCS phase), one of the energy eigenvalues changes sign, as required from the structure of the edge modes. This induces the non-vanishing contribution η_l to Q discussed in (b) above, in the weak-pairing (BCS) phase.

angular momentum is suppressed as $(\Delta/E_F)^\alpha \nu N/2$, where $\alpha>0$. There have been many conflicting papers published over the last several decades on this question, but it still remains controversial.

In order to clarify the long-standing puzzle, we studied chiral superfluids in a two-dimensional circular potential (disk), within the standard Bogoliubov-de Gennes framework but without further approximations or assumptions. The Bogoliubov-de Gennes Hamiltonian has anomalous pairing terms and thus does not conserve particle number N nor the total orbital angular momentum L. Nevertheless, as Volovik pointed out, the combination $Q = L - \nu N/2$ is still conserved and turns out to be a quite useful quantum number. For each value of ν, there are two phases of chiral superfluid: strong-pairing (BEC) and weak-pairing (BCS) phases, separated by a quantum phase transition. Since $L = \nu N/2$ (and thus $Q = 0$) in the strong pairing limit, and no gap closing occurs within the strong-pairing (BEC) phase, the conservation of the quantum number Q immediately implies that the $L = \nu N/2$ holds in the entire strong-pairing (BEC) phase. This is what was naturally expected; the real question is what happens in the weak-pairing (BCS) phase.

We found that, in a *p+ip* -wave (ν=1) chiral superfluid in the weak-pairing (BCS) phase, $L = \nu N/2$ holds exactly for a sufficiently large system. In contrast, in *d+id*, *f+if*, etc. ($\nu \geqq 2$) chiral superfluids in the weak-pairing (BCS) phase, L is strongly suppressed and is at most of $O(\Delta/E_F)$, implying Cooper-pair breaking near the edge. This surprising difference is understood in terms of the spectral flow and the quantum number Q.

Reference

[1] Y. Tada, W. Nie, and M. Oshikawa, Phys. Rev. Lett. **114**, 195301 (2015).

Authors
Y. Tada, W. Nie[a], and M. Oshikawa
[a]Tsinghua University

Quadrupole Orders in Heavy Fermion Systems

Tsunetsugu Group

Heavy fermion compounds PrT_2Zn_{20} (T=Ir, Rh) exhibit an unidentified phase transition at very low temperature of order 0.1K, and this is supposed to be an antiferro-quadrupole ordering. Rare-earth ions Pr^{3+} on the diamond sublattice have the electron configuration $(4f)^2$ and this system is one of the rare cases that the local ionic ground state is a non-Kramers doublet, the degeneracy of which is not related to time-reversal symmetry. This log 2 entropy of Pr ion is released due to inter-site interactions and this is expected to lead to an antiferro order of electric quadrupoles experimentally observed below the transition temperature. First we had investigated this problem by a phenomenological approach [1]. Only two components $\boldsymbol{Q}=(Q_u,Q_v)$ of quadrupole moments are active within the ground-state doublet, and we constructed their Landau free energy based on symmetry analysis. Bond direction to nearest-neighbor sites imposes that only the isotropic coupling $\boldsymbol{Q}_i \cdot \boldsymbol{Q}_j$ is allowed. These seem to imply that the effective model is the antiferro plane rotor model that is known to exhibit a phase transition belonging to the O(2) universality class. However, cubic symmetry around the Pr site is transferred to Z_3 symmetry in the internal two-dimensional $\boldsymbol{Q}$ space, and a special feature in our Landau free energy is the presence of a Z_3 anisotropy term in the $\boldsymbol{Q}$ space. This anisotropy distinguishes the quadrupole physics from a seemingly similar spin system, in which the time-reversal symmetry prohibits the Z_3 anisotropy.

We used a mean-field approach to the Landau theory as well as to a microscopic model for Pr ions and found a phase transition to an antiferro ordered phase. The order parameter is the staggered $\boldsymbol{Q}$ component, but unexpectedly it does not point along a soft direction of the Z_3 anisotropy but is rotated by 90 degrees. The Z_3 anisotropy induces a secondary order parameter, and it is the uniform $\boldsymbol{Q}$ component pointing to a hard direction [1]. An important discovery is that the susceptibility of the secondary order parameter diverges faster than that for the primary order parameter upon approaching the transition temperature in the ordered phase

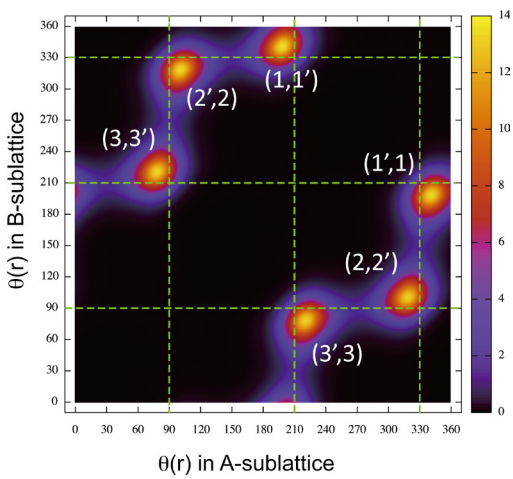

Fig. 1. Monte-Carlo result of the pair distribution of nearest-neighbor order parameters, $\boldsymbol{Q}(\boldsymbol{r}) = (\cos\theta(\boldsymbol{r}), \sin\theta(\boldsymbol{r}))$ in the ordered phase. Index pair (1,1'), etc., represents the directions of the local order parameters in the two-sublattice shown in Fig. 2. Six peaks correspond to the six domains in the ordered phase, the multiplicity of which comes from Z_3 symmetry in the $\boldsymbol{Q}$ space and Z_2 symmetry of exchanging sublattices.

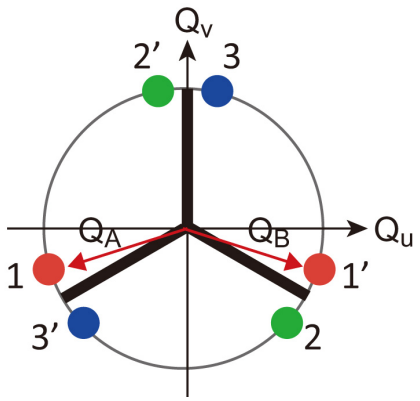

Fig. 2. Schematic picture of order parameters. Bold black lines show soft directions of the Z_3 anisotropy. The primary order parameter is $\boldsymbol{Q}_A - \boldsymbol{Q}_B$, while the secondary order parameter is $\boldsymbol{Q}_A + \boldsymbol{Q}_B$. In each of the six domains, $\boldsymbol{Q}_A$ points to the corresponding direction n or n' (n=1,2,3) and $\boldsymbol{Q}_B$ points to its partner direction n' or n.

[1]. This may explain the observed singularity in the ultrasound experiments.

We continued our study and investigated the effects of thermal fluctuations on this transition. We have performed classical Monte-Carlo simulations for our effective model and compared the results with those for the antiferromagnetic 3-state Potts model on bipartite lattices. Finite-size scaling analysis shows that the transition belongs to the O(2) universality class in three dimensions, which is consistent with simulations for the 3-state Potts model. The difference is about the spatial configuration of order parameter. The 3-state Potts antiferromagnet has a thermodynamic degeneracy in the ground state, and several exotic states have been proposed for the ordered phase. In our results, the local order parameters do not have esoteric macroscopic configurations aside from usual thermal fluctuations. The calculated pair distribution function of local $\boldsymbol{Q}$ direction between nearest-neighbor sites clearly demonstrates that the spatial configuration agrees with the mean-field result. Our result disproves most of the proposals for the Potts model, but the so-called permutationally symmetric sublattice state may be consistent after coarse graining. Understanding the critical behavior of the secondary order parameter is an interesting open issue and needs further investigation.

Reference

[1] K. Hattori and H. Tsunetsugu, J. Phys. Soc. Jpn. **83**, 034709 (2014).

Author
H. Tsunetsugu

Accurate Prediction of Chemical Reaction Systems

Sugino Group

The functional material research, one of the priority subjects of ISSP, investigates the link between (a) various functions of a heterogeneous system and (b) the basic properties of electrons and nuclei. The first-principles simulation can contribute to the research by, for example, (i) obtaining the potential energy surface (PES) for the nuclei and (ii) simulating the non-equilibrium chemical reaction dynamics occurring thereon. Sugino group has been working on the latter subject (ii) by developing algorithms such as the effective screening medium (ESM) [1] for applying the bias potential to the system and the potentiostat molecular dynamics scheme [2] for controlling the bias, with which to study the electrode-electrolyte interface problems. On the other hand, methods for the former subject (i), or obtaining reliable PES, has been left unsolved although crucially important for the present purpose.

Our study in the latter direction began by reformulating the full configuration interaction (FCI) method, or the exact diagonalization method, which is formally exact within the chosen basis set but the application is severely restricted by the combinatorial explosion of the degrees of freedom. It has been occasionally suggested that the key to reducing the degrees of freedom is in a construction of a specialized molecular orbital (MO) set that is non-orthonormal and spatially localized. With this in mind, an efficient and robust algorithm was developed [3, 4], wherein the many-body electronic wavefuntion (WF) is described using a canonical tensor format and the MOs are variationally determined so as to achieve the most compact representation of WF. In the most recent version [4], the resulting WF has a form of a linear combination of the antisymmetrized geminal powers (AGPs), where AGP is equivalent to the Hartree-Fock-Bogoliubov (HFB) state with a fixed particle number. This means that the computational scheme developed herein describes the interacting geminals while the conventional FCI describes the interacting unpaired electrons. The total energy formulas were derived originally for this purpose but many of them are found equivalent to those used in the nuclear physics in a different context.

When the new scheme, called extended symmetric tensor decomposition (ESTD), is applied to, for example, the water molecule that is a benchmark ten-electron system, the WF is accurately described only with ten terms for the decomposition series, i.e., ten for the canonical rank (K) (Fig. 1). The computational time to obtain the total energy within μHartree error scales as $O(K^2M^5)$, where M is the number of MOs that is proportional to the number of electrons, of which the scaling is superior to most of the existing computational schemes. This remarkable result indicates a promise of this scheme in improving the accuracy of PES within reasonable computational time. This scheme will allow further improvements: when a more elaborate tensor format is used instead of the canonical one, one would achieve further accuracy

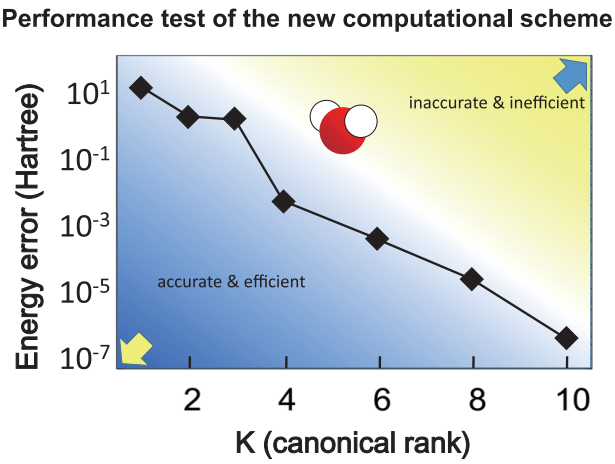

Fig. 1. A version of the extended symmetric tensor decomposition (ESTD) scheme applied to the water molecule. The total energy of the water referred to the full configuration interaction (FCI) is plotted against the canonical rank (K). The total energy converges exponentially to the FCI indicating remarkable efficiency of the computational scheme, which is well beyond most of the conventional schemes.

taking smaller rank; when a mean-field approximation is combined to ESTD to simplify the long ranged correlation that will be weak in some chemical reaction systems, one would achieve further efficiency. The ESTD scheme is general and can be adapted to such modifications. We thus expect ESTD will finally overcome known inaccuracy of the density functional PES and will prove a powerful tool not only to the chemical reaction systems but also many other systems.

References

[1] M. Otani and O. Sugino, Phys. Rev. B **73**, 115407 (2006).
[2] N. Bonnet, T. Morishita, O. Sugino, and M. Otani, Phys. Rev. Lett. **109**, 266101 (2012).
[3] W. Uemura and O. Sugino, Phys. Rev. Lett. **109**, 253001 (2012).
[4] W. Uemura, S. Kasamatsu, and O. Sugino, arXiv:1504.06250v1 (2015); to be published in Phys. Rev. A.

Authors
W. Uemura, S. Kasamatsu, O. Sugino

Effects of Coulomb Interaction on Photon-Assisted Current Noises

Kato Group

Photon-assisted transport through mesoscopic conductors has attracted much attention because the external fields open up additional transport channels via photon absorption and emission. It is known that nonperturbative effects of the time-dependent fields significantly modify the quantum nature of transport processes. In recent years, many studies have revealed that current noises provide significant information about the microscopic processes involved in photon-assisted transport. Photon-assisted current noise has been measured in various systems such as diffusive metals, diffusive normal metal-superconductor junctions, quantum point contacts, and tunnel junctions. Recently, the time-resolved current noise has been measured to evaluate the quantum purity of electrons emitted from on-demand electron sources. The coherent and spectroscopic nature of the photon-assisted current noise of noninteracting electrons has been studied theoretically based on the scattering approach or the Green's function approach [1,2]. These approaches are, however, of limited use to describe the effects of the Coulomb interaction.

We have studied photon-assisted transport in a single-level quantum dot coupled to two electrodes under a periodically oscillating field [3]. A schematic picture of our model is shown in the inset of Fig.1 (a). Hybridization between a dot and a lead is set to be unity ($\Delta_L = \Delta_R = 1$), and the energy level of the quantum dot is denoted with $\varepsilon(t) = \varepsilon_d + \varepsilon_1 \sin(\Omega t)$. We focus on the particle symmetric case ($\varepsilon_d = -U/2$) for simplicity. Photon-assisted current noise in the presence of the Coulomb interaction has been described based on a gauge-invariant formulation of time-dependent transport. The current noises are expressed in this description by two terms, i.e., a bare part and a vertex correction. The latter contribution appears only in the presence of the Coulomb interaction, and reflects internal dynamics of the systems. We have derived the vertex corrections within the self-consistent Hartree-Fock approximation in terms the Floquet-Green's functions and have examined the effects of the Coulomb interaction on the photon-assisted current noise. Within the Hartree-Fock approximation, the vertex correction describes dynamical screening effect induced by the Coulomb interaction.

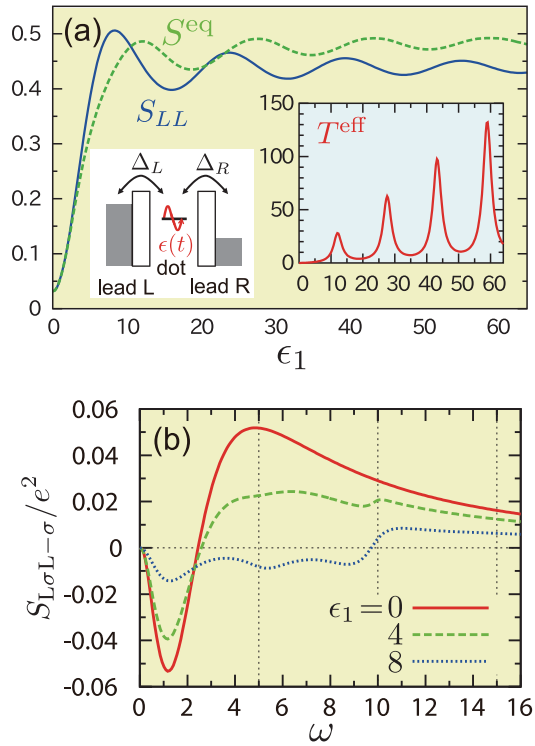

Fig. 1 (a) The photon-assisted zero-bias noise (S_{LL}) and the equilibrium thermal noise evaluated at the corresponding T_{eff} are displayed as a function of ε_1. Parameters are as follows: $\Delta_L = \Delta_R = 1$, $\varepsilon_d = -U/2 = -1$, $k_B T = 0.05$, $V = 0$, and $\Omega = 5$. The left inset: a schematic picture of the present model. The right inset: the effective temperature as a function of ε_1. (b) The vertex corrections to the current noise for antiparallel spins ($S_{L\sigma L\text{-}\sigma}$) are displayed. Parameters are the same as (a).

In Fig. 1(a), we show a current noise (S_{LL}) for zero source-drain voltage bias. From Fig. 1(a), we find that as the amplitude of the oscillating field increases, the zero-bias current noise rapidly increases, and oscillates as a function of ε_1 for large amplitude of the external field. This behavior is understood by considering an effective temperature defined by $T_{eff} = (S_{LL})_{V=0}/4k_B G$ (the inset of Fig.1 (a)), where G is a linear conductance. We note that this definition equals the original temperature for $\varepsilon_1 = 0$ by the dissipation-fluctuation relation, and provides a natural extension of the temperature toward nonequilibrium states. The thermal noise (S_{eq}) estimated from the effective temperature (shown in Fig. 1(a)) qualitatively reproduces the behavior of the zero-bias current noise.

In Fig.1 (b), we show a current noise for antiparallel spins $S_{L\sigma L\text{-}\sigma}$ as a function of the frequency. This noise always vanishes in noninteracting models, and equals the vertex correction in the presence of the Coulomb interaction. $S_{L\sigma L\text{-}\sigma}$ is strongly frequency-dependent, and has structures at integral multiples of the driving frequency Ω in the presence of the external oscillating field. As the amplitude of the oscillating external field increases, the vertex corrections are suppressed on the whole. This suppression of the vertex corrections is understood using the effective temperature as follows. As the amplitude of the oscillating external field increases, the effective temperature rises for $\varepsilon_1 < 12$ as shown in the inset of Fig. 1(a). The rise of the effective temperature leads to suppression of the dynamical screening effect, and weakens the current correlation with different spins. These effects are expected to be general in interacting electron systems. We note that the spin-dependent current noise $S_{L\sigma L\text{-}\sigma}$ is appropriate for study of internal dynamics of interacting systems, and can in principle be measured using a spin

filter.

Our result shows that the effect of Coulomb interaction is modified by external oscillating fields via nonequilibrium distribution functions. Our study will offer a useful viewpoint for understanding photon-assisted transport of other phenomena such as the Coulomb blockade and the Kondo effect.

References

[1] Ya. M. Blanter and M. Büttiker, Phys. Rep. **336**, 1 (2000).
[2] G. H. Ding and B. Dong, Phys. Rev. B **87**, 235303 (2013).
[3] T. J. Suzuki and T. Kato, Phys. Rev. B **91**, 165302 (2015).

Authors

T. J. Suzuki and T. Kato

Spin Transport and Relaxation Mechanism in a Disordered Organic Film

Otani Group

Organic semiconductors (OSCs) consist of relatively light elements such as carbon, hydrogen, and sulfur. Therefore, their spin-orbit (SO) interaction is expected to be weak. OSCs are thus expected to have long-distance spin transport since the spin relaxation is mainly caused by the SO interaction. In most of the OSCs, however, the electron conduction is dominated by hopping transport in the strongly disordered structure. Thus, the spin transport and relaxation mechanism is not well understood compared with the conventional metallic materials where the band-like transport is dominant.

Here we report our systematic studies on the spin transport and relaxation mechanism in an OSC PEDOT:PSS by means of spin pumping, charge transport, and electron paramagnetic resonance (EPR) experiments. The spin pumping experiment enables us to estimate the spin diffusion length (SDL), and the other two experiments to determine the spin diffusion constant (D_S) and the spin lifetime (τ_S), respectively. The OSC used in this study is the conducting polymer PEDOT:PSS in which the conjugated PEDOT molecule is doped with PSS. The film consists of core-shell particles in which a PEDOT-rich core is covered with an insulating PSS shell: the electron transport is dominated by hopping conduction between the PEDOT-rich cores.

Figure 1(a) shows the device structure used in this spin pumping experiment. The device comprises a trilayer of ferromagnetic permalloy (Py), PEDOT:PSS, and platinum (Pt). These layers respectively act as spin injector, transport,

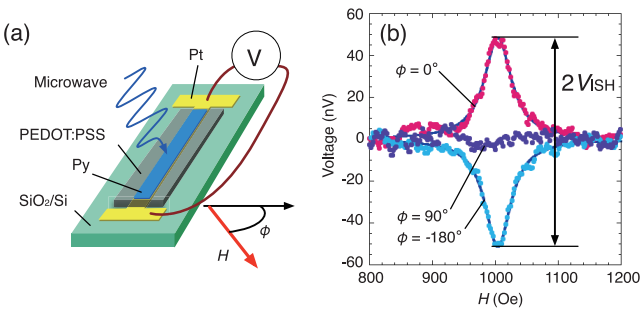

Fig. 1. (a)Schematic of the device structure used for the spin pumping experiment. The applied magnetic field is rotated in the basal plane. (b) Magnetic field dependence of the ISHE voltage signal for ø = 0˚, 90˚ and 180˚. In this figure, only the symmetric voltage component on the FMR field is shown.

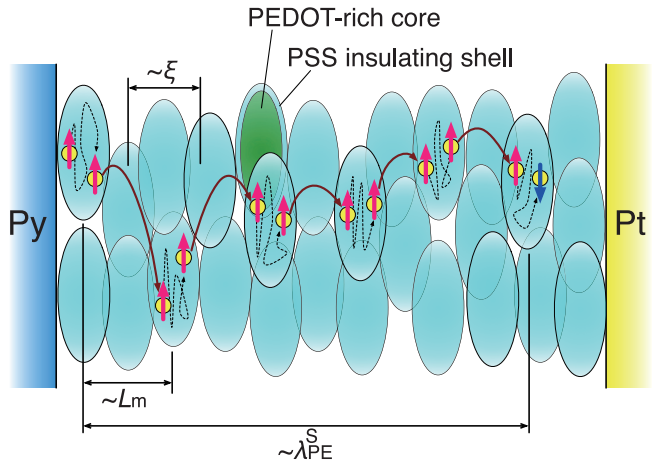

Fig. 2. Expected spin transport mechanism in the PEDOT:PSS layer. ξ, L_m, and λ^S_{PE} denote the localization length, hopping length, and SDL of PEDOT:PSS, respectively. The spins do not flip during hopping conduction, but mostly flip while trapped in the PEDOT-rich cores.

and detector layers. In this experiment, the pure spin current accompanied by no net charge current is induced in the adjacent PEDOT:PSS layer by the interfacial exchange interaction during the ferromagnetic resonance (FMR) excitation. The injected pure spin current through the PEDOT:PSS is absorbed by the Pt layer, and then converted to the electric field via the inverse spin Hall (ISH) effect of the Pt layer. Figure 1(b) shows the magnetic field dependence of voltage signal at the Pt layer for ø = 0˚, 90˚ and 180˚. As can be seen in the figure, a clear voltage peak is observed at the FMR field. The voltage signal changes its sign when the magnetic field direction is inverted, and vanishes at ø = 90˚. This behavior is consistent with the ISH voltage signal (V_{ISH}) given by $V_{ISH} \propto J_S \times \sigma$ where J_S is the spin current and σ is the spin polarization vector. From the PEDOT:PSS thickness dependence of V_{ISH}, we have determined the SDL of PEDOT:PSS layer as 140 ± 20 nm. By using the diffusion constant obtained from the charge transport experiment, we can estimate the spin lifetime (τ_S^t) as 28 ± 20 ns. To confirm this result, we have performed an EPR experiment of PEDOT:PSS which is an alternative method to determine the spin lifetime. The obtained spin lifetime (τ_S^{EPR}) is in the range of 5-100 ns, and this value is reasonably consistent with τ_S^t .

Now we consider the relationship between two spin lifetimes obtained by different experiments. In the present material PEDOT:PSS, the charge transport is dominated by the hopping conduction. Therefore, the electrons are first trapped at the PEDOT-rich core, and occasionally hop to adjacent cores, suggesting τ_S^t is determined by both the trapping and hopping processes. On the other hand, the EPR experiment mainly gives the spin lifetime in the trapping state, i.e., the spin lifetime within the PEDOT-rich cores. The present study indicates that two spin lifetimes determined by two different experimental methods are reasonably consistent with each other. Moreover, we have revealed that the SDL is longer than the average hopping length (L_m) for one hopping process. These results suggest that most of the spins are not flipped during the hopping process, while the spin relaxation mainly takes place in the trapping state of the PEDOT-rich cores (Fig. 2).

Authors

M. Kimata, D. Nozaki, Y. Niimi, H. Tajima[a], and Y. Otani
[a]University of Hyogo

A Low-Dimensional Metallic State on Au-Adsorbed Ge(001) Surface

Komori Group

Surface electronic states on bulk semiconductors are suitable for the study of low-dimensional electronic properties because the metallic state in the bulk band gap can provide an ideal low-dimensional metal. Moreover, we can expect to study one-dimensional (1D) surface electronic properties such as Tomonaga-Lüttinger liquid (TLL) and Peierls instability when the surface atomic structure is highly anisotropic. As one of the surfaces with a 1D atomic structure, the Au-adsorbed Ge(001) surface has recently attracted much attention and its electronic and atomic structures have been studied in detail using scanning tunneling microscopy/spectroscopy (STM/STS), and angle-resolved photoemission spectroscopy (ARPES). An interesting STS result of this system was that the surface local density of states (LDOS) depends on the energy E as $(E - E_F)^{\alpha}$ with $\alpha = 0.5$ [1]. This was attributed to TLL while the metallic surface state has an anisotropic two-dimensional (2D) dispersion in the ARPES study [2]. We have studied this surface state by using high-resolution STS to understand the origins of these interesting features [3].

Figure 1 shows the results of STM/STS for the Au-adsorbed Ge(001) surface consisting of the well-known atomic chain structure. The atomic images largely depend on the sample bias voltage. The symmetry of the surface structure has been considered to be c(8×2) while a short range order of a 4×8 superstructure can be seen on the surface. The tunneling spectra always show a dip at E_F as in Fig. 1d. However, by fitting the data to the $(E-E_F)^{\alpha}$ dependence, α is always larger than 0.7 at the ordered 4×8 area while α is closed to 0.5 at the areas including point defects and domain boundaries of the 4×8 superstructure. Thus, the square-root behavior is ascribed to the surface disorder.

We have measured differential conductivity (dI/dV) maps in the bias-voltage (V_b) region corresponding to the metallic surface state to study the spatial distribution of the surface LDOS. The results shown in Fig. 2 exhibit no 1D channel of high LDOS, which is expected for a 1D surface state. The observed LDOS is consistent with the ARPES observation of the 2D metallic state.

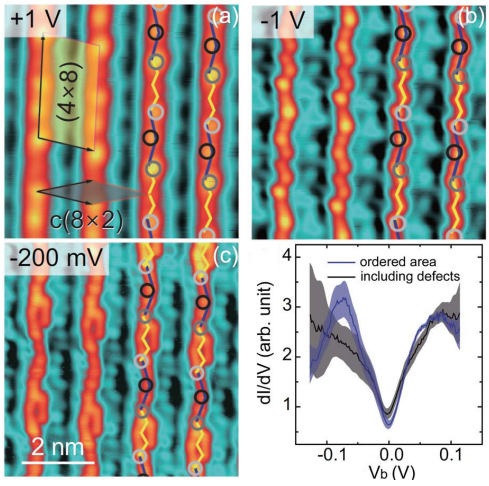

Fig. 1. (a-c) STM images of the Au-adsorbed Ge(001) surface at 78 K for three sample-bias voltages (V_b) shown in the figures. One-dimensional chain structure can be always observed while the image largely depends on V_b. The top of the chain structure consists of a zig-zag part (yellow) and a chevron part (blue) at V_b = -1 V. The both structures are not clear at V_b = 1 V, and the zig-zag structure turns to a double row at V_b = - 200 mV. (d) Spatially-averaged STS measured at 5.5 K over an ordered 4×8 area (blue) and over an area including point defects and the domain boundaries of the 4×8 superstructure (black).

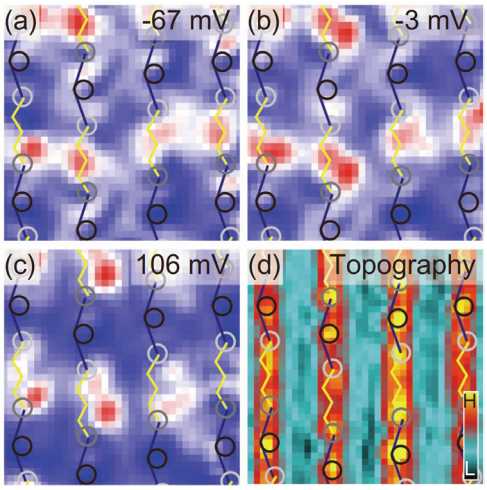

Fig. 2. (a-c) Differential conductance (dI/dV) maps at 78 K for three sample-bias voltages (V_b) shown in the figures. The band bottom of the metallic surface state is located at 150 meV below E_F, and the map indicates LDOS of the metallic state at the corresponding energy. The conductance peaks are on the zig-zag parts of the top of the chain structures. (d) Simultaneously-obtained topography image (6×6 nm^2, V_b = 0.5V).

References

1. C. Blumenstein *et al.*, Nat. Phys. **7**, 776 (2011).
2. K. Nakatsuji *et al.*, Phys. Rev. B **80**, 081406 (2009).
3. J. Park *et al.*, Phys. Rev. B **90**, 165410 (2014).

Authors

F. Komori, J. Park[a], K. Nakatsuji, T.-H.Kim[b] S. K. Song[a,b], and H. W. Yeom[a,b]

[a]Institute for Basic Science

[b]Pohang University of Science and Technology

Conductance Difference in the Atomic Point Contacts Formed on an Atom and Between Atoms

Hasegawa Group

Electronic conduction through atomic-size metal contacts is of fundamental interest as a transport through the ultimately squeezed conductor. Several seminal phenomena, such as quantization and step-wise variation in the conductance, have been reported using a method called break junction by measuring the conductance just before the breaking of a nanometer-width wire. In these measurements, since atomic geometry of the point contact cannot be controlled, the measured conductance fluctuates at every breaking and, therefore, the results are usually analyzed statistically using a conductance histogram.

Here, making most of the capability of the atomically resolved imaging of scanning tunneling microscopy (STM), we directly measured the conductance of the atomic point contact in an atomically controlled manner. We first positioned the STM tip on a specific site, for instance, on-top, bridge, and hollow (fcc and hcp) sites, in the crystallographic lattice of the substrate surface, and then measured the conductance by moving the tip toward the substrate from tunneling to contact regimes. It was found that the conductance evolution depends significantly on the contact site. In the contact regime, the hollow site has the largest conduc-

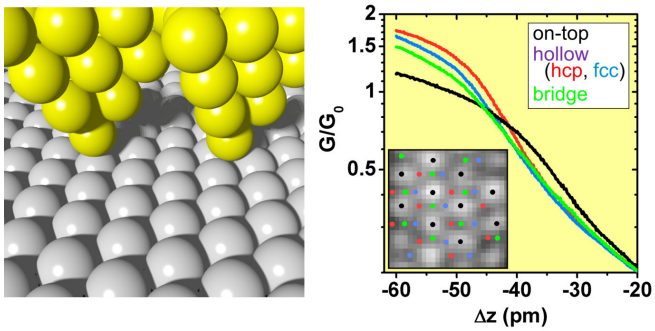

Fig. 1. (left) schematic showing the atomic geometry of the atomic point contacts formed at a on-top site (left) and a 3-fold hollow site (right) of a close-packed surface. (right) electrical conductance measured from tunneling (Δz = -20 pm) to contact (Δz = -60 pm) regimes. The measured conductance G is normalized by the quantum conductance G_0 given by $2e^2/h$ (~77.5 μS). For each conductance trace, 10 traces taken at the corresponding sites marked in the atomically-resolved STM image (inset) are averaged.

tance and among the two hollow sites the hcp site is more conductive than fcc. When the tip is a little bit (20-25 pm!) far from the contact, a crossover occurs and the conductance at on-top site becomes largest.

The traces of the electrical conductance measured from tunneling to contact at on-top, bridge, fcc, and hcp sites of the Pb(111) surface are shown in the right panel of Fig. 1. For each plot, 10 traces obtained from the corresponding marked sites in the inset STM image are averaged. At the tip displacement Δz of -50~-60 pm from the tunneling (Δz = 0), the atomic contact is formed as the conductance shows saturation around the quantum conductance G_0 given by $2e^2/h$ (~77.5 μS). The contact conductance shows strong site dependence; the conductance at the hcp site is largest and more than 50 % larger than the one measured at the on-top site. Around Δz = -30~-40 pm, that is, when the tip is located above the substrate by 20~30 pm from the contact, the figure show the largest conductance at on-top site.

In order to demonstrate the site dependence, we performed real-space mappings of the conductance in the on-top enhancement region and in the contact regime. The upper-left panel of Fig. 2 is an STM image showing the atomic contrast taken simultaneously with the conductance

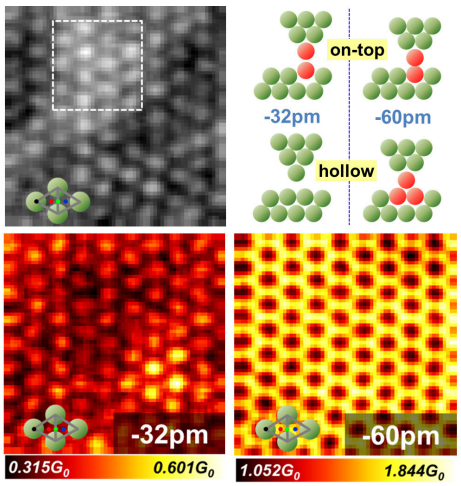

Fig. 2. Spatial mappings of the conductance at various tip displacements. (upper left) topographic STM image (3.0 × 3.0 nm^2) taken simultaneously with 64 × 64 conductance traces. (lower left) conductance mapping at Δz=-32pm, where the conductance at on-top site is enhanced (lower right) conductance mapping at Δz = -60 pm, that is, the contact regime, where hollow site, particularly hcp site, has large conductance. (upper right) schematics explaining the site dependence of the conductance. The atoms on which the chemical interaction is exerted are marked red.

traces. At a tip displacement Δz of -32pm, the conductance mapping (lower-left of Fig. 2) exhibits bright contrast at the on-top site, similarly to that in the topographic image. As the conductance mapping at Δz =0 does not have any contrast, the bright contrast indicates the conductance enhancement at the on-top site. On the other hand, the conductance mapping in the contact regime (lower right of Fig. 2, Δz =-60pm) has its contrast reversed from that of the topographic one, indicating a larger conductance at the hollow site than at the on-top site. These results indicate that the point contact conductance is quite sensitive to the atomic configuration.

When the distance between the tip and substrate is reduced, the attractive chemical interaction is exerted between the surface and tip apex atoms. This interaction presumably opens up the conduction channel and contributes to the development of the conductance. Schematics in the upper right panel of Fig. 2 show how the chemical interaction works in the case of contacts formed at on-top and hollow sites. When the tip approaches from the tunneling regime, the attractive interaction is exerted first at the on-top site (The force-exerted atoms are marked red in the schematics.) because the atom at on-top site is located higher than that of hollow sites, making the on-top conductance enhanced. In the contact regime, however, the attractive force becomes stronger at hollow sites because the number of involved atoms is greater than that at the on-top site. This is probably the reason why conductance becomes larger there at the contact and why the crossover occurs. Obviously further theoretical studies are needed to elucidate the observed conductance behaviors.

Referecce

[1] H. Kim and Y. Hasegawa, Phys. Rev. Lett. **114**, 206801 (2015).

Authors
H. Kim and Y. Hasegawa

Double Perovskite Ferroelectrics

Lippmaa Group

La_2NiMnO_6 is a double perovskite with a pseudo-cubic structure where the Ni and Mn atoms at the perovskite *B*-site form a natural superlattice along the [111] direction (Fig. 1). Such *B*-site-ordered double perovskites open interesting materials design possibilities since transition metals with dissimilar *d*-electron configurations can be integrated in a crystal, allowing for tuning of transport, dielectric, or magnetic properties. In our recent work, we explore the influence of epitaxial strain on the dielectric behavior of the La_2NiMnO_6 perovskite. This material is ferromagnetic in bulk form and, as is common for oxides with non-zero *d*-electron configurations, does not support a polar ferroelectric state. However, first-principles calculations show that when the rhombohedral crystal is strained, a polar state can emerge due to a shift of the *A*-site La atoms from the unstrained equilibrium position, giving rise to macroscopic ferroelectricity. The structural differences between the bulk nonpolar and strained polar structures are illustrated in Fig. 1.

The strained crystal structure can be obtained by growing La_2NiMnO_6 thin films on a lattice-mismatched $SrTiO_3$ substrate. The lattice expansion in an epitaxial thin film does

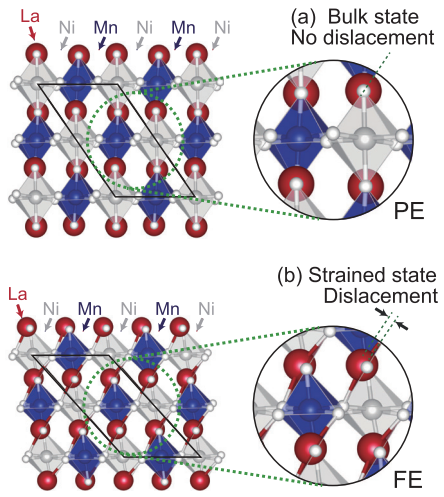

Fig. 1. Crystal structure of an ordered bulk La_2NiMnO_6 double perovskite crystal with Ni (gray) and Mn (blue) atoms arranged in layers along the [111] direction. The rhombohedral unit cell outline is shown in black. The La atoms are at symmetric positions and the lattice is nonpolar (top). Under epitaxial strain of about 6%, the *A*-site La atoms are displaced, inducing a polar state.

not have a significant effect on the magnetism and a clear ferromagnetic hysteresis loop can be observed at low temperatures. The magnetic state survives up to room temperature, with a Curie temperature close to 300 K. The ferroelectric state is observable below about 50 K, as illustrated in Fig. 2. The ferroelectricity in La_2NiMnO_6 films is caused by an offset of the *A*-site cations, while the magnetism originates from the transition metals at the *B*-site of the crystal lattice. The material is thus multiferroic, although there is no direct coupling between the magnetism and the polarity. Double perovskites are thus an interesting class of materials, where multiple ferroic orders can be integrated in the same lattice on a microscopic scale by associating the different types of order with different lattice sites.

A consequence of this differentiation of lattice sites opens the possibility to tune the polarity and the magnetism independently of each other. The ferroelectric polarization is strongly dependent on the magnitude of the applied strain, which has little effect on the magnetic order. The strain sensitivity can be quite dramatically illustrated by a noticeable shift in the pyroelectric polarization measurement

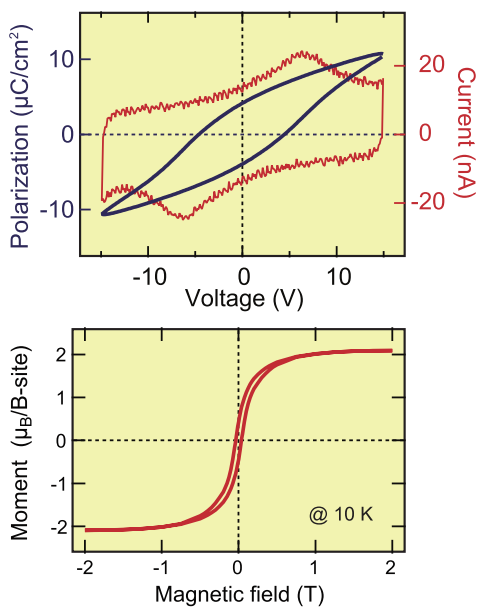

Fig. 2. Ferroelectric and ferromagnetic hysteresis loops of strained La_2NiMnO_6 thin films measured at 10 K, showing that the material is multiferroic.

response when an in plane strain change by just 0.015% is applied. This small strain change can be reliably generated by a structural phase transition that occurs in the $SrTiO_3$ substrate at 105 K. The magnetism, on the other hand, can be controlled by the level of disorder among the *B*-site Ni and Mn cations. For typical thin films, the level of Ni/Mn ordering can be adjusted between about 20% and 80% by adjusting the film growth parameters. This variation leads to a nearly linear change of the saturation magnetization, reaching 2.5 μ_B/*B*-site for a perfectly ordered lattice and vanishing in a completely disordered material.

A potential limitation in the use of double perovskites such as La_2NiMnO_6 is the coexistence of rhombohedral and monoclinic crystal phases. The multiferroic behavior is only observed in a strained rhombohedral lattice, while the monoclinic phase remains paraelectric at all temperatures. The phase distribution can be imaged on a macroscopic scale by scanning nonlinear dielectric microscopy, which visualizes the distribution and polarity of ferroelectric domains in the films. Further work is required to find ways of controlling the phase formation in thin films by process parameter variations and substrate mismatch selection.

Reference

[1] R. Takahashi, I. Ohkubo, K. Yamauchi, M. Kitamura, Y. Sakurai, M. Oshima, T. Oguchi, Y. Cho, and M. Lippmaa, Phys. Rev. B **91**, 134107 (2015).

Authors
R. Takahashi, I. Ohkubo[a], K. Yamauchi[b], M. Kitamura, Y. Sakurai, M. Oshima, T. Oguchi[b], Y. Cho[c], and M. Lippmaa
[a]National Institute for Materials Science
[b]Osaka University
[c]Tohoku University

Pressure Induced Superconductivity in CrAs

Uwatoko Group

The transition-metal pnictide compounds MX (M = 3d transition metal, and X = P, As, Sb) have been studied since 1960s as a paradigm for studying the intimated relationship between magnetism and structural parameters of metallic magnets. Among these compounds, CrAs, stands out due to its peculiar magnetic and structural transitions as detailed below. At room temperature, CrAs adopts the orthorhombic MnP-type structure with lattice parameters a = 5.649Å, b = 3.463 Å, and c = 6.2084 Å. Upon decreasing temperature to T_N = 265 K, it displays an isostructural, first-order transition with discontinuous changes of lattice parameters; the most dramatic change is a sudden jump of lattice constant b by ~ 3% with a net volume expansion. Neutron powder diffraction measurements revealed that this structural transition is accompanied by a double helical antiferromagnetic order with the localized moments of ~1.7 μ_B/Cr lying essentially within the ab plane and propagating along the c axis. The acquisition of localized Cr moment below T_N has been rationalized as an itinerant- (or collective) to localized-electron transition due to the sudden elongation of Cr-Cr separation along the b direction. By monitoring the resistivity anomaly at T_N, subsequent high-pressure studies have shown that this transition is very sensitive to external pressure and it can be suppressed completely at ~ 6 kbar. These observations seem

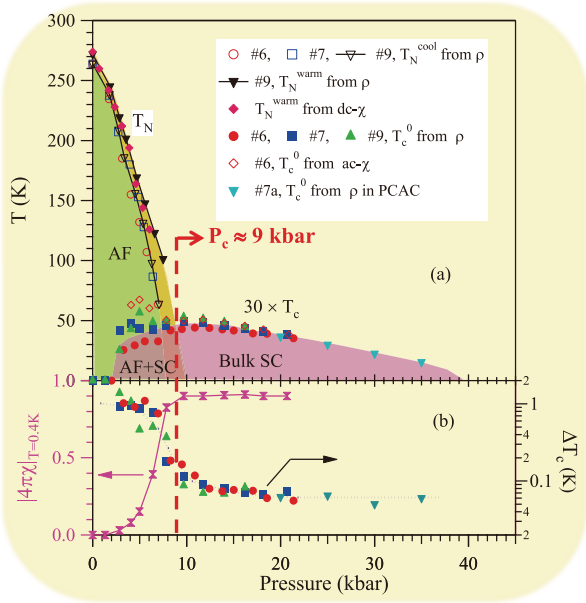

Fig. 1. (a) Temperature-pressure phase diagram of the Pressure-Induced Superconductivity in the antiferromagnetic CrAs. The superconducting transition temperature *Tc* has been scaled by a factor of 30 for clarity. (b) The superconducting shielding fraction at 0.4 K, $|4\pi\chi|_{T=0.4K}$, and the superconducting transition temperature width, ΔTc, as a function of pressure. The symbols of circle (red), square (blue), and triangle (green) in (a, b) represent three independent samples with residual resistivity ratio RRR = 240, 327, and 250, respectively.

to be consistent with the scenario of localized-to-itinerant transition since pressure tends to reduce the b axis and also the volume. Thus, CrAs provides us a unique opportunity to explore the localized-to-itinerant transition as well as the possible quantum critical point by applying minute pressure.

We measured the resistivity $\rho(T)$ and ac magnetic susceptibility $\chi'(T)$ of a number of CrAs single crystals under various hydrostatic pressures up to 21.4 kbar in a wide temperature range from 300 K down to 70 mK. CrAs single crystals were grown out of the Sn flux. We found that CrAs becomes superconducting when its coupled magnetic/structural transition is suppressed by pressure, and CrAs is the first superconductor among the Cr-based compounds. The phase diagram of CrAs is shown in Fig. 1(a). The major findings include: (i) T_N decreases progressively with pressure and vanishes completely at a critical pressure $P_c \approx 9$ kbar; (ii) the transition at T_N remains to be first order until disappears and the thermal hysteresis enlarges with pressure; (iii) the superconducting state emerges upon the application of pressure, and bulk superconductivity with a volume fraction over 90% develops eventually when T_N vanishes completely above 9 kbar, (Fig 1(b); (iv) the established T-P phase diagram resembles those of unconventional superconductors such as the heavy-fermion and iron-based superconductors; and $T_c(P)$ displays a dome shape with a broad maximum around 10±2 kbar; (v) the superconducting state can deteriorate if the level of impurity and/or disorder in the sample is high, a key signature for non-s-wave pairing symmetry; (vi) the normal-state resistivity was found to deviate from the Fermi-liquid behavior in a large pressure range. The above observations indicated that the observed superconductivity in CrAs should fall into the unconventional category [1].

Reference
[1] W. Wu, J.-G. Cheng, K. Matsubayashi, P. P. Kong, F. K. Lin, C. Q. Jin, N. L. Wang, Y. Uwatoko, and J. L. Luo; Nature Communications **5**, 5508 (2014).

Authors
W. Wu[a], J.G. Cheng, K. Matsubayashi, P. P. Kong[a], F. K. Lin[a], C. Q. Jin[a], N. L. Wang[a], Y. Uwatoko, and J. L. Luo[a]
[a]IOP, Chinese Academy of Sciences

Bulk and Edge States in an Atomic Layer Semiconductor, Phosphorene

Osada Group

Phosphorene is a single atomic layer of the layered crystal of black phosphorus. Its realization using the standard mechanical exfoliation technique was reported by Liu *et al.* in 2014. Since then, a great amount of researches have been performed on phosphorene. There exist many first-principle calculations on the electronic structure of phosphorene, but the tight-binding approach is an easier way to extract the physical picture. We have qualitatively investigated the bulk and edge electronic structure of monolayer and bilayer phosphorene under vertical electric fields by employing the Slater-Koster-Harrison tight-binding model, which assumes transfer integrals depending only on the inter-atomic distance.

The crystal structure of monolayer phosphorene is a puckered honeycomb lattice where phosphorus atoms exist on two parallel planes. So, the external vertical electric field can modify the electronic structure by introducing the potential difference between the two planes. The calculated global band structures under the zero and finite fields are shown in Fig. 1(a) and Fig. 1(b), respectively. The electric field decreases the energy gap as seen in the Fig. 1. The band structure of bilayer phosphorene is shown in Fig. 1(c). The energy gap becomes smaller than monolayer, resulting from lifting of valence band top. This unsymmetrical behavior originates from the fact that the valence band top, mainly consisting of $3p_z$ orbitals, is largely raised up by interlayer coupling comparing to the conduction band bottom.

The edge state existing in the gap is a remarkable feature of phosphorene. Figure 2(a) shows the energy spectrum of monolayer phosphorene nanoribbon with the zigzag edge. We can see that a flat edge subband appears in the middle of the main gap. It has two-fold degeneracy and isolated from the conduction and valence bands. Under the electric field, it splits into two subbands corresponding to the two

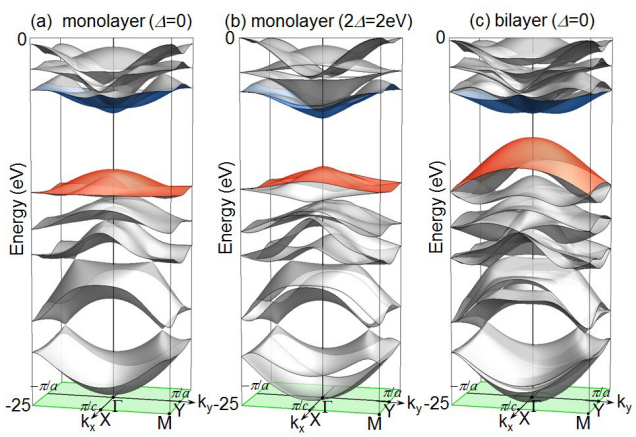

Fig. 1. Band structure of (a) monolayer phosporene, (b) monolayer phosphorene under the vertical electric field, and (c) bilayer phosphorene. The blue and red surfaces indicate the conduction band and the valence band, respectively.

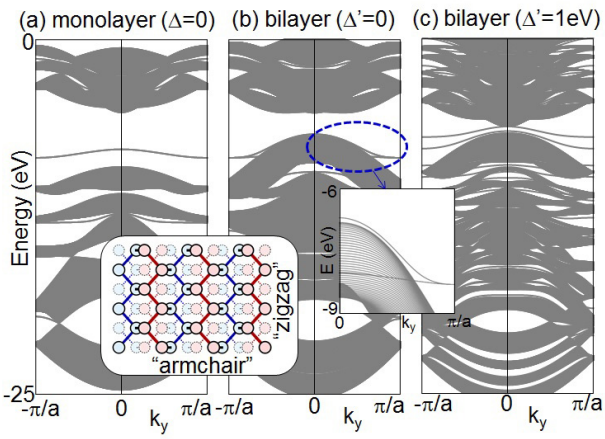

Fig. 2. Energy spectra in phosphorene nanoribbon with the zigzag edge. (a) monolayer nanoribbon. (b) bilayer nanoribbon. (c) bilayer nanoribbon under vertical electric field. Insets show the crystal structure of phosphorene and detail of edge states in bilayer nanoribbon.

phosphorus planes.

In the bilayer phosphorene, two edge subbands, which correspond to bonding and anti-bonding of monolayer edge states, appear around the main gap at the zigzag edge under zero electric field (Fig. 2(b)). Each one is doubly degenerated corresponding to two sides of the nanoribbon. Reflecting the valence band lifting, the upper subband is almost tangent to the valence band top, whereas the lower one penetrates the valence band. So, the most part of both edge states overlap with the valence band in energy. The overlap between the edge state and the valence band causes the hole transfer from the upper edge subband into the valence band. In other words, the upper edge state works as acceptor. This intrinsic hole doping mechanism around the edge might be responsible for the natural p-type doping in the bulk black phosphorus. In fact, the estimated averaged hole density is in good agreement with the reported effective acceptor concentration in black phosphorus.

Under the vertical electric field, the bulk gap is slightly reduced, and the edge states doubly split since edge states at both sides of the nanoribbon lie on different atomic planes (Fig. 2(c)). As the electric field is increased, the upper two split edge states move into the gap separating from the valence band top. This causes the reduction of the intrinsic hole doping from the upper edge state.

In monolayer phosphorene, the existence of the midgap edge state might be crucial for device application, since it causes current leakage at room temperature. In contrast, the bilayer phosphorene has fewer midgap state. Therefore, we can expect better device characteristics in bilayer phosphorene. The level of intrinsic hole doping can be controlled by the vertical electric field. These features of bilayer phosphorene might be better suited for device application.

Reference

[1] T. Osada, J. Phys. Soc. Jpn. **84**, 013703 (2015).

Authors
T. Osada, T. Taen, and S. Fukuoka

A Scaling Relation for Dangerously Irrelevant Symmetry-Breaking Fields

Kawashima Group

We studied the effect of a dangerously irrelevant symmetry-breaking field on critical phenomena and obtained a new scaling relation. We verified the relation by numerical calculation of the classical XY model with Z6-symmetry breaking field in three and four dimensions.

While irrelevant scaling fields play minor roles in most cases, some of them are quite relevant in the usual sense of the word. We studied the cases where such a dangerously-irrelevant scaling field reduces the symmetry of the system, and demonstrated that it yields a new scaling relation. We considered a generic renormalization-group flow diagram (Fig. 1) including two fixed points; one describing the critical point and the other the ordered phase. In the case described by this diagram, the perturbation λ may almost die out at some length scale, say ξ, while it may recover its amplitude at larger length scale, say ξ'. When the system size is between the two scaling lengths, $\xi \ll L \ll \xi'$, the system would seem ordered but still no effect of the symmetry breaking can be detected. It may then appear that an intermediate phase exists where the system acquires an emergent symmetry. A classic example of this type of renormalization group flow is the q-state clock model in three dimensions, and its continuous-spin counterpart.

However, it is now widely accepted that in three dimensions there is no partially ordered phase with the emergent symmetry. Nevertheless, disagreement still persists concerning the scaling relation that relates the scaling exponent ν' and ν that characterize the longer and the shorter correlation length, respectively. Previously, a scaling relation was proposed by Ueno et al. [2] and by Oshikawa [3]. Their arguments are based on the basic assumption that there is a well-defined domain wall splitting the whole system and the excess free-energy caused by the domain walls is the scaling variable. The excess free-energy density per area of the domain wall may be given by the symmetry-breaking field renormalized up to the scale of locally-correlated volume, $\lambda(\xi) \approx \lambda\xi^{y_\lambda}$ (y_λ represents the scaling exponent of the symmetry-breaking field at the critical fixed point). The total domain-wall free-energy, then, may be $L^{d-1}\lambda(\xi)$. This yields a scaling relation $\nu'/\nu = -y_\lambda(d-1)$. Lou, Sandvik, and Balents [4] presented a similar argument, but they argued that the effect of the anisotropy free-energy comes from the volume instead of the domain walls. Therefore, they multiply the

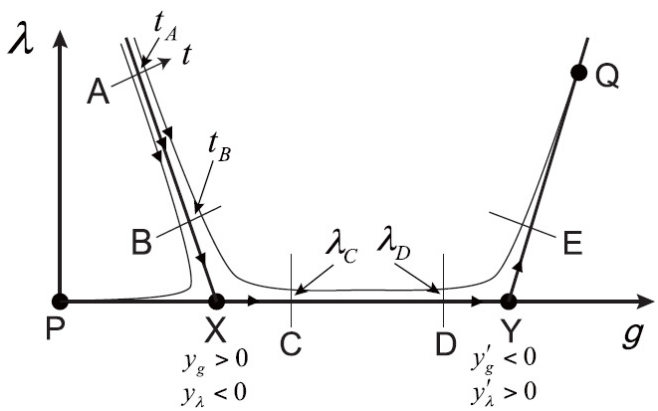

Fig. 1. The generic renormalization flow diagram with four fixed points: P, Q, X, and Y.

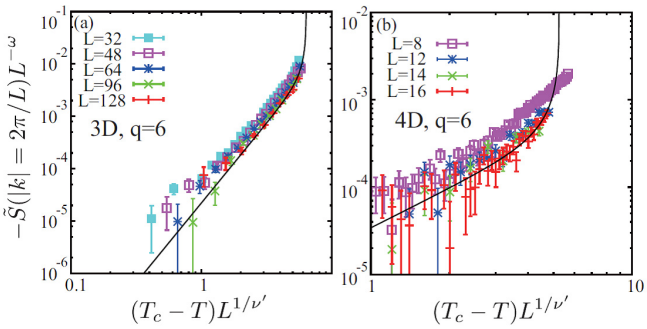

Fig. 2. Log-log plot of the angular Fourier transform of the angle dependent spin-structure factor $\tilde{S}$ for the Z6-anisotropic XY model with $\lambda_6/J = 5$ in three dimensions (a) and in four dimensions (b). For (a) the estimates obtained through the scaling relation $\omega = 1.983$ and $\nu' = 1.511$ are used. (b) The corresponding finite-size scaling plot assuming $\omega = 2.0$ and $\nu' = 1$ in four dimensions. The critical temperatures $Tc/J = 2.202$ for three dimension and $Tc/J = 3.3143$ for four dimentions are estimated from the binder ratios of the magnetization.

renormalized field by the number of correlated volumes, to obtain $\nu'/\nu = 1 - y_\lambda/d$.

We presented a new scaling relation, which is similar to what was speculated previously but is more general and yields different prediction in general. The bare Hamiltonian is along the short line near the point "A" parameterized by t so that $t = 0$ corresponds to the critical point. If we start from the point $t = 0$ on this line, the scaling flow takes us to the critical fixed point "X", where $g = g_X$ and $\lambda = 0$. In the vicinity of X, the RG flow is characterized by $y > 0$ for the variable g and $y_\lambda < 0$ for the variable λ. If we start from a point slightly off A, the scaling flow goes through the points "C", "D", and approaches the second fixed point "Y" around which renormalization group flow is characterized by scaling exponents $y' < 0$ and $y'_\lambda > 0$. Because of the presence of λ, the flow deviates from "Y", and eventually reaches some other fixed point. We obtained the new scaling relation

$$\xi' \propto \xi^a \left(a = 1 - \frac{y_\lambda}{y'_\lambda}\right).$$

To verify the validity of this relation, we computed the structure factor of spin-fluctuation around the mean direction θ_0:

$$S_k(\theta_0) \equiv \frac{1}{N}\left\langle \left| \sum_r e^{ikr} S(r) \right|^2 \right\rangle_{\theta_0},$$

where the expectation value is evaluated with the spontaneous symmetry breaking along the direction specified by θ_0. The Fourrier transformation of this quantity, $\tilde{S}_k \equiv \frac{1}{2\pi}\int d\theta_0 \cos\theta_0\, S_k(\theta_0)$, is suppose to have the scaling behavior $\tilde{S}_k \approx L^\omega g((T_c - T)L^{1/\nu'})$ with $\omega \equiv 2(d - y_\lambda - 2x_h)/(2 - y_\lambda)$. Figure 2 is the scaling plot of our numerical results. The data are scaled with the exponents obtained through the scaling relations quoted above. While there are strong corrections to scaling, the data clearly converging to the expected scaling function as the system is enlarged.

References
[1] T. Okubo, K. Oshikawa, H. Watanabe, and N. Kawashima, Phys. Rev. B **91** 174417 (2015).
[2] Y. Ueno and K. Mitsubo, Phys. Rev. B **43**, 8654 (1991).
[3] M. Oshikawa, Phys. Rev. B **61**, 3430 (2000).
[4] J. Lou, A. W. Sandvik, and L. Balents, Phys. Rev. Lett. **99**, 207203 (2007).

Authors
T. Okubo, K. Oshikawa, H. Watanabe, and N. Kawashima

Kinetic Aspect on Gelation Mechanism of Tetra-PEG Hydrogel

Shibayama Group

Gels are defined as three-dimensional polymer networks swollen in solvent. Because of their high retention capacity of solvents, gels are utilized as super absorbent, contact lenses, drug reservoirs, etc. However, industrial applications of gels are still limited because of their low mechanical strength, which results from inhomogeneity created during the cross-linking process. One of the most popular approaches for removing inhomogeneity is an "end-cross-linking" method, which forms a polymer network from AB-type polycondensation of telechelic prepolymers and multifunctional crosslinkers. Because of simplicity of its network structure, mechanical, structural and simulational studies were conducted on this type of polymer network. However, from these studies, it is found that this network still contains inhomogeneities such as spatial concentration fluctuation, connectivity defects, and entanglements. We developed a novel class of hydrogels by "cross-end-coupling" of two types of tetra-arm poly(ethylene glycol) (PEG) units that have mutually reactive amine (Tetra-PEG-NH_2) and activated ester (Tetra-PEG-NHS) terminal groups, respectively [1]. A schematic illustration of the tetra-PEG gel is shown in Fig. 1, where the red and blue lines represent the component chains.

In order to elucidate the high reactivity and high regularity of the Tetra-PEG gels, we carried out a kinetic study on the gelation reaction of the two tetra-arm poly(ethylene glycol) (Tetra-PEG) prepolymers by ATR-IR and UV spectroscopies [2]. The reaction rate constant for the gelation of Tetra-PEG was determined in aqueous solutions with varying both prepolymer volume fraction, ϕ and molecular weight, M_w, of the prepolymers. The gelation rate constant, k_{gel} was successfully estimated for all the systems. Figure 2(a) clearly shows that the k_{gel} values obtained here are almost constant within experimental error regardless of polymer volume fraction, ϕ, and prepolymer molecular weight, M_w, and their k_{gel} values for Tetra-PEG gel are essentially consistent with those for linearPEG system (Linear5k). The value of k_{gel} for Tetra-PEG gel is obtained to be around 70 $dm^3\ mol^{-1}\ s^{-1}$, which is much smaller than the reaction rate of typical diffusion-controlled reaction (*e.g.*, 10^8 ~ 10^9 $dm^3\ mol^{-1}\ s^{-1}$) and cross-linking photopolymerization (10^4 ~ 10^5 $dm^3\ mol^{-1}\ s^{-1}$). That is, the reaction rate of the

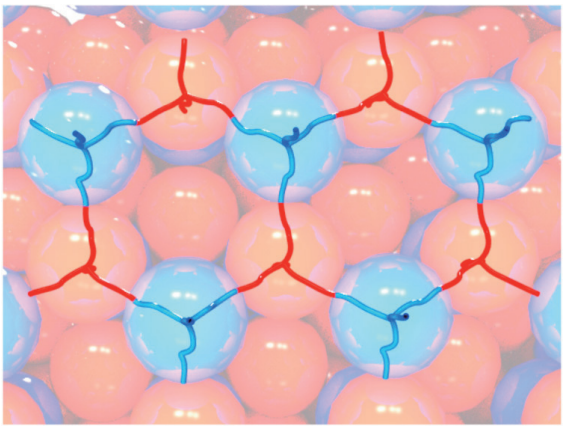

Fig. 1. Schematic illustration showing tetra-arm poly(ethylene glycol) (Tetra-PEG) gel. The red and blue lines represent Tetra-PEG-NH_2 and Tetra-PEG-NHS chains, respectively. Balls denotes the space occupied by the polymer chains.

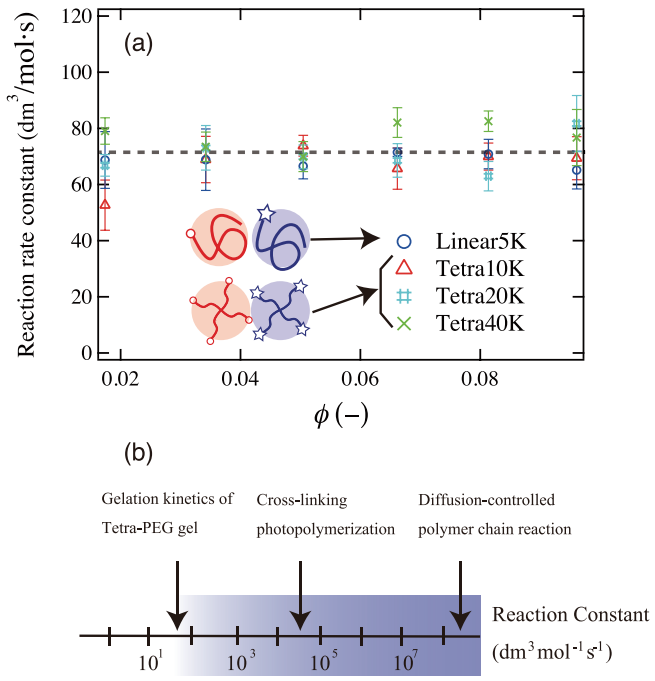

Fig. 2. (a) The reaction rate constant, k_{gel}, plotted against polymer concentration ϕ for 5K LinearPEG, 10K Tetra-PEG, 20K Tetra-PEG, and 40K Tetra-PEG. (b) Comparison of reaction rate constants of Tetra-PEG gel, cross-linking photopolymerization, and diffusion-controlled polymer chain reaction.

amide bond formation is much slower than the collision rate of the terminal NHS and amine groups. From these results, we concluded that the gelation reaction of Tetra-PEG gel is not diffusion-limited but reaction-limited process, i.e. the diffusion motion is much faster than the reaction rate (Fig. 2(b)). It is thus expected that Tetra-PEG prepolymer chains can diffuse in the solution during gelation process, leading to homogeneity and high-strength of Tetra-PEG gel. These discussions imply that, in order to achieve high-efficient and homogeneous gel, it is necessary to choose reaction groups so as to undergo reaction-limited reaction.

References
[1] T. Sakai *et al.*, Macromolecules **41**, 5379 (2008).
[2] K. Nishi *et al.*, Macromolecules **47**, 3274 (2014).

Authors
K. Nishi and M. Shibayama

Neutron Diffraction of Nano-crystalline PdD

Yamamuro Group

Palladium hydride (PdH_x) is the most popular metal hydride which has been investigated by many physicists and chemists. It has been remarked also from industrial points of view, *e.g.*, hydrogen storage, filters, sensors, catalysts, etc. On the adsorption process, a hydrogen molecule (H_2) dissociates into two hydrogen atoms (2H). In the H concentration region higher than x = 0.6, the hydride crystal takes the β phase with an fcc (NaCl-type) structure as show in Fig. 1(a). It is known that the H atoms are located at the octahedral (O) sites (1/2, 1/2, 1/2).

The physical and chemical properties of nanometer-sized materials are of interest since they are often different from bulk properties. As for the nano-particles of palladium hydrides, there are drastic changes of H_2 pressure-composition phase diagram [1], structures [2,3], etc. Inelastic neutron scattering (INS) [4] and quasielastic neutron scattering (QENS) [5] works have also been performed though the size of particles were relatively large (20-30 nm) and there were adhesions between particles. In this work, to clarify the structure including hydrogen atoms, we have performed *in situ* neutron powder diffraction experiments for high-quality nano-crystalline Pd as shown in Fig. 1(b). The nano-particles form an edge-cut octahedron enclosed by {111} and {100} facets, and its diameter is 8.0±0.9 nm.

Figure 2 shows the diffraction pattern of nano-crystalline $PdD_{0.363}$ measured at 300 K on a total scattering diffractometer NOVA at J-PARC. The amount of the absorbed deuterium (D) atoms into nano-crystalline Pd is precisely determined by the hydrogen gas control system installed on NOVA. The data shown in Fig. 2 are obtained after subtracting the large contribution of incoherent scattering from a protection polymer polyvinylpyrrolidone (PVP) which is used to avoid the adhesion between the nano-particles. This is the first neutron diffraction data for nano-crystalline metal hydrides. The crystal structure of nano-crystalline PdD_x has been refined by the Rietveld method as shown by the red curves of Fig. 2. We have examined the following three structural models: (model a) the O sites are occupied by the D atoms homogeneously, (model b) the O sites at the surface and subsurface (a few layers near the surface) are occupied, (model c) both the O sites and tetrahedral (T) sites (1/4,1/4,1/4) are occupied homogeneously. The best fit result was obtained with the model c. The obtained fitting parameters are as follows: lattice constant a = 4.010(4) Å, isotropic atomic displacements B_{Pd} = 0.322(8) Å^2, $B_{D(O)}$ = 1.93(8) Å^2, $B_{D(T)}$ = 14.8(9) Å^2, occupancies of the O and T sites $g_{D(O)}$ = 0.249 and $g_{D(T)}$ = 0.057 under the constraint $x = g_{D(O)} + 2g_{D(T)} = 0.363$.

Thus, our Rietveld analysis has revealed that D atoms

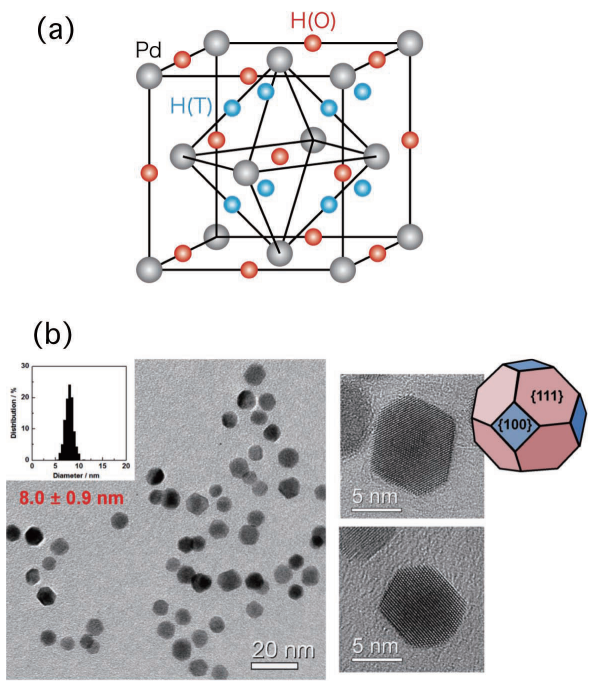

Fig. 1. (a) Structure of the β phase of Pd hydrides. The red and blue spheres show the possible octahedral and tetrahedral sites for hydrogen atoms, respectively. The gray spheres show the Pd fcc lattice. (b) Photographs of transmission electron microscope (TEM) for nano-crystalline Pd. The size distribution of the nano-particles and the schematic drawing of an edge-cut octahedron are also shown.

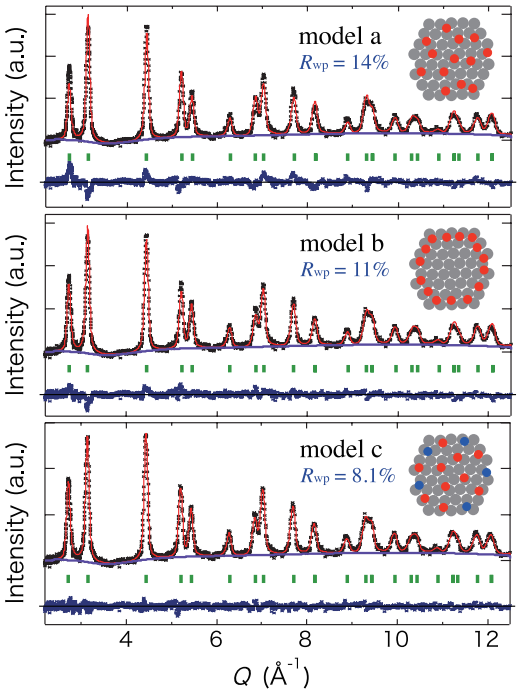

Fig. 2. Neutron powder diffraction pattern of nano-crystalline $PdD_{0.363}$ at 300 K and 0.1 MPa. The Rietveld analysis was performed assuming that D atoms are located at (a) O sites only, (b) O sites around the surface and subsurface, (c) both O and T sites.

occupy not only the O sites but also the T sites in nano-crystalline Pd. We guess that the T site occupation is due to the change in potential energy caused by the surface and/or distortion effects of nano-particles. The present results will give an important clue to the drastic change of the H atom dynamics in Pd nano-particles revealed in our recent preliminary neutron scattering work.

References

[1] M. Yamauchi *et al*., J. Phys. Chem. C **112**, 3294 (2008).
[2] M. Suleiman *et al*., J. Alloys and Compounds **644**, 356 (2003).
[3] J. A. Eastman *et al*., Phys. Rev. B **48**, 84 (1993).
[4] U. Stuhr *et al*., J. Phys.: Condens. Matter **7**, 219 (1995).
[5] S. Janßen *et al*., NanoStruct. Mater. **9**, 579 (1997).

Authors

H. Akiba, M. Kofu, H. Kobayashi[a], H. Kitagawa[a], K. Ikeda[b], T. Otomo[b], and O. Yamamuro
[a]Kyoto University
[b]KEK

Spin Model of O_2-based Magnet in a Nanoporous Metal Complex

Masuda Group

Natural oxygen, the second abundant constituent in the air, is a magnet having spin S = 1 induced by a couple of π_g electrons. Remarkable difference from the magnetism of transition metals is that the geometrical configuration of the O_2 molecules and the spin state are closely correlated because the molecular potential between a pair of O_2 molecules is strongly dependent on the spin state [1]. To manipulate the oxygen molecule and to artificially synthesize a novel type of O_2-based magnet is a challenge in the new field of magnetism.

We focus our attention on a metal complex having one-dimensional nanopores, Cu-Trans-1,4-Cyclohexanedicarboxylic acid abbreviated as Cu-CHD. The adsorbed O_2 molecules form dimer-like structure in the nanopores. Indeed, the magnetic susceptibility of Cu-CHD adsorbing 0.22 mole of O_2 per formula unit showed a rapid decrease with the temperature, suggesting a spin-gap system having non-magnetic ground state. It was, however, explained not by S=1 spin dimer but rather by S = 1/2 spin dimer [2]. To explain the unusual bulk property and to identify the precise energy scheme, a spectroscopic experiment is necessary.

In the present study we carried out inelastic neutron scattering (INS) experiments at low temperatures in order to clarify the spin model of the O_2-based magnet realized in Cu-CHD [3]. We found that the magnetic excitation of Cu-CHD adsorbing less O_2 is explained by a spin-dimers model of which the exchange constants are normally distributed as shown in Figs. 1(a) for experiment and 1(e) for calculation. In contrast, that of Cu-CHD adsorbing more O_2 is explained by a spin-trimers model with the distributed exchange constants as shown in Figs. 1(b) and (c) for experiments and Figs. 1(f) and (g) for calculations. It is noted that additional excitation is observed at 0.4 meV in the high

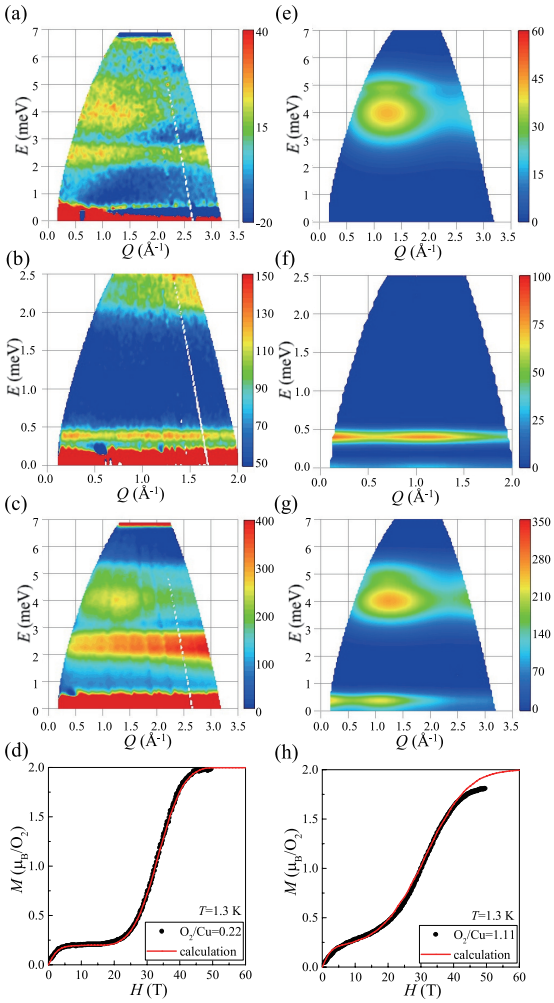

Fig. 1. (a) Inelastic neutron scattering (INS) spectrum for the incident neutron energy of Ei = 7.74 meV in Cu-CHD adsorbing less O_2 molecules. (b) INS spectrum for Ei = 3.14 meV in Cu-CHD adsorbing more O_2 molecules. (c) INS spectrum for Ei = 7.74 meV in Cu-CHD adsorbing more O_2 molecules. (d) Magnetization curve of Cu-CHD adsorbing less O_2 molecules. Experimental and calculation results are shown with black dots and red line. (e) Calculated INS spectrum of spin dimer model for Cu-CHD adsorbing less O_2 molecules. (f) Calculated INS spectrum of spin trimer model for Cu-CHD adsorbing more O_2 molecules in the low energy region. (g) INS spectrum of spin trimer model for Cu-CHD adsorbing more O_2 molecules in the high energy region. (h) Magnetization curve of Cu-CHD adsorbing more O_2 molecules. Experimental and calculation results are shown with black dots and red line.

concentration O_2 sample. The spin model is, thus, tuned by the concentration of O_2 in this system. Based on the spin models with the parameters determined by INS experiments and by considering the spin-dependent molecular potential, we quantitatively explained the magnetization curves as shown in Fig. 1(d) for low O_2 sample and in Fig. (h) for high O_2 sample. The effect of the spin-dependent Van der Waals potential to the anomalous energy scheme is experimentally confirmed.

References

[1] B. Bussery and P. E. S. Wormer, J. Chem. Phys. **99**, 1230 (1993).
[2] W. Mori, T. C. Kobayashi, J. Kurobe, K. Amaya, Y. Narumi, T. Kumada, K. Kindo, H. Aruga Katori, T. Goto, N. Miura, S. Takamizawa, H. Nakayama, and K. Yamaguchi, Mol. Cryst. Liq. Cryst. **306**, 1 (1997).
[3] M. Soda, S. Takamizawa, S.O. Kawamura, K. Nakajima, and T. Masuda, arXiv:1505.03272.

Authors

M. Soda, S. Takamizawa, S. O. Kawamura, K. Nakajima, and T. Masuda

Excitons Bright or Dark ? Revealed by Ultra-High Magnetic Fields in Carbon Nanotubes

Takeyama Group

Optical processes of semiconducting single-walled carbon nanotubes (SWNTs) are well-known to be dominated by pronounced exciton effects at their band edges [1]. Valley degeneracy and the spins in SWNTs connote very complicated exciton structures that comprise of a total of 16 excitonic states, among which only one state is optical dipole active (bright) and all others are optical dipole forbidden (dark) [2]. The ordering and relative energy splitting between these excitonic states, especially the ordering between bright and dark excitons, are crucial for optical device applications, since they essentially determine relaxation processes and thus the fate of optically or electrically generated carriers.

We carried out systematic high-field magneto-optical study on the relative ordering between bright and dark excitons in SWNTs for both 1st (E_{11}) and 2nd (E_{22}) sub-band

Transition	Chirality	Family Type	Environment	Relative Ordering
E_{11}	(6,4)	Type I	PVA	$E_{dark} < E_{bright}$
	(6,5)	Type II	PVA	$E_{dark} < E_{bright}$
	(7,5)	Type I	PFO	$E_{dark} < E_{bright}$
	(7,6)	Type II	PFO	$E_{dark} < E_{bright}$
	(8,3)[c]	Type I	D_2O	$E_{dark} < E_{bright}$
	(8,6)[a,b]	Type I	D_2O / Gelatin	$E_{dark} < E_{bright}$
	(8,7)[a,b]	Type II	D_2O / Gelatin	$E_{dark} < E_{bright}$
	(9,4)[a,b]	Type I	D_2O / Gelatin	$E_{dark} < E_{bright}$
	(9,7)[a]	Type I	D_2O	$E_{dark} < E_{bright}$
	(9,8)[a]	Type II	D_2O	$E_{dark} < E_{bright}$
	(10,2)[b]	Type I	Gelatin	$E_{dark} < E_{bright}$
	(10,5)[a,b]	Type I	D_2O / Gelatin	$E_{dark} < E_{bright}$
	(10,6)[b]	Type II	Gelatin	$E_{dark} < E_{bright}$
	(11,3)[b]	Type I	Gelatin	$E_{dark} < E_{bright}$
	(12,1)[a]	Type I	D_2O	$E_{dark} < E_{bright}$
E_{22}	(6,4)	Type I	PVA	$E_{dark} < E_{bright}$
E_{22}	(6,5)	Type II	PVA	$E_{dark} > E_{bright}$

Table 1. Relative energy position of bright and dark excitons at the band-edge of the first and second sub-band in SWNTs dispersed in various materials. a: I. B. Mortimer *et al.*, PRL **98**, 027404 (2007); b: J. Shaver *et al.*, Nano Lett. **7**, 1851 (2007); c: I. B. Mortimer *et al.*, PRB **76**, 085404 (2007)

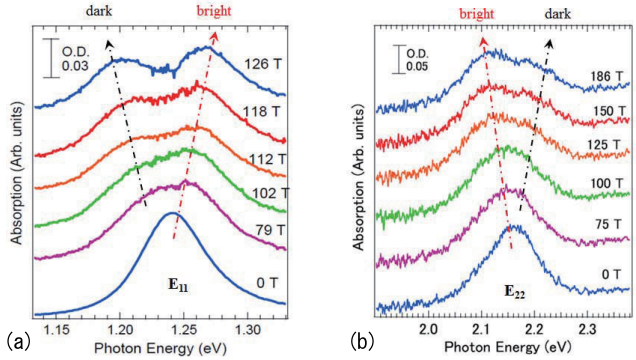

Fig. 1. Absorption spectral evolution of the (6, 5) SWNTs in high magnetic fields up to 186 T. (a) the first sub-band E_{11} transition; (b) the second sub-band E_{22} transition. Difference of the splitting peak evolution without any background contribution is unambiguous due to brightening of the original dark exciton energy position in the absence of magnetic field. O.D. stands for the optical density.

transitions. Considering the fact that electronic properties of SWNTs usually show family patterns, we selected the (6,4) SWNTs as a representative for the Type I species ((2n+m) mod 3 =1) and (6,5) for the Type II species ((2n+m) mod 3=2) in our study. Highly selected chirality (6,4) and (6.5) SWNTs, respectively, were separated from a mixture of HiPco-grown SWNTs by single-surfactant multicolumn gel chromatography, which was recently developed [3]. The magnetic fields up to 190 T were generated in the single-turn coil ultra-high magnetic field generation system at the ISSP International MegaGauss Science Laboratory.

We have identified the relative energy position of the dark exciton by brightening it in ultra-high magnetic fields. We found that the 1st and 2nd sub-band transitions exhibit completely different characteristics [4]. For the 1st sub-band transition, the bright exciton appears to be higher in energy than its dark counterpart for any chiral species and is robust against environmental effect. While for the 2nd sub-band, their relative ordering was found to be chirality-sensitive: the bright exciton can be either higher or lower than the dark one, depending on the specific nanotube structures (summarized in Table 1). Figure 1 shows the absorption spectral evolution in magnetic fields for the case of (6,5) chirality categorized in Type II . E_{22} transition in Fig.1 (b) exhibits the typical behavior that the lowest energy state is bright, which is quite contrast to almost all semiconductor materials, wherein the dark excitons always locate at the lower energy side of the bright one. The unique chirality-sensitive bright-dark excitonic ordering discovered in this study renders us with possible controllability of the optical properties of SWNTs by manipulating the ordering of their exciton states. The choice of the family pattern could serve as a guide to select nanotubes with desired exciton structures. Thus, the findings in this work open up new possibilities for engineering the optical properties of SWNTs and will facilitate future commercial applications

References

[1] F. Wang *et. al.*, Science **308**, 838 (2005).
[2] T. Ando, J. Phys. Soc. Jpn. **75**, 024707 (2006).
[3] H. Liu *et al.*, Nat. Commun. **2**, 309 (2011).
[4] W. Zhou, D. Nakamura, H. Liu, H. Kataura, and S. Takeyama, Scientific Reports **4**, 6999 (2014).

Authors

S. Takeyama, D. Nakamura, and W. Zhou

Optical Access to Frustrated Spin Spinel $HgCr_2O_4$ in Pulsed Strong Magnetic Fields

Takeyama Group

$HgCr_2O_4$ belongs to a series of the chromium spinel oxides ACr_2O_4 (A = Mg, Zn, Cd, Hg), comprising a three-dimensional pyrochlore antiferromagnet, and shows typical characteristics of geometrical spin frustration. When subjected to strong external magnetic fields, successive magnetic phase transitions take place accompanied by discontinuous lattice distortions [1]. This material is known as the first three-dimensional spin frustration system that exhibits a remarkable half-magnetization plateau phase [2], which has been understood using a bilinear–biquadratic model that takes into account the spin–lattice interactions.

Upon decreasing atomic size going from Hg to Zn or Mg at the A cation site in the pyrochlore lattice, much intense magnetic fields are required to reveal all of the rich magnetic phases up to fully saturated magnetization, owing to the increased nearest-neighbor antiferromagnetic exchange interaction. Our group has explored an optical method to approach magnetic phases in extremely high magnetic fields and applied to $CdCr_2O_4$ [3], $ZnCr_2O_4$ [4], and $MgCr_2O_4$ [5]. A novel magnetic phase that is hidden in conventional magnetization data has been detected by the optical method, just prior to the fully polarized moment state. We have termed this as the last ordered phase (LOP). The LOP was concluded to be a phase corresponding to a magnetic "superfluid" state, inferred from an analogy to symmetry breaking of the quantum phases in ^{4}He, whereas the detailed spin structure is not yet clarified. One of the plausible candidate

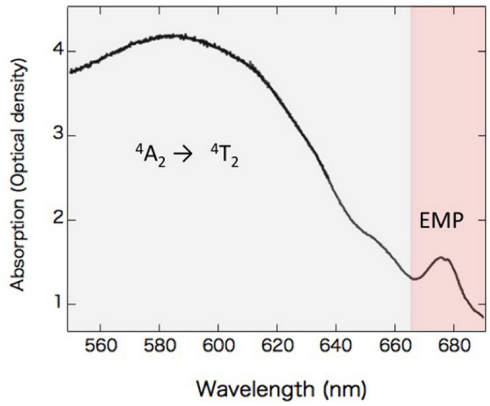

Fig. 1. Absorption spectra obtained at 4.2 K in a region of wavelengths where $^4A_2 \rightarrow {}^4T_2$ and EMP transitions are observed in polycrystalline powder $HgCr_2O_4$ embedded in Stycast solid resin.

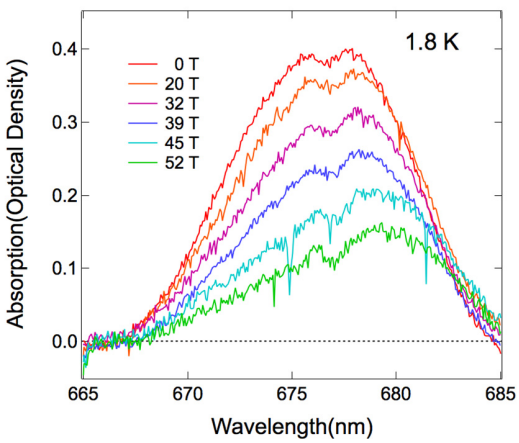

Fig. 2. Change of the EMP absorption spectra in magnetic fields.

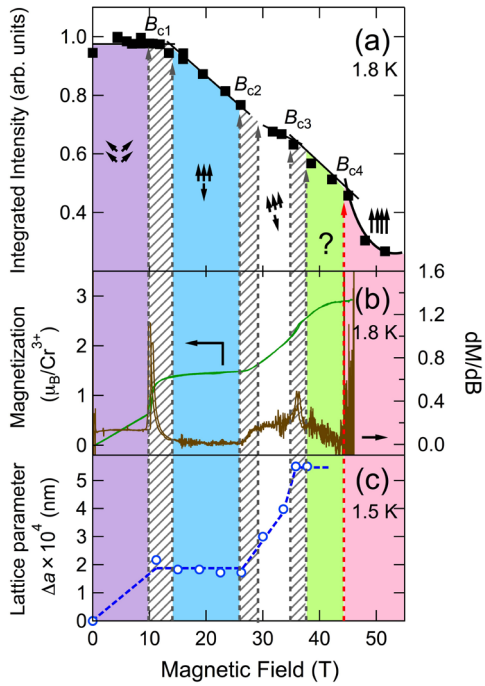

Fig. 3. (a) Changes in an integrated intensity of the EMP absorption peak in magnetic fields. (b) Magnetization M and its derivative dM/dB as a function of magnetic field, measured at 1.8 K [2], and (c) Variation of the lattice parameter Δa plotted against magnetic field. The data (circle) are reproduced from Fig. 2. in ref. [1].

is the spin "nematic" state. There needs, however, various experimental approach for verification. On the other hand, the magnetic-field strengths (B) at which the LOP is realized are extremely large and methods of measurement probes are quite restricted. The LOP in $HgCr_2O_4$ could be detected in magnetic fields around 40 T, much lower than those in $CdCr_2O_4$ and $ZnCr_2O_4$. However, in case of $HgCr_2O_4$, only powdered samples were available, that has been a hurdle for the optical approaches.

An exciton-magnon-phonon (EMP) absorption spectra were detected in a powder sample dispersed in Stycast 1266 transparent sold resin (Fig. 1), and the spectra were measured in magnetic fields up to 55 T (Fig. 2). The EMP absorption, reflecting a magnon density of states, showed the intensity variations corresponding to the point of successive phase transitions consistent with those of magnetization [2], lattice distortions [1], and electron magnetic resonance [6] measurements, where successive anomalies reported by other group. All these data are summarized in Fig. 3. This study has revealed that a fourth phase, termed LOP, also exists in $HgCr_2O_4$ and is related to the magnetic "superfluid" state that has also been observed in $CdCr_2O_4$ and $ZnCr_2O_4$ prior to the full-saturation phase. This study has revealed that the existence of the "superfluid" magnetic state, possibly of the spin "nematic" state is of universal among the chromium spinel magnetic frustrating oxides [7].

References

[1] Y. Tanaka , Y. Narumi , N. Terada , K. Katsumata, H. Ueda, Urs Staub, K. Kindo, T. Fukui, T. Yamamoto, R. Kammuri, M. Hagiwara, A. Kikkawa, Y. Ueda, H. Toyozawa, T. Ishikawa, and H. Kitamura, J. Phys. Soc. Jpn. **76**, 043708 (2007).
[2] H. Ueda, H. Aruga Katori, H. Mitamura, T. Goto, and H. Takagi, Phys. Rev. Lett. **94**, 047202 (2005).
[3] A. Miyata, S. Takeyama, and H. Ueda, Phys. Rev. B **87**, 214424 (2013).
[4] A. Miyata, H. Ueda, Y. Ueda, H. Sawabe, and S. Takeyama, Phys. Rev. Lett. **107**, 207203 (2011).
[5] A. Miyata, H. Ueda, and S. Takeyama, J. Phys. Soc. Jpn. **83**, 063702 (2014) .
[6] S. Kimura, M. Hagiwara, T. Takeuchi, H. Yamaguchi, H. Ueda, Y. Ueda, and K. Kindo, Phys. Rev. B **83**, 214401 (2011).

[7] D. Nakamura, A. Miyata, Y. Aida, H. Ueda and S. Takeyama, J. Phys. Soc. Jpn. **83**, 113703 (2014).

Authors
D. Nakamura and S. Takeyama

High Field Investigation of Field Induced Phase Transitions in $BiCu_2PO_6$

Kindo, Y. Matsuda, and Takeyama Groups

A frustrated two-leg ladder spin-gap system, $BiCu_2PO_6$, has recently attracted intense theoretical and experimental interest [1,2]. An application of a magnetic field along the leg direction of the spin ladder ($H//b$) closes the spin gap at H_{c1} ~ 20T and induces a series of field-induced phase transitions at higher magnetic fields [1]. Recent nuclear magnetic resonance (NMR) experiments by F. Casola have observed a triple-peak NMR profile in the intermediate field range from 20 to 35 T, and they have interpreted it as an appearance of an exotic "quantum soliton phase" [2]. However, since the measurements at high magnetic fields are experimentally challenging, detailed researches above 35 T remain scarce. In this context, we have experimentally investigated the field-induced phase-transitions under ultrahigh magnetic fields, i.e. up to 120 T, for three different crystallographic axes, by means of a combination of state-of-the-art techniques including specific heat (C_p), magnetocaloric effect (MCE), magnetization (M), and Faraday rotation (Θ_M) [3]. Here we have provided the thermodynamic evidence for the formation and the subsequent collapse of this field-induced soliton lattice.

Figure 1 shows the (H,T) phase diagram for $BiCu_2PO_6$. The phase boundaries depicted by open triangles and circles were determined by C_p and MCE measurements, respectively. Here, it should be emphasized that the MCE measurement were carried out under adiabatic conditions. Thus, the obtained MCE curves correspond to isentropic temperature changes as a function of the magnetic field, i.e., the entropy remains constant when collecting reversible MCE curves. Using the isentropic curve and specific heat data, we have succeeded to estimate the magnetic entropy (S_M), as seen in Fig.1(a)-(c) as color contour plots. We find that the Phase II_b (20 T < H < 35 T // b axis) can be characterized by high entropy, which is subsequently observed to disappear when entering phase III_b. This observation is in line with a recent study suggesting the formation and the collapse of a soliton lattice [2], which is predicted to have high entropy due to the short-ranged magnetic order.

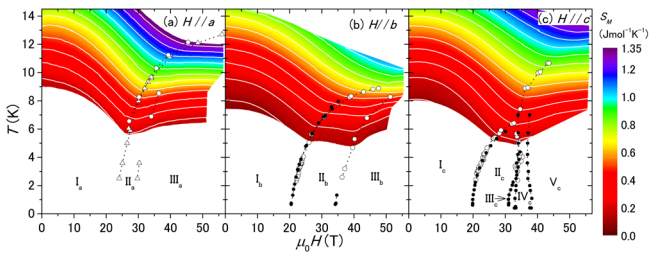

Fig. 1. (a)-(c) Contour map of $S(T,H)$ for $H//a$ (left), $H//b$ (middle), and $H//c$ (right). The contour plot of S_M (T,H) is constructed through linear interpolation of a series of MCE data. The phase boundaries determined by MCE and specific heat are also shown as open circles and open triangles, respectively. The solid dots are the phase boundaries reported in Ref. [1].

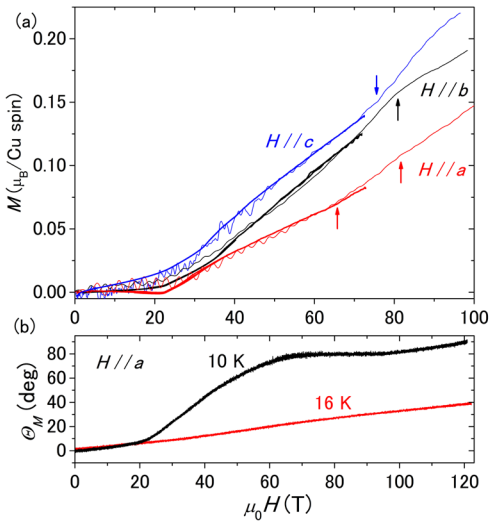

Fig. 2, (a) Magnetization (M) of $BiCu_2PO_6$. Thin curves were obtained by using a single turn coil. Thick curves were measured in a 75 T nondestructive pulsed magnet. (b) Field dependence of Faraday rotation angle (Θ_M) at 10 and 16 K. The magnetic field was applied along the a axis.

The magnetization (M) and Faraday rotation (Θ_M) shown in Fig. 2 captures further features in the ultrahigh magnetic field region. (i) For $H//a$, additional weak anomalies in M are observed in fields exceeding 60 T, a kink and a shoulder in M at 65 and 80 T (red arrows), respectively, indicating further field-induced transitions. This finding is also supported by the Θ_M measurements as a function of H [Fig. 2(b)]. (ii) When the external magnetic field is applied along the b axis, we can find a broad shoulder in M at 80 T (indicated by a black arrow). For $H//c$, an upturn at 75 T is evident in M (blue arrow). Although we observe a strongly anisotropic magnetization, the sequence of field-induced transitions continues above 60 T, regardless of field orientation. Our results indicate that $BiCu_2PO_6$ undergoes a sequence of novel phase transitions from a quantum soliton lattice to other exotic states under fields up to 120 T.

References

[1] Y. Kohama, S. Wang, A. Uchida, K. Prsa, S. Zvyagin, Y. Skourski, R. D. McDonald, L. Balicas, H. M. Ronnow, C. Rüegg, and M. Jaime, Phys. Rev. Lett. **109**, 167204 (2012).
[2] F. Casola, T. Shiroka, A. Feiguin, S. Wang, M. S. Grbić, M. Horvatić, S. Krämer, S. Mukhopadhyay, K. Conder, C. Berthier, H.-R. Ott, H. M. Rønnow, Ch. Rüegg, and J. Mesot, Phys. Rev. Lett. **110**, 187201 (2013).
[3] Y. Kohama, K. Mochidzuki, T. Terashima, A. Miyata, A. DeMuer, T. Klein, C. Marcenat, Z. L. Dun, H. Zhou, G. Li, L. Balicas, N. Abe, Y. H. Matsuda, S. Takeyama, A. Matsuo, and K. Kindo, Phys. Rev. B **90**, 060408(R) (2014).

Authors
Y. Kohama and K. Kindo

Possible Excitonic Phase in the Quantum Limit State of Graphite

Tokunaga and Kindo Groups

The quantum limit state, where all carriers are accommodated in the lowest Landau level, exhibits various anomalous phenomena because of the strong correlation acting on the carriers confined by magnetic fields. This state can be realized only in extremely high magnetic fields, the order of

10^4 T, in ordinary metals.

Graphite is a semimetal having a small number of electrons and holes (~ 3 × 10^{18} cm^{-3} for each) and goes into the quasi-quantum limit state, where only the lowest electron-like (Landau index n = 0, spin ↑ and ↓) and hole-like (n = −1, ↑ and ↓) subbands are populated in magnetic fields above 7.4 T applied along the c-axis. With further increasing the field, emergence and collapse of a density wave state has been claimed through measurements of in-plane (ρ_{xx}) and out-of-plane (ρ_{zz}) resistivity [1]. In addition, recent magnetoresistance measurements up to 80 T suggested emergence and collapse of another gapped state at 53 T and 75 T, respectively [2]. The actual nesting vector in these density wave states and also the underlying structure of the subbands, however, remain unclear as yet because of the limited experimental technique available above 25 T.

We studied Hall resistivity (ρ_{xy}) and magnetization in single crystals and pyrolytic graphite in pulsed high magnetic fields [3]. As the main feature of the results, the ρ_{xy} becomes almost zero as the field approaches 53 T, where ρ_{xx} and ρ_{zz} show anomalies as shown in Fig. 1. In the microscopic point of view, the Hall resistance is given by summation of the matrix elements of the current operator between the states having different Landau indices Δn = 1 and, hence, sensitive to the whole dispersion curves of the relevant subbands. The almost zero Hall resistance seems consistent with the existence of two populated subbands (n = 0↓ and n = −1↑) [1] rather than the less-symmetric three subband model (n = 0↑ , n = 0↓ and n = −1↑) [2]. Thereby, the quantum limit state likely emerges above 53 T. In this quantum limit state, density wave can be formed by the nesting between the Fermi points of the n = 0↓ and n = −1↑ subbands, which is equivalent to the BCS-like pairing state of excitons. Further studies are needed to clarify the nature of the additional phase transition at 75 T in this quantum limit state.

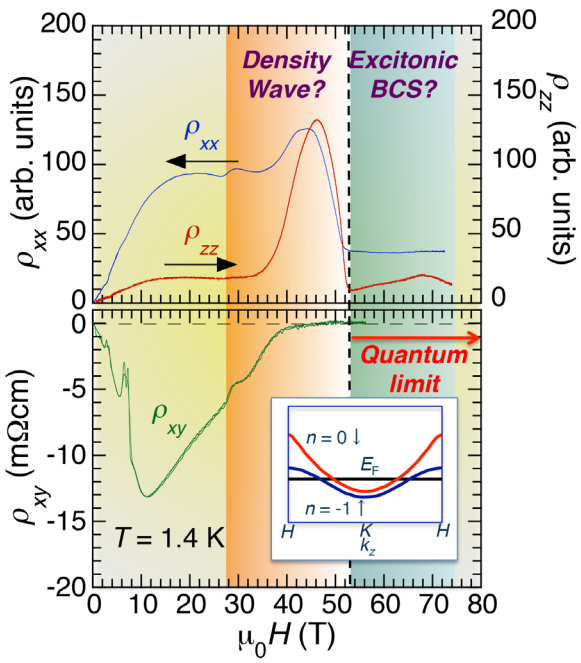

Fig. 1. (upper) In-plane (ρ_{xx}) and out-of-plane (ρ_{zz}) resistivity of graphite single crystals as a function of magnetic field applied along the c-axis at temperature of 1.4 K. (lower) Magnetic field dependence of in-plane Hall resistivity (ρ_{xy}) of graphite at 1.4 K. The colored areas represent different electronic phases suggested by transport measurements. The inset of the lower panel shows schematic illustration of the dispersion curves of the populated subbands above 53 T.

References

[1] H. Yaguchi and J. Singleton, J. Phys.: Condens. Matter **21**, 344207 (2009).

[2] B. Fauqué *et al*, Phys. Rev. Lett. **110**, 266601 (2013).

[3] K. Akiba *et al*, J. Phys. Soc. Jpn. **84**, 054709 (2015).

Authors

K. Akiba, A. Miyake, H. Yaguchi[a], A. Matsuo, K. Kindo, and M. Tokunaga

[a]Tokyo University of Science

Insulator-Metal Transition in Perovskite Cobalt Oxides at Ultrahigh Magnetic Fields

Y. Matsuda and Takeyama Groups

Phase transitions between metal and insulator are a subject that has been fascinating scientists for a long time. According to the one-electron approximation, materials whose energy band is partially occupied by electrons become metal. In 1930's, however, it had already been pointed out that some materials don't obey this rule. Nowadays, it is known that the electron-electron interaction plays an important role for making materials insulating and exotic phenomena such as non-Fermi liquid behavior and unconventional superconductivity emerge in the vicinity of the metal-insulator transition. The insulating phases of many materials appear along with interesting magnetic features such as antiferromagnetic order, spin gap formation and spin state transition [1]. Possible control of metal-insulator transitions by magnetic field is one of the most intriguing research subjects.

In the present work, we studied the magnetic-field-induced insulator–metal transition in perovskite cobalt oxides $(Pr_{1-y}Y_y)_{0.7}Ca_{0.3}CoO_3$ (y = 0.075, 0.10). $(Pr_{1-y}Y_y)_{1-x}Ca_xCoO_3$ is obtained by substitution of Y for a part of Pr in $Pr_{1-x}Ca_xCoO_3$ that shows a sharp first-order spin state (SS) transition of Co only when x is close to 0.5. The striking point is that the metal-insulator (MI) transition and the SS transition take place at the same time at 90 K. It is recently found that $(Pr_{1-y}RE_y)_{1-x}Ca_xCoO_3$ (RE= rare-earth element) also exhibits the first-order MI-SS transition even when x is different from 0.5 and the transition temperature

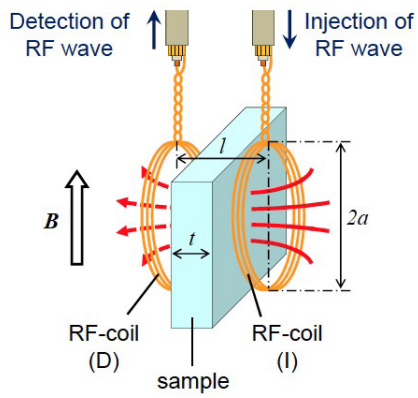

Fig. 1. Schematic view of a pair of coils and a sample for the high-frequency contactless electrical resistivity measurement. The coils are for injection and detection of the electromagnetic wave, respectively. The frequency range employed is 240 – 400 MHz. The magnetic field dependence of the electrical resistivity is obtained as the field variation of the transmission of the electromagnetic wave through the sample.

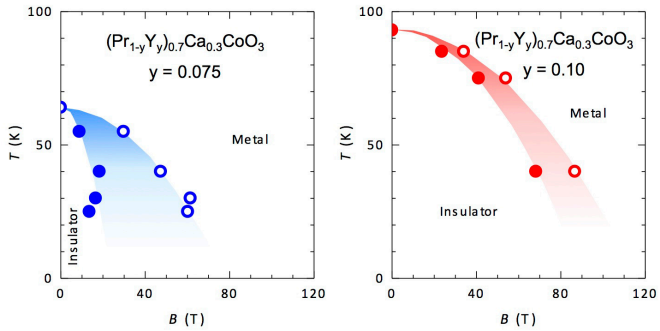

Fig. 2. The magnetic field-temperature (*B-T*) phase diagram determined by the magnetoresistance experiment. The higher field phase boundary (open circles) is obtained in the field-increasing process of the pulsed magnetic field and the lower field phase boundary (filled circles) by the field-descending process. The hysteretic behavior is the evidence of the first-order phase transition. Judging from the width of the hysteresis, the first order nature is more prominent in y=0.075 (a) than y=0.10 (b).

can be tuned by x and y [2]. We employed polycrystals of $(Pr_{1-y}Y_y)_{0.7}Ca_{0.3}CoO_3$ (y=0.075, 0.10) that were grown by a solid-state reaction method. The MI transition temperatures (T_{MI}) at zero magnetic field are 64 and 93 K for y=0.075 and 0.10, respectively. One can expect that a magnetic field induces the metallic phase at low temperatures when the Zeeman energy overcomes the energy gap between the different spin states. In order to realize the phase transition, ultrahigh magnetic fields in the range of 100 T will be required because the T_{MI} is rather high.

The single-turn coil method is utilized for generation of the pulsed magnetic fields over 100 T. We used the high frequency contactless technique to measure the electrical resistivity of $(Pr_{1-y}Y_y)_{0.7}Ca_{0.3}CoO_3$ (y=0.075, 0.10). The sample is sandwiched by two small coils; one coil is for generation of electromagnetic wave and another is for detection of the wave after transmission of the sample. The measured intensity of the transmitted wave is a function of the electrical resistivity of the sample (*e.g.*, the transmission is small when the resistivity is low owing to the shielding effect by the eddy current) and we can obtain the magnetoresistance from the magnetic field variation of the transmission. The schematic view of the coils and sample is shown in Fig. 1. This method was originally developed by Sakakibara *et al.* [3]. We modified the dimensions and used higher frequencies (240 – 400 MHz) to optimize the method for the present work.

As results of the experiment, we found that the transmission showed an abrupt decrease at certain magnetic field when the temperature is lower than T_{MI}, suggesting the insulator–metal transition occurs by magnetic fields. The phenomenon was observed in both samples but the transition magnetic field depends on sample and temperature. Figure 2 shows the magnetic field-temperature (*B-T*) phase diagram for the MI-SS transition in $(Pr_{1-y}Y_y)_{0.7}Ca_{0.3}CoO_3$ (y=0.075, 0.10) [4] . The marks denote the transition magnetic fields at different temperatures. The MI-SS transition is the first-order transition and we observed significant hysteretic behavior. The higher-field values in Fig. 2 are obtained in the field-increasing process and the lower-field values in the field-descending process. Considering the Clausius–Clapeyron relation, the obtained phase boundary indicates that the entropy change is important for the transition. However, the entropy change expected from only the SS transition cannot explain the phase boundary. Moreover, recent discovery of the valence change of Pr at the MI-SS transition [5] suggests that not only Co but also Pr plays an important role for the MI transition. Although the microscopic understanding of the MI-SS transition is still in controversy, the obtained *B-T* phase diagram sheds new light on this problem.

References

[1] M. Imada, A. Fujimori, and Y. Tokura, Rev. Mod. Phys. **70**, 1039 (1998).
[2] T. Naito, H. Sasaki, and H. Fujishiro, J. Phys. Soc. Jpn. **79**, 034710 (2010).
[3] T. Sakakibara, T. Goto, and N. Miura, Rev. Sci. Instrum. **60**, 444 (1989).
[4] S. Lee, Y. H. Matsuda, T. Naito, D. Nakamura, and S. Takeyama, J. Phys. Soc. Jpn. **84**, 044703 (2015).
[5] H. Fujishiro, T. Naito, S. Ogawa, N. Yoshida, K. Nitta, J. Hejtmánek, K. Knížek, and Z. Jirák, J. Phys. Soc. Jpn. **81**, 064709 (2012).

Authors

S. Lee, Y. H. Matsuda, T. Naito[a], D. Nakamura, and S. Takeyama
[a]Iwate University

Electron-Hole Recombination on ZnO(0001) Single-Crystal Surface Studied by Time-Resolved Soft X-Ray Photoelectron Spectroscopy

I. Matsuda Group

Zinc oxide (ZnO) has attracted much attention for its optoelectronic applications, e.g. photovoltaics, light-emitting diode, and photocatalyst. One of the important factors in the photo-induced function is dynamics of photoexcited carriers that govern optical and electronic phenomena, and their lifetime is directly related to efficiency of the optoelectronic functionalities. Recently, time-resolved photoemission spectroscopy has been carried out to trace relaxation of the photovoltage effect on various semiconductor surfaces. The relaxation is a consequence of decay of the photo-excited carriers or electron-hole (e-h) recombination and, thus,

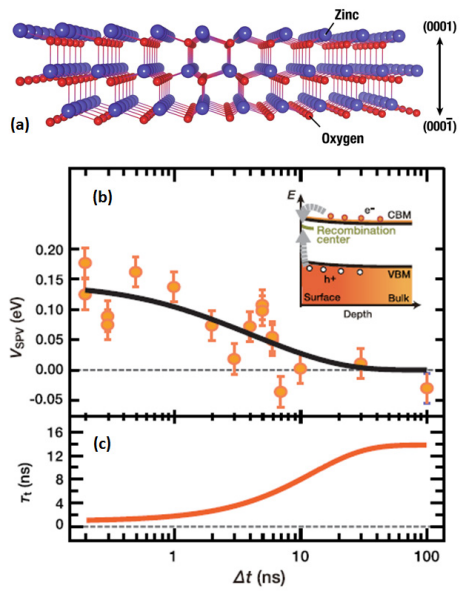

Fig. 1. (a) Atomic structure of an ideal ZnO crystal. Time-dependences of (b) surface photovoltage, V_{SPV}, taken with the laser intensity of 113 mJ/cm^2/pulse, and (c) carrier lifetime (τ_t) during the relaxation of the SPV effect. The inset shows the schematic drawing of electron-hole recombination at or near the surface. In (b), the data points are curve-fitted with the thermionic model. Variation of τ_t is obtained with $\tau_t = \tau_0 \exp\{(V_s - V_{SPV})/\eta kT\}$, where η=2.0 and τ_o=1.7 ps.

the decay constant of surface photovoltage (SPV) directly corresponds to the lifetime of photoexcited carriers. In the present research, we report the detailed investigation of the time-resolved soft X-ray PES experiments on a ZnO(0001) surface to clarify the carrier dynamics [1].

A ZnO crystal has wurtzite structure and the (0001) surface is terminated with zinc atoms (Fig. 1(a)). The e-h pairs are generated by the irradiation of the femtosecond-pulse laser, and the following charge separation leads to the SPV generation. The relaxation of the SPV was found to take nanoseconds, as shown in Fig.1(b). The relaxation process is fairly described by a thermionic model, in which the photoexcited carriers overcome the surface potential, V_s, to be transported to the surface and then recombine with the counterparts accumulated at the surface. The potential, generated by the bulk band-bending effect near the surface and the V_s value, was evaluated by valence band photoemission spectroscopy measurements of the sample surface. By tracing the relaxation of the SPV effect, we determined a photoexcited carrier lifetime at the surface under the flat band condition on the ZnO(0001) surface to be τ_o=1.7 ps and the lifetime exponentially increases with temporal variation of surface potential barrier (Fig.1(c)). The obtained carrier lifetime at the surface matches with values of the surface carrier decay time (~1ps) reported in the literatures of femtoseconds-time-resolved reflectivity and transmissivity experiments [2]. The agreement implies the relaxation of the SPV effect on the ZnO(0001) crystal proceeds with thermal diffusion of photo-excited carriers and the e-h recombination was evaluated to held at the depth of 30–100 nm from the surface. It has been discussed that the density of singly ionized oxygen vacancy traps (which can be the recombination centers) is much higher in such a surface recombination layer than in the interior of the crystal. It is inferred that e-h recombination takes place at the trapping sites at the topmost surface (the surface state) and in the subsurface layer (the impurity states) with the different carrier-capturing cross-sections. The understanding leads to both developments of a new optoelectronically functional materials and improvements of the efficiency.

References

[1] R. Yukawa, S. Yamamoto, K. Ozawa, M. Emori, M. Ogawa, Sh. Yamamoto, K. Fujikawa, R. Hobara, S. Kitagawa, H. Daimon, H. Sakama, and I. Matsuda, Appl. Phys. Lett. **105**, 151602 (2014).

[2] M. A. M. Versteegh, T. Kuis, H. T. C. Stoof, and J. I. Dijkhuis, Phys. Rev. B **84**, 035207 (2011).

Authors

R. Yukawa, S. Yamamoto, and I. Matsuda

15-GHz Optical Frequency Comb as Calibration Source for Astronomical Spectrographs

Kobayashi Group

Optical frequency comb (OFC), based on a frequency-stabilized femtosecond mode-locked pulsed laser, have become an invaluable tool in precision applications, including optical clocks, frequency metrology and spectroscopy. Our group are developing OFCs and studying precision spectroscopies with OFC. Here, we highlight a 15-GHz OFC as a calibration source for astronomical spectrographs.

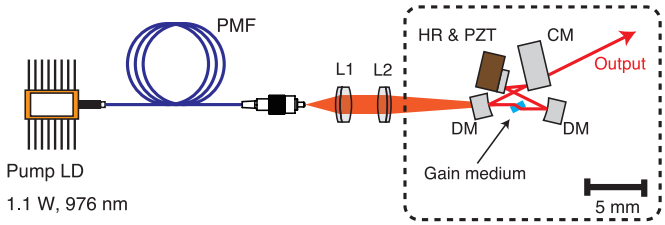

Fig. 1. Layout of the 15-GHz laser.

In astronomy one of the main research topics is searching for Extra-solar planets. Extra-solar planets are detected by a Doppler shift of the absorption spectrum of the fixed star with a carefully-calibrated spectrograph, and then, one can derive the information about the planets, for example its revolution period, distance from the host star and its weight. In order to detect an Earth-like planet around a Sun-like fixed star, the spectrograph needs the calibration level within a velocity of 10 cm/s, corresponding to the wavelength shift of 0.3 femtometer at the center wavelength of 1000 nm, as a Doppler shift during more than one year, which is extremely-difficult task. Although usually I_2 cell or Th-Ar lamp have been used for a conventional calibration sources, they do not satisfy the long-term stability, traceability and the spectral cover range. OFC is one of the alternatives to concur such drawbacks. It is because that OFC emits a broadband comb-like spectrum and the longitudinal modes are evenly spaced by a separation equal to the pulse repetition rate. That is, OFC is an ideal "frequency scale" for spectrographs.

Conventional OFCs, however, cannot be used for a frequency scale. Typically, mode separation is less than the resolution of spectrograph, several hundred MHz and GHz respectively — imagine a ruler with too dense scales to be resolved by your eyes. The mode spacing of 10 to 20 GHz, hundred times higher than that of typical OFCs, is required. One of the methods to obtain such large mode spacing is using several Fabry–Pérot cavities as harmonic mode filters. This scheme, however, significantly increases apparatus complexity and cannot perfectly suppress the unwanted adjacent modes. In our group, an OFC with a mode spacing of 15 GHz has been developed based on a 15-GHz femtosecond laser [1]. This OFC directly produce a comb-like spectrum with sufficiently large mode spacing to be resolved by a conventional spectrograph and it would be a suitable calibration source. Figure 1 shows the 15-GHz femtosecond laser. The laser composed four-mirror ring cavity with a cavity length of only 2 cm, as so far this is the shortest cavity

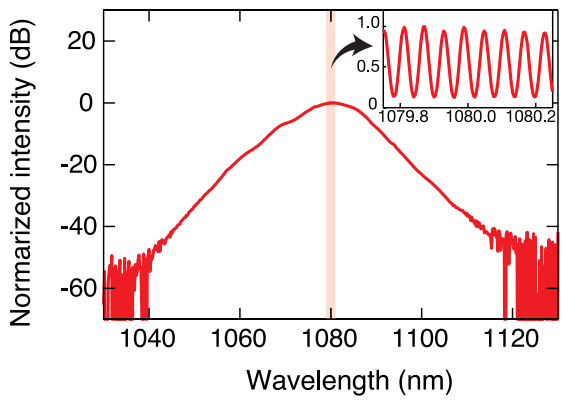

Fig. 2. Optical spectra measured with an optical spectrum analyzer at a resolution of 2 nm and (inset) 16 pm.

length in femtosecond Kerr-lens mode-locked lasers. The gain material was an ytterbium-doped Y_2O_3 ceramic and the laser emitted a pulse with a pulse duration of 152 fs and an average power of 60 mW. The optical spectrum is shown in Fig. 2. Thanks to sufficiently high repetition rate, a commercial spectrometer could resolve comb structure. One of the longitudinal modes of the 15-GHz laser was phase locked to an optical frequency standard, semiconductor laser locked to an ultra-low expansion glass cavity with a frequency drift of less than 0.5 MHz/month. Furthermore our laser was pumped by a reliable semiconductor laser diode, which was suitable for long-term operation.

In this report, we especially focused on a calibration source of spectrograph as a 15-GHz OFC application. The reported 15-GHz OFC also has a potential to expand the comb applications, including optical arbitrary waveform generation, low-phase noise microwave generation.

Reference
[1] M. Endo, I. Ito, and Y. Kobayashi, Opt. Express **23**, 10564 (2015).

Authors
M. Endo, S. Tani, I. Ito, and Y. Kobayashi

Generation of Isolated Attosecond Soft X-Ray Pulses in the Water Window

Itatani Group

High harmonic generation using Ti:sapphire lasers at 800 nm is well established in 1990's, and has opened a way to produce attosecond optical pulses in the extreme ultraviolet (EUV). The spectral range of such attosecond pulses, however, remains in the EUV (< 200 eV in photon energy, or > 5 nm in wavelength). It has been expected that the spectral range of attosecond pulses can be drastically extended to the soft X ray region by using an ultrashort light source in a *longer wavelength* because low-frequency strong fields can accelerate electrons to much higher kinetic energies. The accelerated electron's kinetic energy is then converted to a photon energy in the recombination process of high harmonic generation. However, such ultrashort-pulse infrared (IR) sources have been not available because of the lack of appropriate laser media in the IR or mid IR.

Here we report on the recent breakthrough in producing isolated attosecond pulses in the soft X ray region (up to ~325 eV in photon energy) by using a newly developed IR light source that is based on optical parametric chirped pulse amplification (OPCPA). The OPCPA, unlike chirped pulse amplification in Ti:sapphire lasers, is based on parametric amplification in nonlinear transparent crystals. By appropriately selecting the nonlinear crystals, pump lasers, and phase-matching conditions, we can design the spectral properties of optical amplification. We have developed a full-scale OPCPA system that uses BiB_3O_6 (BIBO) crystals as nonlinear media and a Ti:sapphire laser system around 800 nm as a pump source. With this novel combination of BIBO and Ti:sapphire, the BIBO-based OPCPA exhibits an extremely broad gain bandwidth spanning from 1100 to 2200 nm. This nearly-octave spanning bandwidth enables us to amplify few-cycle IR pulses directly in the OPCPA system. We have successfully produced 0.55-mJ, 10-fs pulses centered at 1600 nm at a repetition rate of 1 kHz. This pulse duration corresponds to sub-two cycles of the carrier wave at 1600 nm. The output of the OPCPA system was focused onto a gas cell containing neon to produce high harmonics. We observed soft X-ray spectra of high harmonics up to 325 eV, which is well reaching the water window or covering the carbon *K* edge. The spectral structure below the cutoff was observed to be extremely sensitive to the carrier envelope phase (CEP) of the driver pulses. By changing the CEP, we observed a drastic shift of the peak structure in the soft X-ray spectra. This behavior is known as a half-cycle cutoff, which is an important signature for the production of isolated attosecond pulses.

This work is indeed a milestone to extend attosecond spectroscopy from the EUV to the soft X ray, where we are aiming the first demonstration of ultrafast soft-X-ray spectroscopy that can probe element-specific electronic states of condensed matters. Such laser-based ultrafast soft X-ray sources are expected to play an important role, which is complementary to other soft X-ray sources such as 3rd generation synchrotrons and X-ray free electron lasers.

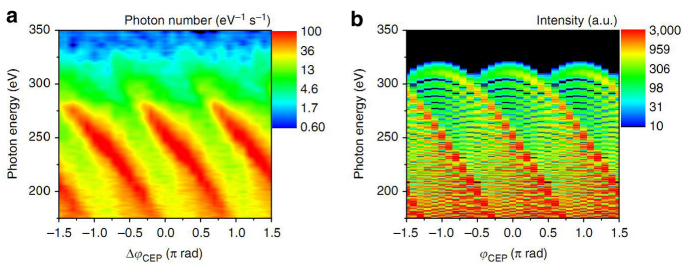

Fig. 1. (a) Experimentally obtained high harmonic spectra recorded with varying the CEP with steps of 0.1 π radian. (b) Simulated high harmonic spectra assuming 10-fs optical pulses at 1600 nm with an intensity of 3.8×10^{14} W/cm^2.

Reference
[1] N. Ishii, K. Kaneshima, K. Kitano, T. Kanai, S. Watanabe, and J. Itatani, Nature Commun. **5**, 3331 (2014).

Authors
N. Ishii, K. Kaneshima, K. Kitano, T. Kanai, S. Watanabe[a], and J. Itatani.
[a]Tokyo University of Science

Highlights of Joint Research

Supercomputer Center

The Supercomputer Center (SCC) is a part of the Materials Design and Characterization Laboratory (MDCL) of ISSP. Its mission is to serve the whole community of computational condensed-matter physics of Japan providing it with high performance computing environment. In particular, the SCC selectively promotes and supports large-scale computations. For this purpose, the SCC invites proposals for supercomputer-aided research projects and hosts the Steering Committee, as mentioned below, that evaluates the proposals.

The ISSP supercomputer system consists of three subsystems: System A, which is intended for a parallel computation with relatively smaller number of nodes connected tightly, and System B, which is intended for more nodes with relatively loose connections. In July, 2010, the SCC replaced the two supercomputer subsystems. The current system B is SGI Altix ICE 8400EX, which consists of 30 racks or 15360 cores whereas the system A is NEC SX-9, which consists of 4 nodes or 64 cpus. They have totally 200 TFlops. System C - FUJITSU PRIMEHPC FX10 was installed in April, 2013. It is highly compatible with K computer, the largest supercomputer in Japan. System C consists of 384 nodes, and each node has 1 SPARC64TM IXfx CPU (16 cores) and 32 GB of memory. The total system achieves 90.8 TFlops theoretical peak performance.

The hardware administration is not the only function of the SCC. The ISSP started hosting Computational Materials Science Initiative (CMSI), a new activity of promoting materials science study with next-generation parallel supercomputing. This activity is financially supported by the MEXT HPCI strategic program, and in CMSI, a number of major Japanese research institutes in various branches of materials science are involved. The SCC supports the activities of CMSI as its major mission.

All staff members of university faculties or public research institutes in Japan are invited to propose research projects (called User Program). The proposals are evaluated by the Steering Committee of SCC. Pre-reviewing is done by the Supercomputer Project Advisory Committee. In school year 2014 totally 247 projects were approved. The total points applied and approved are listed on Table. 1 below.

The research projects are roughly classified into the following three (the number of projects approved):

First-Principles Calculation of Materials Properties (119)
Strongly Correlated Quantum Systems (38)
Cooperative Phenomena in Complex, Macroscopic Systems (90)

All the three involve both methodology of computation and its applications. The results of the projects are reported in 'Activity Report 2014' of the SCC. Every year 3-4 projects are selected for “invited papers” and published at the beginning of the Activity Report. In the Activity Report 2014, the following three invited papers are included:

"All-Electron First-Principles GW+Bethe-Salpeter Program: Development & Applications", Yoshifumi NOGUCHI
"First-Principles Study on Superconductivity in Alkali-Doped Fullerides", Ryotaro ARITA
"Development of Simulation Methods for Membrane Protein Structure Predictions and Replica-Exchange Methods", Ryo URANO and Yuko OKAMOTO

Class	Max/Min Points	Application	Number of Projects	Total Points					
				Applied			Approved		
				System A	System B	System C	System A	System B	System C
A	100	any time	9	500	600	400	500	600	400
B	2k, 1k, 500	twice a year	53	40.8k	44.8k	6.3k	33.8k	29.4k	5.7k
C	20k, 10k, 2.5k	twice a year	151	637.0k	1210.2k	141.2k	429.0k	360.5k	111.4k
D	20k, 10k, 2.5k	any time	10	12.0k	71.7k	0	12.0k	57.6k	0
E	0, 30k, 2.5k	twice a year	23	-	621.0k	42.0k	-	270.0k	37.4k
S		twice a year	1	0	60.0k	0	0	25.0k	0
CMSI			18	-	-	-	-	-	140.0k
Total			265	690.3k	2,008.3k	189.9k	475.3k	743.1k	294.9k

Table 1. Research projects approved in 2014
The maximum points allotted to the project of each class are the sum of the points for the two systems; Computation for 1 CPU· hour corresponds to 0.32, 0.022, and 0.042 points for System-A, System-B, and System C, respectively.

Neutron Science Laboratory

The Neutron Science Laboratory (NSL) has been playing a central role in neutron scattering activities in Japan since 1961 by performing its own research programs as well as providing a strong General User Program for the university-owned various neutron scattering spectrometers installed at the JRR-3 (20MW) operated by Japan Atomic Energy Agency (JAEA) in Tokai (Fig. 1). In 2003, the Neutron Scattering Laboratory was reorganized as the Neutron Science Laboratory to further promote the neutron science with use of the instruments in JRR-3. Under the General User Program supported by NSL, 14 university-group-owned spectrometers in the JRR-3 reactor are available for a wide scope of researches on material science, and proposals close to 300 are submitted each year, and the number of visiting users under this program reaches over 6000 person-day/year. In 2009, NSL and Neutron Science Laboratory (KENS), High Energy Accelerator Research Organization (KEK) built a chopper spectrometer, High Resolution Chopper Spectrometer, HRC, at the beam line BL12 of MLF/J-PARC (Materials and Life Science Experimental Facility, J-PARC). HRC covers a wide energy and Q-range ($10\mu eV < \hbar\omega < 2eV$ and $0.02Å^{-1} < Q < 50Å^{-1}$), and therefore becomes complementary to the existing inelastic spectrometers at JRR-3. HRC started to accept general users through the J-PARC proposal system in FY2011.

Triple axis spectrometers, chopper spectrometer (HRC), and a high resolution powder diffractometer are utilized for a conventional solid state physics and a variety of research fields on hard-condensed matter, while in the field of soft-condensed matter science, researches are mostly carried out by using the small angle neutron scattering (SANS-U) and/or neutron spin echo (iNSE) instruments. The upgraded time-of-flight (TOF) inelastic scattering spectrometer, AGNES, is also available through the ISSP-NSL user program.

On March 11, 2011, a great earthquake with Magnitude 9.0 hit North East Coast of Japan. Fortunately, JRR-3 was under regular inspection and no serious accidents or damages were reported. However, the lifeline of Tokai Village area was lost for more than two weeks, and it took more than two months before damage inspection of JRR-3 could be started. As of May of 2015, JRR-3 has not restarted yet. General User Programs of 2011 - 2014 were cancelled and that of 2015 has been suspended so far. In order to compensate the loss of the activity of NSL, a number of proposals accepted in 2011 - 2014 were transferred to overseas owing to kind offer from the major facilities, namely, ORNL, ILL, ANSTO, and HANARO.

Fig. 1. The reactor of JRR-3. The eight neutron scattering instruments are attached to the horizontal beam tubes in the reactor experimental hall. Two thermal and three cold guides are extracted from the reactor core towards the guide hall located to the left.

Fig. 2. The U.S.-Japan spectrometer, CTAX, installed at the cold guide-line CG4, High Flux Isotope Reactor (HFIR), in Oak Ridge National Laboratory. Members who contributed the relocation project of the U.S.-Japan spectrometer celebrate the completion of the project in October 2010.)

Research topics in FY2013 cover Hydrogen release from Li alanates originates in molecular lattice instability (6G:TOPAN T1-3:HERMES), Direct observation of antiferromagnetic ordering in s electrons confined in regular nanospace of sodalite (5G:PONTA), SANS Studies on Catalyst Ink of Fuel Cell (SANS-U), Neutron scattering studies of Ti-Cr-V bcc alloy with the residual hydrogen and deuterium (AGNES). In addition, there are a variety of activities on fundamental physics, neutron beam optics, developments of neutron scattering techniques.

Progress of HRC spectrometer in FY2014 is the development of the magnetic field environment. We examined a performance test of a superconducting magnet on the HRC goniometer. The magnetic field of 10 T was achieved with normal operation of the related components in the straying field. The magnitude of the field is the highest record in J-PARC/MLF at present. By using radial collimator for the reduction of background scattering from Aluminum supporting ring in the magnet, high-quality data was collected. The magnet is now ready for the general user program.

The NSL also operates the U.S.-Japan Cooperative Program on neutron scattering, providing further research opportunities to material scientists who utilize the neutron scattering technique for their research interests. In 2010, relocation of the U.S.-Japan triple-axis spectrometer, CTAX, was completed, and it is now open to users (Fig. 2).
http://neutrons.ornl.gov/instruments/HFIR/CG4C/

The activity report on Neutron Scattering Research in JFY2011 is given in NSL-ISSP Activity Report vol. 18 (2011), http://quasi.issp.u-tokyo.ac.jp/actrep/actrep-18-2011/index-pub_vol18.html.

International MegaGauss Science Laboratory

The objective of this laboratory (Fig. 1) is to study the physical properties of solid-state materials (such as semiconductors, magnetic materials, metals, insulators, superconducting materials) under ultra-high magnetic field conditions. Such a high magnetic field is also used for controlling the new material phase and functions. Our pulse magnets, at moment, can generate up to 87 Tesla (T) by non-destructive manner, and from 100 T up to 760 T (the world strongest as an in-door record) by destructive methods. The laboratory is opened for scientists both from Japan and from overseas, especially from Asian countries, and many fruitful results are expected to come out not only from collaborative research but also from our in-house activities. One of our ultimate goals is to provide the scientific users as our joint research with magnets capable of a 100 T, milli-second long pulses in a non-destructive mode, and to offer versatile physical precision measurements. The available measuring techniques now involve magneto-optical measurements, cyclotron resonance, spin resonance, magnetization, and transport measurements. Recently, specific heat and calorimetric measurements are also possible to carry out with sufficiently high accuracy.

Our standard non-destructive-type pulse magnets are energized by single capacitor bank and can generate fields up to 75 T for ordinary use. Their simple sinusoidal waveforms are advantageous for precise and reliable measurements of various physical properties. Several on-demand magnets having irregular shapes and sizes are developed for some particular experiments. We open six magnet cells for parallel experiments and accept more than 50 research projects per year in 2013.

A 210 MJ flywheel generator (Fig. 2), which is the world largest DC power supply (recorded in the Guinness Book of World Records) has been installed in the DC flywheel generator station at our laboratory, and used as an energy source of long pulse magnets. The magnet technologies are intensively devoted to the quasi-steady long pulse magnet (an order of 1-10 sec) energized by the giant DC power supply. The latest long-pulse magnet can generate fields up to 36 T with its pulse half-period of 1 sec.

Our interests cover the study on quantum phase transitions (QPTs) induced by high magnetic fields. Field-induced QPTs have been explored in various materials such as quantum spin systems, strongly correlated electron systems and other magnetic materials. Direct thermodynamic evidences of QPTs are obtained through magnetization and recently developed caloric measurements. For some QPTs, changes in symmetry at the transitions are sensitively resolved through measurements of electric polarization or optical imaging using a polarizing microscope. High resolution of electrical measurements realized the observation of quantum oscillations in high quality crystals through measurements of electrical resistivity, contactless impedance, and torque magnetometry.

Magnetic fields higher than 100 T can only be obtained with destructing a magnet coil, where ultra-high magnetic fields are obtained in a microsecond time scale. Our destructive techniques have undergone intensive developments. The project, financed by the ministry of education, culture, sports, science and technology, is now in progress, and goal is to generate 1000 T by the electromagnetic flux compression (EMFC) system (Fig. 3). The system which is unique to ISSP in the world scale is comprised of a power source of 5 MJ main condenser bank and 2 MJ condenser bank and has been accomplished its installation. Two magnet stations are constructed and both are energized from each power source. Both systems are fed with a 2 MJ condenser bank used for a seed-field coil, of which magnetic flux is to be compressed.

As an easy access to the megagauss science and technology, we have the single-turn coil (STC) system capable of generating the fields of up to 300 T by a fast-capacitor of 200 kJ. We have two STC systems, one is a horizontal type (H-type) and the other is a vertical type (V-type, Fig. 4). Various kinds of laser spectroscopy experiments such as the cyclotron resonance and the Faraday rotation using the H-type STC are available. On the other hand, for very low-temperature experiments, a combination of the V-type STC with a liquid helium bath cryostat is very useful and the magnetization measurements at temperature as low as 2 K can be performed up to 120 T with high precision.

Fig. 1. Building view of the International MegaGauss Science Laboratory (C-building) at ISSP.

Fig. 2. The building for the flywheel generator (left hand side) and a long pulse magnet station (right hand side). The flywheel giant DC generator is 350 ton in weight and 5 m high (bottom). The generator, capable of a 51 MW output power with the energy storage 210 MJ, is planned to energize the long pulse magnet generating 100 T without destruction.

	Alias	Type	B_{max}	Pulse width Bore	Power source	Applications	Others
Building C Room 101-113	Electro- Magnetic Flux Compression	destructive	730 T	μs 10 mm	5 MJ, 40kV	Magneto-Optical Magnetization	5 K – Room temperature
	Horizontal Single-Turn Coil	destructive	300 T 200 T	μs 5 mm 10 mm	0.2 MJ, 50 kV	Magneto-Optical measurements Magnetization	5 K – 400 K
	Vertical Single-Turn Coil	destructive	300 T 200 T	μs 5 mm 10 mm	0.2 MJ, 40 kV	Magneto-Optical Magnetization	2 K – Room temperature
Building C Room 114-120	Mid-Pulse Magnet	Non-destructive	60 T 70 T	40 ms 18 mm 40 ms 10 mm	0.9 MJ, 10 kV	Magneto-Optical measurements Magnetization Magneto-Transport Hall resistance Polarization Magneto-Striction Magneto-Imaging Torque Magneto- Calorimetry Heat Capacity	Independent Experiment in 5 site Lowest temperature 0.1 K
Building C Room 121	PPMS	Steady State	14 T			Resistance Heat Capacity	Down to 0.3 K
	MPMS	Steady State	7 T			Magnetization	
Building K	Short-Pulse magnet	Non-destructive	87 T (2-stage pulse) 85 T	5 ms 10 mm 5 ms 18 mm	0.5 MJ, 20 kV	Magnetization Magneto-Transport	2K – Room temperature
	Long-Pulse magnet	Non-destructive	36 T	1 s 30 mm	210 MJ, 2.7 kV	Resistance Magneto-Calorimetry	2K – Room temperature

Table 1. Available Pulse Magnets, Specifications

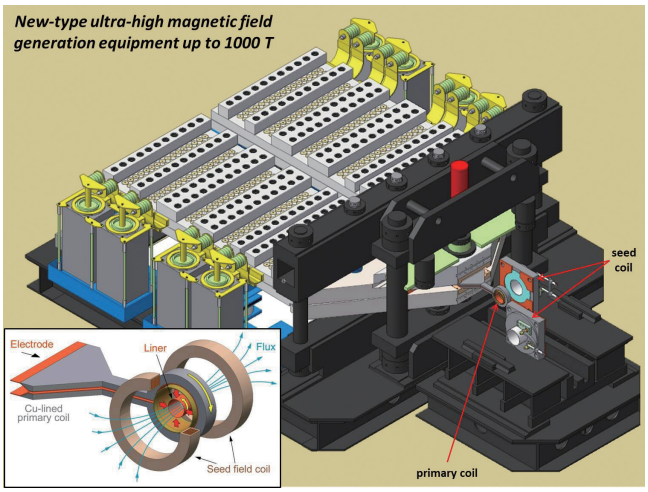

Fig. 3. (Build. C) The building for the electro-magnetic flux compression, generating over 700 T. 1000 T project started since 2010, and finally condenser banks of 9 MJ (5 MJ + 2 MJ +2 MJ) as a main system with the 2 MJ sub bank system for the seed field have been installed, and completed in the year of 2014.

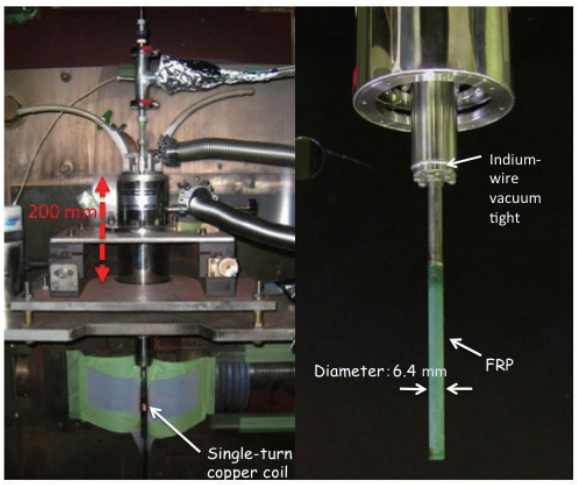

Fig. 4. Fig.4. A photo of the V-type single-turn coil equipped with 40 kV, (A:100+B:100=200 kJ) fast operating pulse power system. Measurements are carried out from room temperature down to 2 K by a specially designed cryostat.

Center of Computational Materials Science

With the advancement of hardware and software technologies, large-scale numerical calculations have been making important contributions to materials science and will have even greater impact on the field in the near future. Center of Computational Materials Science (CCMS) is a specialized research center for promoting computer-aided materials science with massively parallel computers, such as K-computer. The center also functions as the headquarters of Computational Materials Science Initiative (CMSI), which is an inter-institutional organization for computational science of a broad range of disciplines, including molecular science, quantum chemistry, biological materials, and solid state physics. ISSP made contracts with 9 universities and 2 national institutes for supporting the activities of CMSI in which nearly 100 research groups are involved. The main purpose of CMSI is to establish a new community of computational science in which researches from different backgrounds work together on grand challenge problems, thereby developing computational infrastructures (new algorithms, coding styles, standard software packages, etc) and inspire young scientists.

CCMS has a branch office in the RIKEN AICS building on the Port Island Kobe, where K-computer is located, for supporting CMSI researchers getting together at the K-computer site to exchange ideas of computational science, fine-tune various applications software for the K-computer, and develop better contact with staff members of RIKEN, the operating institute of K-computer. Another mission of the Kobe branch of CCMS is to communicate with researchers from other fields of computer science. (There are 5 major fields in the HPCI strategic program of MEXT, "biology", "materials and energy" (our field), "seismology, oceanography and meteorology", "industrial applications", and "high-energy physics and cosmology".)

The following is the selected list of meetings organized by CMSI and CCMS in SY2014:

- "CMSI Hands-On: FU Tutorial" (Apr 28, Aug 18/2014, Kobe)
- "CMSI Hands-On: Version Control System Tutorial" (May 30/2014, Kobe)
- "CMSI Hands-On: ALPS Tutorial" (June 16/2014, Kobe)
- "Workshop: Programming Techniques for K-Computer" (Jul 7-Jul 9/2014, Kobe)
- "CMSI Hands-On: AkaiKKR Tutorial" (June 30/2014, Kashiwa)
- "CMSI Division 1 Summer School" (Aug 18-Aug 22/2014, Biwako)
- "CMSI Hands-On: GPGPU Computing with OpenACC 2.0" (Aug 28/2014, Hongo)
- "Symposium: Collabration with National Experimental Facilities" (Sep. 02, Akihabara)
- "CMSI Hands-On: Rokko Tutorial" (Sep. 18/2014, Kobe)
- "Workshop: Possibilities of Post-K Computing" (Sep. 28, Tokyo)
- "CMSI Hands-On: OpenMX Tutorial" (Oct. 10/2014, Kobe)
- "CMSI Hands-On: ALPS Tutorial" (Oct. 16/2014, Kashiwa)
- "CMSI International Workshop 2014: Tensor Network Algorithms in Materials Science" (Oct. 20-22/2014, Kobe)
- "The 4th Symposium of CCMS" (Nov.12-14, Kashiwa)
- "10sor Network Workshop" (Nov. 25/2014, Kashiwa)
- "The 5th CMSI Symposium" (Dec.08-10/2014, Sendai)
- "CMSI Hands-On: xTAPP Tutorial" (Dec. 12/2014, Kashiwa)
- "CMSI Hands-On: feram Tutorial" (Dec. 17/2014, Kashiwa)
- "CMSI Hands-On: modylas Tutorial" (Jan. 1/2015, Kobe)
- "Workshop: Programming Techniques for K-Computer" (Feb. 4-6/2014, Kakegawa)
- "CMSI Hands-On: SMASH Tutorial" (Feb. 16/2014, Kobe)
- "International Workshop on New Frontier of Numerical Methods for Many-Body Correlations --- Methodologies and Algorithms for Fermion Many-Body Problems" (Feb.18-21/2015, Hongo)
- "CMSI Hands-On: OpenMX Tutorial" (Mar. 11/2015, Kashiwa)

Fig. 1. International Workshop on New Frontier of Numerical Methods for Many-Body Correlations, Feb.18-21/2015, Hongo

Laser and Synchrotron Research Center (LASOR Center)

Laser and Synchrotron Research (LASOR) Center started from October, 2012. LASOR Center aims to promote material sciences using advanced photon technologies at ISSP by combining the "Synchrotron Radiation Laboratory" and "Advanced Spectroscopy Group". These two groups have long histories since 1980's and have kept strong leaderships in each photon science fields for a long time in the world. In the past several decades, the synchrotron-based and laser-based photon sciences have made remarkable progresses independently. However, recent progresses in both fields make it feasible to merge the synchrotron-based and laser based technologies to develop a new direction of photon and materials sciences. In the LASOR Center, extreme laser technologies such as ultrashort-pulse generation, ultraprecise control of optical pulses in the frequency domain, and high power laser sources for the generation of coherent VUV and SX light are intensively under development. The cutting edge soft X-ray beamline is also developed at the synchrotron facility SPring-8.

LASOR center aims three major spectroscopic methods [ultrafast, ultra-high resolution, and operand spectroscopy] by three groups [extreme laser science group, soft-X-ray spectroscopy and materials science group, and coherent photon science group], as illustrated in Fig. 2. Under this framework, various advanced spectroscopy, such as ultra-high resolution photoemission, time-resolved, spin-resolved spectroscopy, diffraction, light scattering, imaging, microscopy and fluorescence spectroscopy are in progress by employing new coherent light sources based on laser and synchrotron technologies that cover a wide spectral range from X-ray to terahertz. In LASOR Center, a variety of materials sciences for semiconductors, strongly-correlated materials, molecular materials, surface and interfaces, and bio-materials are studied using advanced light sources and advanced spectroscopy. Another important aim of LASOR Center is the synergy of photon and materials sciences.

Fig. 1. Open ceremony of LASOR center on October 2012.

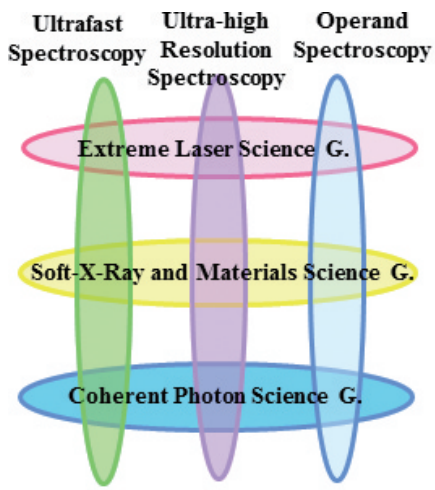

Fig. 2. Developments of advanced spectroscopy at LASOR center by three groups

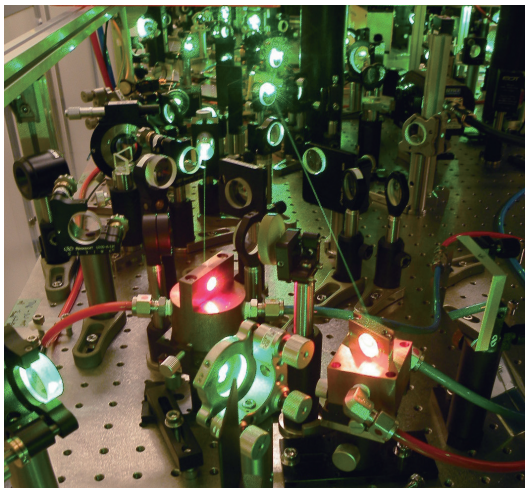

Fig. 3. Close look of a high-peak-power ultrashort-pulse laser

Most of the research activities on the extreme laser development and their applications to materials science are performed in the ISSP buildings D and E at Kashiwa Campus where large clean rooms and the vibration-isolated floor are installed. On the other hand, the experiments utilizing the advanced synchrotron source are performed at a beamline BL07LSU in SPring-8 (Hyogo).

• Extreme Laser Science Group

The advancement of ultrashort-pulse laser technologies in the past decade has transformed the laser development at ISSP into three major directions, (i) towards ultrashort in the time domain, (ii) ultra high resolution in the spectral domain, and (iii) the extension of the spectral range, with extreme controllability of the laser sources. For ultrafast

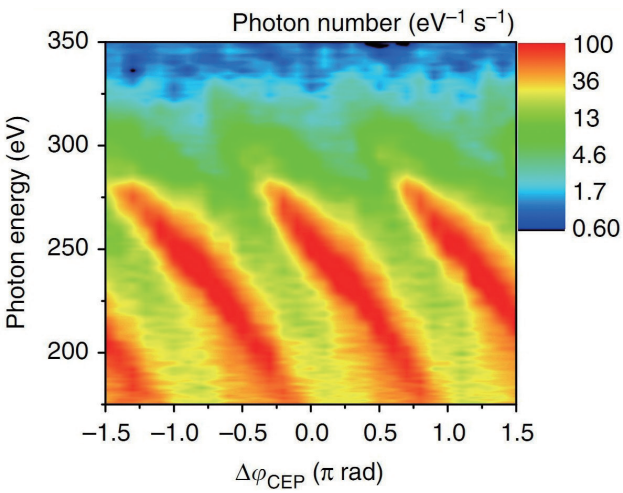

Fig. 4. Phase-dependence of high harmonic spectra in soft X rays.

Fig. 5. 10-MHz high harmonic generation in an enhancement cavity.

spectroscopy, we have developed carrier-envelope phase stable intense infrared light source that can produce sub-two cycle optical pulses for high harmonic and attosecond pulse generation. So far we observed coherent soft-X-ray radiation extending to a photon energy of ~330 eV. The simulation predicts the soft-X-ray field consists of single isolated attosecond pulses. For ultra-high resolution spectroscopy, fiber-laser-based light sources are intensively developed for producing EUV pulses for high resolution and time-resolved photoemission spectroscopy as well as extending the frequency comb to ultraviolet or infrared for various applications. The spectral range of intense optical pulses are being extended from visible to IR, MIR and THz ranges. Various types of high-repetition-rate ultrastable light sources are developed for laser-based ultrahigh resolution photoemission spectroscopy, high-average-power EUV generation in an enhancement cavity, and frequency comb spectroscopy for atomic physics, astronomical application, and frequency standards.

• Soft-X-ray and Materials Science Group

Recently, VUV and SX lasers have progressed very rapidly. They become very powerful for the materials science using the cutting-edge VUV and SX spectroscopy. Especially, angle resolved photoemission spectroscopy (ARPES) is very powerful to know the solid state properties. Laser has excellent properties, such as coherence, monochromaticity, polarization, ultra-short pulse, high intensity, and so on. By using monochromatic laser light, the resolution of ARPES becomes about 70-μeV. The materials science with sub-meV resolution-ARPES is improved drastically by using high resolution laser. For examples, superconducting gap anisotropy of the superconductors and Fermiology of the strongly correlated materials are studied very well. On the other hand, using pulsed laser light, the time-resolved photoemission in fs region becomes powerful to know the relaxation process of photo-excited states of the materials. Furthermore, by using CW laser with circular polarization in VUV region, the photoelectron microscopy (PEEM) is developed. The spatial resolution of nm resolution is very powerful for the study of nanomagnetic materials.

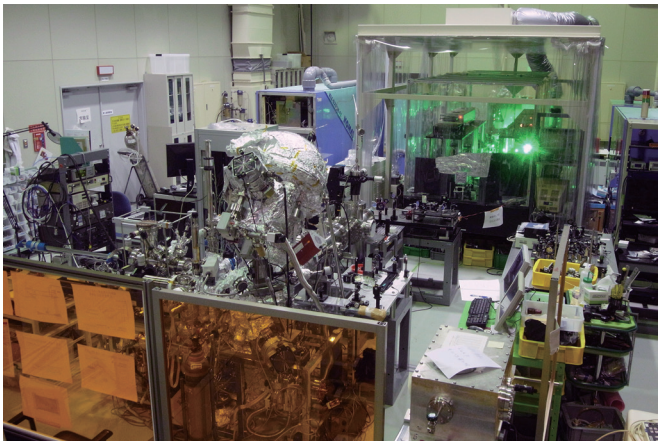

Fig. 6. Pump-probed photoemission system using 60-eV laser

• Coherent Photon Science Group

The coherent-photon science group has main interests in exploring a variety of coherent phenomena and non-equilibrium properties of excited states in condensed matters, in collaborations with research groups in charge of photoemission, operand-spectroscopy and extreme laser science. This group covers a wide range of materials, from semiconductors, ferromagnets, complexes and superconductors to biomaterials. Various ultrafast optics technologies such as femtosecond luminescence and pump-and-probe transmission/reflection spectroscopy are applied to studies on wavepacket dynamics, photo-induced phase transitions and carrier dynamics. Coherent control and observation of spin dynamics in magnetic materials and metamaterial structures by using high power terahertz radiation source is extensively studied. Advanced photonics devices are intensively studied, such as quantum nano-structure lasers with novel low-dimensional gain physics, low-power light-standard LEDs, very efficient multi-junction tandem solar cells for satellite use, and wonderful bio-/chemi-luminescent systems for wide bio-technology applications.

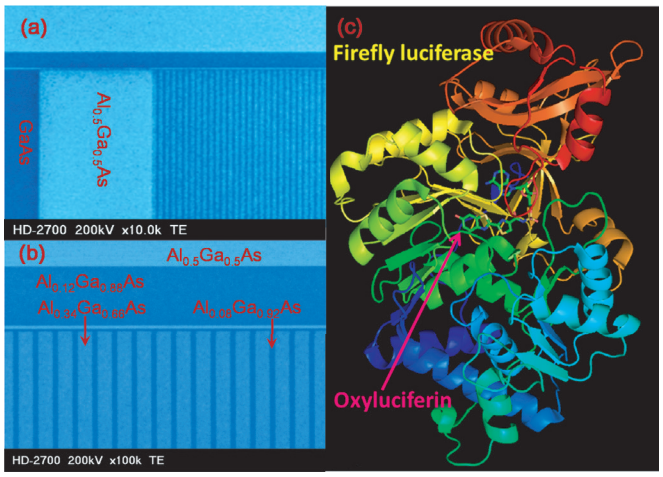

Fig. 7. Photonics devices under study: (left panel) semiconductor quantum wires and (right panel) firefly-bioluminescence system consisting of light emitter (oxyluciferin) and enzyme (luciferase)

Synchrotron Radiation Laboratory

The Synchrotron Radiation Laboratory (SRL) was established in 1975 as a research division dedicated to solid state physics using synchrotron radiation (SR). In 2006, the SRL staffs have joined the Materials Research Division of the Synchrotron Radiation Research Organization (SRRO) of the University of Tokyo and they have played an essential role in constructing a new high brilliant soft X-ray beamline, BL07LSU, in SPring-8. The light source is the polarization-controlled 25-m long soft X-ray undulator with electromagnetic phase shifters that will allow fast switching of the circularly (left, right) and linearly (vertical, horizontal) polarized photons.

The monochromator is equipped with a varied line-spacing plain grating, which covers the photon energy range from 250 eV to 2 keV. At the downstream of the beamline, a lot of experimental stations have been developed for frontier spectroscopy researches: five endstations, i.e. time-resolved soft X-ray spectroscopy (TR-SX) equipped with a two-dimensional angle-resolved time-of-flight (ARTOF) analyzer (Fig. 1), three-dimensional (3D) nano-ESCA station equipped with the Scienta R-4000 analyzer (Fig. 2), high resolution soft X-ray emission spectroscopy (XES) stations (Fig. 3) are regularly maintained by the SRL staffs and open for public use, and at free-port station many novel spectroscopic tools have been developed and installed such as soft X-ray resonant magneto-optical Kerr effect (MOKE) (Fig. 4) and soft X-ray diffraction (Fig. 5), ambient pressure photoemission, two dimensional photoelectron diffraction and so on. The beamline construction was completed in 2009 and SRL established the Harima branch laboratory in SPring-8. At SPring-8 BL07LSU, each end-station has achieved high performance: the TR-SX station have established the laser-pump and SR-probe method with the time-resolution of 50 ps which corresponds to the SR pulse-width; the 3D nano-ESCA station reaches the spatial resolution of 70 nm; the XES station provides spectra with the energy resolution around 70 meV at 400 eV and will enable real ambient pressure experiments in the near future. Soft X-ray resonant MOKE station has been developed to conduct novel magneto-optical experiment using the polarization-controlled 25-m long soft X-ray undulator. The soft X-ray diffraction station was connected to the beamline for the first time in February, 2015, and is preparing for time-resolved diffraction measurements. Each end-station has now been opened fully to outside users. In 2014, 150 researchers made their experiments during the SPring-8 operation time of 3400 hours.

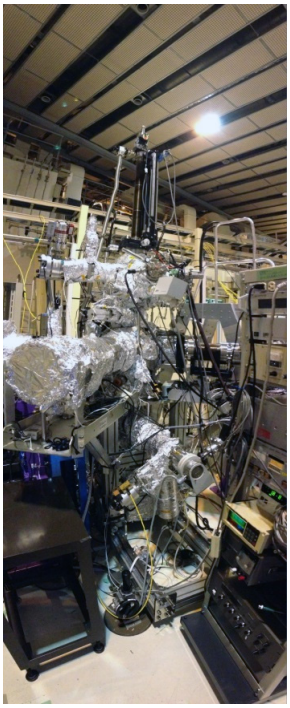

Fig. 1. TR-SX station

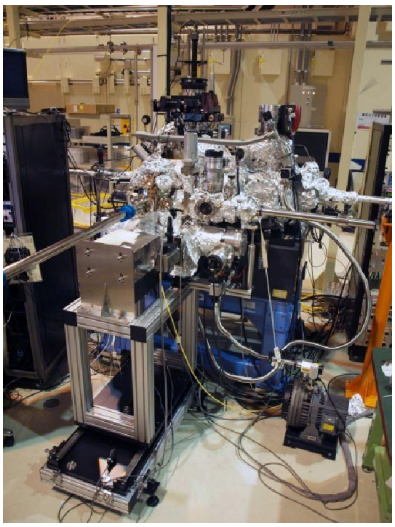

Fig. 2. 3D-nano ESCA station

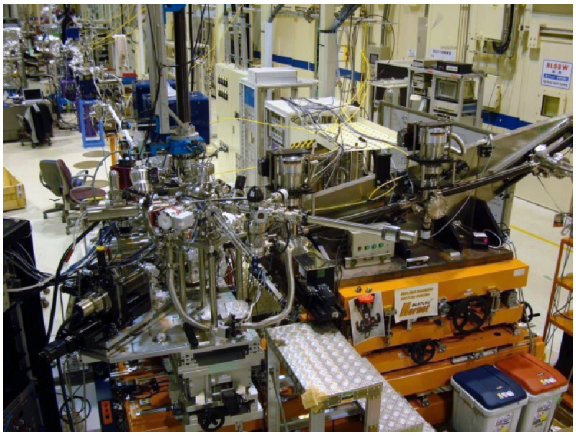

Fig. 3. Soft X-ray emission station

Fig. 4. Soft X-ray MOKE station

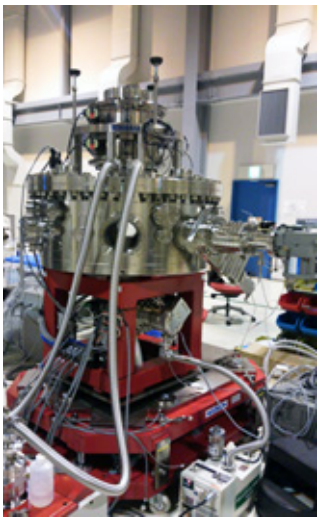

Fig. 5. Soft X-ray diffraction station

Quantum Phase near the Saturation Field in the S=1/2 Frustrated Spin Ladder

H. Yamaguchi and T. Sakakibara

Frustration in spin systems suppresses conventional magnetic orders and induces a variety of exotic quantum phenomena. Much attention has recently been paid to frustrated ferromagnets, in which ferromagnetic (FM) and antiferromagnetic (AFM) interactions strongly compete. In these systems, magnons are expected to form multiple bound states at high magnetic fields near the saturation point, owing to attractive FM interactions. Theoretical works have suggested that correlations between the bound magnons form a spin-multipolar (SM) phase and that a subsequent condensation brings about a hidden order of spin multipoles in various spin systems. Among them, the spin-nematic (quadrupolar) phase has been extensively studied as a possible candidate of the Bose-Einstein condensation of two-magnon bound states, but there is currently no clear experimental evidence of its realization. Regarding the macroscopic behavior, the magnetization curve is predicted to show an anomalous change at the phase transition to the spin-nematic order near the saturation field [1].

Here, we report on a low-temperature study of the S=1/2 organic spin ladder 3-I-V [2], which we recently succeeded in synthesizing and reported as a strong-leg spin ladder with FM leg interactions [3]. *Ab initio* molecular orbital (MO) calculations revealed that the low-temperature spin model in 3-I-V can be regarded as a weakly coupled frustrated spin ladder. Considering the magnetic and thermodynamic properties, we strongly suggest that the observed low-field phase and the phase near the saturation field are, respectively, a longitudinal spin-density-wave (SDW) order and a subsequent SM order like a spin-nematic phase.

The MO calculations indicate four kinds of additional interactions excluding those forming the spin ladder. Considering those additional interactions, we found two types of triangular units inducing frustration through the combination of the signs of the interactions. One combination consists of intraladder interactions J_{leg}, J_{rung}, and J_{diag}, and the other consists of interladder interactions J_1, J_2, and J_3, as shown in Figs. 1(a)–1(c).

The temperature dependence of the magnetization

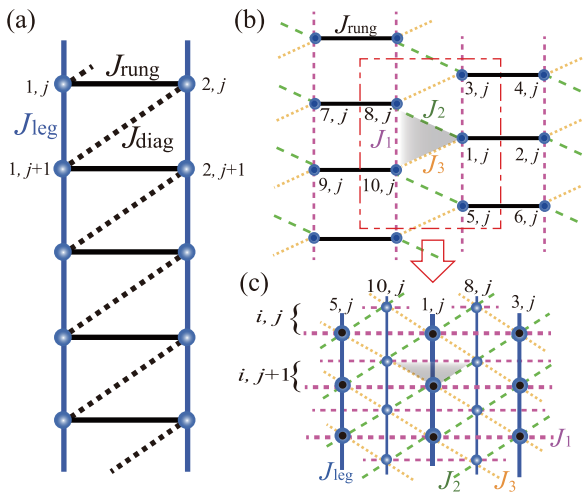

Fig. 1. (a) Frustrated spin ladder formed by J_{leg}, J_{rung} and the additional J_{diag} for 3-I-V. The 3D lattices connected by the interladder interactions J_1, J_2, and J_3 viewed along (b) the leg and (c) the rung directions for 3-I-V. The shadowed plane in each figure shows one of the interladder triangular units, causing frustration.

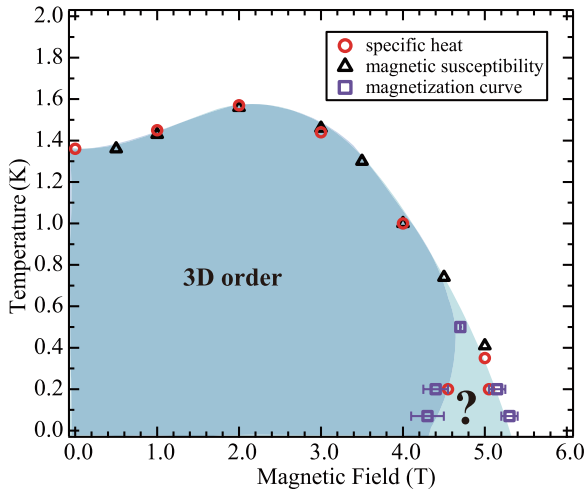

Fig. 2. Magnetic field vs temperature phase diagram showing the 3D order phase and nontrivial phase near the saturation field. The circles, triangles, and squares indicate the phase boundaries determined from the specific heat, the magnetic susceptibility, and the magnetization curve, respectively.

indicates singular cusp-like extremes [2], originating from the Bose-Einstein condensation of magnons. The specific heats consistently exhibite sharp peaks at the temperatures corresponding to these features [2]. On the other hand, we found a broad peak indicating two phase boundaries in the magnetic field dependence of the specific heat at 0.2 K. We plotted these temperatures in the magnetic field-temperature phase diagram in Fig. 2. The obtained phase diagram suggests a low-field three-dimensional (3D) order and a nontrivial phase near the saturation field. Furthermore, we found nonmonotonic behavior of the field derivative of the magnetization curve (dM/dB) near the saturation field [2], which suggests the existence of an intermediate phase with large quantum fluctuations just below the saturation field, as shown in Fig. 2.

We classified the low-field 3D ordered phase on the basis of the presence or absence of a successive phase transition. There is no successive phase transition in the temperature dependence of the specific heat for 3-I-V, while the corresponding curves for isomorphous 3-Cl-4-F-V and 3-Br-4-F-V indicate successive phase transitions accompanied by distinct double peaks. The absence of a successive phase transition in 3-I-V strongly suggests an SDW order with a single-component order parameter along the field direction. The presence of the SDW phase definitely indicates the formation of multi-magnon bound states [1]. Hence, the SM order is one possible explanation of the nontrivial phase near the saturation field, where the magnetization curve indicates large quantum fluctuations. For 3-I-V, the enhanced frustration effect originating from the FM diagonal interaction is considered to stabilize multi-magnon bound states.

References

[1] T. Hikihara, L. Kecke, T. Momoi, and A. Furusaki, Phys. Rev. B **78**, 144404 (2008)
[2] H. Yamaguchi, H. Miyagai, Y. Kono, S. Kittaka, T. Sakakibara, K. Iwase, T. Ono, T. Shimokawa, and Y. Hosokoshi, Phys. Rev. B **91**, 125104 (2015)
[3] H. Yamaguchi, H. Miyagai, T. Shimokawa, K. Iwase, T. Ono, Y. Kono, N. Kase, K. Araki, S. Kittaka, T. Sakakibara, T. Kawakami, K. Okunishi, and Y. Hosokoshi, J. Phys. Soc. Jpn. **83**, 033707 (2014).

Authors
H. Yamaguchi[a], H. Miyagai[a], Y. Kono, S. Kittaka, T. Sakakibara, K. Iwase[a], T. Ono[a], T. Shimokawa[b], and Y. Hosokoshi[a]
[a]Osaka Prefecture University
[b]Osaka University

Magnetic Ordering in the Ising Frustrated Spin-Chain Magnet NaCo(acac)$_3$benzene

Y. Karaki, S. Nakatsuji, and Y. Uwatoko

Geometrical frustration in antiferromagnets has attracted much attention in recent years. The geometrical frustration destroys the conventional Néel state and tends to produce an exotic magnetic phase. Ising spin system with antiferromagnetic nearest-neighbor interactions on a triangular lattice is a simple frustrated system. A partially disordered antiferromagnetic (PDA) phase is a typical example of such exotic phases. [1]

A series of metal chelate compounds having the formula $M^{I}M^{II}$(acac)$_3$benzene, where acac represents acetylacetonate, M^{I} is Na^{+} or K^{+} and M^{II} is divalent metal ion surrounded by the octahedron of oxygen atoms, have a trigonal crystal structure belonging to the space group *P-31c* with a = 10.24 Å and c = 11.95 Å [2]. Since the divalent metal ions form a hexagonal lattice, these compounds are possible candidates for studying the frustration on the triangular lattice.

Here we report on the results of the susceptibility(χ), magnetization and specific heat measurements using single crystals of NaCo(acac)$_3$benzene [2]. ESR and χ measurements (T>2 K) show that Co^{2+} of NaCo(acac)$_3$ benzene has the anisotropic g-factor g_c= 8.12 and g_{perp}= 1.41 for fictitious spin S=1/2. Figure 1(a) shows the temperature dependence of DC χ parallel to the c-axis at H= 5.0 Oe. The inset shows the inverse of AC χ(T) of a needle-shaped sample. Figure 1(b) shows the specific heat at zero field and DC χ at low temperatures. A long range ordering accompanied with a sudden increase of χ appears around 62 mK. Figure 2(a) shows the magnetization curve. Below 60 mK an anomaly of the *M-H* curve appears. A step-wise change of the magnetization becomes clear at 20 mK. At H~ 300 Oe the magnetic moment aligns fully with applied field. The plateau at 1/3 of full moment suggests a ferrimagnetic alignment of the ferromagnetic chains. The ferromagnetic intra-chain interaction J_C/k_B= -0.2 K and the antiferromagnetic inter-chain interaction J/k_B = 0.05 K are deduced from the Weiss temperature 20 mK and the critical field 300 Oe. These results confirm the 1-D nature of NaCo(acac)$_3$benzene. When a 1-D short-range order is well developed at low temperatures, each chain behaves like a magnetic moment and thus a magnetic ordering with two-dimensional character is expected. The mean field theory of a triangular Ising lattice predicts a step-like increase of χ at Tc from a paramagnetic phase to a PDA phase and no anomaly at Tc from the paramagnetic phase to the ferrimagnetic phase [2]. Thus the observed χ anomaly

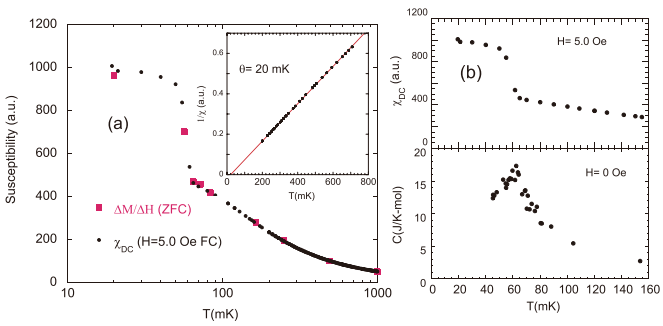

Fig. 1. (a) Temperature dependence of DC χ (FC) and differential χ obtained from *M-H* curves. *M-H* curves are measured after zero field cooling. The inset shows the inverse of AC χ (220 Hz) of a needle-shaped sample at T> 200 mK. (b) Temperature dependence of the specific heat at zero field and DC χ at 5.0 Oe below 160 mK.

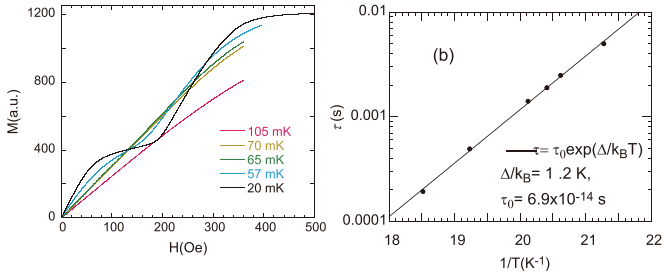

Fig. 2. (a) Magnetization curve for *H// c* at 20mK, 57mK, 65 mK and 105 mK. (b) Temperature dependence of the spin relaxation time.

at 62 mK suggests the existence of the PDA phase around zero field. At the PDA phase, two thirds of chains order into an antiferromagnetic alignment and the resultant chain is incoherent with other chains. Since the molecular fields of the incoherent chain are canceled, the magnetic response of single chain is expected in the PDA phase. Figure 2(b) shows temperature dependence of the spin relaxation time obtained from the frequency dependence of AC χ. The thermal activation process with the gap energy Δ/k_B= 1.2 K is observed. However, obtained gap energy is about 6 times larger than estimated value using $\Delta=4S^2Jc$ given by Glauber for a ferromagnetic Ising chain [3]. The simple chain model in the PDA phase cannot explain the observed spin relaxation well enough. Further microscopic measurements are necessary to clarify the ordered phase and the spin relaxation mechanism.

References

[1] M. Mekata, J. Phys. Soc. Jpn. **42**, 76 (1977).
[2] Y. Karaki, K. Kuga, K. Kimura, S. Nakatsuji , K. Matsubayashi, and Y. Uwatoko, submitted to J. Phys. Soc. Jpn.
[3] R. J. Glauber, J. Math. Phys. **4**, 294 (1963)

Authors
Y. Karaki[a], K. Kuga[b], K. Kimura[b], S. Nakatsuji , K. Matsubayashi, and Y. Uwatoko
[a]University of the Ryukyus
[b]Osaka University

Trivial Yet Distinct

Y. Fuji, F. Pollmann, and M. Oshikawa

Classification of quantum phases is a central subject in statistical mechanics and condensed matter physics. Traditionally, it was based on the notion of spontaneous symmetry breaking, as initiated by Landau. However, recently, a rich variety of quantum phases without any spontaneous symmetry breaking has been recognized. This also requires us to develop new concepts and formulations. One of the novel classes of quantum phases is called Symmetry-Protected Topological (SPT) phases. As the name suggests, they are distinct from the trivial phase only in the presence of an appropriate symmetry. In this regard, SPT phases are similar to the conventional ordered phases with a spontaneously broken symmetry. However, SPT phases do not break the symmetry, and hence are called topological. A well-known example of SPT phases is the topological insulator, which possesses a helical edge state and is distinct from a trivial band insulator. The helical edge state and the distinction from a trivial band insulator however go away once the time-reversal symmetry is broken explicitly. Another example of SPT phases is Haldane phase in S =1

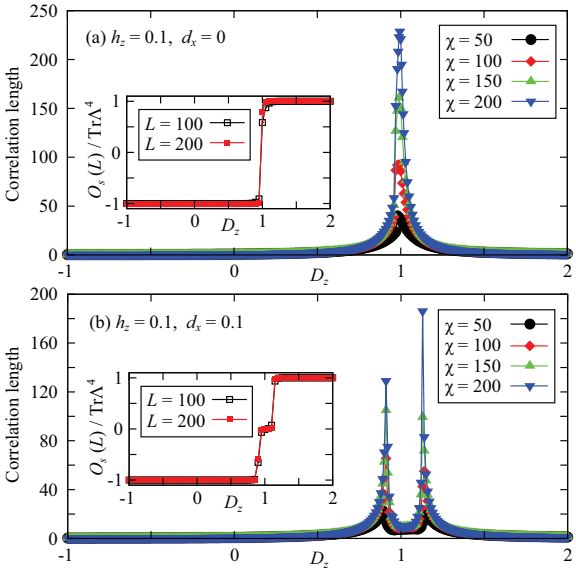

Fig. 1. Divergence of the correlation length demonstrating the existence of the quantum phase transition separating the two trivial phases. Insets show the non-local string order parameter which distinguishes the two phases.

antiferromagnetic chains. There is no long-range order which can be detected by a local order parameter in the Haldane phase. Nevertheless, the Haldane phase is separated by a quantum phase transition from a trivial phase such as "large-D phase" which includes the product of $S^z = 0$ states. The Haldane phase also has a characteristics of edge state (free spin), which is protected by the time-reversal symmetry. It turns out however that the edge states are not the most general characterization of SPT phases. Under the lattice inversion symmetry, there are topological insulator and Haldane phase without any physical edge state. These are most generally characterized by degeneracy in the entanglement spectrum. This implies that they are distinct, in the presence of the symmetry, from a trivial product state without any entanglement.

In a recent joint research [1] we demonstrated that the notion of symmetry protection of quantum phases can be generalized in a somewhat surprising manner. In the standard SPT phases, as we discussed above, there is a nontrivial entanglement which makes the state distinct from a trivial product state. We showed that, in the presence of a certain class of inversion symmetry, there are two trivial phases that are still distinct, in a simple model of $S = 1$ chain. By "trivial phase" we mean the ground state can be adiabatically connected to a product state where there is no entanglement at all. Nevertheless the two trivial phases are distinct in the sense that they are always separated by a quantum phase transition as long as the symmetry is kept. We dubbed them "Symmetry-Protected Trivial (SPt)" phases. We have also formulated a non-local string order parameter which can distinguish these phases and detect the quantum phase transition between them. So, there is something nontrivial even in trivial phases! This would also add a new aspect to the fundamental question "What is phase?".

This work was performed in collaboration between ISSP and Max-Planck Institute for Physics of Complex Systems, which is recently strengthened by the JSPS Strategic International Networks Program No. R2604 "TopoNet."

Reference

[1] Y. Fuji, F. Pollmann, and M. Oshikawa, Phys. Rev. Lett. **114**, 177204 (2015).

Authors
Y. Fuji, F. Pollmann[a], and M. Oshikawa
[a]Max-Planck Institute for Physics of Complex Systems

First-Principles Simulation Program for Excited States

Y. Noguchi, M. Hiyama, and N. Koga

These days the first-principles simulations are commonly used as a basic tool for the material research. Most of the simulation programs have been designed for the ground state only, while excited states are the target of increasing number of spectroscopic measurements demanding thereby the program to cover the excited states. Recently, Noguchi, Hiyama and Koga have shown such extension is possible with the first-principles two-particle Green's function program.

The program has been developed by Noguchi on the basis of the Bethe-Salpeter equation (BSE) combined with the GW approximation (GWA) to the self-energy operator, and the problem originated from the extremely large computational requirement has been overcome by the development of the parallel programming. Thus the remaining problem is to test the accuracy of the program by comparing with reference data and convince it to the users of the first-principles program. In this context, the authors focused on recently synthesized nanomaterials, or the fullerene containing alkali metal inside and a carbon material called warped nanographene, which are extraordinarily suitable for the benchmark. By comparing the measured and calculated spectra, reliability of the GW-BSE calculation was shown [1, 2].

More stringent test was done for the core-excitation spectrum of a molecule [3], which so far has been calculated using the density functional theory together with empirical

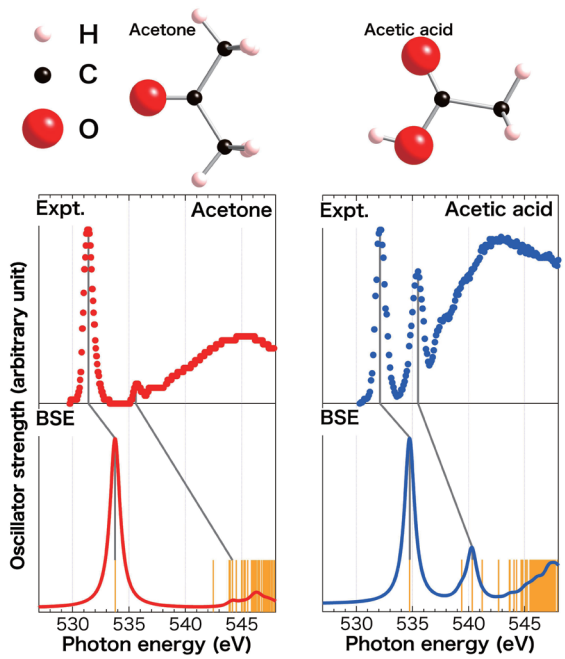

Fig. 1. Comparison of the calculated (bottom) and the measured (top) XAS spectra for benchmark molecules, acetone (left) and acetic acid (right). Using the first-principles Green's function scheme, the excitation energy from the oxygen 1s state to the valence states was calculated for the first time without empirical parameters. The calculated excitation energies are in agreement with experiments within the error of 1 %, or 2-5 eV. This demonstrates that theory is able to provide reliable data that will help analyzing the measurements.

adjustments. By the comparative study, the authors demonstrated that x-ray absorption spectra (XAS) can be reliably assigned fully from first-principles using the program (see Fig. 1).

So far, the program was also applied to other materials such as the firefly liciferin, or the light-emitting compound found in firefly species, to understand the light-emitting mechanism [3]. The GW-BSE program is planned to open to ISSP supercomputer users and is expected to advance our understanding of the excited states of materials.

References

[1] Y. Noguchi, O. Sugino, H. Okada, and Y. Matsuo, J. Phys. Chem. C **117**, 15362 (2013).
[2] Y. Noguchi and O. Sugino, J. Chem. Phys. **142**, 064313 (2015).
[3] Y. Noguchi, M. Hiyama, H. Akiyama, N. Koga, J. Chem. Phys. **141**, 044309 (2014).
[4] Y. Noguchi, M. Hiyama, H. Akiyama, Y. Harada, and N. Koga, J. Chem. Theor. Compt. **11**, 1668 (2015).

Authors
Y. Noguchi, M. Hiyama, and N. Koga[a]
[a]Nagoya Univerisy

Dephasing in Single-Electron Generation Due to Environmental Noise Probed by Hong-Ou-Mandel Interferometry

E. Iyoda, T. Kato, K. Koshino, and T. Martin

Quantum mesoscopic physics, or nanophysics, aims at studying the manifestations of quantum mechanics, such as interference effects and coherence, with electron transport in condensed matter materials. Such manifestations have been studied in the context of quantum optics since the middle of the past century, where fundamental tests of quantum mechanics were explored, for instance, in Hanbury Brown and Twiss [1] (HBT) and Hong-Ou-Mandel [2] (HOM) experiments for photons. The fermionic counterpart of the HOM experiment has been realized quite recently in a setup of a two-electron collider using a quantum point contact (QPC) and two single-electron generators composed of integer quantum Hall edge states and quantum dots [3] (see a schematic figure in Fig. 1(a)). In the fermionic HOM experiment, if two electrons arrive at the QPC simultaneously, the two electrons always scatter into two different output channels because of their fermionic statistics.

In condensed matter settings, the two electrons are always accompanied by the Fermi sea, and as charged particles they interact strongly between themselves and with their environment. The coherence of injected electrons is directly measured by perfectness of anti-correlated scattering in the fermionic HOM experiment. The imperfect anti-correlated scattering reported in [3] includes information about the distinguishability of propagating electrons in the chiral edge channels before arriving at the QPC. At present, the dephasing of propagating electrons has been discussed mostly by considering Coulomb interactions between electrons. The origin of electron decoherence has, however, not yet been determined experimentally. We have examined the effect of electron decoherence by focusing on the role of the energy-level fluctuations of the quantum dot due to this environment [4].

We have employed a simple analytic framework for

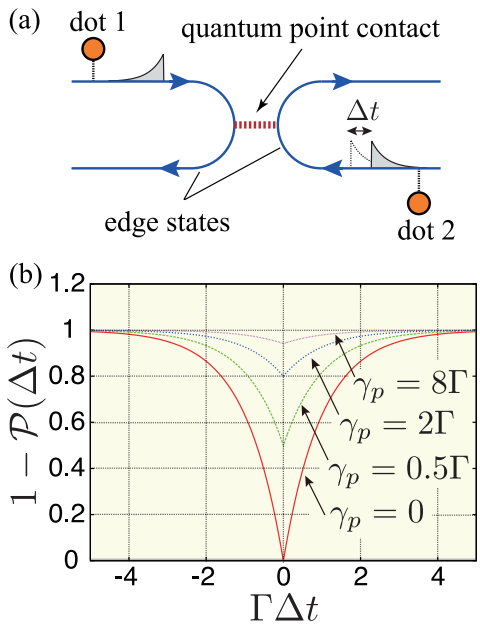

Fig. 1 (a) A schematic figure of the Hong-Ou-Mandel-type two-electron collision experiment. Two electrons injected from two quantum dots propagate along edge states of integer quantum Hall states, and collides at a central quantum point contact (QPC). (b) The probability 1-$P(\Delta t)$, that two electrons scatter into the same edge states, is plotted as a function of a wavepacket delay time Δt. Two electrons always scatter into difference edge states (1-$P(\Delta t)$ = 0) when Δt = 0 and γ_p = 0. On the other hand, as the dephasing rate γ_p increases, the probability 1-$P(\Delta t)$ at Δt = 0 increases, and approaches the classical value.

evaluating the current noises reflecting electron indistinguishability based on the so-called input-output relation, which is a standard theoretical tool in quantum optics. In this approach, the dephasing rate γ_p due to energy-level fluctuations is easily taken into account in the model Hamiltonian. In order to clarify coherence of generated electrons, we have calculated $P(\Delta t) = \mathrm{Tr}(\rho(t)\rho(t+\Delta t))$, where $\rho(t)$ is a density matrix of injected electrons and Δt is the time delay between the two emitted electron wave packets (see Fig. 1(a)), and have obtained an analytic solution, $P(\Delta t) = 1/(1+\gamma_p/\Gamma)\exp(-\Gamma|\Delta t|)$ where Γ is the decay time of electron generators. Figure 1(b) shows a plot of 1-$P(\Delta t)$, which is proportional to the excess current noise measured at one of the output channels, assuming a balanced transmissivity of QPC. If there is no dephasing ($\gamma_p = 0$), the excess noise is completely suppressed for the simultaneous collision ($\Delta t = 0$) between injected electrons. This is the manifestation of the Fermi statistics of the injected electrons. As the pure dephasing rate γ_p increases, the dip of the current noise is reduced and vanishes for $\gamma_p >> \Gamma$. We note that $\mathcal{P} = P(0)$ corresponds to the purity $\mathcal{P} = \mathrm{Tr}(\rho^2)$ of injected electrons, which has the simple form in our case: $\mathcal{P} = \Gamma/(\Gamma+\gamma_p)$. The purity approaches 1 for $\gamma_p << \Gamma$, leading to a perfect suppression of the excess noise.

In our work [4], we have also shown that the time filtering technique helps to enhance the purity, and that a generalization of the present results to an asymmetric setup is possible, with possible implication for measuring the energy detuning of the two injectors in actual experiments. Our calculation provides a useful and comprehensive picture of dephasing effects on the quality of generated single electrons as well as compact formulas for the purity and the current noises in the HOM experiment.

References
[1] R. H. Brown and R. Q. Twiss, Proc. R. Soc. A **242**, 300 (1957).
[2] C. K. Hong, Z. Y. Ou, and L. Mandel, Phys. Rev. Lett. **59**, 2044 (1987).
[3] E. Bocquillon *et al*., Science **339**, 1054 (2013).
[4] E. Iyoda, T. Kato, K. Koshino, and T. Martin, Phys. Rev. B **89**, 205318 (2014).

Authors
E. Iyoda[a], T. Kato, K. Koshino[b], and T. Martin[c]
[a]University of Tokyo
[b]Tokyo Medical and Dental University
[c]Aix Marseille Université, CNRS, CPT

Electrical Conduction in Epitaxial Graphene on Stepped Substrate of Vicinal SiC Surface

A. Endo, F. Komori, and S. Tanaka

Two-dimensional electron system (2DES) in graphene, *i.e.* a single or a few layers of graphitic sheet, has attracted much interest on account of its properties quite distinct from conventional 2DES. Graphene samples are typically produced either by "peel-and-stamp" technique or by epitaxial growth on appropriate substrates. In this study[1] monolayer graphene was grown on a vicinal surface of 6H-SiC(0001) which has a quasi-regular step-and-terrace structure as shown in Fig.1. This is analogous to 2DES in a GaAs/AlAs quantum well fabricated on the (775)B surface of GaAs [2].

Electrical conduction under a magnetic field normal to the plane showed a high degree of anisotropy. The quantum Hall effect (QHE) with zero resistance manifests itself for the current along the steps as shown in Fig.1, whereas the QHE is obscured by pronounced positive magnetoresistance with quadratic magnetic-field dependence for the current across the steps. The latter, as well as the small slope of the Hall resistance, implies the presence of parallel conduction due

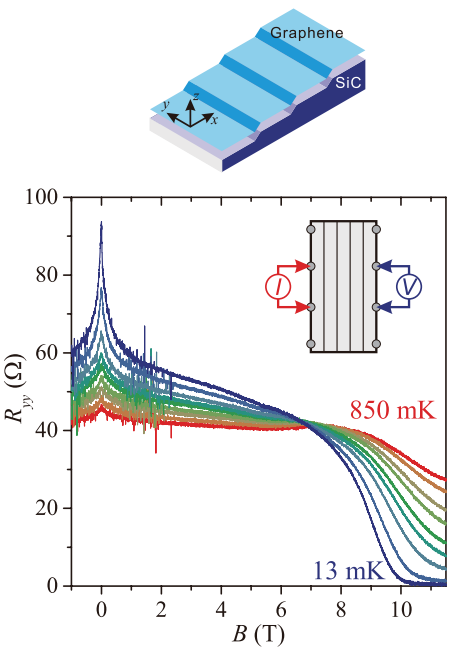

Fig. 1. Epitaxial monolayer graphene grown on a vicinal surface of 6H-SiC(0001) which has a regular step-and-terrace structure. Resistance along the step exhibits negative magnetoresistance characteristic of weak localization at low field and well-developed quantum Hall effect (ν=2) at high field.

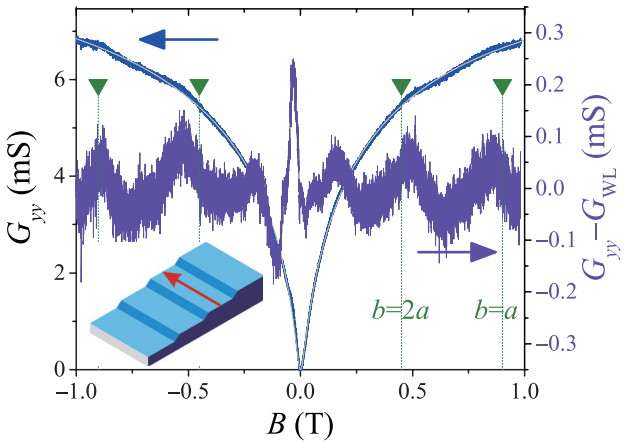

Fig. 2. Low field magnetoconductance with current along the steps exhibits oscillatory behavior superposed on the positive magnetoconduction attributable to the weak localization effect. The vertical dashed lines marked by arrows represent the expected positions of open orbit geometrical resonance.

to remnant carriers in the SiC substrate, albeit with seeming inconsistency with the zero resistance observed for the former current direction. The anisotropic behavior is interpreted by assuming that the parallel conduction is sizable along the steps but is virtually prohibited across the steps

Conspicuous negative magnetoresistance in low field regime can be analysed by the weak localization formula. The phase relaxation time τ_ϕ thus obtained is on the order of a few psec, which considerably exceeds the transport relaxation time $\tau \sim 10^{-2}$ psec. The conductance along the steps is found to exhibit small-amplitude oscillations as shown in Fig. 2, after subtracting out the large positive magnetoconductance of the weak localization origin. This oscillatory behavior is attributed to open-orbit geometrical resonance effect previously elucidated in a GaAs/AlGaAs 2DES subjected to a unidirectional potential modulation [3].

References
[1] A. Endo, F. Komori, K. Morita, T. Kajiwara, and S. Tanaka, J. Low Temp. Phys. **179**, 237 (2015).
[2] Y. Iye, A. Endo, S. Katsumoto, Y. Ohno, S. Shimomura, and S. Hiyamizu, Physica E **12**, 200 (2002).
[3] A. Endo and Y. Iye, Phys. Rev. B **71** 081303(R) (2005).

Authors
A. Endo, F. Komori, K. Morita[a], T. Kajiwara[a], and S. Tanaka[a]
[a]Kyushu University

Methylation of Epitaxial Graphene on SiC(0001) through Two-Step Chlorination Alkylation Reactions

Md. Z. Hossain and J. Yoshinobu

Chemical modification of graphene with varieties of functionalities is vital for anticipated applications such as sensing, detecting, and composite material systems. However, it is not easy to chemically graft the atoms or molecules onto the graphene surface because of the bonding nature of sp^2 C atoms in graphene. Therefore, it is highly desirable to establish a common chemical approach through which the pristine graphene can be modified with varieties of chemical species. In this joint research, we demonstrate the covalent binding of a methyl group on the basal plane

of epitaxial graphene on SiC(0001) through the two-step chlorination and alkylation processes using a Grignard reagent (CH_3MgBr). The modified surfaces are characterized by scanning tunneling microscopy and spectroscopy, X-ray photoelectron spectroscopy (XPS) and Raman spectroscopy.

Figure 1a is an atomic resolution STM image of monolayer epitaxial graphene (EG) on SiC(0001). The hexagonal network of the graphene lattice is clearly seen over the $6\sqrt{3} \times 6\sqrt{3}$ substrate structure. The chlorination of EG was done by exposing the surface to Cl_2 under UV light in N_2 atmosphere. Following the chlorination of graphene, the atomically resolved high-resolution image clearly reveals that the EG contains a large number of small protrusions (Figure 1b). Since the graphene mesh and underlying substrate periodicity are still visible, we ascribe these additional small protrusions to the chemisorbed Cl atoms on EG. Note that the surface morphology shown in Figure 1b is only seen in the monolayer EG region. Figure 1c shows a typical STM image; the hexagonal mesh of the graphene lattice is clearly visible in the lower half of the image, and the upper half contains randomly distributed protrusions ascribed to the chemisorbed Cl. The approximate surface coverage of chemisorbed Cl is estimated to be ~ 8 atom%. Based on the atomic resolution STM and Raman measurements on the different areas of the surface, we conclude that chemisorption of Cl is selective to the monolayer EG on SiC.

The covalent binding of Cl onto the EG is confirmed by the XPS spectra as shown in Figure 1d. The Cl 2p and Cl 2s peaks are observed in the XPS spectrum for chlorinated graphene (Fig. 1d(ii)). The high-resolution Cl 2p spectrum exhibits two components at 200.2 and 201.8 eV (Fig. 1e). When the chlorinated EG is treated with CH_3MgBr in THF, the Cl peaks disappear [Figure 1d(iii), e(iii)] and the height of the C 1s peak slightly increased [Figure 1d(iii)] compared to that of the chlorinated surface. The absence of any Mg or Br peaks in the wide range spectra suggests the clean EG modified with only the C containing group. The STM investigations of CH_3MgBr treated surfaces indicate that only the monolayer graphene regions contain small protrusions randomly distributed over the surface. The density of small protrusions is similar to that of the respective chlorinated

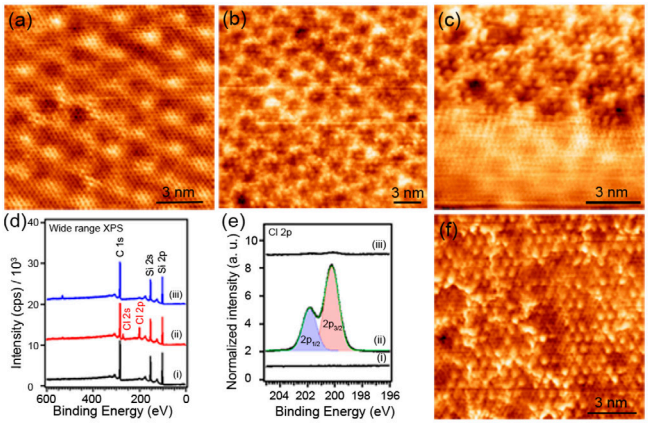

Fig. 1. Typical ambient STM images of (a) the clean epitaxial graphene on the Si-face of the SiC substrate and (b) the same surface after chlorination. (c) Chlorinated and non-chlorinated areas within the same scanning area. (d) Wide range XPS spectra of (i) clean, (ii) chlorinated, and (iii) chlorinated surface treated with CH_3MgBr in THF (tetrahydrofuran) for 2 h at 65 °C. hν = 1486 eV. (e) High-resolution Cl 2p XPS spectra of (i) clean, (ii) chlorinated, and (iii) chlorinated surface treated with CH_3MgBr in THF. hν = 410 eV. (f) Atomic resolution STM image of the chlorinated surface treated with CH_3MgBr. V_{tip} = 0.5 V; I_{tunnel} = 0.5 nA. [© 2014 American Chemical Society]

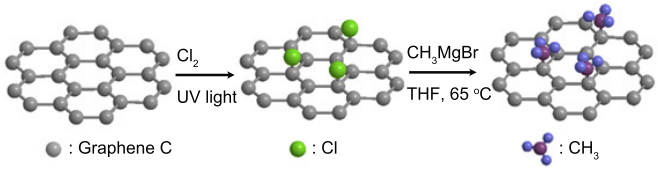

Fig. 2. Schematic of the reaction steps for photochlorination and methylation of epitaxial graphene on SiC using CH_3MgBr in THF. [© 2014 American Chemical Society]

surface. A typical atomically resolved STM image of the CH_3MgBr treated surface is shown in Figure 1f. In addition to the small protrusions, we can clearly see the underlying hexagonal mesh of graphene in Fig. 1f. These small protrusions are found to be stable even after annealing the surface at 300 °C in UHV. Since the surface is free from any other contamination as revealed by XPS, we ascribed these small protrusions to the covalently bonded CH_3 groups.

The scheme for the present two-step reactions is summarized in Fig. 2, and the detailed analysis of experimental data and discussion is found in reference 1.

Reference

[1] Md. Z. Hossain, M. B. A. Razak, H. Noritake, Y. Shiozawa, S. Yoshimoto, K. Mukai, T. Koitaya, J. Yoshinobu, and S. Hosaka, J. Phys. Chem. C **118**, 22096 (2014).

Authors

Md. Z. Hossain, M. B. A. Razak, H. Noritake, Y. Shiozawa, S. Yoshimoto, K. Mukai, T. Koitaya, J. Yoshinobu, and S. Hosaka

Imaging of Josephson Vortices on Surface Superconductor by Scanning Tunneling Microscopy

T. Uchihashi, X. Hu, and Y. Hasegawa

The recent discovery of superconductivity in silicon surface reconstructions with metal adsorbates was an unexpected surprise, and as an ultimately thin 2D superconductor extensive studies on their properties are in progress [1-4]. One ubiquitous feature of these systems is the presence of atomic steps, which may strongly affect electron transport there. Recent direct electron transport measurements indicated that atomic steps work as Josephson junctions [2]. Nevertheless, direct evidence of Josephson coupling has not been obtained yet, and possible local variation of its strength has remained an open issue.

Here, we report on compelling evidence of the Josephson coupling at atomic steps on the surface superconductor Si(111)-($\sqrt{7} \times \sqrt{3}$)-In [5]. Zero-bias conductance (ZBC) images, which correspond to a mapping of the density of states (DOS) at the Fermi level, taken with a low-temperature scanning tunneling microscopy (STM) reveal that vortices are present at atomic steps after magnetic fields are applied. Elongated shapes and significant recovery of superconductivity within their cores, which are characteristic to Josephson vortices (JV), are clearly observed in the images.

Figure 1(a) shows an STM image with an area of 500 nm×1500 nm. The surface consists of flat terraces separated by single atomic height steps. ZBC images taken on the same area under magnetic fields of 0.08, 0.04, 0 T are displayed in Figs. 1(b)-1(d). The imagings were performed

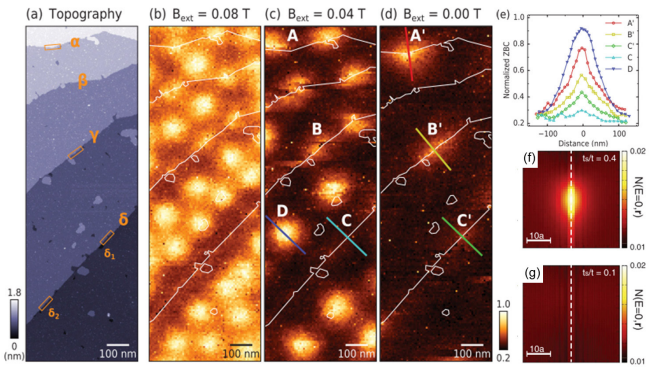

Fig. 1. (a) Large-scale STM image of Si(111)-($\sqrt{7} \times \sqrt{3}$)-In surface, where the terraces are separated by atomic steps marked as α, β, γ, and δ from top to bottom. (b)-(d) ZBC images taken under magnetic fields of (b) 0.08 T, (c) 0.04 T, (d) 0 T. The positions of the atomic steps are depicted by thin solid lines. (e) Spatial profiles of ZBC plotted along the thick solid lines shown in (c) and (d). (f) and (g) numerically obtained spatial profile of the zero energy DOS for the hopping strength t_s/t = 0.4 and 0.1, respectively. The dashed lines indicate the place where the Josephson coupling was modeled.

below 0.5 K, which is sufficiently lower than $T_c \approx 3$ K of the superconducting surface. At 0.08 T, round vortices formed a closely packed triangular lattice within each terrace. Reduction of the magnetic field to 0.04 T decreased the number of vortices as expected. When the magnetic field was set to zero, vortices disappeared from the terraces, but slightly bright regions remained along the steps [Fig. 1(d)]. Note that similar features were also present along the steps at finite fields [Figs. 1(b) and 1(c)]. They are not simply regions where superconductivity is suppressed due to the presence of steps because the features change their positions under different magnetic fields, as seen from A and A'. These observations clearly show that these bright features are vortices trapped at the atomic steps.

The vortices at steps are anomalous compared to the vortices on terraces. First, their shapes are elongated along the steps whereas the vortices on terraces are round. Second, ZBC values measured at the centers are lower than those of the vortices on terraces, as quantitatively depicted in Fig. 1(e). These anomalies are the direct consequences of JV and show that the atomic steps work as Josephson junctions.

Suppose that a vortex is created by penetration of the magnetic field through a Josephson junction line and its surrounding region. At the junction, the critical current density J_c is suppressed from that of the superconducting regions J_0. This leads to two important properties regarding the vortex [6]. First, the circulation of supercurrent near the center is strongly deformed and the vortex core is elongated along the junction line by a factor of $(J_c/J_0)^{-1}$. Second, the breaking of superconductivity around the core is weakened as J_c/J_0 decreases. When the supercurrent distribution near the junction line is nearly parallel and the suppression is sufficiently small, the vortex should be called a JV, like the case of layered superconductors under magnetic field parallel to the layers [7].

To ensure this picture, we numerically calculated the order parameter and DOS using the Bogoliubov-de Gennes (BdG) equation for a 2D tight-binding model with the hopping strength t_s at the Josephson junction reduced from a constant hopping strength t elsewhere. Then the Josephson parameter J_c/J_0 is represented by the ratio t_s/t. Figures 1(f) and 1(g) display zero-energy DOS calculated for t_s/t = 0.4 and 0.1, respectively. The characteristics of zero-energy DOS are different from the case of t_s/t = 1; its magnitude around the center is decreased as t_s/t is reduced, while the spatial distribution becomes strongly elliptic, which directly corresponds to the observed changes for vortices A', B', and C' in Fig. 1(d). From the comparison of the experiment and the theory, J_c/J_0 is estimated to be ~ 0.4 for step γ where vortex B' is located. Because of a weaker coupling at step δ, vortex C' can be safely called a JV.

References

[1] T. Zhang *et al.*, Nat. Phys. **6**, 104 (2010).
[2] T. Uchihashi, P. Mishra, M. Aono, and T. Nakayama, Phys. Rev. Lett. **107**, 207001 (2011).
[3] M. Yamada, T. Hirahara, and S. Hasegawa, Phys. Rev. Lett. **110**, 237001 (2013).
[4] C. Brun *et al.*, Nat. Phys. **10**, 444 (2014).
[5] S. Yoshizawa, H. Kim, T. Kawakami, Y. Nagai, T. Nakayama, X. Hu, Y. Hasegawa, and T. Uchihashi, Phys. Rev. Lett. **113**, 247004 (2014).
[6] G. Blatter, M. V. Feigel'man, V. B. Geshkenbein, A. I. Larkin, and V. M. Vinokur, Rev. Mod. Phys. **66**, 1125 (1994).
[7] P. J. W. Moll, L. Balicas, V. Geshkenbein, G. Blatter, J. Karpinski, N. D. Zhigadlo, and B. Batlogg, Nat. Mater. **12**, 134 (2013).

Authors
S. Yoshizawa[a], H. Kim, T. Kawakami[a], Y. Nagai[b], T. Nakayama[a], X. Hu[a], Y. Hasegawa, and T. Uchihashi[a]
[a]International Center for Materials Nanoarchitectonics, National Institute for Materials Science
[b]CCSE, Japan Atomic Energy Agency

Silver Oxide Clathrate Thin Films

Y. Matsumoto, R. Takahashi, and M. Lippmaa

We have studied the possibility of growing epitaxial films of silver clathrates on single-crystal oxide substrates by photoelectrochemical deposition. The clathrates chosen for this study were $Ag_7O_8NO_3$ and $Ag_7O_8HSO_4$. Both materials consist of a cubic lattice of Ag_6O_8 cages that enclose either NO_3 or HSO_4 anions, as illustrated in Fig. 1(a). Silver clathrates have various interesting properties; $Ag_7O_8NO_3$, for example, becomes superconducting at 1 K. Our purpose was to develop a technique for fabricating epitaxial clathrates with well-defined orientation on a single-crystal substrate. Silver clathrates contain Ag ions in several valence states, including Ag^+, Ag^{2+}, and Ag^{3+}, which means that strongly oxidizing synthesis conditions are needed. One possibility is to use photoelectrochemical deposition on a metallic substrate under a suitable substrate bias in either $AgNO_3$ or Ag_2SO_4 solution. Growth experiments on 0.5 wt% Nb-doped TiO_2 substrates showed that the best selectivity for clathrate

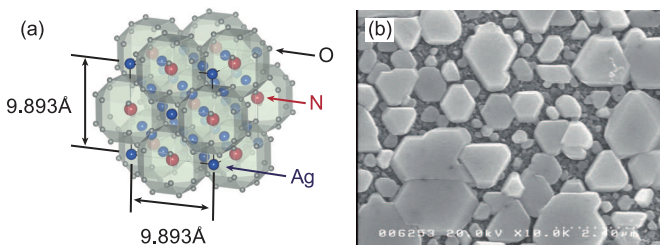

Fig. 1. (a) Structure of $Ag_7O_8NO_3$ silver clathrate crystals that consist of a cubic lattice of Ag_6O_8 cages that enclose NO_3 anions. (b) SEM image of epitaxial (111)-oriented $Ag_7O_8NO_3$ platelets photodeposited on a TiO_2(110) substrate surface in a $AgNO_3$ solution at an electrode potential of +0.3V vs Ag.

formation can be obtained at a bias of +0.2V vs. Ag. The necessary photoexcitation was provided by a high-pressure mercury lamp at a flux of 28 mW/cm^2. X-ray diffraction analysis showed that the best orientation control could be achieved on TiO_2 (110) substrates, yielding micrometer-scale epitaxial platelets, shown in a scanning electron microscope image in Fig. 1(b). It is clear from the image that the platelets tend to assume a hexagonal shape, characteristic of (111)-oriented growth. The growth habit and epitaxial relationship were further studied by x-ray diffraction and epitaxial relationships were found.

The reason for the preferential formation of epitaxial clathrate crystals on TiO_2 (110) surfaces was analyzed in terms of lattice matching between the clathrate Ag_6O_8 cage pseudo lattice and the TiO_2 surface. The (110)-oriented TiO_2 surface has a tetragonal structure where the spacing between adjacent bridging oxygen rows is 6.495 Å. This distance matches reasonably well the clathrate cage spacings of 6.056 Å, when the clathrate lattice is viewed along the (111) direction. It appears that despite the 6% mismatch, an epitaxial relationship is formed during platelet growth. The growth mechanism is thus somewhat similar to the formation of C_{60} films on crystalline substrates, although the growth of a hexagonal (111)-oriented lattice on a tetragonal surface is unusual.

Various different anions can be integrated in the clathrate lattice. We compared the growth habit and growth rates of silver clathrates containing the HNO_3 and HSO_4 anions and found that while the growth rate of $Ag_7O_8HSO_4$ was much higher than for $Ag_7O_8NO_3$, the epitaxial relationship was weaker. Since the lattice parameter of the clathrates is predominantly set by the size of the Ag_6O_8 cages, it appears that the formation of large epitaxial platelets is limited by other factors, with variable anion incorporation kinetics in the Ag_6O_8 cages being the most likely reason. This work showed that epitaxial growth of inorganic cage compounds is possible when commensurate matching between the cage pseudo lattice and a single-crystal substrate occurs.

Reference

[1] R. Tanaka, R. Takahashi, S. Takata, M. Lippmaa, and Y. Matsumoto, CrystEngComm **17**, 3701 (2015).

Authors
R. Tanaka[a], R. Takahashi, S. Takata[a], M. Lippmaa, and Y. Matsumoto[a,b]
[a]Tokyo Institute of Technology
[b]Tohoku University

Vortices of Superfluid ^{3}He in a Narrow Cylinder

O. Ishikawa and T. Kunimatsu

Vortices are well known fluid phenomena, whose size is widely distributed from the scale of a galaxy to that of water vortices in a laundry machine. The vortices familiar to us are classical ones with circulating motion of fluid, which are well described by a classical fluid mechanics. In modern physics, other types of vortices are found in liquid ^{3}He and ^{4}He from a quantum mechanical point of view. Both of quantizing a circulation and having a localized vorticity characterize a vortex in superfluid. Especially superfluid

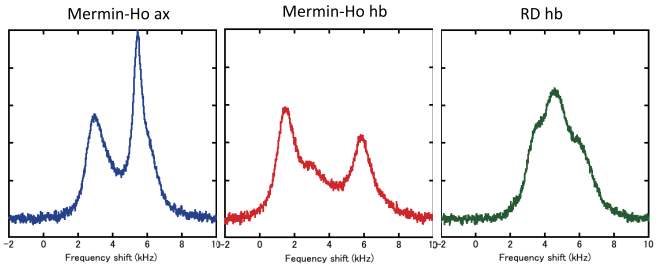

Fig. 1. Three types cw-NMR spectra in superfluid ^{3}He-A phase confined in a single narrow cylinder of 50 μm radius. Each spectrum corresponds to a different texture (spatial structure) of order parameters in the condensate.

^{3}He having many degrees of freedom in a condensate is more interesting than superfluid ^{4}He having only one type of vortex.

You can rotate normal liquid in a bucket by rotating the bucket itself but in the case of superfluid it is not easy to rotate it in such a way. Besides a vortex nucleation problem, stabilizing vortices in the bucket is another problem when the radius of bucket becomes very small, so-called a confined geometry. The necessary angular velocity of rotation to stabilize a vortex depends on the radius of cylinder and the quantity of circulation quantum of vortex. In superfluid ^{3}He-A phase, several types of vortex in bulk liquid have been observed but it was not clear whether another type vortex appears in the thin cylinder, where the angular velocity stabilizing a vortex becomes large. We showed that circulating velocity fields in superfluid ^{3}He–A phase were created in a very narrow cylinder, 100 μm in radius, using the rotating cryostat in ISSP, where three types of vortices were observed [1]. Two of three have the circulation quantum of unity and another had that of two, which was the same vortex as that in bulk liquid. Recently we can manipulate the type of vortex in even narrower cylinder, 50 μm in radius, in which three types of vortices are observed and all vortices correspond to the circulation quantum of unity [2]. A different type of vortex consists of different structures of order parameters of the condensate in a cylinder.

Figure 1 shows that three typical cw-NMR spectra in a single cylinder of 50 μm radius. A spectrum consists of a few spin wave resonances. Spin wave resonances are the low energy excitations in magnetic resonance experiments, whose frequencies are determined by NMR potential created by the dipole-dipole interaction E_D between ^{3}He nuclei in superfluid state. The order parameters in spin space and in orbital space are coupled each other through E_D. Three NMR spectra correspond to three types of textures, which are the spatial structures of order parameters in a cylinder. Our analysis reveals that they are Mermin-Ho hb texture, Mermin-Ho ax texture, and Radial-disgyration (RD) hb texture (see details in ref. [2]). These textures correspond to three types of vortices that can be observed in a narrow cylinder.

We have always observed one of three NMR spectra and

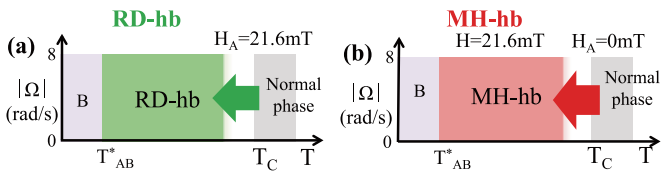

Fig. 2. Stable textures on cooling under rotation at two kinds of magnetic fields. (a) RD hb texture appeared at 21.6 mT. (b) MH hb texture appeared at 21.6 mT after passing through Tc under 0 mT.

have not observed the spectrum where the textures coexist each other. Figure 2 shows the stability of textures in the rotation-temperature phase diagram strongly depends on the magnetic field on cooling through T_C (transition temperature between superfluid and normal fluid) under rotation. The experimental procedure is quite similar to that of field cooling technique in studies of superconducting material. Theoretical calculations have been done about the stability of texture under rotation in magnetic field [3]. There exist qualitative and quantitative discrepancies between calculated results and observed ones on the stability of the texture in varying temperatures, magnetic fields and rotation angular velocities. We think that these discrepancies are attributed to the metastable state of texture because the textural transition needs a higher energy state between textures.

References

[1] R. Ishiguro, O. Ishikawa, M. Yamashita, Y. Sasaki, K. Fukuda, M. Kubota, H. Ishimoto, R.E.Packard, T. Takagi, T. Ohmi, and M. Mizusaki, Phys. Rev. Lett. **93**, 125301 (2004).
[2] T. Kunimatsu, H. Nema, R. Ishiguro, M. Kubota, T. Takagi, Y. Sasaki, and O. Ishikawa, Phys. Rev. B **90**, 214525 (2014).
[3] Y. Tsutsumi and K. Machida, J. Phys. Soc. Jpn. **78**, 114606 (2009).

Authors
O. Ishikawa[a] and T. Kunimatsu[a]
[a]Osaka City University

Development of Metal Ion-Containing Ionic Liquid Catalyst on Mesoporous Silica

T. Sasaki

We have been developing and using metal ion-containing immobilized ionic liquid catalysts in order to design heterogeneous catalysts by utilizing the characteristics of ionic liquids, where ionic liquid molecule with imidazolium cation moiety is immobilized on silica support and the metal halogenate anions are introduced as counter anion serving as reaction centers [1, 2]. It was found that the ImmCu_IL containing $[CuCl_4]^{2-}$ is active for Kharasch addition reaction between styrene and CCl_4. ImmNi_IL was found to be active for Suzuki cross coupling reactions with chlroarenes and phenyl boronic acids. ImmPd_IL was found to be active in a phosphine-free condition for Suzuki cross coupling reaction for bromoarenes [2].

We report the synthesis and application of immobilized palladium metal-containing ionic liquid supported on mesoporous silica such as SBA-15 (ImmPd-IL@SBA-15) as a novel catalyst for organic reactions. There are several advantages by using mesoporous material such as SBA-15 as a support. It has high surface area, easy to prepare, high gas adsorption capacity and high temperature tolerance.

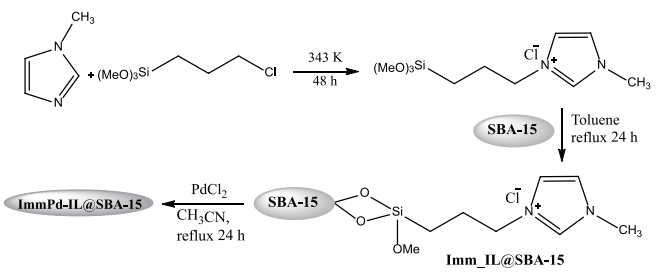

Scheme 1. Synthetic steps for the ImmPd-IL@SBA-15 catalyst.

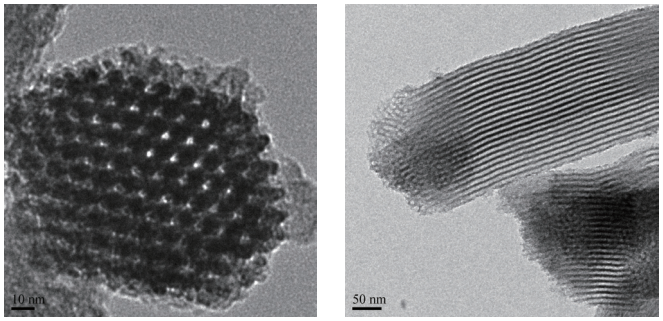

Fig. 1. TEM images of fresh ImmPd-IL@SBA15

The synthesis procedures were adopted from our method [1, 2] and all the reactions were conducted under nitrogen atmosphere (Scheme 1). Immobilized ionic liquid on SBA-15 samples were prepared using 1-methyl-3-(3-trimethoxysilylpropyl) imidazolium chloride (Mtim chloride). Mtim chloride was synthesized by refluxing the mixture of N-methylimidazole and 3-trimethoxysilylpropyl chloride at 70°C for 48 h. Mtim chloride and SBA-15 were dispersed in dehydrate toluene and refluxing, yielding solid products, Imm-IL@SBA-15. $PdCl_2$ and solid product were added to acetonitrile solution. After refluxing for 24 h, the resulting materials are obtained, denoted as ImmPd-IL@SBA-15. Fig. 1 shows TEM images for fresh ImmPd-IL@SBA15. Transmission Electron Microscope (JEOL JEM-2100 in ISSP, Univ. Tokyo) operating at 200 kV was used to obtain bright field images. It is found that uniform hexagonal channel structures are retained after immobilization of imidazolium groups. No Pd nanoparticles are found. The presence of $[PdCl_4]^{2-}$ was also confirmed by EDX analysis and EXAFS measurements.

It was found that the ImmPd-IL@SBA-15 catalyst has significantly improved the catalytic activity for synthesis of urea and oxamate derivatives by oxidative carbonylation of amines under co-catalyst, dehydrating agent and ligand free conditions [3]. ImmPd-IL@SBA-15 was also found to catalyze polyester amide synthesis by carbonylation polycondensation [4].

References

[1] T. Sasaki, C. Zhong, M. Tada, and Y. Iwasawa, Chem. Commun., 2506 (2005).
[2] T. Sasaki, M.Tada, C. Zhong, T. Kume, and Y. Iwasawa, J. Mol. Catal. A-Chem. **279**, 200 (2008).
[3] S. T. Gadge, E. N. Kusumawati, K. Harada, T. Sasaki, D. Nishio-Hamane, and B. M. Bhanage, J. Mol. Catal. A Chemical **400**, 170 (2015).
[4] A. Satapathy, S. T. Gadge, E. N. Kusumawati, K. Harada, T. Sasaki, D. Nishio-Hamane, and B. M. Bhanage, Catal. Lett. **145**, 824 (2015).

Authors
T. Sasaki[a], D. Nishio-Hamane, B. M. Bhanage[b]
[a]The University of Tokyo
[b]Institute of Chemical Technology

Efficient Method for Membrane Protein Structure Predictions

Y. Okamoto

Membrane proteins have essential biological functions based on their structures for life, and atomistic structural information is important to investigate the mechanism of their functions. Computers have been developing for

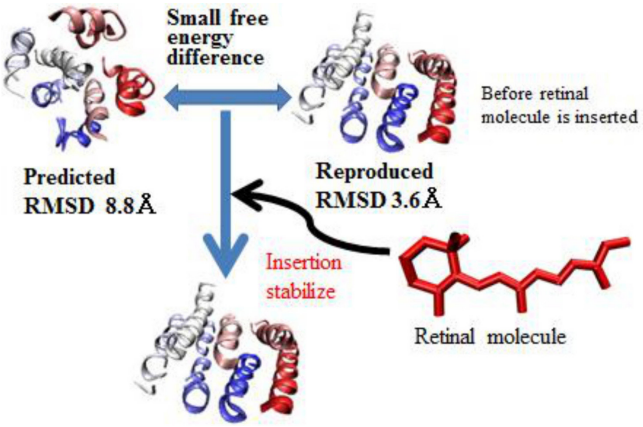

Fig. 1. Two predicted structures from our simulation and hypothesis about the relation between the structures and effects of retinal molecule insertion for the structures. In other words, the hypothesis is as follows: from our simulation without retinal molecule, the difference between above two structures is not large, however, insertion of retinal molecule into the empty space results in the stabilization of native-like structure compared to the other structure. This hypothesis is also consistent with previous experimental results.

decades. However, the resource runs short of structure predictions by brute-force simulations yet. Thus, efficient algorithm for computer simulation is needed to reduce computational resources for the prediction.

There are two fundamental approaches for the developments: decrease of interaction points in system and enhancement of sampling. A former example is to adopt an implicit solvent model. In good models, this method can achieve the structure prediction with simulations. A latter example is to employ replica- exchange method (REM) which enhances sampling of conformations. This method typically accelerates the crossing of free energy barriers using temperature change of replicas.

We developed the method from both approaches. We extended the previous method to target most membrane proteins [1]. Using the method, we performed structure prediction of bacteriorhodopsin and reproduced the native structure. Moreover, we also obtained the expected but unknown structure with empty space structure for retinal insertion, which is related to a hypothesis for co-molecule insertion during membrane protein folding as is shown in Fig. 1. As a result, our simulation produced the consistent results for previous experiments and supported the membrane protein folding hypothesis in co-molecule stage. Because we confirmed the validity of our new method for structure predictions, a next step will be to predict the unknown membrane protein structures or low-resolution protein structures.

We next proposed two new replica-exchange methods to increase efficiency of REM. One is the method of replica exchange with a differential equation without pseudo random numbers [2]. The other is the method that specifies the order of replica exchange and, thus, the trajectory in temperature space among replicas [3]. With 2-dimensional Ising model, we compared results of these new methods and its combination to results of the conventional Metropolis replica-exchange method. Figure 2 shows that specific heat obtained from the conventional Metropolis replica-exchange method (METREM), deterministic replica-exchange method (DETREM), designed-walk replica-exchange method (DEWREM), and their combination. DETREM with random-walk replica-exchange method reproduced the exact quantities including phase transition. Because short interval

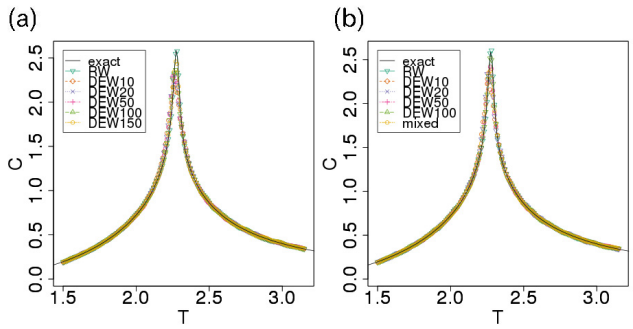

Fig. 2. Specific heat of 2-dimensional Ising model obtained by conventional random walk REM, DEWREM, and mixed simulations with (a) Metropolis replica-exchange method and (b) DETREM. The error bars are smaller than the symbols. In the inset, the labels are as follows. exact: exact solution, RW: random walk, DEW*n*: DEWREM with the interval of *n* MC steps between replica exchanges, and mixed: mixed walk.

causes correlation among replicas, DEWREM requires a longer interval of replica- exchange attempts to reproduce the conventional results. On the other hand, biomolecular simulation generally employs longer time interval between replica-exchange attempts. Hence, this does not cause such a problem in such simulations. In these simulations, DEWREM will result in the increase of efficiency of conformational sampling. For spin system, another implementation such as mixed walk simulation or different pairs in designed walk can improve the interval problem. These are future works to improve these methods.

References

[1] R. Urano, H. Kokubo, and Y. Okamoto, J. Phys. Soc. Jpn., in press.
[2] R. Urano and Y. Okamoto, arXiv:1412.6959.
[3] R. Urano and Y. Okamoto, arXiv:1501.00772.

Authors
R. Urano[a] and Y. Okamoto[a]
[a]Nagoya University

A New Structure Family of Oxide-Ion Conductor $NdBaInO_4$

M. Yashima and K. Fujii

Oxide-ion conducting materials such as pure oxide-ion conductors and mixed oxide ion-electronic conductors have a wide variety of applications in fuel cells, oxygen separation membranes and gas sensors. Since the oxide-ion conductivity is strongly dependent on the crystal structure, the discovery of new oxide-ion conductor belonging to a new structure family may open a new window for further innovative developments in the applications of oxide-ion conductors. Here, we report a new structure family of oxide-ion conductor $NdBaInO_4$ (Fig. 1) [1, 2].

To design a new layered perovskite-related structure, we have examined various chemical compositions of $AA'BO_4$ where A and A' are larger cations and B is smaller cation. After examining a number of chemical compositions, we discovered a new structure family of oxide-ion conducting materials $NdBaInO_4$ [1]. The Nd, Ba and In were chosen as cations, because (i) the different sizes of Nd and Ba can lead to the Ba/Nd cation ordering and (ii) the $BaInO_3$ perovskite layer can form from the view point of the sizes of Ba and In cations. $Nd_{1-x}Sr_xBaInO_{4-x/2}$ samples were prepared by solid-

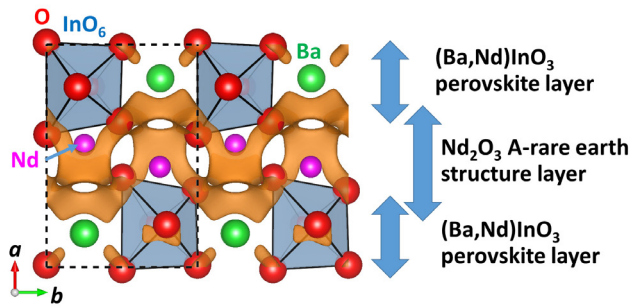

Fig. 1. Refined crystal structure and orange isosurface of the difference bond valence sum distribution for an oxide ion (O^{2-}) of $NdBaInO_4$. The structure consists of (i) Nd_2O_3 A-rare earth structure- and (ii) (Ba,Nd) InO_3 perovskite-layers. The difference bond valence sum map suggests that the oxide-ion conduction occurs in the Nd_2O_3 layer.

state reactions at 1400 °C using $BaCO_3$, $SrCO_3$, In_2O_3 and Nd_2O_3 powders. $NdBaInO_4$ and $Nd_{0.9}Sr_{0.1}BaInO_{3.95}$ exhibit oxide-ion conduction as shown in Figure 2. $NdBaInO_4$ and $Nd_{0.9}Sr_{0.1}BaInO_{3.95}$ samples are a single monoclinic phase with a new crystal structure as described below. Thus, a new structure family of oxide-ion conducting material $NdBaInO_4$ was discovered in this study. The oxide-ion conductivity of $NdBaInO_4$ is improved by Sr substitution at the Nd site (Fig. 2).

Crystal structure of $NdBaInO_4$ was investigated by neutron and synchrotron X-ray powder diffractometry and *ab initio* electronic calculations. We carried out the *ab initio* crystal structure analysis using the X-ray powder diffraction data. Neutron diffraction enables the precise determination of positional parameters of oxygen atoms. The space group was found to be monoclinic $P2_1/c$. The validity of the crystal structure of $NdBaInO_4$ (Figure 1) was confirmed by Rietveld refinements of synchrotron X-ray powder diffraction data measured at (i) SPring-8 and at (ii) PF, by Rietveld analysis of neutron diffraction data measured at (iii) J-PARC at (iv) ANSTO, and at (v) KAERI, (vi) by bond valence sums (BVS) of Nd, Ba and In atoms, and (vii) by the structural optimization based on the density functional theory (DFT) calculations. The refined crystal structure of $NdBaInO_4$ consists of (i) Nd_2O_3 A-rare earth structure- and (ii) (Ba,Nd) InO_3 perovskite-layers (Fig. 1), which indicates a new *A*/*A′* (Nd/Ba) cation ordered perovskite-related layered structure. An outstanding and unique feature of this new structure is that the edge of the InO_6 octahedron faces the A_2O_3 (Nd_2O_3) layer. The oxide-ion diffusion path of $NdBaInO_4$ was studied by the bond valence method (Fig. 1). The oxide ions can diffuse two-dimensionally in the A_2O_3 (Nd_2O_3) layer.

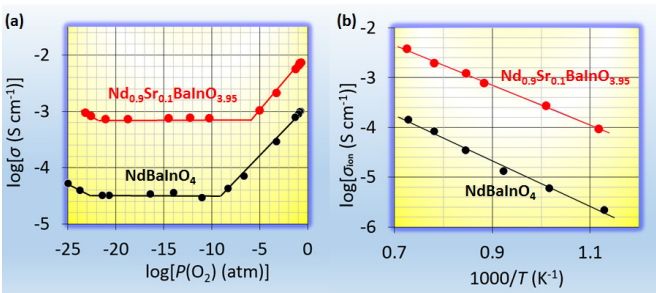

Fig. 2. (a) Oxygen partial pressure dependence of total electrical conductivity at 858 °C of $NdBaInO_4$ (Black) and $Nd_{0.9}Sr_{0.1}BaInO_{3.95}$ (Red). (b) Arrhenius plots of oxide-ion conductivity of $NdBaInO_4$ (Black) and $Nd_{0.9}Sr_{0.1}BaInO_{3.95}$ (Red).

References

[1] K. Fujii, Y. Esaki, K. Omoto, M. Yashima, A. Hoshikawa, T. Ishigaki, and H. R. Hester, Chem. Mater. **26**, 2488 (2014).

[2] K. Fujii, M. Shiraiwa, Y. Esaki, M. Yashima, S. J. Kim, and S. Lee, J. Mater. Chem. A **3**, 11985 (2015).

Authors

M. Yashima[a], K. Fujii[a], M. Shiraiwa[a], Y. Esaki[a], K. Omoto[a], A. Hoshikawa[b], T. Ishigaki[b], H. R. Hester[c], S. J. Kim[d], and S. Lee[d]

[a]Tokyo Institute of Technology

[b]Ibaraki University

[c]Australian Nuclear Science and Technology Organization

[d]Korea Atomic Energy Research Institute

Almost Perfect Frustration in the Dimer Magnet $Ba_2CoSi_2O_6Cl_2$

H. Tanaka and K. Kindo

Coupled spin dimer magnets provide a stage to embody the quantum physics of interacting lattice bosons. These magnets often exhibit a gapped singlet ground state. In an external magnetic field exceeding the energy gap, the $S_z = +1$ component of the spin triplet is created on the dimer. The $S_z = +1$ component, called a magnon, acts as a boson on the dimer lattice. The number of magnons can be tuned via the external magnetic field corresponding to the chemical potential. Magnons move to neighboring dimers and interact with one another owing to the transverse and longitudinal components of the interdimer exchange interactions, respectively. When the hopping term is dominant, magnons can undergo Bose–Einstein condensation while when the hopping term is suppressed so that the repulsive interac-

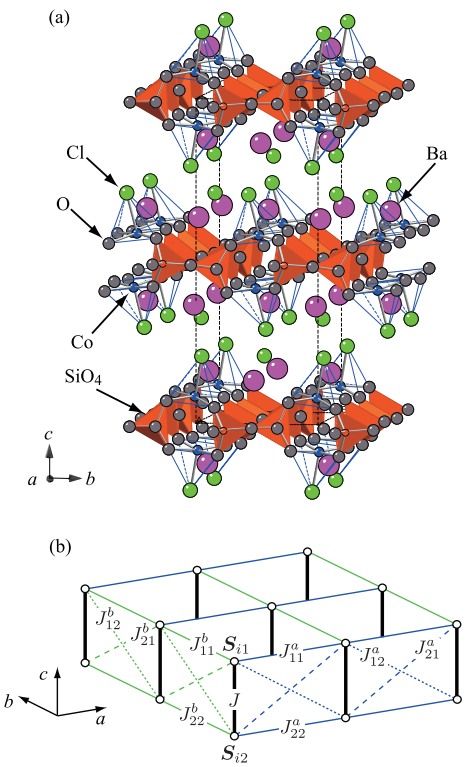

Fig. 1. (a) Perspective view of the crystal structure of $Ba_2CoSi_2O_6Cl_2$. Dotted lines denote the chemical unit cell. A magnetic Co^{2+} ion is located approximately at the center of the base of the CoO_4Cl pyramid, where the pyramids are linked via orange-colored SiO_4 tetrahedra in the *ab* plane. (b) Model of the exchange network for $Ba_2CoSi_2O_6Cl_2$. Thick solid lines represent the intradimer exchange interaction *J*, and thin solid, dashed and dotted lines represent the interdimer exchange interactions

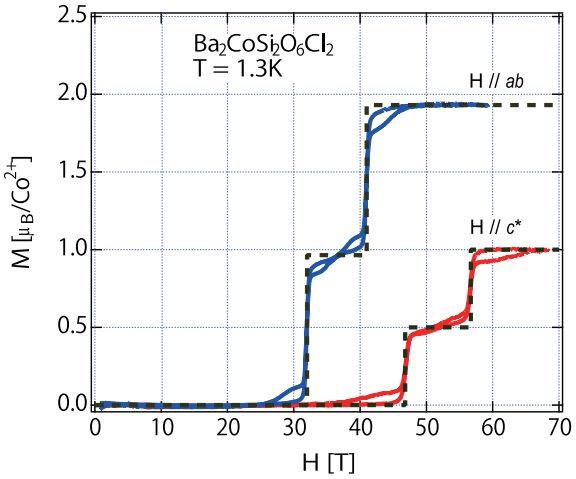

Fig. 2. Magnetization curves measured at 1.3K for $H \parallel c^*$ and $H \parallel ab$ using a piece of single crystal corrected for Van Vleck paramagnetism. Dashed lines are theoretical magnetization curves calculated using the anisotropy of the interdimer exchange interaction and the intradimer exchange interaction.

tion due to the antiferromagnetic interdimer interaction is dominant, magnons can crystallize to form a regular array.

Here we report the crystal structure of the spin dimer magnet $Ba_2CoSi_2O_6Cl_2$ and show that this compound exhibits magnon crystallization in a high magnetic field owing to the strong frustration of interdimer exchange interactions, which is different from the orthogonal dimer model [1]. The crystal structure consists of CoO_4Cl pyramids with a Cl^- ion at the apex, as shown in Fig 1(a). Magnetic Co^{2+} is located approximately at the center of the base composed of O^{2-}, which is approximately parallel to the *ab*-plane. Two CoO_4Cl pyramids form a chemical dimer with their bases facing each other. The magnetic property of Co^{2+} in an octahedral environment is determined by the lowest orbital triplet $^4T_1$. This orbital triplet splits into six Kramers doublets owing to spin–orbit coupling and the low-symmetric crystal field. When the temperature T is much lower than the magnitude of the spin–orbit coupling constant, the magnetic property is determined by the lowest Kramers doublet, and the effective magnetic moment of Co^{2+} is represented by the fictitious spin-1/2 operator [2, 3].

Figure 2 shows the magnetization curves for $Ba_2CoSi_2O_6Cl_2$ single crystal measured at 1.3 K for $H \parallel c^*$ and $H \parallel ab$. The entire magnetization process was observed up to a magnetic field of 70 T. The saturation of the Co^{2+} spin occurs at $H_s \simeq 57$ and 41 T for $H \parallel c^*$ and $H \parallel ab$, respectively. It can be clearly seen that the magnetization processes for both field directions are stepwise with a plateau at $M_s/2$. The singlet ground state is stabilized in a wide field range below H_c. These magnetization processes can be explained to consider that the interdimer exchange interactions are perfectly frustrated, which corresponds to the case $J^{ab}_{11} + J^{ab}_{22} = J^{ab}_{12} + J^{ab}_{21}$ within the exchange network shown in Fig. 1(b). In this case, the magnon cannot move onto the neighboring dimer, because the hopping amplitude is proportional to $J^{ab}_{11} + J^{ab}_{22} - J^{ab}_{12} - J^{ab}_{21}$. Hence, the ground state is determined by the balance between the Zeeman energy and the repulsive interaction between magnons. Consequently, a stepwise magnetization process with the $M_s/2$ plateau occurs, as observed in $Ba_2CoSi_2O_6Cl_2$.

In conclusion, this compound should be described as a 2D coupled spin dimer system with XY-like exchange interactions. $Ba_2CoSi_2O_6Cl_2$ exhibits a stepwise magnetization process with an $M_s/2$ plateau, irrespective of the magnetic field directions. This finding shows that the frustration for the interdimer exchange interactions is almost perfect. The $M_s/2$ plateau state is almost exactly given by the alternate product of singlet and triplet dimers, which corresponds to a Wigner crystal of magnons.

References

[1] H. Tanaka, N. Kurita, M. Okada, E. Kunihiro, Y. Shirata, K. Fujii, H. Uekusa, A. Matsuo, K. Kindo, and H. Nojiri, J. Phys. Soc. Jpn. **83**, 103701 (2014).
[2] A. Abragam and M. H. L Pryce, Proc. R. Soc. London, Ser. A **206**, 173 (1951)
[3] M. E. Lines, Phys. Rev. **131**, 546 (1963)

Authors
H. Tanaka[a], N. Kurita[a], M. Okada[a], E. Kunihiro[a], Y. Shirata[a], K. Fujii[a], H. Uekusa[a], A. Matsuo, K. Kindo, and H. Nojiri[b]
[a]Tokyo Institute of Technology
[b]Tohoku University

Thermal Critical Properties of Two-Dimensional Generalized SU(N) Heisenberg Models

T. Suzuki, K. Harada, and H. Matsuo

In recent years, deconfined critical phenomena (DCP) [1] have attracted much attention in condensed matter physics. The transition that exhibits DCP is expected to take place between a magnetic ordered phase and valence bond solid (VBS) phase. The most famous model family that shows such phase transition is the two-dimensional Heisenberg models with multiple singlet-projection terms for SU(N) spins, namely SU(N) JQ_m models [2]. We investigated the quantum criticality between the Neel phase and the VBS phase in the JQ_2 model on the square lattice and the JQ_3 model on the honeycomb lattice by using quantum Monte Carlo (QMC) calculations [3]. From the finite-size scaling analysis, we found that data collapses for order parameters are obtained by the same scaling function independently of the lattice geometry. This result implies that the quantum phase transition in those models is of the second order transition. However, as the system size increases, the

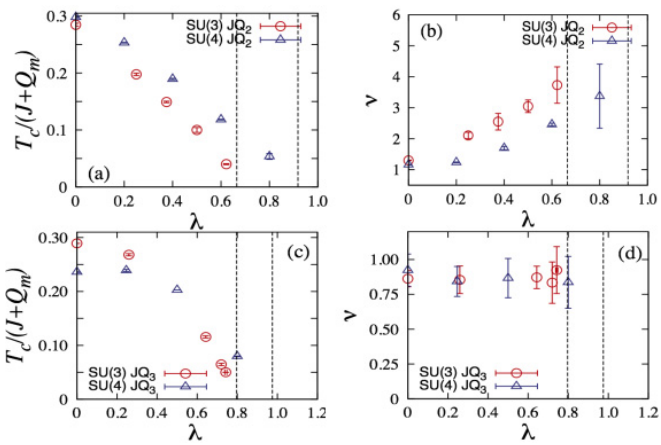

Fig. 1. Critical temperature T_c and critical exponent ν of the SU(N) generalized Heisenberg model. (a) and (c) ((b) and (d)) are results of T_c (ν) for the square-lattice and honeycomb-lattice case, respectively. Vertical dotted lines correspond to the quantum critical point between the Neel phase and VBS phase. The horizontal axis λ is the coupling ratio between Heisenberg interaction J and the amplitude of the multiple singlet-projection term Q_m, $\lambda = J/(J+Q_m)$.

estimated value of the quantum critical exponent ν exhibits a monotonic change and it approaches the phenomenological value for the first order transition. To discuss the quantum criticality from the different viewpoint and clarify the whole phase diagrams, we have studied the thermal critical properties of those models.

When we focus on the thermal properties of the SU(N) JQ_m models, the thermal phase transition to the VBS phase is possible because the VBS phase is characterized by coverings of the singlet dimers on the square or honeycomb lattice. We calculated the temperature dependence of the VBS order parameter by the QMC method. In figure 1, we show the critical temperature T_c and the thermal exponent ν which were evaluated from the finite-size scaling analysis up to L=192 for the square lattice case and L=96 for the honeycomb lattice case. Since the dimer covering state in the VBS phase is related to the rotational symmetry breaking of the lattice, we can expect the presence of the classical spin models that belong to the same universality class. In the present cases, the universality class of the square-lattice case is expected to be the same as that of the classical XY model with π/2-rotational symmetry breaking field, namely the $XY+Z_4$ model. In the honeycomb-lattice case, it may correspond to the three-state Potts model because the transition is characterized by π/3-rotational symmetry breaking. As shown in figure 1, ν increases monotonically in the square-lattice case when the system approaches the quantum critical point. It is obvious that the increase of ν survives in the vicinity of the quantum critical point. The similar behavior of ν is also observed when the classical $XY+Z_4$ model approaches the XY model limit, where the Kosterlitz-Thouless transition is realized. In the honeycomb lattice case, ν is almost constant at ν ~ 5/6, the value of the three-state Potts universality class. If the system shows the first-order transition at a zero temperature, a shift of ν toward the first-order-transition value is expected in both cases. However, we found that the first-order transition is unlikely for $T_c/(J+Q_m) \gtrsim 1/100$.

References

[1] T. Senthil *et al*., Phys. Rev. B **70**, 144407 (2004); T. Senthil *et al*., Science **303**, 1490 (2004).
[2] A. Sandvik, Phys. Rev. Lett. **98**, 227202 (2007).
[3] K. Harada *et al*., Phys. Rev. B **88**, 220408 (2013).
[4] T. Suzuki *et al*., Phys. Rev. B **91**, 094414 (2015); J. Phy.:Conf. Series. **592**, 012114 (2015).

Authors

T. Suzuki[a], K. Harada[b], H. Matsuo[c], S. Todo[d], and N. Kawashima
[a]The University of Hyogo
[b]Kyoto University
[c]RIST
[d]The University of Tokyo

Conferences and Workshops

International Conferences and Workshops

New Horizon of Strongly Correlated Physics (NHSCP2014)

June 16 - July 4, 2014
H. Tsunetsugu, K. Ueda, H. Kusunose, A. Koga, and J. Otsuki

Since 2006, the ISSP has organized an annual series of three-week workshops, with the only exception in 2011 due to the aftermath of the Tohoku earthquake. The last two in the series are "MAterial Simulation in Petaflops eta" (MASP2012) and "Emergent Quantum Phases in Condensed Matter – from topological to first-principles approaches" (EQPCM2013). In 2014, the ISSP organized the eighth workshop, "New Horizon of Strongly Correlated Physics" (NHSCP2014), held for three weeks starting from mid-June. Recent developments in theoretical and numerical studies on strongly correlated systems were discussed, and a special focus was placed on the strong correlation effects on dynamics and non-equilibrium phenomena. The main topics intensively discussed include the non-equilibrium Mott transition and optical response there, spin liquids, frustrated systems, topological insulators in strongly correlated electron systems, multipolar order in heavy fermion systems, multiple-component superfluidity in optical lattices. Dynamical mean field theory is the highlight in the workshop. Its many new progresses and developments were presented, and the dual-fermion and the dual-boson approaches aroused intense interest. The program and presentation materials are available on the web at the URL http://www.issp.u-tokyo.ac.jp/public/nhscp2014/.

Following the tradition of the series, the workshop contained the intensive three-day symposium during Jun. 25–27, and 33 oral and 17 poster presentations were made there. The remaining part was arranged into a more relaxing style providing a long discussion time, and 21 oral presentations were made. This style of workshop attracted many people; the cumulative number of participants during the three weeks summed up to just 600, and 272 of them attended the symposium part.

The NHSCP2014 workshop was organized by the ISSP and it was also supported by Computational Materials Science Initiative (CMSI) and Elements Strategy Initiative Center for Magnetic Materials (ESICMM). The workshop chairman was Hirokazu Tsunetsugu (ISSP) and the other organizers were Kazuo Ueda (ISSP), Hiroaki Kusunose (Ehime Univ.), Akihisa Koga (Tokyo Tech.), and Junya Otsuki (Tohoku Univ.). The organizers acknowledge a significant contribution from the oversea scientific advisor, Philipp Werner of University of Fribourg.

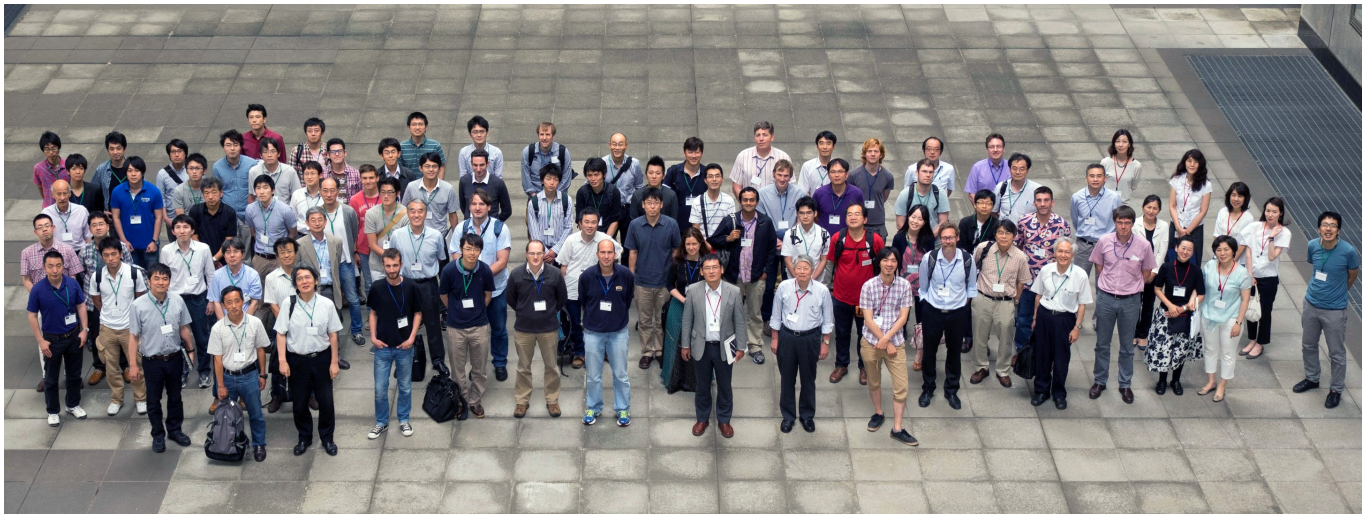

Joint Symposium of Polymer Networks and Research Group on Polymer Gels (PN&G2014)

November 10 - 14, 2014
M. Shibayama

The joint symposium of the 22nd Polymer Networks Group Meeting (PNG) and the 10th Gel Symposium (PN&G2014) was held at Ito International Research Center in Hongo Campus, the University of Tokyo. The PNG Meetings, started in 1975 in Strasburg, France, were held in Europe every other year, and is focusing on the physics of polymer networks and the theory of gelation, the structure and properties of polymer networks. On the other hand, Polymer Gel Symposium, an international symposium on polymer gels launched in 1989, is organized by Research Group on Polymer Gels, the Society of Polymer Science, Japan. It has also been held every other year, but exclusively in Japan. This was the first joint symposium on polymer networks and gels with the theme of "Cutting Edge of Chemistry, Physics, and Engineering in Polymer Networks". The symposium covered all fields of polymer gels and networks and provided a platform for scientific exchange in all areas relevant to theory and simulation, fabrication, structure, properties, and industrial/medical applications of gels.

There were 281 active participants from 23 countries. The oral sessions included 8 plenary lectures, 18 keynote lectures, 5 invited lectures, 56 contributed papers, and 7 Young Investigator Award nominee lectures. The symposium started with a mixer on Nov. 10, where a large number of participants from abroad got together. The scientific session began on Nov. 11 and ended with the concluding remark in the evening of Nov. 14, followed by Symposium Banquet with a large number of participants. Poster sessions were scheduled in the evening session from 19:00 – 20:30 on Nov. 11 and 12, and 134 posters were displayed in the two sessions. In addition to high-quality posters, snack service kept the audience to stay in the session until the last minute. 7 young investigators were awarded to the first PNG Young Investigator Awards sponsored by Sumitomo Bakelite Co. and by German and UK companies. In addition, 10 poster awards sponsored by Soft Matter, Royal Society of Chemistry, UK, and Research Group on Polymer Gels, Japan, were given to young scientists including graduate students and postdoctoral fellows. The next PNG will be held during June 19 – 23, 2016, in Stockholm, Sweden.

http://www.issp.u-tokyo.ac.jp/public/PNandG2014/

Young Investigator Awardees, PNG

Banquet

ISSP–MPIPKS Joint Workshop: Dynamics of Strongly Correlated Systems" (DSCS2015)

March 30 - 31, 2015
H. Tsunetsugu and R. Moessner

The ISSP conducts academic exchange programs with several foreign institutions, and one of the partners is Max Planck Institute for the Physics of Complex System (MPI–PKS) in Dresden, Germany. As a part of this exchange program, the ISSP and MPI–PKS recently started organizing joint workshops, and the first one took place at MPI–PKS in April of 2012. In this March 30–31, the ISSP hosted the second joint workshop, "Dynamics of Strongly Correlated Systems" (DSCS2015), and it was cochaired by Hirokazu Tsunetsugu (ISSP) and Roderich Moessner (MPI-PKS).

The DSCS2015 workshop aimed at overview and discussion on recent developments in theories and experiments on strongly correlated systems with special focus on their dynamical properties, non-equilibrium and transport phenomena, and related topics. Main subjects discussed include the following topics: electric and thermal conductivities, cross response between electric, magnetic, and thermal properties, topological quantum phases in strongly correlated electron systems, and effects of strong correlations on topologically protected surface states. Responses near metal-insulator transition or charge order were another focused topic as well as exotic properties of frustrated magnets/metals and unconventional superconductors. Another important topic was an emerging one and that was thermalization/non-thermalization of strongly correlated systems.

During the two-day workshop, the cumulative number of participants was 128, and there were 15 oral presentations, of which 13 were invited, and 19 poster presentations. The papers presented have stimulated participants and they are expected to yield various further progresses in the future. The program and the abstract booklet are available on the web at the URL http://tsune.issp.u-tokyo.ac.jp/dscs/index.html

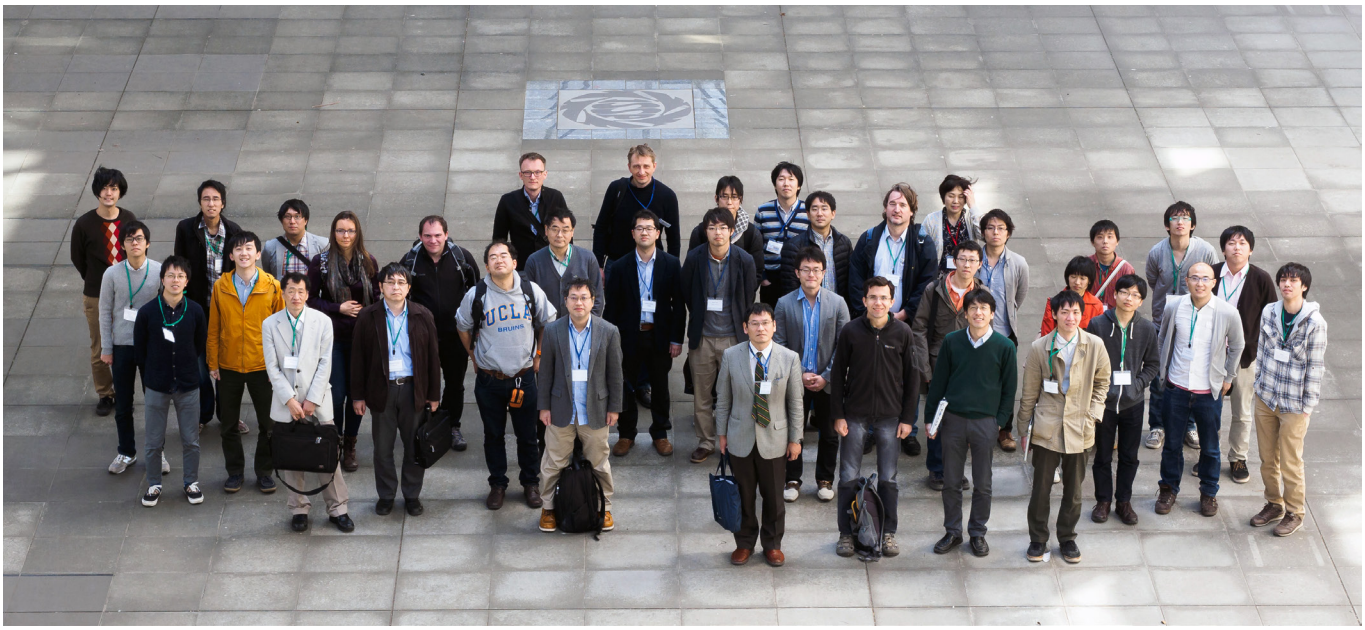

Novel Quantum Phenomena in Supermatter

April 17 - 19, 2014
K. Shirahama, M. Tsubota, M. Oshikawa, and Y. Okuda

Emergent quantum phenomena in matters often lead to universal concepts in science. As a prime example, superfluidity/superconductivity observed at very low temperatures gave a motivation to formulate spontaneous symmetry breaking in field theory and high-energy physics. In order to find a seed of universal concept, it is desirable to control the degrees of freedom and structure of the matter so that the system can be tuned to exhibit a particular phenomenon in a genuine way. This is realized in various systems which we will call "supermatters" with multiple layers of structure. The term was conceived in analogy to superlattice, which is made by stacking different crystals. Examples of supermatters include quantum vortices in superfluids/superconductors, ultracold atoms and liquid Helium in periodic potentials, quantum spin liquid with exotic elementary excitations, collective excitations in superfluid Helium 3, and exciton-polariton condensates with highly tunable parameters. We hope that the development and investigation of various supermatter systems will contribute to elucidation of fundamental problems in physics and to construction of novel universal concepts.

This workshop was organized with the purpose of sharing the common perspective of supermatter among scientists from various backgrounds, and of discussing future directions. Although the workshop was held at the beginning of the Japanese academic year, there were 244 cumulative participants over 3 days, attending 40 oral and 27 poster presentations and lively discussions. It was indeed a very useful meeting to exchange ideas based on studies of many different systems which had been pursued independently, and to seek new directions.

Details on the workshop can be found in the web page (in Japanese):
URL http://www.issp.u-tokyo.ac.jp/public/SuperMatter/

New Horizon of Strongly Correlated Physics (NHSCP2014)

June 25 - 27, 2014
H. Tsunetsugu, K. Ueda, H. Kusunose, A. Koga, J. Otsuki, and Z. Hiroi

This ISSP workshop was held as the symposium part of the international workshop of the same title. See the section of "International Conferences and Workshops".

Toward a Paradigm Shift of Synchrotron Radiation Based Materials Science in the VUV-SX Region

September 20 - 21, 2014

Y. Harada, A. Fujimori, S. Shin, F. Komori, and I. Matsuda

In order to encourage a motivation and discussions that demand an internationally competitive vacuum ultra-violet-soft X-ray (VUV-SX) light source in Japan in addition to the present synchrotron light sources, it is now necessary to accelerate mutual communications not only within the present VUV-SX community but also with broad scientific community. This workshop was held aiming to boost a paradigm shift of synchrotron radiation based materials science and further of all the scientific community in Japan by broad-ranging discussions beyond the concept of community such as ultra-violet, soft X-ray, hard X-ray and even inside/outside synchrotron radiation. The program was categorized into four sessions by "catalyst/battery", "soft matter/biomaterial", "solid and surface physics" and "materials science" and representative or energetic and pioneering young researchers in each field were selected as speakers of review-talks.

In all sessions there were a lot of questions and comments, regarding such as new scientific directions by a combination of different synchrotron techniques, actual scientific requests for the energy/spatial resolution that much exceed the ability of the present synchrotron techniques, possible collaborative synchrotron and neutron studies and so on. The workshop dealt with issues mostly aiming at real applications, thus it was unique among workshops held in ISSP and will contribute to establish a new scientific trends in ISSP.

ISSP Workshop: Physical Chemistry Revealed by Advanced Operando Observations

September 29 - 30, 2014.

I. Matsuda, J. Yoshinobu, Y. Harada, S. Yamamoto, Y. Takagi, and M. Nagasaka

Today there is strong demand in our society towards developing novel catalysts and devices that will solve energy and environmental problems. In recent years the importance of the spectroscopic/microscopic characterization of materials during operation with confirming their operation at the same time starts to be realized. For example, chemical reactions on a catalyst surface involve a variety of dynamic processes such as adsorption, diffusion, desorption of molecules. To gain the fundamental understanding on a reaction mechanism, the heterogeneous catalysts under real reaction conditions have to be studied. This approach is called "*Operando* observation", which becomes a key topic in catalysis and device researches. Very recently, "*Operando* observation" in X-ray region becomes possible by the development of high-brilliant synchrotron light sources and novel instruments.

This workshop thus aimed to discuss the latest results both from experimental and theoretical studies on the catalysts and devices using "*Operando* observation", and to create new human network among the researchers' community and promote the scientific collaborations. The workshop covered a broad range of related topics including X-ray spectroscopies, electron microscopies, vibrational spectroscopies as well as theoretical studies. The workshop welcomed 102 participants, notably 30% of which are from private companies. The program of the workshop consisted of 1 invited lecture, 13 invited oral presentations and 16 poster presentations.

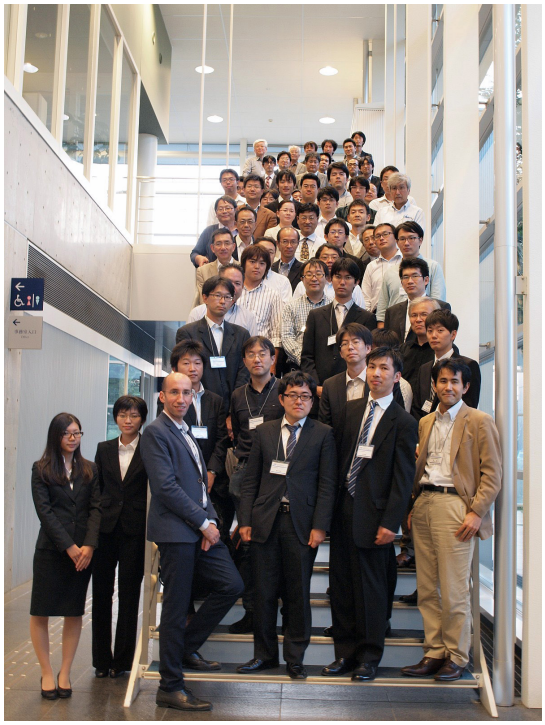

Recent Advances in Physics of Strongly Correlated Electrons in Skutterudite and Related Compounds

October 10 - 12, 2014

C. Sekine, T. Sakakibara, H. Harima, Y. Aoki, R. Shiina, and K. Iwasa

Filled skutterudite compounds, in particular Pr- and Sm-based ones having more than two 4*f* electrons, exhibit a variety of many-body quantum phenomena. Extensive studies were done on these systems during the MEXT project, Grant-in-Aid for Scientific Research on Priority Area "Evolution of New Quantum Phenomena Realized in the Filled Skutterudite Structure" (2003-2007), and the basic physical picture of those phenomena was partly clarified. Seven years have past after the end of the project, and there has been substantial progress in the research on filled skutterudites and the related systems having a similar caged structure. This workshop was aimed to further advance the physics of strongly correlated systems realized in those caged systems, and covered a broad range of topics including pyrochlores, clathrates, and RT_2X_{20}. The presentations included 4 review talks, 13 invited talks and 22 poster presentations. Recent advances and some remaining issues in this field were discussed intensively.

Supercomputer Users Meeting

Novermber 13 - 14, 2014

T. Oguchi, S. Yunoki, R. Yamamoto, S. Tsuneyuki, S. Todo, H. Noguchi, O. Sugino, H. Akai, T. Ozaki, H. Watanabe, H. Kasamatsu, Y. Noguchi, S. Morita, I. Matsuda, S. Harada, and N. Kawashima

This is the meeting for the ISSP supercomputer general use held annually to exchange information on the latest developments in condensed matter physics achieved by the use of ISSP supercomputer. This year's meeting was held also for the CCMS annual activity report. The selection of speakers is based on suggestions made by three unaffiliated scientists appointed as the program committee members. Since SY2014 is the last year of the current supercomputer system that started operation in 2010, the meeting was a good opportunity for surveying what have been achieved by the current system, and indeed an active discussion was held among the audience, of which the cumulative total number was 154. Having made the keyword of this year's meeting "Industrial Applications of Computational Sciences", we had speakers who have close contact with researchers in industry and their industry partners, such as Taisuke Ozaki (ISSP) and Hideaki Sawada (Nippon Steel & Sumitomo Metal). Yoshitaka Tateyama (NIMS) gave a presentation on his recent work of the first-principles calculation concerning solid battery. We also invited three speakers who wrote invited articles in the annual report of ISSP supercomputer general use: Shiro Sakai (RIKEN), Takeo Hoshi (Tottori) and Hayato Shiba (ISSP). Also notable was the presentation on software developments and their public release in the field of condensed matter physics.

ISSP Series Workshop on Synergetic Science for Functional Material Systems: (1) Optical Functions

December 4 - 5, 2014

H. Akiyama, H. Mori, J. Yoshinobu, F. Komori, M. Shibayama, T. Suemoto, O. Yamamuro, O. Sugino, H. Noguchi, Y. Harada, I. Matsuda, and M. Lippmaa

This workshop focusing on optical functions is the first one among series workshops on synergetic science for functional material systems, which were proposed and organized by the 12 members of ISSP working group for a future plan on a new research center of interdisciplinary area. We collected presentations consisting of 16 invited talks and 19 contributed posters. The topics of the workshop covered functional optical properties of various material systems, functional optical imaging, and bio-medical imaging. Protein was one of the most frequently discussed material systems, which enable ion pumping, photo-synthesis, photo-sensing, and bio-luminescence in biological systems. Novel bio-medical imaging was also hot topic in the workshop. Though they had been exotic subjects in ISSP seminars, we sincerely realized that those are important subjects that ISSP must watch and challenge. We had 76 and 57 attendances for the first and the second days, respectively, including young researchers and students from other universities.

ISSP Workshop: Status of SPring-8 BL07LSU and Prospects for the Next Generation Synchrotron Light Sources

March 5, 2015

H. Wadati, S. Shin, F. Komori, I. Matsuda, and Y. Harada

Synchrotron radiation laboratory has a Harima branch to maintain and develop a high-brilliance soft X-ray beamline BL07LSU at SPring-8. There we are performing time-resolved, spatial-resolved and energy-resolved soft X-ray spectroscopy to study electronic states and their dynamics of new materials. In this workshop, recent research activities at our beamline were reported and our future prospects toward the next generation synchrotron light sources were discussed. The speakers talked about their recent results from each end station (time-resolved spectroscopy, 3D nano-ESCA, emission spectroscopy, and so on). There were two invited talks; one is about synthesizing new materials and the advantage of using synchrotron x-rays for this synthesis process, and the other is about the upgrade plan of the light source to SPring-8 II. There were a lot of discussions for each talk, and we successfully started to obtain a clear vision about how we can utilize the next generation synchrotron light sources for the condensed-matter research. We also encouraged the young generation in this research field by awarding the best poster prizes to two graduate students.

ISSP Workshop: Topological Aspects in Correlated Electron Systems

March 26, 2015

S. Nakatsuji, M. Oshikawa, T. Sakakibara, and M. Takigawa

This workshop was intended to deepen our understanding on novel phenomena that have been seen in many correlated electrons and its possible relation to topology of electronic structure and spin texture. Experts from the field provided us both pedagogical and advanced talks on topical subjects covering iridates, heavy fermions, Bismuth, Axion and Weyl anomalies in metals. Another purpose of the workshop was to enhance the collaborative research activities among participants. For the latter perspective, the workshop was supported by both the ISSP workshop series, and by our JSPS project for Strategic International Networks Project on Topological Phenomena in Novel Quantum Materials.

In spite of a short announcement, a large number of on/off-campus researchers reaching 75 attended this workshop. The workshop consisted of two parts. The morning part was a pedagogical lecture for non-experts on "Novel correlated topological phases in correlated materials." by Prof. Leon Balents (UCSB), which gave an introduction on the concept of the topology in condensed matter physics and its application to correlated electron systems.

The afternoon part was made by three sessions with a series of talks intended for experts. As the first speaker in the first session, Prof. Luis Balicas (NHMFL, Florida) gave a talk on the discovery of the axial anomaly in the quasi-two-dimensional metal $PdCoO_2$. This talk was followed by Prof. Masaki Oshikawa (ISSP), who made a theory talk on the chiral magnetic effect in an insulator. Then, the next session focused on the recent development in understanding of Bismuth. First talk was given by Prof. Yuki Fuseya (UEC, Tokyo) on Spin Hall Effect and Large Anisotropic g-Factor of Bismuth. This was followed by an experimental talk by Dr. Robert Kuechler (MPI-CPfS, Dresden), on the thermodynamic evidence for valley-dependent density of states in bulk bismuth. Finally, in the last session, the topological aspects in strongly correlated electron systems were discussed. In particular, two talks were given focusing on the quantum critical phenomena in the mixed valent system β-$YbAlB_4$. Distinct quantum critical behaviors were discussed in the first talk by Dr. Takahiro Tomita (ISSP), which were found to form a strange metal without magnetic criticality. It was pointed out that these quantum critical behaviors are clearly different from the typical non-Fermi liquid behaviors observed in the vicinity of the antiferromagnetic quantum critical point. Finally, Prof. Andriy Nevidomskyy (Rice Univ., Houston) introduced a novel topological viewpoint to understand anomalous properties and superconductivities in the heavy fermion systems such as β-$YbAlB_4$ and UPt_3. Throughout this workshop, very active discussions were made and the future direction was addressed to shed further light on the emergent topological phenomena in correlated electron systems.

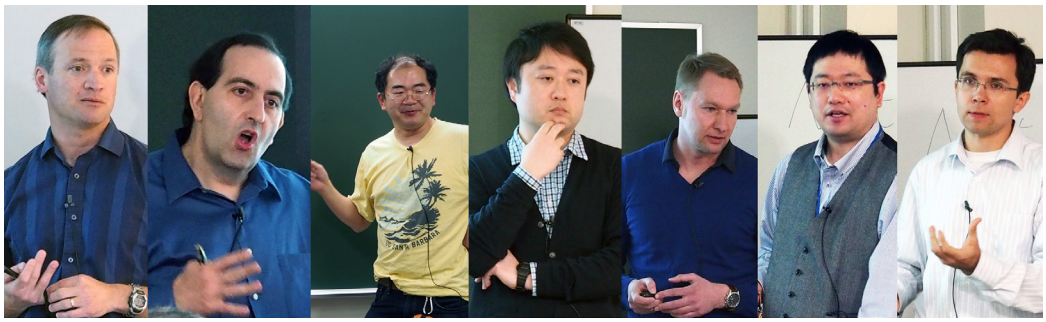

Subjects of Joint Research

平成 26 年度　共同利用課題一覧（前期）/ Joint Research List (2014 First Term)

嘱託研究員 / Commission Researcher

No.	課題名	氏名	所属		Title	Name	Organization
担当所員：中辻　知							
1	X 線回析実験による軌道状態の研究とその化学的置換効果の解明	澤　博	名古屋大学	大学院工学研究科	X-ray diffraction study of orbital state and its control by chemical substitution	Hiroshi Sawa	Nagoya University
2	価数異常を伴う量子臨界現象	三宅　和正	豊田理化学研究所		Quantum criticality associated with valence instability	Kazumasa Miyake	Toyota Physical and Chemical Research Institute
3	幾何学的フラストレート磁性体における量子物性の研究	木村　健太	大阪大学	大学院基礎工学研究科	Quantum state of matter in geometrically-frustrated magnets	Kenta Kimura	Osaka University
4	超伝導と核強磁性の共存	柄木　良友	琉球大学	教育学部	Interplay between superconductivity and nuclear ferromagnetizm	Yoshitomo Karaki	University of the Ryukyus
担当所員：榊原　俊郎							
5	強相関遷移金属化合物の開拓	大串　研也	東北大学	大学院理学研究科	Exploration of strongly correlated transition-metal compounds	Kenya Ohgushi	Tohoku University
担当所員：吉信　淳							
6	HREELS によるシリセンの化学的性質の解明	アントワーヌ　フロランス	北陸先端科学技術大学院大学	マテリアルサイエンス研究科	Exploring chemical properties of silicene using HREELS	Fleurence Antoine	Japan Advanced Institute of Science and Technology
7	固体表面に吸着した有機分子の電子・光学物性評価	桑原　裕司	大阪大学	大学院工学研究科	Investigation of electronic/optical properties of organic molecules on sold surfaces	Yuji Kuwahara	Osaka University
8	極低温非弾性トンネル分光と高分解能電子エネルギー損失分光による吸着分子の素励起過程	米田　忠弘	東北大学	多元物質科学研究所	Elementary excitations of adsorbed molecules using low-temperature scanning tunneling spectroscopy and high-resolution electron energy loss spectroscopy	Tadahiro Komeda	Tohoku University

No.	課題名	氏名	所属		Title	Name	Organization
9	酸化物半導体光触媒における水分解反応の研究	松本　吉泰	京都大学	大学院理学研究科	Study of water splitting reaction on oxide semiconductor catalysts	Yoshiyasu Matsumoto	Kyoto University
10	二酸化炭素還元触媒反応に関する研究	森川　良忠	大阪大学	大学院工学研究科	Study on catalytic reactions of reduction of CO_2	Yoshitada Morikawa	Osaka University
11	銅表面上に吸着した一酸化窒素の振動状態	奥山　弘	京都大学	大学院理学研究科	Vibrational states of nitric oxide adsorbed on Cu surfaces	Hiroshi Okuyama	Kyoto University
担当所員：上床　美也							
12	有機伝導体の圧力効果	村田　惠三	大阪市立大学	大学院理学研究科	Effect of pressure on the organic conductor	Keizo Murata	Osaka City University
13	多重極限関連圧力装置の調整	高橋　博樹	日本大学	文理学部	Adjustment of cubic anvil apparatus	Hiroki Takahashi	Nihon University
14	希土類化合物の単結晶試料評価とその圧力効果	藤原　哲也	山口大学	大学院理工学研究科	Effect of pressure on the Ce compounds	Tetsuya Fujiwara	Yamaguchi University
15	磁性体の圧力効果	巨海　玄道	久留米工業大学		Effect of pressure on the magnetic materials	Gendo Oomi	Kurume Institute of Technology
16	圧力下 NMR 測定法に関する開発	藤原　直樹	京都大学	大学院人間・環境学研究科	Development of NMR measurement method under high pressure	Naoki Fujiwara	Kyoto University
17	低温用マルチアンビル装置の開発	辺土　正人	琉球大学	理学部	Development of multi-anvil apparatus for low temperature	Masato Hedo	University of the Ryukyus
18	中性子回析に用いる圧力装置の開発	片野　進	埼玉大学	大学院理工学研究科	Developments of high pressure cell for neutron diffraction	Susumu Katano	Saitama University
19	擬一次元有機物質の圧力下物性研究	糸井　充穂	日本大学	医学部	Study on pressure induced superconductivity of quasi organic conductor	Miho Itoi	Nihon University
20	高圧下の比熱測定装置の開発	梅原　出	横浜国立大学	工学部	Development of apparatus for specific heat measurements under high pressure	Izuru Umehara	Yokohama National University
21	磁化測定装置の開発	名嘉　節	物質・材料研究機構		Development of the magnetometer	Takashi Naka	National Institute for Materials Science
22	重い電子系物質における圧力下電気抵抗測定	礒田　誠	香川大学	教育学部	Effect of pressure on the electrical resistivity of heavy fermi on compounds	Makoto Isoda	Kagawa University
担当所員：柴山　充弘							
23	小型集束型小角散乱装置の高性能化及びそれによる応用研究	古坂　道弘	北海道大学	大学院工学研究院	Development of a compact focusing small-angle neutron scattering instrument and application research using the instrument	Michihiro Furusaka	Hokkaido University

No.	課題名	氏名	所属		Title	Name	Organization
24	中性子散乱装置の共同利用・開発による強相関電子系物質の構造物性の研究	岩佐　和晃	東北大学	大学院理学研究科	Structural studies of strongly correlated electron systems by neutron scattering method and instrumental development	Kazuaki Iwasa	Tohoku University
25	中性子モノクロメータの改良と中性子４軸回折計 FONDER の制御プログラムの改良	木村　宏之	東北大学	多元物質科学研究所	Improvement of neutron monochromator and control program for four circle neutron diffractometer FONDER	Hiroyuki Kimura	Tohoku University
26	中性子散乱装置のアップグレードと共同利用研究の推進	藤田　全基	東北大学	金属材料研究所	Upgrading of the neutron scattering device and promotion of the research and public use	Masaki Fujita	Tohoku University
27	中性子散乱装置のアップグレード後の研究計画の実施と共同利用の推進	平賀　晴弘	高エネルギー加速器研究機構	物質構造科学研究所	Implementation of the research plan under the cooperation-use program after upgrading neutron scattering instruments	Haruhiro Hiraka	KEK
28	中性子散乱装置のアップグレード後の研究計画の実施と共同利用の推進	田畑　吉計	京都大学	大学院工学研究科	Progress of the joint research by using the neutron scattering instruments	Yoshikazu Tabata	Kyoto University
29	中性子散乱装置のアップグレード後の研究計画の実施と共同利用の推進	松村　武	広島大学	大学院先端物質科学研究科	Promotion of joint research after the upgrade of neutron scattering instruments	Takeshi Matsumura	Hiroshima University
30	J-PARC/MLF と JRR-3 共存時代に向けた３軸型中性子散乱装置の高度化	松浦　直人	総合科学研究機構		Upgrade of 3-axis neutron spectrometer for the oncoming coexistence of J-PARC/MLF and JRR-3	Masato Matsuura	CROSS
31	中性子分光器を用いた強相関電子系物質の微視的研究	桑原　慶太郎	茨城大学	大学院理工学研究科	Neutron scattering study of strongly correlated electron systems by using neutron spectrometers	Keitaro Kuwahara	Ibaraki University
32	高度化した３軸分光器を用いた共同利用の推進と物質科学研究の実施	横山　淳	茨城大学	理学部	Executing user program and study of material science with the advanced triple-axis spectrometers	Makoto Yokoyama	Ibaraki University
33	冷中性子スピン干渉計の応用と MINE ビームラインの整備	田崎　誠司	京都大学	大学院工学研究科	Development of cold neutron spin interferometry and improvements of MINE beam line	Seiji Tasaki	Kyoto University
34	膜貫通ペプチドのフリップフロップ誘起能の評価	中野　実	富山大学	大学院医学薬学研究部（薬学）	Induction of phospholipid flip-flop by transmembrane peptides	Minoru Nakano	University of Toyama
35	C_1-3　ULS 極小角散乱装置 IRT	杉山　正明	京都大学	原子炉実験所	Development of micro-focusing small-angle neutron scattering spectrometer	Masaaki Sugiyama	Kyoto University
36	集光テスト用小型 SANS の開発及び冷中性子反射率計・干渉計のアップグレード	日野　正裕	京都大学	原子炉実験所	Improvement of MIEZE spectrometer and cold neutron reflectometer and interferometer	Masahiro Hino	Kyoto University
37	集光テスト用小型 SANS の開発及び冷中性子反射率計・干渉計のアップグレード	北口　雅暁	名古屋大学	現象解析研究センター	Development of compact SANS and improvement of cold neutron reflectometer and interferometer	Masaaki Kitaguchi	Nagoya University
38	中性子散乱用高圧セルの開発および高圧下における中性子散乱実験	藤原　哲也	山口大学	大学院理工学研究科	Neutron scattering experiments under high pressure and development of high pressure cell for neutron scattering	Tetsuya Fujiwara	Yamaguchi University
39	流動場でのソフトマターの構造変化に関する研究	高橋　良彰	九州大学	先導物質化学研究所	Studies on structural change of soft matter under flow field	Yoshiaki Takahashi	Kyushu University
40	三軸分光器を用いた極端条件下における物質科学研究の実施	阿曽　尚文	琉球大学	理学部	Material science studies under extreme conditions by using triple-axis spectrometers	Naofumi Aso	University of the Ryukyus

No.	課題名	氏名	所属		Title	Name	Organization
41	圧力誘起ベシクルにおける２分子膜の相転移	川端　庸平	首都大学東京	大学院理工学研究科	Phase transition of bilayers in a pressure-induced vesicle	Youhei Kawabata	Tokyo Metropolitan University
42	中性子散乱研究計画の実施と共同利用の推進	伊藤　晋一	高エネルギー加速器研究機構	物質構造科学研究所	Propelling the inter university research cooperation	Shinichi Itoh	KEK
43	冷中性子干渉イメージング装置開発研究	大竹　淑恵	理化学研究所	光量子工学研究領域	Research and development of interferometric imaging instruments for cold neutron	Yoshie Otake	RIKEN
44	高度化した三軸分光器を用いた共同利用の推進とスピンダイナミクスの研究	佐藤　卓	東北大学	多元物質科学研究所	Promoting user program and investigating spin dynamics using advanced triple-axis spectrometers	Taku Sato	Tohoku University
45	高度化した三軸分光器を用いた強相関電子系物質の研究	南部　雄亮	東北大学	多元物質科学研究所	Study of strongly correlated electron systems using advanced triple-axis spectrometers	Yusuke Nambu	Tohoku University
担当所員：金道　浩一							
46	強磁場量子ビーム科学のためのパルスマグネットの開発	鳴海　康雄	東北大学	金属材料研究所	Developments of pulse magnets for synchrotron and neutron experiments in pulsed high magnetic fields	Yasuo Narumi	Tohoku University
担当所員：辛　埴							
47	高温超伝導体の高分解能光電子分光	藤森　淳	東京大学	大学院理学系研究科	Ultra-high resolution photoemission spectroscopy on high Tc superconductor	Atsushi Fujimori	The University of Tokyo
48	60-eV レーザーを用いた時間分解光電子分光の開発	石坂　香子	東京大学	大学院工学系研究科	The development of time-resolved photoemission using 60eV laser	Kyoko Ishizaka	The University of Tokyo
49	鉄系超伝導体のレーザー光電子分光	下志万　貴博	東京大学	大学院工学系研究科	Laser-ARPES on Fe superconductor	Takahiro Shimojima	The University of Tokyo
50	Bi 系超伝導体の角度分解光電子分光	竹内　恒博	豊田工業大学		Angle-resolved photoemission study on high Tc cuprate	Tsunehiro Takeuchi	Toyota Technological Institute
51	高分解能光電子分光による強相関物質の研究	横谷　尚睦	岡山大学	大学院自然科学研究科	Ultra-high resolution study on strongly correlated materials	Takayoshi Yokoya	Okayama University
52	酸化バナジウムの高分解能光電子分光	江口　律子	岡山大学	大学院自然科学研究科	Photoemission study on vanadium oxides	Ritsuko Eguchi	Okayama University
53	有機化合物の光電子分光	金井　要	東京理科大学	理工学部	Photoemission study on organic compounds	Kaname Kanai	Tokyo University of Science
54	重い電子系ウラン化合物の高分解能光電子分光	藤森　伸一	日本原子力研究開発機構	量子ビーム応用研究部門	Ultra high resolution photoemission study on heavy fermion Uranium compounds	Shinichi Fujimori	Japan Atomic Energy Agency
55	レーザー光電子分光による酸化物薄膜の研究	津田　俊輔	物質・材料研究機構		Laser-photoemission study on oxide films	Shunsuke Tsuda	National Institute for Materials Science

No.	課題名	氏名	所属		Title	Name	Organization
56	４ｆ電子系物質の高分解能光電子分光	松波　雅治	自然科学研究機構	分子科学研究所	Photoemission study on 4f materials	Masaharu Matsunami	National Institutes of Natural Sciences
57	超高空間分解能光電子顕微鏡による磁区構造観察	中川　剛志	九州大学	大学院総合理工学府	Observation of magnetic domain structures by ultra-high resolution photoemission electron microscopy	Takeshi Nakagawa	Kyushu University
58	Mn 化合物の時間分解光電子分光	大川　万里生	東京理科大学	理学部	Time resolved photoemission on Mn compounds	Mario Okawa	Tokyo University of Science
59	極低温・超高分解能光電子分光を用いた超伝導機構の研究	岡崎　浩三	東京大学	大学院理学系研究科	Study of the mechanism of superconductivity by low temperature and high resolution photoemission spectroscopy	Kozo Okazaki	The University of Tokyo
60	収差補正型光電子顕微鏡の建設と利用研究	小嗣　真人	高輝度光科学研究センター		Construction and utilization research of aberration correction photoelectron emission microscopy	Masato Kotsugi	Japan Synchrotron Radiation Institute
61	時間分解・マイクロビームラインの開発と研究	室　隆桂之	高輝度光科学研究センター		Development of micro- and time-resolved beamline	Takayuki Muro	Japan Synchrotron Radiation Institute
62	光電子分光法を用いた各種分子性結晶の電子状態の研究及び装置の低温化	木須　孝幸	大阪大学	大学院基礎工学研究科	Research on electron state of molecular crystals using photoemission spectroscopy	Takayuki Kisu	Osaka University
担当所員：松田　巌							
63	高輝度放射光軟Ｘ線を用いた時間分解光電子分光による表面ダイナミクス研究	近藤　寛	慶應義塾大学	理工学部	Study of surface dynamics by time-resolved photoemission spectroscopy with high-brilliant soft x-ray synchrotron radiation	Hiroshi Kondoh	Keio University
64	軟Ｘ線アンジュレータビームラインの分光光学系の開発研究	雨宮　健太	高エネルギー加速器研究機構	物質構造科学研究所	Research and development of soft X-ray undulator beamline	Kenta Amemiya	KEK
65	光電子スピン検出器の開発・研究	奥田　太一	広島大学	放射光科学研究センター	Research and development of a new photoelectron spin detector	Taichi Okuda	Hiroshima University
66	光電子顕微鏡による磁性ナノ構造物質の磁化過程	木下　豊彦	高輝度光科学研究センター		Magnetization in process of magnetic nano structure by PEEM	Toyohiko Kinoshita	Japan Synchrotron Radiation Institute
67	高輝度軟Ｘ線を利用した強相関物質の電子状態研究	組頭　広志	高エネルギー加速器研究機構	物質構造科学研究所	Study of electronic states in strongly correlated materials with high brilliant soft-Xray	Hiroshi Kumigashira	KEK
68	時間分解光電子分光法による光触媒材料のキャリアダイナミクス研究	小澤　健一	東京工業大学	大学院理工学研究科	Study of carrier dynamics in photocatalysis materials by time-resolved photoemission spectroscopy	Kenichi Ozawa	Tokyo Institute of Technology
69	軟Ｘ線時間分解分光実験による磁性研究	木村　昭夫	広島大学	大学院理学研究科	Study of magnetic properties by time-resolved soft X-ray spectroscopy	Akio Kimura	Hiroshima University
70	高輝度軟Ｘ線を利用する光電子顕微鏡装置の設計・開発	坂本　一之	千葉大学	大学院融合科学研究科	Research and designing of a PEEM spectrometer for high brilliance soft X ray	Kazuyuki Sakamoto	Chiba University
71	二次元表示型スピン分解光電子エネルギー分析器の開発	大門　寛	奈良先端科学技術大学院大学	物質創成科学研究科	Development of 2D display type spin resolved photoelectron energy analyzer	Hiroshi Daimon	Nara Institute of Science and Technology

No.	課題名	氏名	所属		Title	Name	Organization
72	時間分解光電子回析実験の要素技術開発	林　好一	東北大学	金属材料研究所	Technical development of time-resolved photoelectron diffraction experiment	Koichi Hayashi	Tohoku University
担当所員：原田　慈久							
73	軟 X 線吸収／発光分光法によるリチウムイオン電池電極材料の電子物性研究	細野　英司	産業技術総合研究所	エネルギー技術研究部門	Study on the electronic property of electrode materials for Li-ion batteries by soft X-ray absorption/emission spectroscopy	Eiji Hosono	National Institute of Advanced Industrial Science and Technology
74	〃	朝倉　大輔	産業技術総合研究所	エネルギー技術研究部門	〃	Daisuke Asakura	National Institute of Advanced Industrial Science and Technology
75	超高分解能軟 X 線発光分光による水素吸蔵合金中の水素の波動関数の局在性に関する研究	関場　大一郎	筑波大学	数理物質系	Study on the localization of wave functions of hydrogen atom in hydrogen storage alloys using ultrahigh resolution soft X-ray emission spectroscopy	Daiichiro Sekiba	University of Tsukuba
76	時間分解光電子分光による重い電子系の研究	関山　明	大阪大学	大学院基礎工学研究科	Study on heavy Fermion materials by time-resolved photoemission	Akira Sekiyama	Osaka University
77	高分解能光電子分光による酸化バナジウムの研究	藤原　秀紀	大阪大学	大学院基礎工学研究科	Study on vanadium oxides by high resolution photoemission	Hidenori Fujiwara	Osaka University
78	軟 X 線発光・共鳴非弾性散乱分光の磁気円・線二色性測定システムの構築	菅　滋正	大阪大学	産業科学研究所	Construction of a noble system for circular and linear dichroism in soft X-ray emission and RIXS spectroscopy	Shigemasa Suga	Osaka University
79	極小角 X 線散乱と軟 X 線吸収・発光分光の融合によるソフトマテリアルの物性研究	雨宮　慶幸	東京大学	大学院新領域創成科学研究科	Study on the physical properties of soft materials by a combination of ultra-small-angle X-ray scattering and soft X-ray absorption/emission spectroscopy	Yoshiyuki Amemiya	The University of Tokyo
80	二次元原子薄膜トランジスタの電子状態のナノ分析 (I)	吹留　博一	東北大学	電気通信研究所	Nanoscale analysis of electronic states of graphene device	Hirokazu Fukidome	Tohoku University
担当所員：和達							
81	三次元 nanoESCA による実デバイスのオペランド電子状態解析	永村　直佳	東北大学	多元物質科学研究所	Operando analysis of the electronic structure of actual devices by 3DnanoESCA	Naoka Nagamura	Tohoku University

一般研究員 / General Researcher

No.	課題名	氏名	所属		Title	Name	Organization
担当所員：榊原　俊郎							
1	CuO_2 リボン鎖系 $Cs_2Cu_2Mo_3O_{12}$ の磁気的基底状態	安井　幸夫	明治大学	理工学部	Magnetic Ground State of CuO_2 ribbon Chain system $Cs_2Cu_2Mo_3O_{12}$	Yukio Yasui	Meiji University
2	パイロクロア磁性体 $Tb_{2-x}Ti_{2+x}O_7$ の比熱測定	高津　浩	首都大学東京	大学院理工学研究科	Specific heat measurements of the pyrochlore magnet $Tb_{2-x}Ti_{2+x}O_7$	Hiroshi Takatsu	Tokyo Metropolitan University

No.	課題名	氏名	所属		Title	Name	Organization
3	〃	脇田　美香	首都大学東京	大学院理工学研究科	〃	Mika Wakita	Tokyo Metropolitan University
4	強相関伝導系のパルス磁場中の超音波測定	吉澤　正人	岩手大学	大学院工学研究科	Ultrasonic measurements of strongly correlated electron systems in pulsed magnetic field	Masahito Yoshizawa	Iwate University
5	〃	赤坂　直哉	岩手大学	大学院工学研究科	〃	Naoya Akasaka	Iwate University
6	強相関電子系化合物の秩序相に対する結晶対称性および軌道縮退の効果	横山　淳	茨城大学	理学部	Effects of crystal symmetry and orbital degeneracy in ordered states of strongly correlated electron systems	Makoto Yokoyama	Ibaraki University
7	〃	藤村　健司	茨城大学	大学院理工学研究科	〃	Kenji Fujimura	Ibaraki University
8	極低温磁化測定による $SmRh_2Zn_{20}$ の磁場誘起相転移の検証	加瀬　直樹	新潟大学	大学院自然科学研究科	Study of field-induced order of $SmRh_2Zn_{20}$ by low-temperature magnetization measurements	Naoki Kase	Niigata University
9	〃	安達　季並	新潟大学	大学院自然科学研究科	〃	Kinami Adachi	Niigata University
10	重い電子系超伝導体の対関数の対称性決定理論	町田　一成	岡山大学	大学院自然科学研究科	Theoretical studies of pair symmetry in heavy fermion superconductors	Kazushige Machida	Okayama University
11	有機ラジカルを用いた新規磁性体の低温磁気測定	山口　博則	大阪府立大学	大学院理学系研究科	Low temperature magnetic properties of new organic radical compounds	Hironori Yamaguchi	Osaka Prefecture University
12	〃	岩瀬　賢治	大阪府立大学	大学院理学系研究科	〃	Kenji Iwase	Osaka Prefecture University
13	〃	菊地　健太郎	大阪府立大学	大学院理学系研究科	〃	Kentaro Kikuchi	Osaka Prefecture University
14	高圧合成法による新規パイロクロア型遷移金属化合物の探索	有馬　孝尚	東京大学	大学院新領域創成科学研究科	Exploration of new transition metal compounds of pyrochlore structure by means of high-pressure syntheses	Taka-hisa Arima	The University of Tokyo
15	〃	阿部　伸行	東京大学	大学院新領域創成科学研究科	〃	Nobuyuki Abe	The University of Tokyo
16	高圧合成法による新規パイロクロア型遷移金属化合物の探索	鷲見　浩樹	東京大学	大学院新領域創成科学研究科	Exploration of new transition metal compounds of pyrochlore structure by means of high-pressure syntheses	Hiroki Sumi	The University of Tokyo
担当所員：森　初果							
17	プロトン - 電子相関系分子性導体における重水素効果	西尾　豊	東邦大学	理学部	Deuteration effect of proton-electron correlated molecular Conductor	Yutaka Nishio	Toho University
18	〃	山田　翔太	東邦大学	大学院理学研究科	〃	Shota Yamada	Toho University

No.	課題名	氏名	所属		Title	Name	Organization
19	水素結合型分子性機能物質における重水素効果の理論的解析	立川　仁典	横浜市立大学	大学院生命ナノシステム科学研究科	Theoretical analysis of deuterated effect on hydrogen-bonded molecular materials	Masanori Tachikawa	Yokohama City University
20	〃	兼松　佑典	横浜市立大学	大学院生命ナノシステム科学研究科	〃	Yusuke Kanematsu	Yokohama City University
21	〃	緒方　勇大	横浜市立大学	大学院生命ナノシステム科学研究科	〃	Yudai Ogata	Yokohama City University
22	鉄錯体からなる分子性導電体の磁気・光物性研究	松田　真生	熊本大学	大学院自然科学研究科	Studies on magnetic and optical properties of molecular conductors coposed of a Fe complex	Masaki Matsuda	Kumamoto University
23	〃	西　美樹	熊本大学	大学院自然科学研究科	〃	Miki Nishi	Kumamoto University
24	熱耐久性を有する高性能塗布型有機トランジスタ材料の開発	岡本　敏宏	東京大学	大学院新領域創成科学研究科	Development of solution-processable high performance organic semiconductos with thermal durability	Toshihiro Okamoto	The University of Tokyo
25	〃	三津井　親彦	東京大学	大学院新領域創成科学研究科	〃	Chikahiko Mitsui	The University of Tokyo
26	〃	山岸　正和	東京大学	大学院新領域創成科学研究科	〃	Masakazu Yamagishi	The University of Tokyo
27	〃	吉本　和美	東京大学	大学院新領域創成科学研究科	〃	Kazumi Yoshimoto	The University of Tokyo
28	強相関パラメーターを制御した拡張および縮小π系分子性伝導体の物質合成と物性研究	白旗　崇	愛媛大学	大学院理工学研究科	Synthesis and properties of new molecular conductors based on extended and reduced π-electron donors, in which electron correlation parameters are controlled	Takashi Shirahata	Ehime University
29	〃	古田　圭介	愛媛大学	大学院理工学研究科	〃	Keisuke Furuta	Ehime University
担当所員：瀧川　仁							
30	13C NMR による有機三角格子物質の基底状態の研究	清水　康弘	名古屋大学	大学院理学研究科	13C NMR study for the ground state of the organic triangular lattice	Yasuhiro Shimizu	Nagoya University
担当所員：中辻　知							
31	$CeAl_2$ の臨界磁場近傍での低温電気抵抗測定	海老原　孝雄	静岡大学	大学院理学研究科	Electrical resistivity measurements in $CeAl_2$ by dilution refrigerator	Takao Ebihara	Shizuoka University
32	〃	土屋　政人	静岡大学	大学院理学研究科	〃	Masato Tsuchiya	Shizuoka University
33	Si 置換 Mn_2GeO_4 における新奇マルチフェロイック特性の起源解明	本田　孝志	高エネルギー加速器研究機構	物質構造科学研究所	Study on the origin of unusual multiferroicity in Si-substituted Mn_2GeO_4	Takashi Honda	KEK

No.	課題名	氏名	所属		Title	Name	Organization
担当所員：上田　和夫							
34	コランダム構造における量子相転移	宮原　慎	福岡大学	理学部	Quantum phase transition in corundum structure	Shin Miyahara	Fukuoka University
担当所員：常次　宏一							
35	電子凝縮系における新奇現象	御領　潤	弘前大学	大学院理工学研究科	Novel phenomena in electronic condensed matter systems	Jun Goryo	Hirosaki University
担当所員：リップマー　ミック							
36	ダブルペロブスカイト酸化物薄膜における秩序構造制御とその輸送・誘電特性評価	北村　未歩	東京大学	大学院工学系研究科	Control of ordered-structure and evaluations of transport and dielectric properties in double perovskite oxide films	Miho Kitamura	The University of Tokyo
37	パルスレーザー堆積法による多成分系ナノ相分離酸化物薄膜の構造と物性	松本　祐司	東北大学	大学院工学研究科	Structural and material-property characterization of multi component oxide lms with nano-scale phase separation	Yuji Matsumoto	Tohoku University
38	〃	丸山　伸伍	東北大学	大学院工学研究科	〃	Shingo Maruyama	Tohoku University
39	太陽電池用シリコンプロセスにおける触媒効果	伊高　健治	弘前大学	北日本新エネルギー研究所	Catalysis effect on the direct silica reduction process for solar cells	Kenji Itaka	Hirosaki University
担当所員：家　泰弘							
40	Bi ナノワイヤーにおける量子振動実験	長谷川　靖洋	埼玉大学	工学部	Experiment of quantum oscillations by Bi nanowire	Yasuhiro Hasegawa	Saitama University
担当所員：吉信　淳							
41	HREELS によるグラファイト・グラフェンにおける電子格子散乱の直接測定	田中　慎一郎	大阪大学	産業科学研究所	Direct measurement for the electron-phonon scattering in graphite and graphite using HREELS	Shin-ichiro Tanaka	Osaka University
42	Ag(110) 上に作成した TiO_2 単結晶薄膜の STM 観察	枝元　一之	立教大学	理学部	STM study of the TiO_2 single-crystal film on Ag(110)	Kazuyuki Edamoto	Rikkyo University
43	Ag（111）表面に合成したシリセンの格子ダイナミクスに関する研究	高木　紀明	東京大学	大学院新領域創成科学研究科	Lattice dynamics of silicene grown on Ag(111)	Noriaki Takagi	The University of Tokyo
担当所員：小森　文夫							
44	金属／半導体表面上ナノ構造の形成とその光学応答の時間分解測定	河村　紀一	日本放送協会	放送技術研究所	Time resolved spectroscopy of optical responses from nano-structures on metal / semiconductor surfaces	Norikazu Kawamura	NHK Science & Technical Research Laboratories

No.	課題名	氏名	所属		Title	Name	Organization
45	再放出低速陽電子による酸化物表面近傍の欠陥の動的研究	松本　益明	東京学芸大学	教育学部	Study of the dynamics of defects near the surface of oxides by reemitted slow positron	Masuaki Matsumoto	Tokyo Gakugei University
担当所員：長谷川　幸雄							
46	圧縮応力下における金単原子接点の高バイアス安定性	酒井　明	京都大学	大学院工学研究科	High-bias stability of gold single-atom contacts under compressive stresses	Akira Sakai	Kyoto University
47	二ホウ化物薄膜上のエピタキシャルシリセン及びゲルマニウム層の低温走査トンネル顕微鏡観察	高村　由起子	北陸先端科学技術大学院大学	マテリアルサイエンス研究科	Low temperature scanning tunneling microscopy investigations of epitaxial silicene and germanium layer on diboride thin films	Yukiko Takamura	Japan Advanced Institute of Science and Technology
48	〃	アントワーヌ　フロランス	北陸先端科学技術大学院大学	マテリアルサイエンス研究科	〃	Antoine Fleurence	Japan Advanced Institute of Science and Technology
49	〃	青柳　航平	北陸先端科学技術大学院大学	マテリアルサイエンス研究科	〃	Kohei Aoyagi	Japan Advanced Institute of Science and Technology
50	圧縮応力下における金単原子接点の高バイアス安定性	若杉　晋作	京都大学	大学院工学研究科	High-bias stability of gold single-atom contacts under compressive stresses	Shinsaku Wakasugi	Kyoto University
担当所員：上床　美也							
51	$(Ho,Y)Rh_2Si_2$ 単結晶の磁気転移の圧力効果	繁岡　透	山口大学	大学院理工学研究科	Pressure effect on magnetic transitions of $(Ho,Y)Rh_2Si_2$ single crystal	Toru Shigeoka	Yamaguchi University
52	〃	藤井　洋	山口大学	大学院理工学研究科	〃	Yoh Fujii	Yamaguchi University
53	CDW 有機伝導体の圧力下磁場誘起相の普遍化の探索	村田　惠三	大阪市立大学	大学院理学研究科	Search of generalization of field-induced phase of CDW organic conductor	Keizo Murata	Osaka City University
54	〃	平山　光	大阪市立大学	大学院理学研究科	〃	Hikaru Hirayama	Osaka City University
55	$EuCo_2P_2$ の高圧力下磁化測定 (2)	藤原　哲也	山口大学	大学院理工学研究科	Magnetization measurements of $EuCo_2P_2$ under high pressures II	Tetsuya Fujiwara	Yamaguchi University
56	〃	田端　克好	山口大学	大学院理工学研究科	〃	Katsuyoshi Tabata	Yamaguchi University
57	$LaFe_{2-x}Mn_xGe_2$ の単結晶育成	藤原　哲也	山口大学	大学院理工学研究科	Single crystal growth of $LaFe_{2-x}Mn_2Ge_2$	Tetsuya Fujiwara	Yamaguchi University
58	〃	中田　琢也	山口大学	大学院理工学研究科	〃	Takuya Nakada	Yamaguchi University
59	Mn 基磁気一次相転移物質の高圧下磁化測定	小山　佳一	鹿児島大学	大学院理工学研究科	Magnetization measurement of Mn based compounds under high pressure	Keiichi Koyama	Kagoshima University

No.	課題名	氏名	所属		Title	Name	Organization
60	〃	吉峰　裕貴	鹿児島大学	大学院理工学研究科	〃	Yuki Yoshimine	Kagoshima University
61	Ni-Mn-Ga 系強磁性形状記憶合金の磁化の圧力依存性	安達　義也	山形大学	大学院理工学研究科	Pressure dependence of magnetization for the ferromagnetic shape-mem ory alloys of Ni-Mn-Ga system	Yoshiya Adachi	Yamagata University
62	〃	池田　大地	山形大学	大学院理工学研究科	〃	Daichi Ikeda	Yamagata University
63	Pr 系銅酸化物及びその関連物質における超伝導の圧力効果	久田　旭彦	徳島大学	大学院ソシオ・アーツ・アンド・サイエンス研究部	Pressure effects on superconductivity in Pr-based copper oxide and related materials	Akihiko Hisada	The University of Tokushima
64	$YbCo_2Zn_{20}$ 置換系物質の基本物性評価	阿曽　尚文	琉球大学	理学部	Evaluation of fundamental physical properties in doped $YbCo_2Zn_{20}$	Naofumi Aso	University of the Ryukyus
65	〃	比嘉　泰之	琉球大学	大学院理工学研究科	〃	Yasuyuki Higa	University of the Ryukyus
66	$YbMn_2Ge_2$ の高圧力下磁化測定	藤原　哲也	山口大学	大学院理工学研究科	Magnetization measurements under high pressures in $YbMn_2Ge_2$	Tetsuya Fujiwara	Yamaguchi University
67	〃	中田　琢也	山口大学	大学院理工学研究科	〃	Takuya Nakada	Yamaguchi University
68	カゴ状構造を有する超伝導体 $Sc_5Rh_6Sn_{18}$ の高圧下電気抵抗測定	加瀬　直樹	新潟大学	大学院自然科学研究科	Electrical resistivity measurements under high pressure of $Sc_5Rh_6Sn_{18}$ with caged structure	Naoki Kase	Niigata University
69	〃	鈴木　陽史	新潟大学	大学院自然科学研究科	〃	Harufumi Suzuki	Niigata University
70	〃	新井　宏典	新潟大学	大学院自然科学研究科	〃	Hironori Arai	Niigata University
71	セリウムおよびユーロピウム化合物 $R_2T_3Ge_5$ (R: Ce, Eu) の高圧下物性	中島　美帆	信州大学	理学部	Physical properties of cerium and europium coumpound $R_2T_3Ge_5$ (R: Ce, Eu) under high pressure	Miho Nakashima	Shinshu University
72	〃	岡崎　友哉	信州大学	大学院理工学系研究科	〃	Tomoya Okazaki	Shinshu University
73	セリウム系化合物における微小磁気モーメントの圧力下磁化測定 II	阿曽　尚文	琉球大学	理学部	Magnetization studies under pressure in Ce-based compounds with small magnetic moments II	Naofumi Aso	University of the Ryukyus
74	〃	比嘉　泰之	琉球大学	大学院理工学研究科	〃	Yasuyuki Higa	University of the Ryukyus
75	〃	藤原　哲也	山口大学	大学院理工学研究科	〃	Tetsuya Fujiwara	Yamaguchi University
76	ホイスラー化合物 Ni_2MnGa の高圧下電気抵抗	伊藤　昌和	鹿児島大学	大学院理工学研究科	Electrical resistivity of Heusler alloy Ni_2MnGa in high pressure	Masakazu Ito	Kagoshima University

No.	課題名	氏名	所属		Title	Name	Organization
77	ホイスラー合金 Pd_2MnIn の反強磁性とマルテンサイト変態の圧力効果	岡田　宏成	東北学院大学	工学部	Pressure effect on antiferromagnetic and martensitic transition in Heusler alloy Pd_2MnIn	Hironari Okada	Tohoku Gakuin University
78	圧力下における CeSe の磁気相転移と近藤効果	松村　武	広島大学	大学院先端物質科学研究科	Magnetic order and Kondo effect in CeSe under high pressure	Takeshi Matsumura	Hiroshima University
79	〃	林　佑弥	広島大学	大学院先端物質科学研究科	〃	Yuya Hayashi	Hiroshima University
80	圧力誘起価数転移の探索と高圧下輸送特性	辺土　正人	琉球大学	理学部	Searching of pressure-induced valence transition and transport properties under high pressure	Masato Hedo	University of the Ryukyus
81	〃	垣花　将司	琉球大学	大学院理工学研究科	〃	Masashi Kakihana	University of the Ryukyus
82	価数揺動物質の高圧力中輸送特性の研究	仲間　隆男	琉球大学	理学部	Transport properties of valence fluctuating compounds under pressure	Takao Nakama	University of the Ryukyus
83	〃	仲村　愛	琉球大学	大学院理工学研究科	〃	Ai Nakamura	University of the Ryukyus
84	〃	赤嶺　拡	琉球大学	大学院理工学研究科	〃	Hiromu Akamine	University of the Ryukyus
85	回転希釈冷凍機を用いた量子固体・量子液体研究	白濱　圭也	慶應義塾大学	理工学部	Studies of quantum fluids and solids using rotating dilution refrigerators	Keiya Shirahama	Keio University
86	希土類磁性体の異方的磁気体積効果	大橋　政司	金沢大学	理工研究域	Anisotropic magnetovolume effect of rare earth compounds	Masashi Ohashi	Kanazawa University
87	〃	立野　翔大	金沢大学	大学院自然科学研究科	〃	Shota Tateno	Kanazawa University
88	強磁性体 RCu_9Sn_4(R: 希土類) の圧力下電気抵抗測定	広瀬　雄介	新潟大学	理学部	Electrical resistivity measurement of ferromagnet RCu_9Sn_4 (R:rare earth) under high pressure	Yusuke Hirose	Niigata University
89	〃	倉橋　秀平	新潟大学	大学院自然科学研究科	〃	Shuhei Kurahashi	Niigata University
90	〃	都丸　駿	新潟大学	大学院自然科学研究科	〃	Shun Tomaru	Niigata University
91	強相関型セリウム化合物および合金の量子相転移と磁性	村山　茂幸	室蘭工業大学	大学院工学研究科	Quantum phase transition and magnetism in the strongly correlated Ce compounds and alloys	Shigeyuki Murayama	Muroran Institute of Technology
92	〃	雨海　有佑	室蘭工業大学	大学院工学研究科	〃	Yusuke Amakai	Muroran Institute of Technology
93	〃	荒川　恵理	室蘭工業大学	大学院工学研究科	〃	Eri Arakawa	Muroran Institute of Technology

No.	課題名	氏名	所属		Title	Name	Organization
94	固体ヘリウム４の界面近傍におけるずれ弾性測定	青木　悠樹	東京工業大学	大学院総合理工学研究科	Shear modulus measurement of solid helium-4 at near interface	Yuki Aoki	Tokyo Institute of Technology
95	〃	岩佐　泉	神奈川大学	理学部	〃	Izumi Iwasa	Kanagawa University
96	固体ヘリウムの超流動に見られる様な「新規超流動現象の基礎研究」	久保田　実	芝浦工業大学	総合研究所	Fundamental study of new types of superfluidity, as seen in solid 4He	Minoru Kubota	Shibaura Institute of Technology
97	高圧下における Eu 化合物の価数転移の探索	本多　史憲	東北大学	金属材料研究所	Investigation of valence transition on Eu compounds under high pressure	Fuminori Honda	Tohoku University
98	〃	大貫　惇睦	琉球大学	理学部	〃	Yoshichika Onuki	University of the Ryukyus
99	三角格子磁性体 $NaM(Acac)_3benzen$(M=Fe,Ni,Co,Mn) の低温磁性	柄木　良友	琉球大学	教育学部	Low temperature magnetizm of triangular lattice antiferromagnet $NaM(acac)_3benzen$	Yoshitomo Karaki	University of the Ryukyus
100	磁化測定用対向アンビル型高圧力発生装置の開発 (4)	藤原　哲也	山口大学	大学院理工学研究科	Development of opposed-anvil type high pressure apparatus for magnetization measurement IV	Tetsuya Fujiwara	Yamaguchi University
101	〃	田端　克好	山口大学	大学院理工学研究科	〃	Katsuyoshi Tabata	Yamaguchi University
102	磁性単層膜の電気伝導	大橋　政司	金沢大学	理工研究域	Electronic transport properties of magnetic monolayer	Masashi Ohashi	Kanazawa University
103	〃	岸井　信也	金沢大学	大学院自然科学研究科	〃	Nobuya Kishii	Kanazawa University
104	重い電子系反強磁性体 $CeNiIn_4$ の高圧下電子状態の研究	松本　裕司	名古屋工業大学	大学院工学研究科	The study of electronic state for antiferromagnet heavy fermion $CeNiIn_4$ under high pressure	Yuji Matsumoto	Nagoya Institute of Technology
105	〃	浅野　雄平	名古屋工業大学	大学院工学研究科	〃	Yuhei Asano	Nagoya Institute of Technology
106	重い電子系物質における 3He 温度領域での磁化測定	佐藤　由昌	九州大学	大学院工学府	Magnetization measurements in 3He temperature region for heavy fermion systems	Yoshiaki Sato	Kyushu University
107	正方晶の V_2Ga_5 の圧力下の輸送特性	仲間　隆男	琉球大学	理学部	Transport properties of the single crystal V_2Ga_5 with tetragonal structure	Takao Nakama	University of the Ryukyus
108	〃	照屋　淳志	琉球大学	大学院理工学研究科	〃	Atsushi Teruya	University of the Ryukyus
109	〃	上門　太郎	琉球大学	大学院理工学研究科	〃	Taro Uejyo	University of the Ryukyus
110	多形化合物 RIr_2Si_2(R= 希土類）の磁気転移２	繁岡　透	山口大学	大学院理工学研究科	Magnetic transition of polymorphic compound RIr_2Si_2 (R=rera earth)$_2$	Toru Shigeoka	Yamaguchi University

No.	課題名	氏名	所属		Title	Name	Organization
111	〃	森田　哲広	山口大学	大学院理工学研究科	〃	Tetsuhiro Morita	Yamaguchi University
112	多重極限下のゼーベック係数測定システムの開発	辺土　正人	琉球大学	理学部	Development of new Seebeck coefficient measurement system under multiple extreme conditions	Masato Hedo	University of the Ryukyus
113	〃	友利　圭佑	琉球大学	大学院理工学研究科	〃	Keisuke Tomori	University of the Ryukyus
114	超流動 He-3,A1 相中のジョセフソン接合の作成と量子干渉効果の検出	山口　明	兵庫県立大学	大学院物質理学研究科	Development of Josephson device and search for novel quantum interference effects in superfluid He-3 A1 phase	Akira Yamaguchi	The Univerisity of Hyogo
115	超流動ヘリウム 3-A 相の半整数量子渦の検出	石川　修六	大阪市立大学	大学院理学研究科	Investigation of the half quantized vortex in superfluid 3He-A phase	Osamu Ishikawa	Osaka City University
116	〃	國松　貴之	大阪市立大学	大学院理学研究科	〃	Takayuki Kunimatsu	Osaka City University
117	超流動ヘリウム A1 相におけるジョセフソン効果	白濱　圭也	慶應義塾大学	理工学部	Josephson effect in superfluid He-3 A1 phase	Keiya Shirahama	Keio University
118	導電性ラングミュア・ブロジェット膜の高圧下の電気的性質に関する研究	三浦　康弘	桐蔭横浜大学	大学院工学研究科	Studies on electrical properties of conductive langmuir-blodgett films under high pressure	Yasuhiro Miura	Toin University of Yokohama
119	有機分子性導体の高圧物性の研究	鳥塚　潔	法政大学	理工学部	Studies on high pressure properties of organic molecular conductors	Kiyoshi Torizuka	Hosei University
120	Co 基ホイスラー合金における圧力誘起マルテンサイト変態に関する研究	重田　出	鹿児島大学	大学院理工学研究科	Study on pressure-induced martensitic phase transformation in Co-based Heusler alloys	Iduru Shigeta	Kagoshima University
121	〃	藤本　祐太郎	鹿児島大学	大学院理工学研究科	〃	Yutaro Fujimoto	Kagoshima University
122	高圧下での Yb_4As_3 の電気抵抗測定	中村　修	岡山理科大学	学外連携推進室	Transport properties of Yb_4As_3 under high pressure	Osamu Nakamura	Okayama University of Science
123	回転希釈冷凍機を用いた量子固体・量子液体研究	高橋　大輔	足利工業大学	共通過程	Studies of quantum fluids and solids using rotating dilution refrigerators	Daisuke Takahashi	Ashikaga Institute of Technology
124	〃	村川　智	慶應義塾大学	理工学部	〃	Satoshi Murakawa	Keio University
125	〃	立木　智也	慶應義塾大学	大学院理工学研究科	〃	Tomoya Tsuiki	Keio University
担当所員：廣井　善二							
126	3d 遷移金属多窒化物の高圧合成	丹羽　健	名古屋大学	大学院工学研究科	High pressure synthesis of 3d transition metal pernitride	Ken Niwa	Nagoya University

No.	課題名	氏名	所属		Title	Name	Organization
127	〃	寺部　俊紀	名古屋大学	大学院工学研究科	〃	Toshiki Terabe	Nagoya University
128	マルチフェロイック特性を有する新規ペロブスカイト型酸化物の高圧合成	丹羽　健	名古屋大学	大学院工学研究科	High pressure synthesis of new multiferroic oxides with perovskite-type structure	Ken Niwa	Nagoya University
129	〃	志村　元	名古屋大学	大学院工学研究科	〃	Gen Shimura	Nagoya University
130	下部マントル条件において、水素がケイ酸塩鉱物の相関係に与える影響	篠崎　彩子	東京大学	大学院理学系研究科	Influence of H_2 fluid on the stability of silicate minerals under lower mantle condition	Ayako Shiozaki	The University of Tokyo
131	空間反転対称性のない結晶構造を有する新超伝導体の物質探索	関根　ちひろ	室蘭工業大学	大学院工学研究科	Search for new superconductors with noncentrosymmetric structure	Chihiro Sekine	Muroran Institute of Technology
132	〃	崔　云	室蘭工業大学	大学院工学研究科	〃	Un Sai	Muroran Institute of Technology
133	高圧下におけるベンゼンからの多環芳香族炭化水素の生成条件	篠崎　彩子	東京大学	大学院理学系研究科	Formation of polycyclic aromatic hydrocarbons from benzene under high pressure condition	Ayako Shiozaki	The University of Tokyo
134	新規イオン伝導性化合物の超高圧合成	長谷川　正	名古屋大学	大学院工学研究科	High pressure syntheses of novel ion conductors	Masashi Hasegawa	Nagoya University
135	〃	廣瀬　瑛一	名古屋大学	大学院工学研究科	〃	Eiichi Hirose	Nagoya University
136	層状酸化物 $HLaNb_2O_7$ における圧力誘起アモルファス化	陰山　洋	京都大学	大学院工学研究科	Pressure-induced amorphization of layered metal oxides	Hiroshi Kageyama	Kyoto University
137	〃	山本　隆文	京都大学	大学院工学研究科	〃	Takafumi Yamamoto	Kyoto University
138	〃	セドリック　タッセル	京都大学	白眉センター	〃	Cedric Tassel	Kyoto University
139	〃	村上　泰斗	京都大学	大学院工学研究科	〃	Taito Murakami	Kyoto University
140	核−マントル境界における金属鉄−ケイ酸塩メルト間の塩素分配に関する実験的研究	桑原　秀治	東京大学	大学院新領域創成科学研究科	An experimental study on metal-silicate partitioning of chlorine at core-mantle boundary conditions	Hideharu Kuwahara	The University of Tokyo
担当所員：川島　直輝							
141	テンソルネットワーク変分法の数値アルゴリズムの開発	原田　健自	京都大学	大学院情報学研究科	Development of numerical algorithm of tensor network variational method	Kenji Harada	Kyoto University
142	蜂の巣格子上反強磁性 Heisenberg-Kitaev 模型の磁気的性質	鈴木　隆史	兵庫県立大学	大学院工学研究科	Magnetic properties of the antiferromagnetic Heisenberg-Kitaev model on a honeycomb lattice	Takafumi Suzuki	The Univerisity of Hyogo

No.	課題名	氏名	所属		Title	Name	Organization
担当所員：益田　隆嗣							
143	希土類化合物単結晶の物質評価	繁岡　透	山口大学	大学院理工学研究科	Characterization of rare earth single crystal compounds	Toru Shigeoka	Yamaguchi University
144	〃	中田　琢也	山口大学	大学院理工学研究科	〃	Takuya Nakada	Yamaguchi University
145	非磁性不純物による三角スピンチューブのスピンダイナミクスの変化	真中　浩貴	鹿児島大学	大学院理工学研究科	Non-magnetic impurity effect on spin dynamics of triangular spin tubes	Hirotaka Manaka	Kagoshima University
146	スピネル型バナジウム酸化物における磁気励起の観測	阿部　伸行	東京大学	大学院新領域創成科学研究科	Measurement of magnetic excitation in spinel type vanadate	Nobuyuki Abe	The University of Tokyo
147	〃	松浦　慧介	東京大学	大学院新領域創成科学研究科	〃	Keisuke Matsuura	The University of Tokyo
148	高エネルギー X 線ラウエ法を用いたヘリカル磁性合金 Gd-RE (RE=Y,La) の単結晶試料の評価	山崎　照夫	東京理科大学	理工学部	Evaluation of the single crystalline samples of helical magnetic alloys Gd-RE (RE=Y,La) by high-energy X-ray Laue method	Teruo Yamazaki	Tokyo University of Science
149	〃	栗原　舞	東京理科大学	大学院理工学研究科	〃	Mai Kurihara	Tokyo University of Science
担当所員：吉澤　英樹							
150	$(Ho,Y)Rh_2Si_2$ 単結晶の磁気特性	繁岡　透	山口大学	大学院理工学研究科	Magnetic characteristics of $(Ho,Y)Rh_2Si_2$ single crystal	Toru Shigeoka	Yamaguchi University
151	〃	藤井　洋	山口大学	大学院理工学研究科	〃	Yoh Fujii	Yamaguchi University
152	パイロクロア酸化物磁性体 $Tb_2Ti_2O_7$ の比熱測定	高津　浩	首都大学東京	大学院理工学研究科	Specific heat measurements on a pyrochlore oxide $Tb_2Ti_2O_7$	Hiroshi Takatsu	Tokyo Metropolitan University
153	〃	布山　直樹	首都大学東京	大学院理工学研究科	〃	Naoki Nunoyama	Tokyo Metropolitan University
154	金属ヘリカル磁性体 $Gd_{1-x}Y_x$ 合金の H-T 相図	山崎　照夫	東京理科大学	理工学部	H-T phase diagram of the metallic helimagnet $Gd_{1-x}Y_x$	Teruo Yamazaki	Tokyo University of Science
155	〃	栗原　舞	東京理科大学	大学院理工学研究科	〃	Mai Kurihara	Tokyo University of Science
担当所員：金道　浩一							
156	$(Cu,Zn)_3(Mo,W)_2O_9$ のパルス磁場中の熱力学的性質	黒江　晴彦	上智大学	理工学部	Thermodynamic properties in $(Cu,Zn)_3(Mo,W)_2O_9$ under pulsed magnetic fields	Haruhiko Kuroe	Sophia University

No.	課題名	氏名	所属		Title	Name	Organization
157	(Ho,Gd)Rh_2Si_2 単結晶の高磁場磁化２	繁岡　透	山口大学	大学院理工学研究科	High field magnetization of (Ho,Gd)Rh_2Si_2 single crystal2	Toru Shigeoka	Yamaguchi University
158	〃	森田　哲広	山口大学	大学院理工学研究科	〃	Tetsuhiro Morita	Yamaguchi University
159	10MJ コンデンサーバンク用大型ワイドボアパルスマグネットの開発	萩原　政幸	大阪大学	大学院理学研究科	Development of a large wide-bore pulse magnet for a 10MJ capacitor bank	Masayuki Hagiwara	Osaka University
160	〃	谷口　一也	大阪大学	大学院理学研究科	〃	Kazuya Taniguchi	Osaka University
161	$YbInCu_4$ の置換系における強磁場磁化過程	道岡　千城	京都大学	大学院理学研究科	High-field magnetization in the substituted system of $YbInCu_4$	Chishiro Michioka	Kyoto University
162	〃	今井　正樹	京都大学	大学院理学研究科	〃	Masaki Imai	Kyoto University
163	〃	中東　太一	京都大学	大学院理学研究科	〃	Taichi Nakahigashi	Kyoto University
164	カゴメ格子をもつ 3d 遷移金属フッ化物の磁性	植田　浩明	京都大学	大学院理学研究科	Magnetic studies of 3d transition metal fluorides with a kagome lattice	Hiroaki Ueda	Kyoto University
165	〃	後藤　真人	京都大学	大学院理学研究科	〃	Masato Goto	Kyoto University
166	〃	山川　智大	京都大学	大学院理学研究科	〃	Tomohiro Yamakawa	Kyoto University
167	ホイスラー化合物 Ni_2MnGa の強磁場磁化測定	伊藤　昌和	鹿児島大学	大学院理工学研究科	Magnetization of Heusler alloy Ni_2MnGa in high magnetic field	Masakazu Ito	Kagoshima University
168	ホイスラー化合物の強磁場磁化	廣井　政彦	鹿児島大学	大学院理工学研究科	Magnetizaiton of some Heusler compounds in high magnetic field	Masahiko Hiroi	Kagoshima University
169	〃	佐野　紘晃	鹿児島大学	大学院理工学研究科	〃	Hiroaki Sano	Kagoshima University
170	希土類金属間化合物の強磁場物性研究	海老原　孝雄	静岡大学	大学院理学研究科	Physical phenomena at high magnetic fields in rear earth intermetallic compounds	Takao Ebihara	Shizuoka University
171	〃	土屋　政人	静岡大学	大学院理学研究科	〃	Masato Tsuchiya	Shizuoka University
172	金属ナノ結晶の磁化特性	稲田　貢	関西大学	システム理工学部	Magnetic properties of metal nanocrystals	Mitsuru Inada	Kansai University
173	高温超伝導体のパルス強磁場下輸送現象	掛谷　一弘	京都大学	大学院工学研究科	Transport phenomena in high-Tc superconductors under pulsed high magnetic fields	Itsuhiro Kakeya	Kyoto University

No.	課題名	氏名	所属		Title	Name	Organization
174	高ドープ高温超伝導体のパルス強磁場下輸送現象	渡辺　孝夫	弘前大学	大学院理工学研究科	Transport properties in heavily overdoped high-Tc superconductors under pulsed high magnetic fields	Takao Watanabe	Hirosaki University
175	〃	臼井　友洋	弘前大学	大学院理工学研究科	〃	Tomohiro Usui	Hirosaki University
176	新規 S=1/2 擬カゴメ格子磁性体の強磁場磁化過程	浅野　貴行	福井大学	大学院工学研究科	Magnetization process in novel S=1/2 pseudo-kagome lattice magnets	Takayuki Asano	University of Fukui
177	〃	川見　洋一郎	九州大学	大学院理学府	〃	Yoichiro Kawami	Kyushu University
178	単結晶 $LaCo_{1-x}Rh_xO_3$ の強磁場誘起スピン転移	佐藤　桂輔	茨城工業高等専門学校		Field induced spin-state transition in single crystal $LaCo_{1-x}Rh_xO_3$	Keisuke Sato	Ibaraki National College of Technology
179	有機／無機スピン源を有する新規量子スピン系の強磁場磁化測定	小野　俊雄	大阪府立大学	大学院理学系研究科	High field magnetization measurements on the new quantum spin systems with organic/inorganic spin sources	Toshio Ono	Osaka Prefecture University
180	〃	天谷　直樹	大阪府立大学	大学院理学系研究科	〃	Naoki Amaya	Osaka Prefecture University
181	〃	菊地　健太郎	大阪府立大学	大学院理学系研究科	〃	Kentaro Kikuchi	Osaka Prefecture University
182	〃	笠谷　和宏	大阪府立大学	大学院理学系研究科	〃	Kazuhiro Kasatani	Osaka Prefecture University
担当所員：松田　康弘							
183	固体酸素の磁場−温度相図の決定	小林　達生	岡山大学	大学院自然科学研究科	Field-temperature phase diagram in solid oxygen	Tatsuo C. Kobayashi	Okayama University
184	磁性強誘電体における強磁場下方向複屈折	有馬　孝尚	東京大学	大学院新領域創成科学研究科	Directional birefringence in magnetic ferroelectrics in a high magnetic field	Takahisa Arima	The University of Tokyo
185	〃	阿部　伸行	東京大学	大学院新領域創成科学研究科	〃	Nobuyuki Abe	The University of Tokyo
186	磁性強誘電体における強磁場下方向複屈折	豊田　新悟	東京大学	大学院新領域創成科学研究科	Directional birefringence in magnetic ferroelectrics in a high magnetic field	Shingo Toyoda	The University of Tokyo
担当所員：徳永　将史							
187	$(Cu,Zn)_3(Mo,W)_2O_9$ のパルス磁場中の格子歪・磁化・電気分極測定	黒江　晴彦	上智大学	理工学部	Magnetostriction-, magnetization-, and electric-polarization-measurements in $(Cu,Zn)_3(Mo,W)_2O_9$ under pulsed magnetic fields	Haruhiko Kuroe	Sophia University
188	$Pr_{1-x}AxMnO_3$ (A=Ca or Sr) の反強磁性と熱電特性に関する研究	中津川　博	横浜国立大学	大学院工学研究院	Antiferromagnetism and thermoelectric properties in $Pr_{1-x}AxMnO_3$ (A=Ca or Sr)	Hiroshi Nakatsugawa	Yokohama National University

No.	課題名	氏名	所属		Title	Name	Organization
189	〃	窪田　正照	横浜国立大学	大学院工学府	〃	Masaki Kubota	Yokohama National University
190	パイロクロア型イリジウム酸化物の強磁場下の物性研究	松平　和之	九州工業大学	大学院工学研究院	Transport and magnetic properties of pyrochlore iridates under high field magnetic field	Kazuyuki Matsuhira	Kyushu Institute of Technology
191	フラストレーションを有する磁性体の強磁場磁化過程	香取　浩子	東京農工大学	大学院工学研究院	High-field magnetization of frustrated magnets	Hiroko Katori	Tokyo University of Agriculture and Technology
192	〃	斉藤　大地	東京農工大学	大学院工学府	〃	Daichi Saito	Tokyo University of Agriculture and Technology
193	圧力誘起超伝導体 $CePt_2In_7$ の強磁場物性研究	摂待　力生	新潟大学	理学部	High-magnetic-field study of pressure-induced superconductor $CePt_2In_7$	Rikio Settai	Niigata University
194	〃	太田　俊平	新潟大学	大学院自然科学研究科	〃	Shunpei Ota	Niigata University
195	三元系コバルトニクタイドの強磁場磁化過程	太田　寛人	東京農工大学	大学院工学研究院	Magnetic behavior of ternary cobalt pnictogen compounds	Hiroto Ohta	Tokyo University of Agriculture and Technology
196	〃	赤羽　栄介	東京農工大学	大学院工学府	〃	Eisuke Akabane	Tokyo University of Agriculture and Technology
197	超強磁場を利用した CoCr 基合金におけるリエントラント挙動を示すマルテンサイト変態の観察および起源解明	キョキョウ	東北大学	大学院工学研究科	Observation and clarification of the origin of re-entrant martensitic transformation using strong magnetic field in CoCr based alloys	Xiao XU	Tohoku University
198	電界誘起量子相の強磁場物性	笠原　裕一	東京大学	大学院工学系研究科	High-field properties of electric-field-induced quantum phases	Yuichi Kasahara	The University of Tokyo
199	非破壊パルスマグネットを用いたグラファイトの強磁場誘起密度波相の研究	矢口　宏	東京理科大学	理工学部	Study of the high-magnetic-field-induced density-wave phase in graphite using non-destructive pulsed magnets	Hiroshi Yaguchi	Tokyo University of Science
200	正 20 面体対称クラスターを持つ複雑合金の磁化過程	廣戸　孝信	東京理科大学	大学院基礎工学研究科	Magnetization study on complex metallic alloys with icosahedral symmetry cluster	Takanobu Hiroto	Tokyo University of Science
201	ビスマス正方格子を有する新規ディラック系層状物質における量子振動の観測	酒井　英明	東京大学	大学院工学系研究科	Observation of quantum oscillation for a Dirac metal with Bi square nets	Hideaki Sakai	The University of Tokyo
202	マルチフェロイック物質 $LiNiPO_4$ の非整合磁気秩序相における電気分極測定	木原　工	東北大学	金属材料研究所	Electric polarization measurements in incommensurate magnetic ordered phase of the multiferroic material $LiNiPO_4$	Takumi Kihara	Tohoku University
担当所員：辛　埴							
203	2 光子 ARPES を用いた $GeTe/Sb_2Te_3$ 超構造におけるディラックフェルミオンの観測	木村　昭夫	広島大学	大学院理学研究科	Study of Dirac fermions in $GeTe/Sb_2Te_3$ superlattices by two-photon ARPES	Akio Kimura	Hiroshima University
204	2 光子 ARPES を用いた相変化物質 Ge-Sb-Te おけるディラックフェルミオンの観測	朱　思源	広島大学	大学院理学研究科	Study of Dirac ferimions in phase change materials Ge-Sb-Te by two-photon ARPES	Zhu, Siyuan	Hiroshima University

No.	課題名	氏名	所属		Title	Name	Organization
205	極性半導体の表面およびバルクにおける電子構造	石坂　香子	東京大学	大学院工学系研究科	Bulk and surface electronic structures of polar semiconductors	Kyoko Ishizaka	The University of Tokyo
206	空間反転対称性の破れたビスマス化合物超伝導体における電子構造	坂野　昌人	東京大学	大学院工学系研究科	Electronic structure of noncentrosymmetric bismuth compound superconductor	Masato Sakano	The University of Tokyo
207	新奇量子異常ホール系トポロジカル絶縁体の２光子 ARPES	木村　昭夫	広島大学	大学院理学研究科	Two photon ARPES of quantum anomalous Hall topological insulators	Akio Kimura	Hiroshima University
担当所員：高橋　敏男							
208	希薄磁性半導体 GaGdAs 単層ならびに GaGdAs/GaAa 超格子の界面および結晶構造に及ぼす成長条件の影響	宮川　勇人	香川大学	工学部	Growth condition effect on interfaces and crystal structure of diluted magnetic semiconductor GaGdAs single layer and GaGdAs/GaAs superlattices	Hayato Miyagawa	Kagawa University
209	〃	山野　高史	香川大学	大学院工学研究科	〃	Takashi Yamano	Kagawa University
210	〃	大西　吉行	香川大学	大学院工学研究科	〃	Yoshiyuki Onishi	Kagawa University
211	Si 基板上における GaN/GaNAs 超格子の構造評価	小柴　俊	香川大学	工学部	Structural evaluation of GaN/GaAs superlattice on Si	Shyun Koshiba	Kagawa University
212	〃	加太　俊	香川大学	大学院工学研究科	〃	Shun Kabuto	Kagawa University
担当所員：秋山　英文							
213	GaAs/GaAsN 超格子の電子構造に関する研究	矢口　裕之	埼玉大学	大学院理工学研究科	Electronic structure of GaAs/GaAsN superlattices	Hiroyuki Yaguchi	Saitama University
214	〃	高宮　健吾	埼玉大学	大学院理工学研究科	〃	Kengo Takamiya	Saitama University
215	〃	山崎　泰由	埼玉大学	大学院理工学研究科	〃	Yasuyuki Yamazaki	Saitama University
216	Si 基板上における GaN/GaNAs 超格子の光学評価	小柴　俊	香川大学	工学部	Optical assessment of structural evaluation of GaN/GaAs superlattice on Si	Shyun Koshiba	Kagawa University
217	〃	加太　俊	香川大学	大学院工学研究科	〃	Shun Kabuto	Kagawa University
担当所員：末元　徹							
218	テラヘルツ分光装置を用いた酸化物磁性材料の研究	大越　慎一	東京大学	大学院理学系研究科	Study of magnetic oxide using terahertz spectroscopy	Shinichi Ohkoshi	The University of Tokyo

No.	課題名	氏名	所属		Title	Name	Organization
219	〃	生井　飛鳥	東京大学	大学院理学系研究科	〃	Asuka Namai	The University of Tokyo
220	〃	吉清　まりえ	東京大学	大学院理学系研究科	〃	Marie Yoshikiyo	The University of Tokyo
221	(BEDT-TTF)(TCNQ) 結晶における可視 - 近赤外反射スペクトルの温度変化	三野　弘文	千葉大学	普遍教育センター	Temperature dependence of visible to near-infrared reflectance spectra in (BEDT-TTF)(TCNQ) crystals	Hirofumi Mino	Chiba University
222	〃	貞本　貢汰	千葉大学	大学院理学研究科	〃	Kota Sadamoto	Chiba University

物質合成・評価設備 P クラス / Materials Synthesis and Characterization P Class Researcher

No.	課題名	氏名	所属		Title	Name	Organization
1	遷移金属酸窒化物、金属間化合物における構造物性研究	山浦　淳一	東京工業大学	元素戦略研究センター	Structural physics on the transition metal oxynitrides and intermetallic compounds	Junichi Yamaura	Tokyo Institute of Technology
2	低温脱硫処理で得られた不定比性硫化物の構造と組成	陰山　洋	京都大学	大学院工学研究科	Composition and structure of non-stoichiometric sulfides obtained by low temperature desulfurization	Hiroshi Kageyama	Kyoto University
3	〃	小林　洋治	京都大学	大学院工学研究科	〃	Yoji Kobayashi	Kyoto University
4	〃	ギヨーム　ブイー	京都大学	大学院工学研究科	〃	Guillaume Bouilly	Kyoto University
5	〃	増田　直也	京都大学	大学院工学研究科	〃	Naoya Masuda	Kyoto University
6	超臨界流体を含む高密度溶媒中レーザーアブレーションプラズマの分光解析	シュタウス　スヴェン	東京大学	大学院新領域創成科学研究科	Spectroscopic investigation of laser ablation plasmas generated in high-density fluids up to supercritical fluid state	Sven Stauss	The University of Tokyo
7	〃	姫野　翔平	東京大学	大学院新領域創成科学研究科	〃	Shohei Himeno	The University of Tokyo
8	パイロクロア型希土類酸化物の単結晶育成と磁気フラストレーションの研究	松平　和之	九州工業大学	大学院工学研究院	Single crystal growth and study of frustrated magnetism in pyrochlore rare-earth oxides	Kazuyuki Matsuhira	Kyushu Institute of Technology
9	軌道とスピンの自由度を有する遷移金属系物質の純良単結晶育成と物性評価	片山　尚幸	名古屋大学	大学院工学研究科	Growth of single crystals of transition metal compounds with orbital and spin degrees of freedom	Naoyuki Katayama	Nagoya University
10	〃	中埜　彰俊	名古屋大学	大学院工学研究科	〃	Akitoshi Nakano	Nagoya University
11	〃	杉山　由季	名古屋大学	大学院工学研究科	〃	Yuki Sugiyama	Nagoya University

物質合成・評価設備 G クラス / Materials Synthesis and Characterization G Class Researcher

No.	課題名	氏名	所属		Title	Name	Organization
1	高温高圧水を用いた医療廃棄物の小型オンサイト処理システムの開発	大友　順一郎	東京大学	大学院新領域創成科学研究科	Development of small size on-site disposal system in sub- and supercritical water for medical waste	Junichiro Otomo	The University of Tokyo
2	〃	長澤　祐介	東京大学	大学院新領域創成科学研究科	〃	Yusuke Nagasawa	The University of Tokyo
3	ペロブスカイト型酸化物を用いたケミカルルーピングシステムの開発	大友　順一郎	東京大学	大学院新領域創成科学研究科	The study of perovskite based oxygen carrier materials for CLC/CLR applications	Junichiro Otomo	The University of Tokyo
4	〃	オーチェン ジェームズ オーチェン	東京大学	大学院新領域創成科学研究科	〃	Ochieng James Ochieng	The University of Tokyo
5	金属酸化物の酸化還元反応における担体効果の検討	大友　順一郎	東京大学	大学院新領域創成科学研究科	Effect of support materials on redox reaction of metal oxides	Junichiro Otomo	The University of Tokyo
6	〃	高坂　文彦	東京大学	大学院新領域創成科学研究科	〃	Fumihiko Kosaka	The University of Tokyo
7	高温高圧水中における固体酸・塩基触媒反応の速度論的解析	大友　順一郎	東京大学	大学院新領域創成科学研究科	Kinetic analysis of solid acid and base catalyzed reactions in sub- and supercritical water	Junichiro Otomo	The University of Tokyo
8	〃	秋月　信	東京大学	大学院新領域創成科学研究科	〃	Makoto Akizuki	The University of Tokyo
9	酸化セリウム・メソポーラスマテリアル・グラフェンオキサイド - 金属微粒子系のキャラクタリゼーション	佐々木　岳彦	東京大学	大学院新領域創成科学研究科	Characterization for metal nanoparticles dispersed on ceria, mesoporous materials and graphene oxide	Takehiko Sasaki	The University of Tokyo
10	〃	原田　慧	東京大学	大学院新領域創成科学研究科	〃	Kei Harada	The University of Tokyo
11	〃	Etty Nurlia Kusumawati	東京大学	大学院理学系研究科	〃	Etty Nurlia Kusumawati	The University of Tokyo
12	フラストレート磁性とスピン軌道相互作用の協調・競合効果	有馬　孝尚	東京大学	大学院新領域創成科学研究科	Interplay between frustrated magnetism and spin-orbit interaction	Takahisa Arima	The University of Tokyo
13	〃	阿部　伸行	東京大学	大学院新領域創成科学研究科	〃	Nobuyuki Abe	The University of Tokyo
14	〃	植松　大介	東京大学	大学院新領域創成科学研究科	〃	Daisuke Uematsu	The University of Tokyo
15	〃	塩澤　俊介	東京大学	大学院新領域創成科学研究科	〃	Shunnsuke Shiozawa	The University of Tokyo
16	〃	松浦　慧介	東京大学	大学院新領域創成科学研究科	〃	Keisuke Matsuura	The University of Tokyo

No.	課題名	氏名	所属		Title	Name	Organization
17	パイロクロア格子またはカゴメ格子をもつ遷移金属フッ化物の物性評価	植田　浩明	京都大学	大学院理学研究科	Characterization of transition metal fluorides with pyrochlore or kagome lattice	Hiroaki Ueda	Kyoto University
18	〃	小林　慎太郎	京都大学	大学院理学研究科	〃	Shintaro Kobayashi	Kyoto University
19	〃	田口　篤史	京都大学	大学院理学研究科	〃	Atsushi Taguchi	Kyoto University
20	LSCF 空気極酸素還元反応に対する SOFC 製造工程由来微量成分の影響評価	大友　順一郎	東京大学	大学院新領域創成科学研究科	The effects of minor components in LSCF cathode on oxygen reduction reaction	Junichiro Otomo	The University of Tokyo
21	〃	大石　淳矢	東京大学	大学院新領域創成科学研究科	〃	Junya Oishi	The University of Tokyo
22	アンモニア分解及び合成反応における電気化学特性と速度論解析	大友　順一郎	東京大学	大学院新領域創成科学研究科	Electrochemical reaction and its kinetic analysis in ammonia decomposition and synthesis	Junichiro Otomo	The University of Tokyo
23	〃	野田　直人	東京大学	大学院新領域創成科学研究科	〃	Naoto Noda	The University of Tokyo
24	ケミカルループ法における酸化物イオン伝導体を用いた酸素キャリア材料の寿命評価	大友　順一郎	東京大学	大学院新領域創成科学研究科	Evaluation of life time of metal oxides supported by oxide ion conductors in chemical looping combustion	Junichiro Otomo	The University of Tokyo
25	〃	菊池　典晃	東京大学	大学院新領域創成科学研究科	〃	Noriaki Kikuchi	The University of Tokyo
26	プロトン伝導性リン酸ガラス - セラミックス薄膜の微構造観察とイオン伝導特性	大友　順一郎	東京大学	大学院新領域創成科学研究科	Evaluation of microstructure and proton conductivity in phosphate glass-ceramics thin films	Junichiro Otomo	The University of Tokyo
27	〃	門田　稔	東京大学	大学院新領域創成科学研究科	〃	Minoru Kadota	The University of Tokyo
28	結晶界面における無機複合型プロトン電解質の合成とイオン伝導度の評価	大友　順一郎	東京大学	大学院新領域創成科学研究科	Synthesis of proton conducting electrolyte and evaluation of ion conductivity of grain boundary	Junichiro Otomo	The University of Tokyo
29	〃	岩永　愛季	東京大学	大学院新領域創成科学研究科	〃	Aki Iwanaga	The University of Tokyo
30	高温高圧水中における層状固体酸触媒反応	大友　順一郎	東京大学	大学院新領域創成科学研究科	Study of layered solid acid catalyzed reaction in sub- and supercritical water	Junichiro Otomo	The University of Tokyo
31	〃	名越　詩織	東京大学	大学院新領域創成科学研究科	〃	Shiori Nagoya	The University of Tokyo
32	超臨界水熱合成による複合酸化物ナノ粒子の合成とその生成機構解明	大友　順一郎	東京大学	大学院新領域創成科学研究科	Elucidation of formation mechanism for mixed oxide nanoparticles under supercritical hydrothermal synthesis	Junichiro Otomo	The University of Tokyo
33	〃	横　哲	東京大学	大学院新領域創成科学研究科	〃	Akira Yoko	The University of Tokyo

No.	課題名	氏名	所属		Title	Name	Organization
34	有機ハイドライドの電極酸化還元反応における電極開発と速度論解析	大友　順一郎	東京大学	大学院新領域創成科学研究科	Development of electrode catalyst and kinetic analysis in redox reactions of organic hydrides on electrode	Junichiro Otomo	The University of Tokyo
35	〃	酒井　良輔	東京大学	大学院新領域創成科学研究科	〃	Ryosuke Sakai	The University of Tokyo
36	触媒反応の in situ ラマン散乱測定	佐々木　岳彦	東京大学	大学院新領域創成科学研究科	In situ measurement of Raman scattering for heterogeneous catalytic reactions	Takehiko Sasaki	The University of Tokyo
37	〃	板子　健太郎	東京大学	大学院新領域創成科学研究科	〃	Kentaro Itako	The University of Tokyo
38	超臨界二酸化炭素中パルスレーザーアブレーションのイメージング分光	占部　継一郎	東京大学	大学院新領域創成科学研究科	Imaging spectroscopy for pulsed laser ablation plasma in supercritical carbon-dioxide	Keiichiro Urabe	The University of Tokyo
39	Si 基ナノ複合熱電材料の TEM による微細組織評価	宮崎　吉宣	大阪大学	大学院工学研究科	Microstructural analysis of Si-based nanocomposite thermoelectric materials using TEM	Yoshinobu Miyazaki	Osaka University
40	スピンクロスオーバー転移におけるドメイン成長の直接観測	糸井　充穂	日本大学	医学部	Direct observation of domain growth upon thermal spin crossover phenomena	Miho Itoi	Nihon University
41	形態制御に基づく蓄電池材料開発	細野　英司	産業技術総合研究所	エネルギー技術研究部門	Development of the battery materials based on the morphology control	Eiji Hosono	National Institute of Advanced Industrial Science and Technology
42	新規磁石材料の微細構造解析	齋藤　哲治	千葉工業大学	工学部	Microstructural studies of newly developed permanent magnet materials	Tetsuji Saito	Chiba Institute of Technology
43	天然鉱物の微細組織と結晶性の実態	永嶌　真理子	山口大学	大学院理工学研究科	Evaluation of micro-texture and crystallinity of natural minerals	Mariko Nagashima	Yamaguchi University
44	溶融成長バルク超伝導体の磁性と構造組織に関する研究	和泉　充	東京海洋大学	大学院海洋科学技術研究科	Magnetic properties and microstructural organization of melt-growth bulk superconductors	Mitsuru Izumi	Tokyo University of Marine Science and Technology
45	〃	周　迪帆	弓削商船高等専門学校		〃	Difan Zhou	Yuge National College of Maritime Technology
46	ハーフメタル型 Mn 基ホイスラー合金の磁性と輸送特性に関する研究	重田　出	鹿児島大学	大学院理工学研究科	Study on the magnetic and transport properties of half-metallic Mn-based Heusler alloys	Iduru Shigeta	Kagoshima University
47	〃	重松　理史	鹿児島大学	大学院理工学研究科	〃	Satoshi Shigematsu	Kagoshima University
48	ホイスラー型化合物の磁性と伝導の研究	廣井　政彦	鹿児島大学	大学院理工学研究科	Study on the magnetic and electrical properties of Heusler compounds	Masahiko Hiroi	Kagoshima University
49	〃	西井上　創羅	鹿児島大学	大学院理工学研究科	〃	Soura Nishiinoue	Kagoshima University
50	新規ペロブスカイト系関連酸化物の磁気物性	長谷川　正	名古屋大学	大学院工学研究科	Magnetism of novel perovskite-type oxides	Masashi Hasegawa	Nagoya University

No.	課題名	氏名	所属		Title	Name	Organization
51	〃	志村　元	名古屋大学	大学院工学研究科	〃	Gen Shimura	Nagoya University
52	正 20 面体準結晶および近似結晶の磁性	廣戸　孝信	東京理科大学	大学院基礎工学研究科	Magnetic properties of icosahedral quasicrystals and its approximants	Takanobu Hiroto	Tokyo University of Science
53	Cu－Ni－X（X=Co,Fe）系単結晶性合金中の磁性微粒子析出過程と磁気特性の関係	竹田　真帆人	横浜国立大学	大学院工学研究院	Precipitation behavior and magnetic properties of fine magnetic particles in Cu - Ni base alloys single crystal	Mahoto Takeda	Yokohama National University
54	〃	李　東海	横浜国立大学	大学院工学府	〃	Lee donghae	Yokohama National University
55	〃	金　俊燮	横浜国立大学	大学院工学府	〃	Kim Junseop	Yokohama National University
56	フラストレート磁性とスピン軌道相互作用の協調・競合効果	豊田　新悟	東京大学	大学院新領域創成科学研究科	Interplay between frustrated magnetism and spin-orbit interaction	Shingo Toyoda	The University of Tokyo
57	〃	鷲見　浩樹	東京大学	大学院新領域創成科学研究科	〃	Hiroki Sumi	The University of Tokyo
58	〃	根津　正謙	東京大学	大学院新領域創成科学研究科	〃	Naoaki Netsu	The University of Tokyo

物質合成・評価設備 U クラス / Materials Synthesis and Characterization U Class Researcher

No.	課題名	氏名	所属		Title	Name	Organization
1	マイクロミキサを用いた機能性酸化物ナノ粒子の連続合成	陶　究	産業技術総合研究所	ナノシステム研究部門	Continuous synthesis of functional metal oxide nanoparticles using a micromxer	Kiwamu Sue	National Institute of Advanced Industrial Science and Technology
2	カーボンファイバーの高分解能透過電子顕微鏡による微細構造解析	斎藤　幸恵	東京大学	大学院農学生命科学研究科	Structural analysis of carbon fibers using high resolution transmission electron microscopy	Yukie Saito	The University of Tokyo
3	Si 置換 Mn_2GeO_4 における新奇マルチフェロイック特性の起源解明	本田　孝志	高エネルギー加速器研究機構	物質構造科学研究所	Study on the origin of unusual multiferroicity in Si-substituted Mn_2GeO_4	Takashi Honda	KEK

長期留学研究員 / Long Term Young Researcher

No.	課題名	氏名	所属		Title	Name	Organization
1	超流動ヘリウム 3-A 相の半整数量子渦の研究	木村　豊	大阪市立大学	大学院理学研究科	Study of the half quantized vortex in superfluid 3He-A phase	Yutaka Kimura	Osaka City University
2	熱輸送測定を用いたスピン液体の研究	渡邊　大樹	京都大学	大学院理学研究科	Study of spin liquids by thermal transport measurement	Daiki Watanabe	Kyoto University

No.	課題名	氏名	所属		Title	Name	Organization
3	高次高調波発生チャンバー及び多層膜鏡切り替えチャンバーの開発	山本　貴士	東京理科大学	大学院理学研究科	Development of high harmonics generation and multi layer mirror chamber	Takashi Yamanoto	Tokyo University of Science
4	窒素ドープ炭素材料の酸素還元反応メカニズムの解明	木内　久雄	東京大学	大学院工学系研究科	Study on the oxygen reduction reaction of nitrogen-doped carbon material	Hisao Kiuchi	The University of Tokyo

平成 26 年度　共同利用課題一覧（後期）/ Joint Research List (2014 Latter Term)

嘱託研究員 / Commission Researcher

No.	課題名	氏名	所属		Title	Name	Organization
担当所員：中辻　知							
1	X 線回析実験による軌道状態の研究とその化学的置換効果の解明	澤　博	名古屋大学	大学院工学研究科	X-ray diffraction study of orbital state and its control by chemical substitution	Hiroshi Sawa	Nagoya University
2	価数異常を伴う量子臨界現象	三宅　和正	豊田理化学研究所		Quantum criticality associated with valence instability	Kazumasa Miyake	Toyota Physical and Chemical Research Institute
3	幾何学的フラストレート磁性体における量子物性の研究	木村　健太	大阪大学	大学院基礎工学研究科	Quantum state of matter in geometrically-frustrated magnets	Kenta Kimura	Osaka University
4	超伝導と核強磁性の共存	柄木　良友	琉球大学	教育学部	Interplay between superconductivity and nuclear ferromagnetism	Yoshitomo Karaki	University of the Ryukyus
5	価数揺動重い電子イッテルビウム化合物における価数クロスオーバーと量子臨界現象	久我　健太郎	大阪大学	大学院理学研究科	Valence crossover and quantum critical phenomena in valence fluctuating and heavy fermion Yb-based compound	Kentarou Kuga	Osaka University
担当所員：吉信　淳							
6	固体表面に吸着した有機分子の光学物性及び振動状態評価	桑原　裕司	大阪大学	大学院工学研究科	Investigation of optical and vibrational properties of organic molecules on sold surfaces	Yuji Kuwahara	Osaka University
7	極低温非弾性トンネル分光と高分解能電子エネルギー損失分光による吸着分子の素励起過程	米田　忠弘	東北大学	多元物質科学研究所	Elementary excitations of adsorbed molecules using low-temperature scanning tunneling spectroscopy and high-resolution electron energy loss spectroscopy	Tadahiro Komeda	Tohoku University
8	酸化物半導体光触媒における水分解反応の研究	松本　吉泰	京都大学	大学院理学研究科	Study of water splitting reaction on oxide semiconductor catalysts	Yoshiyasu Matsumoto	Kyoto University
9	グラフェンの化学修飾とその評価	Md. Zakir Hossain	群馬大学	先端科学研究指導者育成ユニット	Chemical modification of graphene and its characterization	Md. Zakir Hossain	Gunma University
担当所員：上床　美也							
10	有機伝導体の圧力効果	村田　惠三	大阪市立大学	大学院理学研究科	Effect of pressure on the organic conductor	Keizo Murata	Osaka City University
11	多重極限関連圧力装置の調整	高橋　博樹	日本大学	文理学部	Adjustment of cubic anvil apparatus	Hiroki Takahashi	Nihon University
12	希土類化合物の単結晶試料評価とその圧力効果	藤原　哲也	山口大学	大学院理工学研究科	Effect of pressure on the Ce compounds	Tetsuya Fujiwara	Yamaguchi University

No.	課題名	氏名	所属		Title	Name	Organization
13	磁性体の圧力効果	巨海　玄道	久留米工業大学		Effect of pressure on the magnetic materials	Gendo Oomi	Kurume Institute of Technology
14	圧力下 NMR 測定法に関する開発	藤原　直樹	京都大学	大学院人間・環境学研究科	Development of NMR measurement method under high pressure	Naoki Fujiwara	Kyoto University
15	低温用マルチアンビル装置の開発	辺土　正人	琉球大学	理学部	Development of multi-anvil apparatus for low temperature	Masato Hedo	University of the Ryukyus
16	中性子回析に用いる圧力装置の開発	片野　進	埼玉大学	大学院理工学研究科	Developments of high pressure cell for neutron diffraction	Susumu Katano	Saitama University
17	擬一次元有機物質の圧力下物性研究	糸井　充穂	日本大学	医学部	Study on pressure induced superconductivity of quasi organic conductor	Miho Itoi	Nihon University
18	高圧下の比熱測定装置の開発	梅原　出	横浜国立大学	工学部	Development of apparatus for specific heat measurements under high pressure	Izuru Umehara	Yokohama National University
19	磁化測定装置の開発	名嘉　節	物質・材料研究機構		Development of the magnetometer	Takashi Naka	National Institute for Materials Science
20	重い電子系物質における圧力下電気抵抗測定	礒田　誠	香川大学	教育学部	Effect of pressure on the electrical resistivity of heavy fermi on compounds	Makoto Isoda	Kagawa University
21	圧力下における遷移金属化合物の量子物性研究	大串　研也	東北大学	大学院理学研究科	Study of quantum phenomena under high-pressure in transition-metal compounds	Kenya Ohgushi	Tohoku University
担当所員：山下　穣							
22	超低温強磁場装置を用いた強相関電子系の研究	山口　明	兵庫県立大学	大学院物質理学研究科	Study of strongly-correlated systems under ultra-low temperatures and high fields environments	Akira Yamaguchi	The Univerisity of Hyogo
担当所員：柴山　充弘							
23	小型集束型小角散乱装置の高性能化及びそれによる応用研究	古坂　道弘	北海道大学	大学院工学研究院	Development of a compact focusing small-angle neutron scattering instrument and application research using the instrument	Michihiro Furusaka	Hokkaido University
24	中性子散乱装置の共同利用・開発による強相関電子系物質の構造物性の研究	岩佐　和晃	東北大学	大学院理学研究科	Structural studies of strongly correlated electron systems by usage of neutron scattering and instrumental developments	Kazuaki Iwasa	Tohoku University
25	中性子モノクロメータの改良と中性子４軸回折計 FONDER の制御プログラムの改良	木村　宏之	東北大学	多元物質科学研究所	Improvement of neutron monochromator and control program for four circle neutron diffractometer FONDER	Hiroyuki Kimura	Tohoku University
26	中性子散乱装置のアップグレードと共同利用研究の推進	藤田　全基	東北大学	金属材料研究所	Upgrading of the neutron scattering device and promotion of the research and public use	Masaki Fujita	Tohoku University
27	中性子散乱装置のアップグレード後の研究計画の実施と共同利用の推進	大山　研司	東北大学	原子分子材料科学高等研究機構	Propelling the inter university research cooperation	Keji Ohoyama	Tohoku University

No.	課題名	氏名	所属		Title	Name	Organization
28	中性子散乱装置のアップグレード後の研究計画の実施と共同利用の推進	田畑　吉計	京都大学	大学院工学研究科	Progress of the joint research by using the neutron scattering instruments	Yoshikazu Tabata	Kyoto University
29	中性子散乱装置のアップグレード後の研究計画の実施と共同利用の推進	松村　武	広島大学	大学院先端物質科学研究科	Promotion of joint research after the upgrade of neutron scattering instruments	Takeshi Matsumura	Hiroshima University
30	J-PARC/MLF と JRR-3 共存時代に向けた３軸型中性子散乱装置の高度化	松浦　直人	総合科学研究機構		Upgrade of 3-axis neutron spectrometer for the oncoming coexistence of J-PARC/MLF and JRR-3	Masato Matsuura	CROSS
31	中性子分光器を用いた強相関電子系物質の微視的研究	桑原　慶太郎	茨城大学	大学院理工学研究科	Neutron scattering study of strongly correlated electron systems by using neutron spectrometers	Keitaro Kuwahara	Ibaraki University
32	高度化した３軸分光器を用いた共同利用の推進と物質科学研究の実施	横山　淳	茨城大学	理学部	Executing user program and study of material science with the advanced triple-axis spectrometers	Makoto Yokoyama	Ibaraki University
33	冷中性子スピン干渉計の応用と MINE ビームラインの整備	田崎　誠司	京都大学	大学院工学研究科	Development of cold neutron spin interferometry and improvements of MINE beam line	Seiji Tasaki	Kyoto University
34	膜貫通ペプチドのフリップフロップ誘起能の評価	中野　実	富山大学	大学院医学薬学研究部（薬学）	Induction of phospholipid Flip-Flop by transmembrane peptides	Minoru Nakano	University of Toyama
35	C_1-3　ULS 極小角散乱装置 IRT	杉山　正明	京都大学	原子炉実験所	Development of micro-focusing small-angle neutron scattering spectrometer	Masaaki Sugiyama	Kyoto University
36	集光テスト用小型 SANS の開発及び冷中性子反射率計 / 干渉計のアップグレード	日野　正裕	京都大学	原子炉実験所	Improvement of MIEZE spectrometer and cold neutron reflectometer and interferometer	Masahiro Hino	Kyoto University
37	集光テスト用小型 SANS の開発及び冷中性子反射率計・干渉計のアップグレード	北口　雅暁	名古屋大学	現象解析研究センター	Development of compact SANS and improvement of cold neutron reflectometer and interferometer	Masaaki Kitaguchi	Nagoya University
38	中性子散乱用高圧セルの開発および高圧下における中性子散乱実験	藤原　哲也	山口大学	大学院理工学研究科	Neutron scattering experiments under high pressure and development of high pressure cell for neutron scattering	Tetsuya Fujiwara	Yamaguchi University
39	流動場でのソフトマターの構造変化に関する研究	高橋　良彰	九州大学	先導物質化学研究所	Studies on structural change of soft matter under flow field	Yoshiaki Takahashi	Kyushu University
40	三軸分光器を用いた極端条件下における物質科学研究の実施	阿曽　尚文	琉球大学	理学部	Material science studies under extreme conditions by using triple-axis spectrometers	Naofumi Aso	University of the Ryukyus
41	非イオン界面活性剤水溶液のクラフト転移に伴うベシクルの粒径に対するアルキル鎖長効果	川端　庸平	首都大学東京	大学院理工学研究科	Effects of alkyl tail length on the vesicle size in a nonionic surfactant aqueous solution below the Krafft temperature	Youhei Kawabata	Tokyo Metropolitan University
42	中性子散乱研究計画の実施と共同利用の推進	伊藤　晋一	高エネルギー加速器研究機構	物質構造科学研究所	Propelling the inter university research cooperation	Shinichi Itoh	KEK
43	冷中性子干渉イメージング装置開発研究	大竹　淑恵	理化学研究所	光量子工学研究領域	Research and development of interferometric imaging instruments for cold neutron	Yoshie Otake	RIKEN
44	高度化した三軸分光器を用いた強相関電子系物質の研究	南部　雄亮	東北大学	多元物質科学研究所	Study of strongly correlated electron systems using advanced triple-axis spectrometers	Yusuke Nambu	Tohoku University

No.	課題名	氏名	所属		Title	Name	Organization
45	中性子散乱実験による高強度イオンゲルの精密構造解析	藤井　健太	山口大学	大学院理工学研究科	Structural analysis of high toughness ion gels by SANS	Kenta Fujii	Yamaguchi University
担当所員：金道　浩一							
46	強磁場量子ビーム科学のためのパルスマグネットの開発	鳴海　康雄	東北大学	金属材料研究所	Developments of pulse magnets for synchrotron and neutron experiments in pulsed high magnetic fields	Yasuo Narumi	Tohoku University
担当所員：辛　埴							
47	高温超伝導体の高分解能光電子分光	藤森　淳	東京大学	大学院理学系研究科	Ultra-high resolution photoemission spectroscopy on high Tc superconductor	Atsushi Fujimori	The University of Tokyo
48	60-eV レーザーを用いた時間分解光電子分光の開発	石坂　香子	東京大学	大学院工学系研究科	The development of time-resolved photoemission using 60eV laser	Kyoko Ishizaka	The University of Tokyo
49	鉄系超伝導体のレーザー光電子分光	下志万　貴博	東京大学	大学院工学系研究科	Laser-ARPES on Fe superconductor	Takahiro Shimojima	The University of Tokyo
50	Bi 系超伝導体の角度分解光電子分光	竹内　恒博	豊田工業大学		Angle-resolved photoemission study on high Tc cuprate	Tsunehiro Takeuchi	Toyota Technological Institute
51	高分解能光電子分光による強相関物質の研究	横谷　尚睦	岡山大学	大学院自然科学研究科	Ultra-high resolution study on strongly correlated materials	Takayoshi Yokoya	Okayama University
52	酸化バナジウムの高分解能光電子分光	江口　律子	岡山大学	大学院自然科学研究科	Photoemission study on vanadium oxides	Ritsuko Eguchi	Okayama University
53	有機化合物の光電子分光	金井　要	東京理科大学	理工学部	Photoemission study on organic compounds	Kaname Kanai	Tokyo University of Science
54	重い電子系ウラン化合物の高分解能光電子分光	藤森　伸一	日本原子力研究開発機構	量子ビーム応用研究センター	Ultra high resolution photoemission study on heavy fermion Uranium compounds	Shinichi Fujimori	Japan Atomic Energy Agency
55	レーザー光電子分光による酸化物薄膜の研究	津田　俊輔	物質・材料研究機構		Laser-photoemission study on oxide films	Shunsuke Tsuda	National Institute for Materials Science
56	４ｆ電子系物質の高分解能光電子分光	松波　雅治	自然科学研究機構	分子科学研究所	Photoemission study on 4f materials	Masaharu Matsunami	National Institutes of Natural Sciences
57	超高空間分解能光電子顕微鏡による磁区構造観察	中川　剛志	九州大学	大学院総合理工学府	Observation of magnetic domain structures by ultra-high resolution photoemission electron microscopy	Takeshi Nakagawa	Kyushu University
58	Mn 化合物の時間分解光電子分光	大川　万里生	東京理科大学	理学部	Time resolved photoemission on Mn compounds	Mario Okawa	Tokyo University of Science
59	収差補正型光電子顕微鏡の建設と利用研究	小嗣　真人	高輝度光科学研究センター		Construction and utilization research of aberration correction photoelectron emission microscopy	Masato Kotsugi	Japan Synchrotron Radiation Institute

No.	課題名	氏名	所属		Title	Name	Organization
60	時間分解・マイクロビームラインの開発と研究	室　隆桂之	高輝度光科学研究センター		Development of micr- and time-resolved beamline	Takayuki Muro	Japan Synchrotron Radiation Institute
61	光電子分光法を用いた各種分子性結晶の電子状態の研究及び装置の低温化	木須　孝幸	大阪大学	大学院基礎工学研究科	Research on electron state of molecular crystals using photoemission spectroscopy	Takayuki Kisu	Osaka University
62	時間分解光電子分光を用いた VO_2 の研究と装置の高度化	吉田　力矢	北海道大学	電子科学研究所	Time-resolved photoemission study of VO_2 and upgrade of experimental apparatus	Rikiya Yoshida	Hokkaido University
担当所員：秋山　英文							
63	半導体光デバイスにおける光学遷移強度の定量評価と基礎理論	鈴浦　秀勝	北海道大学	大学院工学研究院	Quantitative measurements and their basic theory of optical transition intensity in semiconductor optical devices	Hidekatsu Suzuura	Hokkaido University
64	半導体光デバイスにおける光学遷移強度の定量評価とその応用	金光　義彦	京都大学	化学研究所	Quantitative measurements and their applications of optical transition intensity in semiconductor optical devices	Yoshihiko Kanemitsu	Kyoto University
担当所員：松田　巌							
65	高輝度放射光軟 X 線を用いた時間分解光電子分光による表面ダイナミクス研究	近藤　寛	慶應義塾大学	理工学部	Study of surface dynamics by time-resolved photoemission spectroscopy with high-brilliant soft x-ray synchrotron radiation	Hiroshi Kondoh	Keio University
66	軟 X 線アンジュレータビームラインの分光光学系の開発研究	雨宮　健太	高エネルギー加速器研究機構	物質構造科学研究所	Research and development of soft X-ray undulator beamline	Kenta Amemiya	KEK
67	光電子スピン検出器の開発・研究	奥田　太一	広島大学	放射光科学研究センター	Research and development of a new photoelectron spin detector	Taichi Okuda	Hiroshima University
68	光電子顕微鏡による磁性ナノ構造物質の磁化過程	木下　豊彦	高輝度光科学研究センター		Magnetization in process of magnetic nano structure by PEEM	Toyohiko Kinoshita	Japan Synchrotron Radiation Institute
69	高輝度軟 X 線を利用した強相関物質の電子状態研究	組頭　広志	高エネルギー加速器研究機構	物質構造科学研究所	Study of electronic states in strongly correlated materials with high brilliant soft-Xray.	Hiroshi Kumigashira	KEK
70	時間分解光電子分光法による光触媒材料のキャリアダイナミクス研究	小澤　健一	東京工業大学	大学院理工学研究科	Study of carrier dynamics in photocatalysis materials by time-resolved photoemission spectroscopy	Kenichi Ozawa	Tokyo Institute of Technology
71	軟 X 線時間分解分光実験による磁性研究	木村　昭夫	広島大学	大学院理学研究科	Study of magnetic properties by time-resolved soft X-ray spectroscopy	Akio Kimura	Hiroshima University
72	高輝度軟 X 線を利用する光電子顕微鏡装置の設計・開発	坂本　一之	千葉大学	大学院融合科学研究科	Research and designing of a PEEM spectrometer for high brilliance soft X ray	Kazuyuki Sakamoto	Chiba University
73	二次元表示型スピン分解光電子エネルギー分析器の開発	大門　寛	奈良先端科学技術大学院大学	物質創成科学研究科	Development of 2D display type spin resolved photoelectron energy analyzer	Hiroshi Daimon	Nara Institute of Science and Technology
74	時間分解光電子回析実験の要素技術開発	林　好一	東北大学	金属材料研究所	Technical development of time-resolved photoelectron diffraction experiment	Koichi Hayashi	Tohoku University

No.	課題名	氏名	所属		Title	Name	Organization
75	分子吸着系における時間分解光電子分光の研究	間瀬　一彦	高エネルギー加速器研究機構	物質構造科学研究所	Study of time-resolved photoemission spectroscopy for molecular adsorption system	Kazuhiko Mase	KEK
76	共鳴磁気光学カー効果の散乱理論研究	田口　宗孝	奈良先端科学技術大学院大学	物質創成科学研究科	Study of scattering theory for the resonant magneto-optical Kerr effect	Munetaka Taguchi	Nara Institute of Science and Technology
担当所員：原田　慈久							
77	軟 X 線吸収／発光分光法によるリチウムイオン電池電極材料の電子物性研究	細野　英司	産業技術総合研究所	エネルギー技術研究部門	Study on the electronic property of electrode materials for Li-ion batteries by soft X-ray absorption/emission spectroscopy	Eiji Hosono	National Institute of Advanced Industrial Science and Technology
78	〃	朝倉　大輔	産業技術総合研究所	エネルギー技術研究部門	〃	Daisuke Asakura	National Institute of Advanced Industrial Science and Technology
79	超高分解能軟 X 線発光分光による水素吸蔵合金中の水素の波動関数の局在性に関する研究	関場　大一郎	筑波大学	数理物質系	Study on the localization of wave functions of hydrogen atom in hydrogen storage alloys using ultrahigh resolution soft X-ray emission spectroscopy	Daiichiro Sekiba	University of Tsukuba
80	時間分解光電子分光による重い電子系の研究	関山　明	大阪大学	大学院基礎工学研究科	Study on heavy Fermion materials by time-resolved Photoemission	Akira Sekiyama	Osaka University
81	高分解能光電子分光による酸化バナジウムの研究	藤原　秀紀	大阪大学	大学院基礎工学研究科	Study on vanadium oxides by high resolution photoemission	Hidenori Fujiwara	Osaka University
82	軟 X 線発光・共鳴非弾性散乱分光の磁気円・線二色性測定システムの構築	菅　滋正	大阪大学	産業科学研究所	Construction of a noble system for circular and linear dichroism in soft X-ray emission and RIXS spectroscopy	Shigemasa Suga	Osaka University
83	極小角 X 線散乱と軟 X 線吸収・発光分光によるソフトマテリアルの物性研究	雨宮　慶幸	東京大学	大学院新領域創成科学研究科	Study on the physical properties of soft materials by a combination of ultra-small-angle X-ray scattering and soft X-ray absorption/emission spectroscopy	Yoshiyuki Amemiya	The University of Tokyo
84	二次元原子薄膜トランジスタの電子状態のナノ分析 (I)	吹留　博一	東北大学	電気通信研究所	Nanoscale analysis of electronic states of graphene device	Hirokazu Fukidome	Tohoku University
85	省エネ・創エネ・蓄電デバイスのオペランド分光	尾嶋　正治	東京大学	放射光連携研究機構	Operando nano-spectroscopy for energy efficient, power generation and energy storage devices	Masaharu Oshima	The University of Tokyo
担当所員：和達　大樹							
86	共鳴硬・軟 X 線散乱による構造物性と磁性研究	村上　洋一	高エネルギー加速器研究機構	物質構造科学研究所	Studying structures and magnetism of materials by resonant hard and soft x-ray scattering	Youichi Murakami	KEK
87	三次元 nanoESCA による実デバイスのオペランド電子状態解析	永村　直佳	東北大学	多元物質科学研究所	Operando analysis of the electronic structure of actual devices by 3DnanoESCA	Naoka Nagamura	Tohoku University

一般研究員 / General Researcher

No.	課題名	氏名	所属		Title	Name	Organization
担当所員：榊原　俊郎							
1	$PrZn_{11}$ の極低温磁気・比熱測定	大原　繁男	名古屋工業大学	大学院工学研究科	Magnetization and specific heat of $PrZn_{11}$ in sub-Kelvin temperature region	Shigeo Ohara	Nagoya Institute of Technology
2	〃	佐藤　嵩晃	名古屋工業大学	大学院工学研究科	〃	Takaaki Sato	Nagoya Institute of Technology
3	Pr 内包カゴ状化合物 $PrOs_2Zn_{20}$ の極低温比熱測定	鬼丸　孝博	広島大学	大学院先端物質科学研究科	Specific heat measurements of a caged compound $PrOs_2Zn_{20}$	Takahiro Onimaru	Hiroshima University
4	〃	松本　圭介	広島大学	大学院先端物質科学研究科	〃	Keisuke Matsumoto	Hiroshima University
5	〃	脇舎　和平	広島大学	大学院先端物質科学研究科	〃	Kazuhei Wakiya	Hiroshima University
6	カゴ状構造を有する $SmTr_2Zn_{20}$ の極低温磁化測定	加瀬　直樹	新潟大学	大学院自然科学研究科	Low temperature magnetization measurements of the caged compound $SmTr_2Zn_{20}$	Naoki Kase	Niigata University
7	〃	安達　季並	新潟大学	大学院自然科学研究科	〃	Kinami Adachi	Niigata University
8	高圧合成法による新規パイロクロア型遷移金属化合物の探索	有馬　孝尚	東京大学	大学院新領域創成科学研究科	Exploration of new transition metal compounds of pyrochlore structure by means of high-pressure syntheses	Taka-hisa Arima	The University of Tokyo
9	〃	鷲見　浩樹	東京大学	大学院新領域創成科学研究科	〃	Hiroki Sumi	The University of Tokyo
10	磁低温磁化測定による希土類アンチモン化合物の磁場誘起秩序	田山　孝	富山大学	大学院理工学研究部（理学）	Field-induced ordering of rare-earth monoantimonides studied by low-temperature magnetization	Takashi Tayama	University of Toyama
11	重い電子系アクチノイド化合物における極低温電子比熱	芳賀　芳範	日本原子力研究開発機構	先端基礎研究センター	Electronic specific heat of heavy fermion actinide compounds at low temperatures	Yoshinori Haga	Japan Atomic Energy Agency
12	〃	松本　裕司	名古屋工業大学	大学院工学研究科	〃	Yuji Matsumoto	Nagoya Institute of Technology
13	重い電子系超伝導体の対関数の対称性決定理論	町田　一成	岡山大学	大学院自然科学研究科	Theoretical studies of pair symmetry in heavy fermion superconductors	Kazushige Machida	Okayama University
14	正方晶 $PrZn_{11}$ の極低温磁気・比熱測定	松本　裕司	名古屋工業大学	大学院工学研究科	Magnetic and specific heat measurements of tetragonal $PrZn_{11}$	Yuji Matsumoto	Nagoya Institute of Technology
15	層状ルテニウム酸化物 Sr_2RuO_4 における一軸性圧力下比熱	矢口　宏	東京理科大学	理工学部	Specific heat of the layered ruthenate Sr_2RuO_4 under uniaxial pressure	Hiroshi Yaguchi	Tokyo University of Science

No.	課題名	氏名	所属		Title	Name	Organization
16	〃	山崎　照夫	東京理科大学	理工学部	〃	Teruo Yamazaki	Tokyo University of Science
17	有機ラジカルを用いた新規磁性体の低温磁気測定	山口　博則	大阪府立大学	大学院理学系研究科	Low temperature magnetic properties of new organic radical compounds	Hironori Yamaguchi	Osaka Prefecture University
18	〃	岩瀬　賢治	大阪府立大学	大学院理学系研究科	〃	Kenji Iwase	Osaka Prefecture University
19	〃	菊地　健太郎	大阪府立大学	大学院理学系研究科	〃	Kentaro Kikuchi	Osaka Prefecture University
20	$Tb_2Ti_2O_7$ の純良単結晶を用いた低温磁化測定	高津　浩	首都大学東京	大学院理工学研究科	Magnetization measurements on the single crystal of $Tb_2Ti_2O_7$	Hiroshi Takatsu	Tokyo Metropolitan University
担当所員：森　初果							
21	プロトン - 電子相関系分子性導体における重水素効果	西尾　豊	東邦大学	理学部	Deuteration effect of proton-electron correlated molecular conductor	Yutaka Nishio	Toho University
22	〃	山田　翔太	東邦大学	大学院理学研究科	〃	Shota Yamada	Toho University
担当所員：中辻　知							
23	Ce および Yb 系強相関化合物における磁場中ミリケルビン領域での物性測定	海老原　孝雄	静岡大学	大学院理学研究科	Low temperature physical properties at magnetic fields in strongly correlated electron system	Takao Ebihara	Shizuoka University
24	〃	土屋　政人	静岡大学	大学院理学研究科	〃	Masato Tsuchiya	Shizuoka University
25	電子ドープを施した $Ag_{5-x}Sr_xPb_2O_6$ の低温超伝導相の探索	秋光　純	青山学院大学	理工学部	Investigation of superconducting phase in electron doped $Ag_{5-x}Sr_xPb_2O_6$	Jun Akimitsu	Aoyama Gakuin University
26	〃	東　幸正	青山学院大学	大学院理工学研究科	〃	Yukimasa Azuma	Aoyama Gakuin University
担当所員：常次　宏一							
27	電子凝縮系における新奇現象	御領　潤	弘前大学	大学院理工学研究科	Novel phenomena in electronic condensed matter systems	Jun Goryo	Hirosaki University
担当所員：リップマー　ミック							
28	太陽電池用シリコン製造プロセスにおける副生成物の評価	伊高　健治	弘前大学	北日本新エネルギー研究所	Analysis of the by-product under the direct reduction process for solar grade silicon	Kenji Itaka	Hirosaki University

No.	課題名	氏名	所属		Title	Name	Organization
29	新規ウルツァイト型四面体強誘電体材料の創成	安井　伸太郎	東京工業大学	応用セラミックス研究所	The creation of novel wurtzite-type tetrahedral ferroelectric materials	Shintaro Yasui	Tokyo Institute of Technology
担当所員：家　泰弘							
30	Pb 置換 Bi 系超伝導体のホール係数測定（2）	神戸　士郎	山形大学	大学院理工学研究科	Hall coefficient measurement of Pb-substituted Bi-based superconductors (2)	Shiro Kambe	Yamagata University
31	〃	鈴木　沙耶	山形大学	大学院理工学研究科	〃	Saya Suzuki	Yamagata University
担当所員：吉信　淳							
32	HREELS によるグラファイトにおける電子格子散乱の直接測定	田中　慎一郎	大阪大学	産業科学研究所	Direct measurement for the electron-phonon scattering in graphite using HREELS	Shin-ichiro Tanaka	Osaka University
33	Ag(111) 表面におけるシリセンの化学活性の研究	高木　紀明	東京大学	大学院新領域創成科学研究科	Chemical reactivity of silicene grown on Ag(111)	Noriaki Takagi	The University of Tokyo
34	Si(001) 表面上の CO 吸着脱離過程の透過 FTIR 測定	大野　真也	横浜国立大学	大学院工学研究院	FTIR measurements of CO adsorption and desorption processes on Si(001)	Shinya Ohno	Yokohama National University
35	〃	田中　一馬	横浜国立大学	大学院工学府	〃	Kazuma Tanaka	Yokohama National University
36	STM による Ag(110) 上の二次元 TiO_2 単結晶の構造解析	枝元　一之	立教大学	理学部	STM study on the structure of a two-dimensional TiO_2 single crystal on Ag(110)	Kazuyuki Edamoto	Rikkyo University
37	金表面に吸着したドーパミン分子の高分解能振動分光	米田　忠弘	東北大学	多元物質科学研究所	High resolution vibration spectroscopy of dopamine molecules adsorbed on Au(111)	Tadahiro Komeda	Tohoku University
38	水の光分解触媒物質 $BiVO_4$ 及び $La_5Ti_2CuS_5O_7$ の構造と物性の研究	山田　太郎	東京大学	大学院工学系研究科	Studies on the structure and physical properties of $BiVO_4$ and $La_5Ti_2CuS_5O_7$ — photoactive materials for water splitting catalysis	Taro Yamada	The University of Tokyo
39	二酸化炭素還元触媒反応に関する研究	森川　良忠	大阪大学	大学院工学研究科	Study on catalytic reactions of reduction of CO_2	Yoshitada Morikawa	Osaka University
担当所員：小森　文夫							
40	STM と XPS による Si(111)-7×7 表面上における Fe クラスター構造の成長過程に関する研究	巨　東英	埼玉工業大学	先端科学研究所	Study on the growth process of Fe cluster structure in the Si(111)-7x7 surface by STM and XPS	Ju Dong-Ying	Saitama Institute of Technology
41	〃	楊　昊宇	埼玉工業大学	大学院工学研究科	〃	Yang Haoyu	Saitama Institute of Technology
42	TiO_2(110) 表面における低速陽電子の対消滅と水素効果の測定	松本　益明	東京学芸大学	教育学部	Measurements of annihilation of positron and effect of hydrogen on the TiO_2(110) surface	Masuaki Matsumoto	Tokyo Gakugei University

No.	課題名	氏名	所属		Title	Name	Organization
43	〃	稲村　直晃	東京学芸大学	大学院教育学研究科	〃	Naoaki Inamura	Tokyo Gakugei University
44	グラフェンナノ構造の電子状態解析	田中　悟	九州大学	大学院工学研究院	Electronic structure analysis of graphene nanostructures	Satoru Tanaka	Kyushu University
45	金属／半導体表面上ナノ構造の形成とその光学応答の時間分解測定	河村　紀一	日本放送協会	放送技術研究所	Time resolved spectroscopy of optical responses from nano-structures on metal / semiconductor surfaces	Norikazu Kawamura	NHK Science & Technical Research Laboratories
46	半導体基板上に成長したシリセンの電子状態	中辻　寛	東京工業大学	大学院総合理工学研究科	Electronic structure of silicene grown on semiconductor substrates	Kan Nakatsuji	Tokyo Institute of Technology
47	陽電子消滅法によるボロン正二十面体クラスター固体の金属結合−共有結合転換研究	金沢　育三	東京学芸大学	教育学部	Metallic-covalent bonding conversion research in boron icosahedral cluster solids using positron annihilation	Ikuzo Kanazawa	Tokyo Gakugei University
48	〃	今井　恵利華	東京学芸大学	大学院教育学研究科	〃	Erika Imai	Tokyo Gakugei University
担当所員：長谷川　幸雄							
49	二ホウ化物薄膜上エピタキシャルシリセン及びゲルマニウム層の低温走査トンネル顕微鏡観察	高村　由起子	北陸先端科学技術大学院大学	マテリアルサイエンス研究科	Low temp. STM investigation of epitaxial silicene and germanium on diboride	Yukiko Takamura	Japan Advanced Institute of Science and Technology
50	〃	アントワーヌ　フロランス	北陸先端科学技術大学院大学	マテリアルサイエンス研究科	〃	Antoine Fleurence	Japan Advanced Institute of Science and Technology
51	〃	フローリアン　ジャンベール	北陸先端科学技術大学院大学	マテリアルサイエンス研究科	〃	Florian Gimbert	Japan Advanced Institute of Science and Technology
52	〃	青柳　航平	北陸先端科学技術大学院大学	マテリアルサイエンス研究科	〃	Kohei Aoyagi	Japan Advanced Institute of Science and Technology
担当所員：山下　穣							
53	準２次元有機超伝導体の渦糸格子状態におけるディラック型ランダウバンド構造の探索	佐々木　孝彦	東北大学	金属材料研究所	Search for Dirac-shaped Landau band structure in the vortex lattice state of quasi 2D organic superconductors	Takahiko Sasaki	Tohoku University
54	〃	橋本　顕一郎	東北大学	金属材料研究所	〃	Kenichiro Hashimoto	Tohoku University
55	〃	佐々木　智	東北大学	大学院理学研究科	〃	Satoru Sasaki	Tohoku University
担当所員：上床　美也							
56	Ce-Zn-Ge 三元系新規化合物の合成および単結晶育成	藤原　哲也	山口大学	大学院理工学研究科	Synthesis and single crystal growth of Ce-Zn-Ge novel ternary intermetallics	Tetsuya Fujiwara	Yamaguchi University

No.	課題名	氏名	所属		Title	Name	Organization
57	〃	中田　琢也	山口大学	大学院理工学研究科	〃	Takuya Nakada	Yamaguchi University
58	Co 基ホイスラー合金における圧力誘起マルテンサイト変態に関する研究	重田　出	鹿児島大学	大学院理工学研究科	Study on pressure-induced martensitic phase transformation in Co-based Heusler alloys	Iduru Shigeta	Kagoshima University
59	〃	藤本　祐太郎	鹿児島大学	大学院理工学研究科	〃	Yutaro Fujimoto	Kagoshima University
60	$EuFe_2P_2$ の高圧力下磁化測定 (2)	藤原　哲也	山口大学	大学院理工学研究科	Magnetization measurements under high pressures in $EuFe_2P_2$ II	Tetsuya Fujiwara	Yamaguchi University
61	〃	森田　哲広	山口大学	大学院理工学研究科	〃	Tetsuhiro Morita	Yamaguchi University
62	$EuRu_2P_2$ の輸送特性の圧力効果	藤原　哲也	山口大学	大学院理工学研究科	Pressure effect on the transport property of $EuRu_2P_2$	Tetsuya Fujiwara	Yamaguchi University
63	〃	中田　琢也	山口大学	大学院理工学研究科	〃	Takuya Nakada	Yamaguchi University
64	Mn 基強磁性体の一次相転移の圧力効果	小山　佳一	鹿児島大学	大学院理工学研究科	Pressure effect on first order phase transition of Mn based ferromagnet	Keiichi Koyama	Kagoshima University
65	〃	大園　康介	鹿児島大学	大学院理工学研究科	〃	Kosuke Ozono	Kagoshima University
66	$Ni_{2-x}MnGa$ の高圧化電気抵抗測定	伊藤　昌和	鹿児島大学	大学院理工学研究科	Electric resistivity of Heusler compounds $Ni_{2-x}MnGa$ under high pressure	Masakazu Ito	Kagoshima University
67	〃	桑原　脩人	鹿児島大学	大学院理工学研究科	〃	Syuto Kuwahara	Kagoshima University
68	Ni-Mn-Ga 系強磁性形状記憶合金の磁化の圧力依存性	安達　義也	山形大学	大学院理工学研究科	Pressure dependence of magnetization for the ferromagnetic shape-memory alloys of Ni-Mn-Ga system	Yoshiya Adachi	Yamagata University
69	〃	池田　大地	山形大学	大学院理工学研究科	〃	Daichi Ikeda	Yamagata University
70	$RTIn_5$ の高圧物性測定	胡　光輝	横浜国立大学	大学院工学府	Magnetic properties under high pressure of $RTIn_5$	Guanghui Hu	Yokohama National University
71	TmB_4 の磁気準周期秩序相における圧力効果	伊賀　文俊	茨城大学	理学部	Pressure effect on the magnetic quasi-period ordered phase in TmB_4	Fumitoshi Iga	Ibaraki University
72	〃	道村　真司	埼玉大学	研究機構	〃	Shinji Michimura	Saitama University
73	$YbCo_2Zn_{20}$ 置換系物質の基本物性評価 II	阿曽　尚文	琉球大学	理学部	Evaluation of fundamental physical properties in doped $YbCo_2Zn_{20}$ II	Naofumi Aso	University of the Ryukyus

No.	課題名	氏名	所属		Title	Name	Organization
74	〃	比嘉　泰之	琉球大学	大学院理工学研究科	〃	Yasuyuki Higa	University of the Ryukyus
75	カゴ状構造を有する超伝導体 $Y_5Rh_6Sn_{18}$ の高圧下電気抵抗測定	加瀬　直樹	新潟大学	大学院自然科学研究科	Electrical resistivity measurements of $Y_5Rh_6Sn_{18}$ with caged compound under high pressure	Naoki Kase	Niigata University
76	〃	佐藤　凌	新潟大学	大学院自然科学研究科	〃	Ryo Sato	Niigata University
77	セリウム系化合物における微小磁気モーメントの圧力下磁化測定 III	阿曽　尚文	琉球大学	理学部	Magnetization studies under pressure in Ce-based compounds with small magnetic moments III	Naofumi Aso	University of the Ryukyus
78	〃	藤原　哲也	山口大学	大学院理工学研究科	〃	Tetsuya Fujiwara	Yamaguchi University
79	〃	比嘉　泰之	琉球大学	大学院理工学研究科	〃	Yasuyuki Higa	University of the Ryukyus
80	ペロブスカイト型ブロック層を有する鉄ニクタイド系超伝導関連物質の圧力効果	余　珊	物質・材料研究機構		Pressure effects of iron pnictide compounds with perovskite type block layers	Yu Shan	National Institute for Materials Science
81	圧力下における CeS の磁気相転移と近藤効果	松村　武	広島大学	大学院先端物質科学研究科	Magnetic order and Kondo effect in CeS under high pressure	Takeshi Matsumura	Hiroshima University
82	〃	林　佑弥	広島大学	大学院先端物質科学研究科	〃	Yuya Hayashi	Hiroshima University
83	圧力下磁場中点接合分光実験の試み	本山　岳	島根大学	大学院総合理工学研究科	Development of a new method of point-contact-spectroscopy under pressure	Gaku Motoyama	Shimane University
84	〃	小川　翔平	島根大学	大学院総合理工学研究科	〃	Shohei Ogawa	Shimane University
85	圧力誘起価数転移の探索と高圧下輸送特性	辺土　正人	琉球大学	理学部	Searching of pressure-induced valence transition and transport properties under high pressure	Masato Hedo	University of the Ryukyus
86	〃	垣花　将司	琉球大学	大学院理工学研究科	〃	Masashi Kakihana	University of the Ryukyus
87	価数揺動物質の圧力下電子状態研究	井村　敬一郎	名古屋大学	大学院理学研究科	Study of electronical state in valence-fluctuation materials under high-pressure	Keiichiro Imura	Nagoya University
88	〃	齋藤　真衣	名古屋大学	大学院理学研究科	〃	Mai Saito	Nagoya University
89	価数揺動物質の高圧力中輸送特性の研究	仲間　隆男	琉球大学	理学部	Transport properties of valence fluctuating compounds under pressure	Takao Nakama	University of the Ryukyus
90	〃	赤嶺　拡	琉球大学	大学院理工学研究科	〃	Hiromu Akamine	University of the Ryukyus

No.	課題名	氏名	所属		Title	Name	Organization
91	回転希釈冷凍機を用いた量子液体・固体研究	白濱　圭也	慶應義塾大学	理工学部	Study of quantum fluids and solids using rotating dilution refrigerator	Keiya Shirahama	Keio University
92	〃	高橋　大輔	足利工業大学	共通課程	〃	Daisuke Takahashi	Ashikaga Institute of Technology
93	〃	村川　智	慶應義塾大学	理工学部	〃	Satoshi Murakawa	Keio University
94	〃	立木　智也	慶應義塾大学	大学院理工学研究科	〃	Tomoya Tsuiki	Keio University
95	希土類化合物の単結晶育成と圧力下輸送特性	中野　智仁	新潟大学	大学院自然科学研究科	Single-crystal growth of the rare-earth compound and its transport properties under pressure	Tomohito Nakano	Niigata University
96	〃	寺島　宗一郎	新潟大学	大学院自然科学研究科	〃	Soichiro Terashima	Niigata University
97	強磁性 Eu 化合物の圧力下電気抵抗測定	光田　暁弘	九州大学	大学院理学研究院	Electrical resistivity of a ferromagnetic Eu compound under high pressure	Akihiro Mitsuda	Kyushu University
98	〃	藤本　巧	九州大学	大学院理学府	〃	Takumi Fujimoto	Kyushu University
99	強相関型セリウム化合物および合金の量子相転移と磁性	村山　茂幸	室蘭工業大学	大学院工学研究科	Quantum phase transition and magnetism in the strongly correlated Ce compounds and alloys	Shigeyuki Murayama	Muroran Institute of Technology
100	〃	雨海　有佑	室蘭工業大学	大学院工学研究科	〃	Yusuke Amakai	Muroran Institute of Technology
101	〃	荒川　恵理	室蘭工業大学	大学院工学研究科	〃	Eri Arakawa	Muroran Institute of Technology
102	高圧下での Yb_4As_3 の電気抵抗測定	中村　修	岡山理科大学	学外連携推進室	Tranport properties of Yb_4As_3 under high pressure	Osamu Nakamura	Okayama University of Science
103	磁性半導体 Yb_5Ge_4 における電気抵抗の圧力効果	小坂　昌史	埼玉大学	大学院理工学研究科	Effect of pressure on the electrical resistivity of magnetic semiconductor Yb_5Ge_4	Masashi Kosaka	Saitama University
104	〃	道村　真司	埼玉大学	研究機構	〃	Shinji Michimura	Saitama University
105	〃	切金　大介	埼玉大学	大学院理工学研究科	〃	Tomoyuki Kirigane	Saitama University
106	重い電子系物質における 3He 温度領域での磁化測定	佐藤　由昌	九州大学	大学院工学府	Magnetization measurements in 3He temperature region for heavy fermion systems	Yoshiaki Sato	Kyushu University
107	三角格子磁性体 $NaM(Acac)_3benzen$(M=Fe,Ni,Co,Mn) の低温磁性	柄木　良友	琉球大学	教育学部	Low temperature magnetizm of triangular lattice antiferromagnet $NaM(acac)_3benzen$	Yoshitomo Karaki	University of the Ryukyus

No.	課題名	氏名	所属		Title	Name	Organization
108	新規な窒化炭素の高圧高温合成とその評価	財部　健一	岡山理科大学	理学部	High-pressure high-temperature synthesis of carbon nitiride and its characterization	Kenichi Takarabe	Okayama University of Science
109	〃	安井　望	岡山理科大学	大学院理学研究科	〃	Nozomu Yasui	Okayama University of Science
110	新規三元化合物 $EuCuP_2$ の磁化測定	藤原　哲也	山口大学	大学院理工学研究科	Magnetization measurement on the novel ternary compound $EuCuP_2$	Tetsuya Fujiwara	Yamaguchi University
111	〃	森田　哲広	山口大学	大学院理工学研究科	〃	Tetsuhiro Morita	Yamaguchi University
112	新構造を持つ RCo_2Ge_4 重希土類化合物の物性評価	北川　健太郎	高知大学	教育研究部	Investigation for physical properties in RCo_2Ge_4 heavy rare-earth compounds with new structure	Kentaro Kitagawa	Kochi University
113	〃	岸本　恭来	高知大学	大学院総合人間自然科学研究科	〃	Yasuki Kishimoto	Kochi University
114	正方晶の V_2Ga_5 と関連物質の圧力下の輸送特性	仲間　隆男	琉球大学	理学部	Transport properties of the single crystal V_2Ga_5 and related compounds with tetragonal structure	Takao Nakama	University of the Ryukyus
115	〃	照屋　淳志	琉球大学	大学院理工学研究科	〃	Atsushi Teruya	University of the Ryukyus
116	〃	上門　太郎	琉球大学	大学院理工学研究科	〃	Taro Uejyo	University of the Ryukyus
117	多形化合物 RIr_2Si_2(R= 希土類）の磁気転移　3	繁岡　透	山口大学	大学院理工学研究科	Magnetic transition of polymorphic compound RIr_2Si_2 (R=rare earth) 3	Toru Shigeoka	Yamaguchi University
118	〃	田端　克好	山口大学	大学院理工学研究科	〃	Katsuyoshi Tabata	Yamaguchi University
119	多形化合物 RIr_2Si_2（R= 希土類）の磁気特性　2	繁岡　透	山口大学	大学院理工学研究科	Magnetic property of polymorphic compound RIr_2Si_2 (R=rare earth) 2	Toru Shigeoka	Yamaguchi University
120	〃	藤井　洋	山口大学	大学院理工学研究科	〃	Yoh Fujii	Yamaguchi University
121	多重極限下のゼーベック係数測定システムの開発	辺土　正人	琉球大学	理学部	Development of new Seebeck coefficient measurement system under multiple extreme conditions	Masato Hedo	University of the Ryukyus
122	〃	友利　圭佑	琉球大学	大学院理工学研究科	〃	Keisuke Tomori	University of the Ryukyus
123	超流動 He-3,A1 相中のスピン流れと電場の交差相関の探索	山口　明	兵庫県立大学	大学院物質理学研究科	Study of cross-correlation between spin flow and electric field in superfluid He-3 A1	Akira Yamaguchi	The University of Hyogo
124	〃	白濱　圭也	慶應義塾大学	理工学部	〃	Keiya Shirahama	Keio University

No.	課題名	氏名	所属		Title	Name	Organization
125	〃	村川　智	慶應義塾大学	理工学部	〃	Satoshi Murakawa	Keio University
126	〃	巻内　崇彦	慶應義塾大学	大学院理工学研究科	〃	Takahiko Makiuchi	Keio University
127	超流動ヘリウム３－Ａ相での半整数量子渦の検出	石川　修六	大阪市立大学	大学院理学研究科	Investigation of the half quantized vortices in superfluid 3He-A phase	Osamu Ishikawa	Osaka City University
128	分子薄膜の高圧下の電気的性質に関する研究	三浦　康弘	桐蔭横浜大学	大学院工学研究科	Studies on electrical properties of molecular thin films under high pressure	Yasuhiro Miura	Toin University of Yokohama
129	有機伝導体の温度圧力相図における圧力媒体の効果	村田　惠三	大阪市立大学	大学院理学研究科	Effect of the properties of high pressure medium on the temperature-pressure phase diagram in organic conductors	Keizo Murata	Osaka City University
130	〃	平山　光	大阪市立大学	大学院理学研究科	〃	Hikaru Hirayama	Osaka City University
131	有機分子性導体の高圧物性の研究	鳥塚　潔	法政大学	理工学部	Studies on high pressure properties of organic molecular conductors	Kiyoshi Torizuka	Hosei University
132	立法晶の結晶構造を持つ希土類化合物の異方的磁気体積効果	大橋　政司	金沢大学	理工研究域	Anisotropic magnetovolume effect of rare earth compounds	Masashi Ohashi	Kanazawa University
133	〃	立野　翔大	金沢大学	大学院自然科学研究科	〃	Shota Tateno	Kanazawa University
134	量子臨界現象の探索と圧力下輸送測定	中野　智仁	新潟大学	大学院自然科学研究科	Investigation of quantum critical phenomena and its transport measurement under pressure	Tomohito Nakano	Niigata University
135	〃	山田　和弘	新潟大学	大学院自然科学研究科	〃	Kazuhiro Yamada	Niigata University
136	固体ヘリウムの超流動に見られる様な「新規超流動現象の基礎研究」	久保田　実	芝浦工業大学	工学部	Fundamental study of new types of superfluidity, as seen in solid 4He	Minoru Kubota	Shibaura Institute of Technology
担当所員：川島　直輝							
137	テンソルネットワーク変分法の実装に関する研究	原田　健自	京都大学	大学院情報学研究科	Implementation of tensor network variational methods	Kenji Harada	Kyoto University
138	蜂の巣格子上反強磁性 Heisenberg-Kitaev 模型の磁気的性質	鈴木　隆史	兵庫県立大学	大学院工学研究科	Magnetic properties of the antiferromagnetic Heisenberg-Kitaev model on a honeycomb lattice	Takafumi Suzuki	The University of Hyogo
担当所員：廣井　善二							
139	Al を含む Zintl 相の超高圧合成	白子　雄一	名古屋大学	大学院工学研究科	High-pressure synthesis of Zintl phase containing Al	Yuichi Shirako	Nagoya University

No.	課題名	氏名	所属		Title	Name	Organization
140	〃	齋藤　雄太	名古屋大学	大学院工学研究科	〃	Yuta Saito	Nagoya University
141	Fe-$MgSiO_3$-H_2 系の高温高圧下におけるふるまいの解明	八木　健彦	東京大学	大学院理学系研究科	Behavior of Fe-$MgSiO_3$-H_2 system under high pressure and temperature condition	Takehiko Yagi	The University of Tokyo
142	〃	飯塚　理子	愛媛大学	地球深部ダイナミクス研究センター	〃	Riko Iizuka	Ehime University
143	Y 系充填スクッテルダイト超伝導体の高圧合成	関根　ちひろ	室蘭工業大学	大学院工学研究科	High-pressure synthesis Y-based filled-skutterudite superconductors	Chihiro Sekine	Muroran Institute of Technology
144	〃	三影　勇人	室蘭工業大学	大学院工学研究科	〃	Hayato Mikage	Muroran Institute of Technology
145	核−マントル境界における金属鉄−ケイ酸塩メルト間の塩素分配に関する実験的研究	桑原　秀治	東京大学	大学院新領域創成科学研究科	An experimental study on metal-silicate partitioning of chlorine at core -mantle boundary conditions	Hideharu Kuwahara	The University of Tokyo
146	下部マントル条件における MgO-SiO_2-H_2 系の相関係	篠崎　彩子	東京大学	大学院理学系研究科	Phase relation of MgO-SiO_2-H_2 system under the lower mantle condition.	Ayako Shinozaki	The University of Tokyo
147	高圧下におけるアミノ酸のラセミ化ならびにペプチド化	鍵　裕之	東京大学	大学院理学系研究科	Racemization and peptide formation of amino acids under high pressure	Hiroyuki Kagi	The University of Tokyo
148	〃	藤本　千賀子	東京大学	大学院理学系研究科	〃	Chikako Fujimoto	The University of Tokyo
149	高圧下におけるガス物質充填型スクッテルダイト型リン化物の探査	丹羽　健	名古屋大学	大学院工学研究科	Exploration for gas-filled skutterudite compounds under high pressure	Ken Niwa	Nagoya University
150	室温高圧下における環状炭化水素の重合反応	篠崎　彩子	東京大学	大学院理学系研究科	Pressure induced polymerization of cyclic organic compounds	Ayako Shinozaki	The University of Tokyo
151	新規イオン伝導性化合物の超高圧合成	長谷川　正	名古屋大学	大学院工学研究科	High pressure syntheses of novel ion conductors	Masashi Hasegawa	Nagoya University
152	〃	廣瀬　瑛一	名古屋大学	大学院工学研究科	〃	Eiichi Hirose	Nagoya University
153	新規ペロブスカイト型複酸化物の高圧高温合成	志村　元	名古屋大学	大学院工学研究科	High pressure and temperature synthesis of novel perovskite oxide	Gen Shimura	Nagoya University
154	新規超伝導体 $BaTi_2(As_{1-x}Sb_x)_2O$ における圧力誘起相転移	陰山　洋	京都大学	大学院工学研究科	Pressure indured transition in $BaTi_2(As_{1-x}Sb_x)_2O$	Hiroshi Kageyama	Kyoto University
155	〃	小林　洋治	京都大学	大学院工学研究科	〃	Yoji Kobayashi	Kyoto University
156	〃	山本　隆文	京都大学	大学院工学研究科	〃	Takafumi Yamamoto	Kyoto University

No.	課題名	氏名	所属		Title	Name	Organization
157	〃	セドリック タッセル	京都大学	白眉センター	〃	Cedric Tassel	Kyoto University
158	超高圧プレスを用いた新規プロトニクス酸化物のソフト化学的合成法の検討	山口　周	東京大学	大学院工学系研究科	Oxide-protonics materials synthesis by combined use of soft chemical method and high pressure	Shu Yamaguchi	The University of Tokyo
159	〃	三好　正悟	東京大学	大学院工学系研究科	〃	Shogo Miyoshi	The University of Tokyo
160	〃	田中　和彦	東京大学	大学院工学系研究科	〃	Kazuhiko Tanaka	The University of Tokyo
161	直接窒化による 3d 遷移金属多窒化物の高圧合成	丹羽　健	名古屋大学	大学院工学研究科	High pressure synthesis of 3d transition metal pernitride via direct nitriding method	Ken Niwa	Nagoya University
162	〃	寺部　俊紀	名古屋大学	大学院工学研究科	〃	Toshiki Terabe	Nagoya University
163	溶融亜鉛メッキ合金相の応力誘起変態	山口　周	東京大学	大学院工学系研究科	Stress-induced phase transformation of Fe-Zn alloy formed in hot-dip process	Shu Yamaguchi	The University of Tokyo
164	〃	三好　正悟	東京大学	大学院工学系研究科	〃	Shogo Miyoshi	The University of Tokyo
165	〃	田中　和彦	東京大学	大学院工学系研究科	〃	Kazuhiko Tanaka	The University of Tokyo
166	〃	上田　涼平	東京大学	大学院工学系研究科	〃	Ryohei Ueda	The University of Tokyo
担当所員：柴山　充弘							
167	ポリオキシエチレン系非イオン性界面活性剤のレオロジーに関する研究	吉村　倫一	奈良女子大学	研究院自然科学系	Study on rheology of polyoxyethylene-type nonionic surfactants	Tomokazu Yoshimura	Nara Women’s University
168	〃	矢田　詩歩	奈良女子大学	大学院人間文化研究科	〃	Shiho Yada	Nara Women’s University
担当所員：益田　隆嗣							
169	3 本鎖量子磁性体 $Cu_3(OD)_3SO_4$ の磁気構造解析	萩原　雅人	東京理科大学	理工学部	Magnetic structure study of three-legged ribbons $Cu_3(OD)_4SO_4$	Masato Hagihala	Tokyo University of Science
170	マルチフェロイック物質 $Cu_3Mo_2O_9$ 単結晶の方位の確認	長谷　正司	物質・材料研究機構		Confirmation of axis-directions of multiferroic substance $Cu_3Mo_2O_9$ single crystals	Masashi Hase	National Institute for Materials Science
171	一次元フラストレート鎖 $AM(VO_4)(OH)$ (A = Ca, Sr;M = Cu, Ni, Co) の磁性	萩原　雅人	東京理科大学	理工学部	Magnetic property of frustrated spin chain system $AM(VO_4)(OH)$	Masato Hagihara	Tokyo University of Science

No.	課題名	氏名	所属		Title	Name	Organization
172	希土類化合物単結晶の物質評価	繁岡　透	山口大学	大学院理工学研究科	Characterization of rare earth single crystal compounds	Toru Shigeoka	Yamaguchi University
173	〃	中田　琢也	山口大学	大学院理工学研究科	〃	Takuya Nakada	Yamaguchi University
174	空間反転対称性の破れた超伝導体の結晶性評価	古川　はづき	お茶の水女子大学	大学院人間文化創成科学研究科	Evaluation of single crystal quality of non-centrosymmetric superconductors	Hazuki Furukawa	Ochanomizu University
175	高エネルギー X 線回折による $CsCuCl_3$ の単一結晶カイラリティ結晶の試料内部評価	高阪　勇輔	青山学院大学	理工学部	Single crystalline $CsCuCl_3$ with homo-crystalline chiral domain, probed by high energy X-ray diffraction	Yusuke Kousaka	Aoyama Gakuin University
176	非磁性不純物による三角スピンチューブのスピンダイナミクスの変化	真中　浩貴	鹿児島大学	大学院理工学研究科	Non-magnetic impurity effect on spin dynamics of triangular spin tubes	Hirotaka Manaka	Kagoshima University
177	高エネルギー X 線ラウエ法を用いたヘリカル磁性合金 Gd-RE (RE=Y,La) の単結晶試料の評価	山崎　照夫	東京理科大学	理工学部	Evaluation of the single crystalline samples of helical magnetic alloys Gd-RE (RE=Y,La) by high-energy X-ray Laue method.	Teruo Yamazaki	Tokyo University of Science
178	〃	栗原　舞	東京理科大学	大学院理工学研究科	〃	Mai Kurihara	Tokyo University of Science
179	スピネル型バナジウム酸化物における磁気励起の観測	阿部　伸行	東京大学	大学院新領域創成科学研究科	Measurement of magnetic excitation in spinel type vanadate	Nobuyuki Abe	The University of Tokyo
180	〃	松浦　慧介	東京大学	大学院新領域創成科学研究科	〃	Keisuke Matsuura	The University of Tokyo
181	〃	塩澤　俊介	東京大学	大学院新領域創成科学研究科	〃	Shunnsuke Shiozawa	The University of Tokyo
担当所員：吉澤　英樹							
182	$(Ho,Y)Rh_2Si_2$ 単結晶の磁気特性 2	繁岡　透	山口大学	大学院理工学研究科	Magnetic characteristics of $(Ho,Y)Rh_2Si_2$ single crystal 2	Toru Shigeoka	Yamaguchi University
183	〃	田端　克好	山口大学	大学院理工学研究科	〃	Katsuyoshi Tabata	Yamaguchi University
184	$ErNi_2B_2C$ とその関連物質における自発的磁束格子の観測	古川　はづき	お茶の水女子大学	大学院人間文化創成科学研究科	Spontaneous vortex lattice in $ErNi_2B_2C$ and its related compounds	Hazuki Furukawa	Ochanomizu University
185	逐次相転移を示す磁性合金 $Gd_{1-x}La_x$ の比熱測定	矢口　宏	東京理科大学	理工学部	Specific heat measurements for the magnetic alloy $Gd_{1-x}La_x$ showing successive phase transition	Hiroshi Yaguchi	Tokyo University of Science
186	〃	山崎　照夫	東京理科大学	理工学部	〃	Teruo Yamazaki	Tokyo University of Science
187	〃	栗原　舞	東京理科大学	大学院理工学研究科	〃	Mai Kurihara	Tokyo University of Science

No.	課題名	氏名	所属		Title	Name	Organization
188	鉄系超伝導体 $FeTe_{1-x}S_x$ の Te 雰囲気中アニール効果	矢口　宏	東京理科大学	理工学部	Effect of Te-annealing in the Fe-based superconductor $FeTe_{1-x}S_x$	Hiroshi Yaguchi	Tokyo University of Science
189	〃	山崎　照夫	東京理科大学	理工学部	〃	Teruo Yamazaki	Tokyo University of Science
190	〃	久保田　聡	東京理科大学	大学院理工学研究科	〃	Satoshi Kubota	Tokyo University of Science
担当所員：嶽山　正二郎							
191	強磁場におけるフラストレート磁性体 $K_2Mn_3(OH)_2(VO_4)_2$ の磁気光学特性	佐藤　博彦	中央大学	理工学部	Magneto-optical properties of frustrated magnet $K_2Mn_3(OH)_2(VO_4)_2$ in high magnetic field	Hirohiko Sato	Chuo University
192	〃	大塚　大祐	中央大学	大学院理工学研究科	〃	Daisuke Otsuka	Chuo University
193	〃	長尾　有紀	中央大学	大学院理工学研究科	〃	Yuki Nagao	Chuo University
194	〃	池戸　優太	中央大学	大学院理工学研究科	〃	Yuta Ikedo	Chuo University
195	〃	原田　景	中央大学	大学院理工学研究科	〃	Kei Harada	Chuo University
担当所員：金道　浩一							
196	$(Ho,Gd)Rh_2Si_2$ 単結晶の高磁場磁化	繁岡　透	山口大学	大学院理工学研究科	High field magnetization of $(Ho,Gd)Rh_2Si_2$ single crystal	Toru Shigeoka	Yamaguchi University
197	〃	藤井　洋	山口大学	大学院理工学研究科	〃	Yoh Fujii	Yamaguchi University
198	10MJ コンデンサーバンク用大型ワイドボアパルスマグネットの開発	萩原　政幸	大阪大学	大学院理学研究科	Development of a large wide-bore pulse magnet for a 10 MJ capacitor bank	Masayuki Hagiwara	Osaka University
199	〃	谷口　一也	大阪大学	大学院理学研究科	〃	Kazuya Taniguchi	Osaka University
200	$Ni_{2-x}MnGa$ の強磁場磁化測定	伊藤　昌和	鹿児島大学	大学院理工学研究科	Magnetization of Heusler compounds $Ni_{2-x}MnGa$ in high magnetic field	Masakazu Ito	Kagoshima University
201	〃	桑原　脩人	鹿児島大学	大学院理工学研究科	〃	Syuto Kuwahara	Kagoshima University
202	$Yb_{1+x}In_{1-x}Cu_4$ における強磁場磁化過程	道岡　千城	京都大学	大学院理学研究科	High-field magnetization measurements in $Yb_{1+x}In_{1-x}Cu_4$	Chishiro Michioka	Kyoto University

No.	課題名	氏名	所属		Title	Name	Organization
203	〃	今井　正樹	京都大学	大学院理学研究科	〃	Masaki Imai	Kyoto University
204	〃	原口　祐哉	京都大学	大学院理学研究科	〃	Yuya Haraguchi	Kyoto University
205	〃	中東　太一	京都大学	大学院理学研究科	〃	Taichi Nakahigashi	Kyoto University
206	カゴメ格子をもつ遷移金属フッ化物単結晶の磁性	植田　浩明	京都大学	大学院理学研究科	Magnetic studies of single crystals of transition metal fluorides with a kagome lattice	Hiroaki Ueda	Kyoto University
207	〃	後藤　真人	京都大学	大学院理学研究科	〃	Masato Goto	Kyoto University
208	〃	山川　智大	京都大学	大学院理学研究科	〃	Tomohiro Yamakawa	Kyoto University
209	スピン 3/2 反強磁性交替鎖物質 $RCrGeO_5$ (R = Tb, Ho, Er, Dy or Gd) の強磁場磁化測定	長谷　正司	物質・材料研究機構		High-field magnetization measurements of spin-3/2 antiferromagnetic alternating chain substances $RCrGeO_5$ (R = Tb, Ho, Er, Dy or Gd)	Masashi Hase	National Institute for Materials Science
210	希土類金属間化合物の強磁場物性研究	海老原　孝雄	静岡大学	大学院理学研究科	Physical phenomena at high magnetic fields in rare earth intermetallic compounds	Takao Ebihara	Shizuoka University
211	〃	土屋　政人	静岡大学	大学院理学研究科	〃	Masato Tsuchiya	Shizuoka University
212	幾何学的フラストレート磁性体の強磁場磁化測定	菊池　彦光	福井大学	大学院工学研究科	Magnetization studies of the frustrated magnets	Hikomitsu Kikuchi	University of Fukui
213	〃	国枝　賢治	福井大学	大学院工学研究科	〃	Kenji Kunieda	University of Fukui
214	強磁場を用いたトポロジカル絶縁体の輸送特性に関する研究	鈴木　悠介	筑波大学	大学院数理物質科学研究科	Study of the transport properties of topological insulator under high magnetic fields	Yusuke Suzuki	University of Tsukuba
215	強相関電子系化合物の秩序相に対する結晶対称性および軌道縮退の効果	横山　淳	茨城大学	理学部	Effects of crystal symmetry and orbital degeneracy in ordered states of strongly correlated electron systems	Makoto Yokoyama	Ibaraki University
216	〃	藤村　健司	茨城大学	大学院理工学研究科	〃	Kenji Fujimura	Ibaraki University
217	近藤半導体 $(Yb, R)B_{12}$ (R=Zr, Sc, Y) の 80T 級磁場下での強磁場物性	伊賀　文俊	茨城大学	理学部	High field physical property of Kondo insulator $(Yb, R)B_{12}$ (R=Zr, Sc, Y) up to 80T class by using the pulse magnet	Fumitoshi Iga	Ibaraki University
218	〃	石井　克弥	茨城大学	大学院理工学研究科	〃	Katsuya Ishii	Ibaraki University
219	高圧合成希土類 12 ホウ化物及び valence skipping 超伝導参照物質 $(Ca,Sr)FeO_3$ の磁化特性と比熱	伊賀　文俊	茨城大学	理学部	Magnetic and thermal properties of rare earth dodeca-borides produced by high pressure synthesis and valence-skipping superconductor reference $(Ca,Sr)FeO_3$	Fumitoshi Iga	Ibaraki University

No.	課題名	氏名	所属		Title	Name	Organization
220	〃	川和　英司	茨城大学	大学院理工学研究科	〃	Eiji Kawawa	Ibaraki University
221	高磁場下における高フッ素濃度 SmFeAs(O,F) 単結晶の超伝導特性	藤岡　正弥	物質・材料研究機構		Superconductivity for SmFeAs(O,F) with high fluorine concentration under high magnetic field	Masaya Fujioka	National Institute for Materials Science
222	新規積層三角格子反強磁性体の強磁場磁化過程と磁気相図	浅野　貴行	福井大学	大学院工学研究科	Magnetization process and magnetic phase diagram of novel stacked triangular lattice antiferromagnets	Takayuki Asano	University of Fukui
223	〃	川見　洋一郎	九州大学	大学院理学府	〃	Yoichiro Kawami	Kyushu University
224	単結晶 $LaCo_{1-x}Rh_xO_3$ の強磁場磁化の結晶方位依存	佐藤　桂輔	茨城工業高等専門学校		Crystal orientation dependence of high field magnetization in $LaCo_{1-x}Rh_xO_3$	Keisuke Sato	Ibaraki National College of Technology
225	低次元新規量子スピン系の強磁場中における量子相転移現象	小野　俊雄	大阪府立大学	大学院理学系研究科	Quantum phase transition phenomena on the low dimensional quantum spin systems in high magnetic field	Toshio Ono	Osaka Prefecture University
226	〃	井川　直哉	大阪府立大学	大学院理学系研究科	〃	Naoya Ikawa	Osaka Prefecture University
227	〃	笠谷　和宏	大阪府立大学	大学院理学系研究科	〃	Kazuhiro Kasatani	Osaka Prefecture University
228	フラストレート磁性体 $K_2Mn_3(OH)_2(VO_4)_2$ の強磁場磁化	佐藤　博彦	中央大学	理工学部	High field magnetization of frustrated magnet $K_2Mn_3(OH)_2(VO_4)_2$	Hirohiko Sato	Chuo University
229	〃	大塚　大祐	中央大学	大学院理工学研究科	〃	Daisuke Otsuka	Chuo University
230	〃	長尾　有紀	中央大学	大学院理工学研究科	〃	Yuki Nagao	Chuo University
231	〃	池戸　優太	中央大学	大学院理工学研究科	〃	Yuta Ikedo	Chuo University
232	〃	原田　景	中央大学	大学院理工学研究科	〃	Kei Harada	Chuo University
233	スピン液体物質 $Tb_2Ti_2O_7$ の熱力学的研究	気谷　卓	東京工業大学	応用セラミックス研究所	Thermodynamic study of spin liquid $Tb_2Ti_2O_7$	Suguru Kitani	Tokyo Institute of Technology
234	ダイヤモンド型量子スピン鎖新モデル物質のパルス強磁場中磁化測定	満田　節生	東京理科大学	理学部	Magnetization study on new model compound of S =1/2 diamond chain system in pulsed high magnetic fields	Setsuo Mitsuda	Tokyo University of Science
担当所員：松田　康弘							
235	メタホウ酸銅における強磁場下の非相反方向二色性	有馬　孝尚	東京大学	大学院新領域創成科学研究科	Nonreciprocal directional dichroism in magnetic ferroelectrics in a high magnetic field	Taka-hisa Arima	The University of Tokyo

No.	課題名	氏名	所属		Title	Name	Organization
236	〃	阿部　伸行	東京大学	大学院新領域創成科学研究科	〃	Nobuyuki Abe	The University of Tokyo
237	〃	豊田　新悟	東京大学	大学院新領域創成科学研究科	〃	Shingo Toyoda	The University of Tokyo
238	〃	根津　正謙	東京大学	大学院新領域創成科学研究科	〃	Naoaki Netsu	The University of Tokyo
239	近藤半導体 (Yb,R)B_{12} および価数揺動物質 (Y,Tm)B_6 のワンターンコイル 120T パルス磁場下での強磁場磁化過程	伊賀　文俊	茨城大学	理学部	High field magnetization of Kondo insulator (Yb,R)B_{12} and valence fluctuation material (Y,Tm)B_6 by using one-turn coil in a 120 T pulse magnet	Fumitoshi Iga	Ibaraki University
240	〃	林　健人	茨城大学	大学院理工学研究科	〃	Kento Hayashi	Ibaraki University
担当所員：徳永　将史							
241	BiS_2 系新層状超伝導体の超伝導機構解明に向けた強磁場下物性評価	水口　佳一	首都大学東京	大学院理工学研究科	Elucidation of mechanisms of superconductivity in novel BiS_2-based layered superconductors using high-field measurements	Yoshikazu Mizuguchi	Tokyo Metropolitan University
242	$Pr_{1-x}(Sr_1\text{-}yCay)_xMnO_3$ の反強磁性と熱電特性に関する研究	中津川　博	横浜国立大学	理工学部	Antiferromagnetism and thermoelectric properties in $Pr_{1-x}(Sr_1\text{-}yCay)_xMnO_3$	Hiroshi Nakatsugawa	Yokohama National University
243	カゴ状物質 SmT_2Al_{20} における磁場に鈍感な強相関電子物性の起源探索	東中　隆二	首都大学東京	大学院理工学研究科	Investigation of field-insensitive nature of heavy-fermion compounds SmT_2Al_{20}	Ryuji Higashinaka	Tokyo Metropolitan University
244	〃	山田　瑛	首都大学東京	大学院理工学研究科	〃	Akira Yamada	Tokyo Metropolitan University
245	超強磁場を利用した CoCr 基合金におけるリエントラント挙動を示すマルテンサイト変態の観察および起源解明	キョキョウ	東北大学	大学院工学研究科	Observation and clarification of the origin of re-entrant martensitic transformation using strong magnetic field in CoCr based alloys	Xiao XU	Tohoku University
246	導電性パイロクロア型酸化物の強磁場下の物性研究	松平　和之	九州工業大学	大学院工学研究院	Transport and magnetic properties of conductive pyrochlore oxides under high field magnetic field	Kazuyuki Matsuhira	Kyushu Institute of Technology
247	〃	前田　賢	九州工業大学	大学院工学府	〃	Satoru Maeda	Kyushu Institute of Technology
248	二次元ディラック系層状物質における磁気トルク測定による量子振動の観測	酒井　英明	東京大学	大学院工学系研究科	Observation of dHvA oscillation for a layered Dirac metal by measuring magnetic torque	Hideaki Sakai	The University of Tokyo
249	非破壊パルス強磁場を用いたグラファイトの磁場誘起密度波相における輸送現象の研究	矢口　宏	東京理科大学	理工学部	Study of the transport properties of the magnetic-field-induced density-wave state in graphite	Hiroshi Yaguchi	Tokyo University of Science
250	強磁場磁化測定によるピーナツ型カゴ状化合物 $R_6T_4Al_{43}$ 系における低温秩序相の解明	青木　勇二	首都大学東京	大学院理工学研究科	High-field magnetization measurements on the low-temperature ordered phases of peanut-shaped cage material $R_6T_4Al_{43}$	Yuji Aoki	Tokyo Metropolitan University
251	〃	伏屋　健吾	首都大学東京	大学院理工学研究科	〃	Kengo Fushiya	Tokyo Metropolitan University

No.	課題名	氏名	所属		Title	Name	Organization
252	強磁場磁化測定による量子磁性体 $SmPt_2Si_2$ の低温秩序相の解明	松田　達磨	首都大学東京	大学院理工学研究科	High-field magnetization measurements on the low-temperature ordered phases of quantum magnet $SmPt_2Si_2$	Tatsuma Matsuda	Tokyo Metropolitan University
253	〃	伏屋　健吾	首都大学東京	大学院理工学研究科	〃	Kengo Fushiya	Tokyo Metropolitan University
担当所員：秋山　英文							
254	フォトルミネッセンス励起分光による GaAs/GaAsN 超格子の電子構造解析	矢口　裕之	埼玉大学	大学院理工学研究科	Photoluminescence excitation spectroscopy study on the electronic structure of GaAs/GaAsN superlattices	Hiroyuki Yaguchi	Saitama University
255	〃	高宮　健吾	埼玉大学	研究機構	〃	Kengo Takamiya	Saitama University
256	〃	須藤　真樹	埼玉大学	大学院理工学研究科	〃	Masaki Sutou	Saitama University
担当所員：辛　埴							
257	角度分解光電子分光による鉄系超伝導体における擬ギャップの研究	園部　竜也	東京大学	大学院工学系研究科	ARPES study on pseudogap in iron-pnictides	Tatsuya Sonobe	The University of Tokyo
258	強いスピン軌道相互作用を有するビスマス化合物超伝導体の研究	坂野　昌人	東京大学	大学院工学系研究科	Investigation of bismuth compound superconductor with strong spin-orbit interaction	Masato Sakano	The University of Tokyo
259	極低温超高分解能レーザー光電子分光装置による超伝導ギャップ測定	鈴木　博人	東京大学	大学院理学系研究科	Superconducting gap measurements by low-temperature high-resolution laser angle-resolved photoemision spectroscopy	Hakuto Suzuki	The University of Tokyo
260	新規な半導体および半金属の時間分解光電子分光	石坂　香子	東京大学	大学院工学系研究科	Time-resolved photoemission spectroscopy on new semiconductors and semimetals	Kyoko Ishizaka	The University of Tokyo
261	〃	辻　英徳	東京大学	大学院工学系研究科	〃	Hidenori Tsuji	The University of Tokyo
262	〃	中村　飛鳥	東京大学	大学院工学系研究科	〃	Asuka Nakamura	The University of Tokyo
263	〃	鈴木　裕也	東京大学	大学院工学系研究科	〃	Yuya Suzuki	The University of Tokyo
264	鉄系超伝導体の時間分解角度分解光電子分光	下志万　貴博	東京大学	大学院工学系研究科	Time-resolved angle-resolved photoemission study on iron-based superconductors	Takahiro Shimojima	The University of Tokyo
265	〃	鈴木　裕也	東京大学	大学院工学系研究科	〃	Yuya Suzuki	The University of Tokyo
266	〃	中村　飛鳥	東京大学	大学院工学系研究科	〃	Asuka Nakamura	The University of Tokyo

No.	課題名	氏名	所属		Title	Name	Organization
267	トポロジカル絶縁体表面のディラック電子におけるキャリア濃度に依存した非平衡ダイナミクスの解明	朱　思源	広島大学	大学院理学研究科	Unveiling carrier concentration dependent nonequilibrium dynamics of Dirac fermions in topological insulators	Zhu Siyuan	Hiroshima University
担当所員：末元　徹							
268	$KNiCl_3$ 族化合物結晶における可視 - 近赤外光学スペクトルの温度変化	三野　弘文	千葉大学	普遍教育センター	Temperature dependence of visible to near-infrared optical spectra in $KNiCl_3$ -family crystals	Hirofumi Mino	Chiba University
269	〃	上村　翔太	千葉大学	大学院理学研究科	〃	Shota Kamimura	Chiba University
270	〃	貞本　貢汰	千葉大学	大学院理学研究科	〃	Kota Sadamoto	Chiba University
271	テラヘルツ分光装置を用いた酸化物磁性材料の研究	大越　慎一	東京大学	大学院理学系研究科	Study of magnetic oxide using terahertz spectroscopy	Shin-ichi Ohkoshi	The University of Tokyo
272	〃	生井　飛鳥	東京大学	大学院理学系研究科	〃	Asuka Namai	The University of Tokyo
273	〃	吉清　まりえ	東京大学	大学院理学系研究科	〃	Marie Yoshikiyo	The University of Tokyo
274	還元型酸化チタンにおける光誘起相転移過程の研究	上岡　隼人	日本大学	文理学部	Study for photo-induced phase transition processes in reduced-type titanium oxides	Hayato Kamioka	Nihon University
275	太陽電池の層間移動ダイナミクス	牧野　哲征	福井大学	工学部	Layer transfer dynamics of solar cells	Takayuki Makino	University of Fukui
276	〃	山口　洋脩	福井大学	大学院工学研究科	〃	Yosuke Yamaguchi	University of Fukui
277	Li ドープ ZnO のエキシトン発光の時間分解発光測定	内野　隆司	神戸大学	大学院理学研究科	Time-resolved photoluminescence measurements on the exciton emission in Li-doped ZnO	Takashi Uchino	Kobe University

物質合成・評価設備 P クラス / Materials Synthesis and Characterization P Class Researcher

No.	課題名	氏名	所属		Title	Name	Organization
1	遷移金属酸窒化物、金属間化合物における構造物性研究	山浦　淳一	東京工業大学	元素戦略研究センター	Structural physics on the transition metal oxynitrides and intermetallic compounds	Junichi Yamaura	Tokyo Institute of Technology
2	〃	真木　祥千子	東京工業大学	元素戦略研究センター	〃	Sachiko Maki	Tokyo Institute of Technology
3	超臨界二酸化炭素中レーザーアブレーションプラズマの分光イメージング	シュタウス スヴェン	東京大学	大学院新領域創成科学研究科	Spectroscopic imaging of laser ablation plasmas in supercritical carbon dioxide	Sven Stauss	The University of Tokyo

No.	課題名	氏名	所属		Title	Name	Organization
4	〃	姫野　翔平	東京大学	大学院新領域創成科学研究科	〃	Shohei Himeno	The University of Tokyo
5	パイロクロア型希土類酸化物の単結晶育成と磁気フラストレーションの研究	松平　和之	九州工業大学	大学院工学研究院	Single crystal growth and study of frustrated magnetism in pyrochlore rare-earth oxides	Kazuyuki Matsuhira	Kyushu Institute of Technology
6	電子が複合自由度を持つ遷移金属系物質の純良単結晶育成と物性評価	片山　尚幸	名古屋大学	大学院工学研究科	Growth of single crystals of transition metal compounds with charge, orbital and spin degrees of freedom	Naoyuki Katayama	Nagoya University
7	〃	杉山　由季	名古屋大学	大学院工学研究科	〃	Yuki Sugiyama	Nagoya University
8	〃	中埜　彰俊	名古屋大学	大学院工学研究科	〃	Akitoshi Nakano	Nagoya University

物質合成・評価設備 G クラス / Materials Synthesis and Characterization G Class Researcher

No.	課題名	氏名	所属		Title	Name	Organization
1	高温高圧水を反応場とした多段階有機合成反応	大友　順一郎	東京大学	大学院新領域創成科学研究科	Multi-step organic synthesis in sub- and supercritical water	Junichiro Otomo	The University of Tokyo
2	〃	中井　佑輔	東京大学	大学院新領域創成科学研究科	〃	Yusuke Nakai	The University of Tokyo
3	高温高圧水を用いた医療廃棄物の小型オンサイト処理システムの開発	大友　順一郎	東京大学	大学院新領域創成科学研究科	Development of a small on-site disposal system for medical waste in sub- and supercritical water	Junichiro Otomo	The University of Tokyo
4	〃	長澤　祐介	東京大学	大学院新領域創成科学研究科	〃	Yusuke Nagasawa	The University of Tokyo
5	高温高圧水中における固体酸・塩基触媒反応の速度論的解析	大友　順一郎	東京大学	大学院新領域創成科学研究科	Kinetic analysis of solid acid and base catalyzed reactions in sub- and supercritical water	Junichiro Otomo	The University of Tokyo
6	〃	秋月　信	東京大学	大学院新領域創成科学研究科	〃	Makoto Akizuki	The University of Tokyo
7	超臨界水を用いた有機・無機複合廃棄物からのマテリアルリサイクル	大友　順一郎	東京大学	大学院新領域創成科学研究科	Material recycling from organic-inorganic composite waste using supercritical water	Junichiro Otomo	The University of Tokyo
8	〃	松本　祐太	東京大学	大学院新領域創成科学研究科	〃	Yuta Matsumoto	The University of Tokyo
9	アンモニア電気化学的合成反応における新規電極触媒開発と速度論解析	大友　順一郎	東京大学	大学院新領域創成科学研究科	Development of electro-catalysts and kinetic analysis for electrochemical synthesis of ammonia	Junichiro Otomo	The University of Tokyo
10	〃	野田　直人	東京大学	大学院新領域創成科学研究科	〃	Naoto Noda	The University of Tokyo

No.	課題名	氏名	所属		Title	Name	Organization
11	ケミカルループ法における酸化物イオン伝導体を用いた酸素キャリア材料の寿命評価	大友　順一郎	東京大学	大学院新領域創成科学研究科	Evaluation of life time of metal oxides supported by oxide ion conductors in chemical looping combustion	Junichiro Otomo	The University of Tokyo
12	〃	菊池　典晃	東京大学	大学院新領域創成科学研究科	〃	Noriaki Kikuchi	The University of Tokyo
13	ペロブスカイト型酸化物を用いたケミカルループピングシステムの開発	大友　順一郎	東京大学	大学院新領域創成科学研究科	The study of perovskite based oxygen carrier materials for CLC/CLR applications.	Junichiro Otomo	The University of Tokyo
14	〃	オーチェン ジェームス オーチェン	東京大学	大学院新領域創成科学研究科	〃	Ochieng James Ochieng	The University of Tokyo
15	メソポーラスマテリアル・グラフェンオキサイドに担持した金属触媒のキャラクタリゼーション	佐々木　岳彦	東京大学	大学院新領域創成科学研究科	Characterization for metal catalysts supported on mesoporous materials and graphene oxides	Takehiko Sasaki	The University of Tokyo
16	リン酸チタニウムガラス - セラミックスの微構造観察とプロトン伝導特性	大友　順一郎	東京大学	大学院新領域創成科学研究科	Evaluation of microstructure and proton conductivity in titanium phosphate glass-ceramics	Junichiro Otomo	The University of Tokyo
17	〃	門田　稔	東京大学	大学院新領域創成科学研究科	〃	Minoru Kadota	The University of Tokyo
18	金属酸化物の酸化還元反応における担体効果の検討	大友　順一郎	東京大学	大学院新領域創成科学研究科	Effect of support materials on redox reaction of metal oxides	Junichiro Otomo	The University of Tokyo
19	〃	高坂　文彦	東京大学	大学院新領域創成科学研究科	〃	Fumihiko Kosaka	The University of Tokyo
20	結晶界面における無機複合型プロトン電解質の合成とイオン伝導度の評価	大友　順一郎	東京大学	大学院新領域創成科学研究科	Synthesis of proton conducting electrolyte and evaluation of ion conductivity at grain boundaries	Junichiro Otomo	The University of Tokyo
21	〃	岩永　愛季	東京大学	大学院新領域創成科学研究科	〃	Aki Iwanaga	The University of Tokyo
22	固体酸化物形燃料電池の電極 / 電解質界面における反応輸送物性の評価	大友　順一郎	東京大学	大学院新領域創成科学研究科	Evaluation of transportation phenomena in the electrode/ electrolyte interface of solid oxide fuel cells	Junichiro Otomo	The University of Tokyo
23	〃	橋北　直人	東京大学	大学院新領域創成科学研究科	〃	Naoto Hashikita	The University of Tokyo
24	高温高圧水を利用した微粒子の in situ 有機修飾および還元技術の開発	大友　順一郎	東京大学	大学院新領域創成科学研究科	The development of in situ organic modification and reduction technology of particles in high temperature and pressure water	Junichiro Otomo	The University of Tokyo
25	〃	岳　磊	東京大学	大学院新領域創成科学研究科	〃	Yue Lei	The University of Tokyo
26	高温高圧水中における層状固体酸触媒反応	大友　順一郎	東京大学	大学院新領域創成科学研究科	Study on layered solid acid catalyzed reaction in sub- and supercritical water	Junichiro Otomo	The University of Tokyo
27	〃	名越　詩織	東京大学	大学院新領域創成科学研究科	〃	Shiori Nagoya	The University of Tokyo

No.	課題名	氏名	所属		Title	Name	Organization
28	中温作動燃料電池におけるプロトン伝導体の材料設計および触媒開発	大友　順一郎	東京大学	大学院新領域創成科学研究科	Material design of proton conductor for ITFC and development of catalyst	Junichiro Otomo	The University of Tokyo
29	〃	小城　元	東京大学	大学院新領域創成科学研究科	〃	Gen Kojo	The University of Tokyo
30	超臨界水熱合成による担持触媒の合成	大友　順一郎	東京大学	大学院新領域創成科学研究科	The preparation of support catalyst under supercritical hydrothermal synthesis	Junichiro Otomo	The University of Tokyo
31	〃	李　夢婷	東京大学	大学院新領域創成科学研究科	〃	li mengting	The University of Tokyo
32	有限要素法シミュレーションと材料物性評価に基づく、SOFC システムの性能評価	大友　順一郎	東京大学	大学院新領域創成科学研究科	Evaluation of SOFC performance by finite element method simulation and material properties	Junichiro Otomo	The University of Tokyo
33	〃	宮崎　顕也	東京大学	大学院新領域創成科学研究科	〃	Kenya Miyazaki	The University of Tokyo
34	宇宙往還機の熱防御システム (TPS) に向けた SiC，ZrB_2-SiC の動的酸化に関する研究	桃沢　愛	東京都市大学	工学部	Dynamic oxidation research of SiC, ZrB_2-SiC for reusable launch vehicle	Ai Momozawa	Tokyo City University
35	〃	横手　寛大	東京大学	大学院新領域創成科学研究科	〃	Norihiro Yokote	The University of Tokyo
36	高圧合成法による新規パイロクロア型遷移金属化合物の探索	有馬　孝尚	東京大学	大学院新領域創成科学研究科	Exploration of new transition metal compounds of pyrochlore structure by means of high-pressure syntheses	Taka-hisa Arima	The University of Tokyo
37	〃	阿部　伸行	東京大学	大学院新領域創成科学研究科	〃	Nobuyuki Abe	The University of Tokyo
38	〃	塩澤　俊介	東京大学	大学院新領域創成科学研究科	〃	Shunnsuke Shiozawa	The University of Tokyo
39	〃	鷲見　浩樹	東京大学	大学院新領域創成科学研究科	〃	Hiroki Sumi	The University of Tokyo
40	アルミ系近似結晶中の正 20 面体クラスターの金属結合–共有結合転換	木村　薫	東京大学	大学院新領域創成科学研究科	Metallic-covalent bonding conversion of icosahedral cluster in Al-based approximant crystals	Kaoru Kimura	The University of Tokyo
41	〃	高際　良樹	東京大学	大学院新領域創成科学研究科	〃	Yoshiki Takagiwa	The University of Tokyo
42	パイロクロア格子またはカゴメ格子をもつ遷移金属フッ化物の構造解析	植田　浩明	京都大学	大学院理学研究科	Structural analysis of transition metal fluorides with a pyrochlore lattice or a kagome lattice	Hiroaki Ueda	Kyoto University
43	〃	小林　慎太郎	京都大学	大学院理学研究科	〃	Shintaro Kobayashi	Kyoto University
44	〃	山川　智大	京都大学	大学院理学研究科	〃	Tomohiro Yamakawa	Kyoto University

No.	課題名	氏名	所属		Title	Name	Organization
45	SOFC 空気極酸素還元反応に対する SOFC 製造プロセス由来微量成分の影響評価	大友　順一郎	東京大学	大学院新領域創成科学研究科	The effects of minor components in SOFC cathode on oxygen reduction reaction	Junichiro Otomo	The University of Tokyo
46	〃	大石　淳矢	東京大学	大学院新領域創成科学研究科	〃	Junya Oishi	The University of Tokyo
47	超臨界水熱合成による酸化物コンポジットナノ粒子の合成とその生成ダイナミクス解明	大友　順一郎	東京大学	大学院新領域創成科学研究科	Elucidation of formation dynamics for oxide composite nanoparticles under supercritical hydrothermal synthesis	Junichiro Otomo	The University of Tokyo
48	〃	横　哲	東京大学	大学院新領域創成科学研究科	〃	Akira Yoko	The University of Tokyo
49	複合酸化物ナノ粒子の超臨界水熱合成手法の検討	大友　順一郎	東京大学	大学院新領域創成科学研究科	Study of compound oxide nano-particles using supercritical hydrothermal synthesis	Junichiro Otomo	The University of Tokyo
50	〃	加藤　進介	東京大学	大学院新領域創成科学研究科	〃	Shinsuke Kato	The University of Tokyo
51	Rutile 型 TiO_2 の酸素欠陥分布観測	有賀　寛子	北海道大学	触媒化学研究センター	Detection of oxygen vacancy in rutile TiO_2 single crystal	Hiroko Ariga	Hokkaido University
52	触媒反応の insitu ラマン散乱測定	佐々木　岳彦	東京大学	大学院新領域創成科学研究科	In situ measurement of Raman scattering for heterogeneous catalytic reactions	Takehiko Sasaki	The University of Tokyo
53	〃	板子　健太郎	東京大学	大学院新領域創成科学研究科	〃	Kentaro Itako	The University of Tokyo
54	有機薄膜の反射率測定	田島　裕之	兵庫県立大学	大学院物質理学研究科	Reflectivity measurement of organic thin films	Hiroyuki Tajima	The Univerisity of Hyogo
55	〃	佐藤　井一	兵庫県立大学	大学院物質理学研究科	〃	Seiichi Sato	The Univerisity of Hyogo
56	〃	西岡　友輔	兵庫県立大学	大学院物質理学研究科	〃	Yusuke Nishioka	The Univerisity of Hyogo
57	〃	宮尾　文啓	兵庫県立大学	大学院物質理学研究科	〃	Fumitaka Miyao	The Univerisity of Hyogo
58	ナノ構造制御による二次電池材料開発	細野　英司	産業技術総合研究所	エネルギー技術研究部門	Development of secondary battery materials by the nanostructure control	Eiji Hosono	National Institute of Advanced Industrial Science and Technology
59	マイクロミキサを用いた機能性酸化物ナノ粒子の連続合成	陶　究	産業技術総合研究所	ナノシステム研究部門	Continuous synthesis of functional metal oxide nanoparticles using a micromixer	Kiwamu Sue	National Institute of Advanced Industrial Science and Technology
60	新規磁石材料の微細構造解析	齋藤　哲治	千葉工業大学	工学部	Microstructural studies of newly developed permanent magnet materials	Tetsuji Saito	Chiba Institute of Technology
61	天然鉱物の微細組織と結晶性の実態	永嶌　真理子	山口大学	大学院理工学研究科	Evaluation of micro-texture and crystallinity of natural minerals	Mariko Nagashima	Yamaguchi University

No.	課題名	氏名	所属		Title	Name	Organization
62	ハーフメタル型 Mn 基ホイスラー合金の磁性と輸送特性に関する研究	重田　出	鹿児島大学	大学院理工学研究科	Study on the magnetic and transport properties of half-metallic Mn-based Heusler alloys	Iduru Shigeta	Kagoshima University
63	〃	重松　理史	鹿児島大学	大学院理工学研究科	〃	Satoshi Shigematsu	Kagoshima University
64	ホイスラー型化合物の磁性と伝導の研究	廣井　政彦	鹿児島大学	大学院理工学研究科	Study on the magnetic and electrical properties of Heusler compounds	Masahiko Hiroi	Kagoshima University
65	〃	田底　知也	鹿児島大学	大学院理工学研究科	〃	Tomoya Tazoko	Kagoshima University
66	価数揺動を起こす希土類元素を含む Zintl 相の磁気特性	白子　雄一	名古屋大学	大学院工学研究科	Magnetic properties of Zintl phase including mixed valence rare earth element.	Yuichi Shirako	Nagoya University
67	〃	齋藤　雄太	名古屋大学	大学院工学研究科	〃	Yuta Saito	Nagoya University
68	新規 A サイト秩序型ペロブスカイト複酸化物の物性	志村　元	名古屋大学	大学院工学研究科	Properties of novel A-site ordered perovskite oxides	Gen Shimura	Nagoya University
69	新規遷移金属硫化物固溶体の磁気物性	長谷川　正	名古屋大学	大学院工学研究科	Magnetism of novel transition metal sulfide solid solutions	Masashi Hasegawa	Nagoya University
70	〃	秋田　貴弘	名古屋大学	大学院工学研究科	〃	Takahiro Akita	Nagoya University
71	水熱合成法による新しい幾何学的フラストレート磁性体の探索	岡本　佳比古	名古屋大学	大学院工学研究科	Hydrothermal synthesis of novel geometrically frustrated antiferromagnets	Yoshihiko Okamoto	Nagoya University
72	正 20 面体準結晶と近似結晶の磁性	田村　隆治	東京理科大学	基礎工学部	Magnetic properties of icosahedral quasicrystal and its approximant crystals	Ryuji Tamura	Tokyo University of Science
73	〃	廣戸　孝信	東京理科大学	大学院基礎工学研究科	〃	Takanobu Hiroto	Tokyo University of Science
74	〃	木下　雄太	東京理科大学	大学院基礎工学研究科	〃	Yuta Kinoshita	Tokyo University of Science
75	〃	古田島　尭宏	東京理科大学	大学院基礎工学研究科	〃	Takahiro Kotajima	Tokyo University of Science
76	Cu－Ni－X（X=Co,Fe）系単結晶性合金中の磁性微粒子析出過程と磁気特性の関係	竹田　真帆人	横浜国立大学	大学院工学研究院	Precipitation behavior and magnetic properties of fine magnetic particles in Cu - Ni base alloys single crystal	Mahoto Takeda	Yokohama National University
77	〃	李　東海	横浜国立大学	大学院工学府	〃	Lee donghae	Yokohama National University
78	〃	金　俊燮	横浜国立大学	大学院工学府	〃	Kim Junseop	Yokohama National University

No.	課題名	氏名	所属		Title	Name	Organization
79	アルミ系近似結晶中の正 20 面体クラスターの金属結合–共有結合転換	佐々木　友彰	東京学芸大学	大学院教育学研究科	Metallic-covalent bonding conversion of icosahedral cluster in Al-based approximant crystals	Tomoaki Sasaki	Tokyo Gakugei University

物質合成・評価設備 U クラス / Materials Synthesis and Characterization U Class Researcher

No.	課題名	氏名	所属		Title	Name	Organization
1	土壌中のフッ素反応輸送の評価	パディ　サカンバリ	東京大学	大学院新領域創成科学研究科	Evaluating reactive transport of fluorine in soil	Padhi Sakambari	The University of Tokyo
2	水の光分解触媒物質上の修飾薄膜物質の電子物性の研究	山田　太郎	東京大学	大学院工学系研究科	Electronic physics of thin layers fabricated on water-splitting photocatalysts	Taro Yamada	The University of Tokyo
3	FTIR を用いて，古人骨より抽出したコラーゲンの組成を確認する	蔦谷　匠	東京大学	大学院新領域創成科学研究科	Checking the composition of collagen extracted from ancient human bones by using FTIR	Takumi Tsutaya	The University of Tokyo
4	超臨界水を用いた連続式下水汚泥ガス化プロセスの検討	布浦　鉄平	東京大学	環境安全研究センター	Investigation of continuous gasification of sewage using supercritical water	Teppei Nunoura	The University of Tokyo
5	〃	福井　啓祐	東京大学	大学院新領域創成科学研究科	〃	Keisuke Fukui	The University of Tokyo

長期留学研究員 / Long Term Young Researcher

No.	課題名	氏名	所属		Title	Name	Organization
1	窒素ドープ炭素材料の酸素還元反応メカニズムの解明	木内　久雄	東京大学	大学院工学系研究科	Study of the oxygen reduction reaction of nitrogen-doped carbon materials	Hisao Kiuchi	The University of Tokyo
2	第一原理計算による希土類磁性材料の磁気特性に関する研究	山之内　佑也	北陸先端科学技術大学院大学	マテリアルサイエンス研究科	Studies on the magnetic properties of rare earth magnetic material by first-principles calculations	Yuya Yamanouchi	Japan Advanced Institute of Science and Technology
3	結晶場解析による磁気異方性の解明	山内　圭	北陸先端科学技術大学院大学	マテリアルサイエンス研究科	Elucidation of the magnetic anisotropy due to the crystal field analysis	Kei Yamauchi	Japan Advanced Institute of Science and Technology

平成 26 年度　中性子科学研究施設　共同利用課題一覧 / Joint Research List of Neutron Scattering Researcher 2014

No.	課題名	指名	所属		Title	Name	Organization
・申請装置 4G: GPTAS							
1	GPTAS（汎用 3 軸中性子分光器）IRT 課題	佐藤　卓	東北大学	多元物質科学研究所	IRT: GPTAS (Triple Axis Spectrometer)	Taku J Sato	Tohoku University
2	中性子 - X 線データの同時解析によるナトリウムイオンの水和構造の解明	亀田 恭男	山形大学	理学部	Hydration structure of Na+ by means of simultaneous analysis of neutron and X-ray diffraction data	KAMEDA Yasuo	Yamagata University
3	$Dy_3Al_5O_{12}$ ガーネットにおけるクーロン相の探索	佐藤 卓	東北大学	多元物質科学研究所	Search for Coulomb phase in the $Dy_3Al_5O_{12}$ garnet	Taku J Sato	Tohoku University
4	共晶組成 Au-Si 合金固体の構造	佐藤 卓	東北大学	多元物質科学研究所	Structure determination of the solidified Au-Si Alloys at eutectic composition	Taku J Sato	Tohoku University
5	強磁性超伝導体 UCoGe におけるスピン揺らぎの研究	佐藤 憲昭	名古屋大学	理学研究科物質理学専攻（物理）	Study on spin fluctuations of the superconducting ferromagnet UCoGe	Noriaki Sato	Nagoya University
6	$CeTe_3$ および $TbTe_3$ における量子臨界現象および磁性と超伝導の相関の研究	佐藤 憲昭	名古屋大学	理学研究科物質理学専攻（物理）	Study on the quantum criticality and correlation of magnetism and superconductivity in $CeTe_3$ and $TbTe_3$	Noriaki Sato	Nagoya University
7	重い電子系超伝導体 $CeRh_xIr(1-x)In_5$ における磁性と超伝導の相関の研究	佐藤 憲昭	名古屋大学	理学研究科物質理学専攻（物理）	Study on the correlation of magnetism and superconductivity in $CeRh_xIr(1-x)In_5$	Noriaki Sato	Nagoya University
8	時間分割中性子散乱測定による磁気構造変化過程の実時間追跡	元屋 清一郎	東京理科大学	理工学部　物理学科	Real-time observation of magnetic structural change by means of time-resolved neutron scattering experiments	Kiyoichiro Motoya	Tokyo University of Science
9	中性子回折法による六方晶フェライト $Ba_2Zn_2Fe_{12}O_{22}$ および $BaFe_{12}O_{19}$ 系の超交換相互作用に関する研究	内海 重宜	諏訪東京理科大学	システム工学部　機械システム工学科	Study on superexchange interaction of $Ba_2Zn_2Fe_{12}O_{22}$ and $BaFe_{12}O_{19}$ systems by neutron diffraction	Shigenori Utsumi	Tokyo University of Science, Suwa
10	AFeAs (A = Li, Na) の超伝導対称性	南部 雄亮	東北大学	多元物質科学研究所	Superconducting pairing symmetry in AFeAs (A = Li, Na)	Yusuke Nambu	Tohoku University
11	パイロクロア磁性体における格子ー軌道ースピン観測とスピン流、異常 ホール効果への影響	古川 はづき	お茶の水女子大学	大学院人間文化創成科学研究科	Neutron study on pyrochlore oxide materials	Hazuki Furukawa	Ochanomizu University
12	強磁性超伝導体における自発的磁束格子構造の研究	古川 はづき	お茶の水女子大学	大学院人間文化創成科学研究科	Spontaneous vortex phase in ferromagnetic superconductors	Hazuki Furukawa	Ochanomizu University
13	Sr_2Ruo_4 の非弾性散乱	古川 はづき	お茶の水女子大学	大学院人間文化創成科学研究科	Inelastic neutron scattering experiments on Sr_2RuO_4	Hazuki Furukawa	Ochanomizu University
14	$YbCo_2Zn_{20}$ における圧力誘起磁気秩序相の研究	松林 和幸	東京大学	物性研究所	Pressure-induced magnetic phase transition in $YbCo_2Zn_{20}$	MATSUBAYASHI, Kazuyuki	The University of Tokyo
15	強磁性量子臨界点近傍の遍歴電子フラストレート磁性体 Fe_3Mo_3N およびその Co 置換系の動的スピン相関	田畑 吉計	京都大学	大学院工学研究科	Dynamic spin correlations in novel itinerant-electron frustrated magnets Fe_3Mo_3N and its Co-substituted systems	Yoshikazu Tabata	Kyoto University

No.	課題名	氏名	所属		Title	Name	Organization
16	$EuRu_2P_2$ の磁気構造解析	藤原 哲也	山口大学	大学院理工学研究科	Magnetic structure analysis of $EuRu_2P_2$	Tetsuya Fujiwara	Yamaguchi University
17	$EuCo_2P_2$ の磁気構造解析	藤原 哲也	山口大学	大学院理工学研究科	Magnetic structure analysis of $EuCo_2P_2$	Tetsuya Fujiwara	Yamaguchi University
18	強誘電体の相転移機構（変位型及び秩序–無秩序型）に関する統一的理解の確立	重松 宏武	山口大学	教育学部	Establishment of the unified explanation about the phase transition mechanism (displacive and order-disorder type) in Ferroelectrics	Hirotake Shigematsu	Yamaguchi University
19	スピンアイスにおけるトポロジカル相転移	門脇 広明	首都大学東京	理工学研究科物理学専攻		Hiroaki Kadowaki	Tokyo Metropolitan University
20	ホールドープ型鉄系超伝導体のスピン揺動	李 哲虎	産業技術総合研究所	エネルギー技術研究部門	Spin fluctuations of hole-doped Fe-based superconductors	Chul-Ho Lee	National Institute of Advanced Industrial Science and Technology
21	ダイマーモット絶縁体 κ-(BEDT-TTF)$_2$Cu[N(CN)$_2$]Cl におけるマルチフェロイクスと電荷揺らぎ・分子格子ダイナミクス	松浦 直人	総合科学研究機構	東海事業センター利用研究促進部		Masato Matsuura	CROSS-Tokai
22	$Ca_{10}Pt_4As_8(Fe_{1-x}Pt_xAs)_{10}$ (x ~ 0.2) の光学フォノンと軌道揺らぎ	池内 和彦	総合科学研究機構	東海事業センター		Kazuhiko Ikeuchi	CROSS-Tokai
・申請装置 5G: PONTA							
23	PONTA（高性能偏極中性子散乱装置）IRT 課題	益田　隆嗣	東京大学	物性研究所	IRT: PONTA (Polarized Neutron Triple Axis Spectrometer)	Takatsugu Masuda	The University of Tokyo
24	PONTA（高性能偏極中性子散乱装置）IRT 課題 偏極中性子線を用いた磁気散乱中性子線ホログラフィー	林　好一	東北大学	金属材料研究所	IRT: PONTA (Polarized Neutron Triple Axis Spectrometer)	Koichi Hayashi	Tohoku University
25	中性子回折によるアルカリ金属ナノクラスター強磁性体の研究	中野 岳仁	大阪大学	理学研究科物理学専攻	Neutron diffraction study on ferromagnetism of alkali-metal nanoclusters arrayed in zeolite crystal	Takehito Nakano	Osaka University
26	時間分割中性子散乱測定による磁気構造変化過程の実時間追跡	元屋 清一郎	東京理科大学	理工学部　物理学科	Real-time observation of magnetic structural change by means of time-resolved neutron scattering experiments	Kiyoichiro Motoya	Tokyo University of Science
27	$NiGa_2S_4$ におけるスピンネマティック相関の検出	南部 雄亮	東北大学	多元物質科学研究所	Detection of spin nematic correlation in the 2D magnet $NiGa_2S_4$	Yusuke Nambu	Tohoku University
28	マルチフェロイックス $Ba_2CoGe_2O_7$ におけるエレクトロマグノンの偏極解析	左右田 稔	東京大学	物性研究所	Polarization Analyses of Electromagnon in Multiferroics $Ba_2CoGe_2O_7$	Minoru Soda	The University of Tokyo
29	S=1/2 正四面体をもつ $Ba_3Yb_2Zn_5O_{11}$ の磁気励起	左右田 稔	東京大学	物性研究所	Magnetic excitation of $Ba_3Yb_2Zn_5O_{11}$ having perfect S=1/2 tetrahedra	Minoru Soda	The University of Tokyo
30	スピン格子結合系における磁気相転移と電気分極の一軸応力制御	満田 節生	東京理科大学	理学部　物理	Uniaxial-stress control of magnetic phase transition and electric polarization in a spin-lattice coupled system	Setsuo Mitsuda	Tokyo University of Science
31	希釈反強磁性体 $Ho_xY_{1-x}Ru_2Si_2$ における動的長距離磁気相関状態とパーコレーション転移	田畑 吉計	京都大学	大学院工学研究科	Dynamically-fluctuating long-range correlated state and percolation transition in the diluted antiferromagnet $Ho_xY_{1-x}Ru_2Si_2$	Yoshikazu Tabata	Kyoto University

No.	課題名	氏名	所属		Title	Name	Organization
32	秩序型ペロブスカイト $CaCu_3Ti_4O_{12}$ のフォノン	留野 泉	秋田大学		Phonons in ordered perovskite $CaCu_3Ti_4O_{12}$	Izumi Tomeno	Akita University
33	混晶系 $Ba_{1-x}Ca_xTiO_3$ のフォノン	留野 泉	秋田大学		Phonons in $Ba_{1-x}Ca_xTiO_3$	Izumi Tomeno	Akita University
34	$NdCoO_3$ の格子ダイナミックス	留野 泉	秋田大学		Lattice dynamics in $NdCoO_3$	Izumi Tomeno	Akita University
35	カゴメ三角格子反強磁性体 $NaBa_2Mn_3F_{11}$ の磁気状態	益田 隆嗣	東京大学		Magnetic state in Kagome-Triangular antiferromagnet $NaBa_2Mn_3F_{11}$	Takatsugu Masuda	The University of Tokyo
36	アルカリ超酸化物 KO_2 の磁気励起	益田 隆嗣	東京大学	物性研究所	Magnetic excitation in Alkali superoxide KO_2	Takatsugu Masuda	The University of Tokyo
37	URu_2Si_2 の隠れた秩序に伴う多重極秩序の直接観測	秋光 純	青山学院大学	理工学部	Direct observation of the “Hidden Order” due to multipole ordering in URu_2Si_2	Jun Akimitsu	Aoyama-Gakuin University
38	導電性三角格子磁性体 $PdCrO_2$ の反強磁性秩序とスピンカイラリティ	高津 浩	首都大学東京	理工学研究科	Antiferromagnetism and its relation to the spin chirality in the metallic triangular-lattice magnet $PdCrO_2$	Hiroshi Takatsu	Tokyo Metropolitan University
39	カイラル磁性体 $CsCuCl_3$ のカイラルらせん磁気構造の検出	高阪 勇輔	青山学院大学	理工学部	Chiral helimagnetic structure in Chiral inorganic compound $CsCuCl_3$	Yusuke Kousaka	Aoyama-Gakuin University
40	$Ca_{10}Pt_4As_8(Fe_{1-x}Pt_xAs)_{10}$ (x ~ 0.2) の光学フォノンと軌道揺らぎ	池内 和彦	総合科学研究機構	東海事業センター		Kazuhiko Ikeuchi	CROSS-Tokai
41	$Ca_{10}Pt_4As_8(Fe_{1-x}Pt_xAs)_{10}$ (x ~ 0.2) の偏極中性ビームによる磁気非弾性散乱	池内 和彦	総合科学研究機構	東海事業センター		Kazuhiko Ikeuchi	CROSS-Tokai
42	スピンフラストレート系 1147 フェライトの磁気励起 - 中性子散乱による -	蒲沢 和也	総合科学研究機構	利用研究促進部		Kazuya Kamazawa	CROSS-Tokai
43	偏極中性子を用いた $Cu_3Mo_2O_9$ 単結晶の磁気構造の決定	長谷 正司	物質材料研究機構	中性子散乱グループ	Determination of the magnetic structure of a $Cu_3Mo_2O_9$ single crystal using polarized neutrons	Masashi Hase	National Institute for Materials Science
44	$(CuZn)_3Mo_2O_9$ 単結晶の磁気反射の測定	長谷 正司	物質材料研究機構	中性子散乱グループ	Measurements of magnetic reflections in a $(CuZn)_3Mo_2O_9$ single crystal	Masashi Hase	National Institute for Materials Science
・申請装置 6G: TOPAN							
45	TOPAN（東北大理：３軸型偏極中性子分光器）IRT 課題	岩佐　和晃	東北大学	大学院理学研究科	IRT: TOPAN (Tohoku-University Polarization Analysis Neutron Spectrometer)	Kazuaki Iwasa	Tohoku University
46		富安 啓輔	東北大学	大学院理学研究科	Magnetic structure and excitations in frustrated 5d pyrochlore oxide $Nd_2Ir_2O_7$ with metal- insulator transition	Keisuke Tomiyasu	Tohoku University
47	全対称型多極子秩序による金属–非金属転移に対する磁気不純物効果	岩佐 和晃	東北大学	大学院理学研究科	Magnetic impurity effect on the metal-nonmetal transition with totally-symmetric electron multipole ordering	Kazuaki Iwasa	Tohoku University

No.	課題名	氏名	所属		Title	Name	Organization
48	$Ce_3Co_4Sn_{13}$ における磁気励起：強相関電子系の候補として	岩佐 和晃	東北大学	大学院理学研究科	Magnetic excitation in $Ce_3Co_4Sn_{13}$: a candidate for strong electronic correlation system	Kazuaki Iwasa	Tohoku University
49	PrT_2Zn_{20} (T = Ru, Rh, Os, Ir) における非 Kramers 二重項基底状態のエントロピー解放過程	岩佐 和晃	東北大学	大学院理学研究科	Entropy releases of the non-Kramers doublet ground states in PrT_2Zn_{20} (T = Ru, Rh, Os, Ir)	Kazuaki Iwasa	Tohoku University
50	質量勾配をもつ非一様系での偏在的原子振動モードであるグレードンの検証	岩佐 和晃	東北大学	大学院理学研究科	Gradon as a localized atomic motion in mass-graded inhomogeneous systems	Kazuaki Iwasa	Tohoku University
51	遍歴電子反強磁性体 Mn_3Si における動的スピン階層構造の研究	平賀 晴弘	高エネルギー加速器研究機構	物質構造科学研究所		Haruhiro Hiraka	KEK
52	CeTe における圧力誘起反強四極子秩序	松村 武	広島大学	大学院先端物質科学研究科	Pressure induced antiferroquadrupole order in CeTe	Takeshi Matsumura	Hiroshima University
53	$Ce_{0.5}La_{0.5}B_6$ における磁気八極子秩序の検証	松村 武	広島大学	大学院先端物質科学研究科	Magnetic octupole order in $Ce_{0.5}La_{0.5}B_6$	Takeshi Matsumura	Hiroshima University
54	$Ce_{0.7}La_{0.3}B_6$ の一軸圧下中性子回折	桑原 慶太郎	茨城大学	大学院理工学研究科	Neutron diffraction study of $Ce_{0.7}La_{0.3}B_6$ under uniaxial pressure	Keitaro Kuwahara	Ibaraki University
55	新規 T' 構造ホールドープ銅酸化物 $Pr_{2-x}Ca_xCuO_4$ における磁気相関の研究	藤田 全基	東北大学	金属材料研究所	Study of spin correlations in novel T' -structured cuprate oxide $Pr_{2-x}Ca_xCuO_4$	Masaki Fujita	Tohoku university
56	高精度測定による Fe-LSCO の異方的磁気秩序ピークの起源の研究	藤田 全基	東北大学	金属材料研究所	Origin of anisotropic magnetic peak in Fe-LSCO studied by high resolution neutron-scattering measurement	Masaki Fujita	Tohoku university
57	新規スピンラダー系 $BiCu_2PO_6$ の磁気相関の研究	藤田 全基	東北大学	金属材料研究所	Study of magnetic correlations in novel spin-ladder system $BiCu_2PO_6$	Masaki Fujita	Tohoku university
・申請装置 C1-1: HER							
58	HER (高エネルギー分解能 3 軸型中性子分光器) IRT 課題	横山　淳	茨城大学	理学部理学科	IRT: HER(High Energy Resolution Triple-Axis Spectrometer)	Makoto Yokoyama	Ibaraki University
59	$Dy_3Al_5O_{12}$ ガーネットにおけるクーロン相の探索	佐藤 卓	東北大学	多元物質科学研究所	Search for coulomb phase in the $Dy_3Al_5O_{12}$ garnet	Taku J Sato	Tohoku University
60	強磁性超伝導体 UCoGe におけるスピン揺らぎの研究	佐藤 憲昭	名古屋大学	理学研究科物質理学専攻 (物理)	Study on spin fluctuations of the superconducting ferromagnet UCoGe	Noriaki Sato	Nagoya University
61	$CeTe_3$ および $TbTe_3$ における量子臨界現象および磁性と超伝導の相関の研究	佐藤 憲昭	名古屋大学	理学研究科物質理学専攻 (物理)	Study on the quantum criticality and correlation of magnetism and superconductivity in $CeTe_3$ and $TbTe_3$	Noriaki Sato	Nagoya University
62	重い電子系超伝導体 $CeRh_xIr_{(1-x)}In_5$ における磁性と超伝導の相関の研究	佐藤 憲昭	名古屋大学	理学研究科物質理学専攻 (物理)	Study on the correlation of magnetism and superconductivity in $CeRh_xIr_{(1-x)}In_5$	Noriaki Sato	Nagoya University
63	鉄系梯子型物質 $BaFe_2Se_3$ の磁気揺動	南部 雄亮	東北大学	多元物質科学研究所	Spin dynamics of the iron-based ladder compound $BaFe_2Se_3$	Yusuke Nambu	Tohoku University

No.	課題名	氏名	所属		Title	Name	Organization
64	AFeAs (A = Li, Na) の超伝導対称性	南部 雄亮	東北大学	多元物質科学研究所	Superconducting pairing symmetry in AFeAs (A = Li, Na)	Yusuke Nambu	Tohoku University
65	Sr_2RuO_4 の非弾性散乱	古川 はづき	お茶の水女子大学	大学院人間文化創成科学研究科	Inelastic neutron scattering experiments on Sr_2RuO_4	Hazuki Furukawa	Ochanomizu University
66	全対称型多極子秩序による金属–非金属転移に対する磁気不純物効果	岩佐 和晃	東北大学	大学院理学研究科	Magnetic impurity effect on the metal-nonmetal transition with totally-symmetric electron multipole ordering	Kazuaki Iwasa	Tohoku University
67	$Ce_3Co_4Sn_{13}$ における磁気励起：強相関電子系の候補として	岩佐 和晃	東北大学	大学院理学研究科	Magnetic excitation in $Ce_3Co_4Sn_{13}$: a candidate for strong electronic correlation system	Kazuaki Iwasa	Tohoku University
68	PrT_2Zn_{20} (T = Ru, Rh, Os, Ir) における非 Kramers 二重項基底状態のエントロピー解放過程	岩佐 和晃	東北大学	大学院理学研究科	Entropy releases of the non-Kramers doublet ground states in PrT_2Zn_{20} (T = Ru, Rh, Os, Ir)	Kazuaki Iwasa	Tohoku University
69	$DyFe_2Zn_{20}$ における異方性変化を伴う逐次磁気相転移	岩佐 和晃	東北大学	大学院理学研究科	Successive magnetic phase transition accompanying switch in magnetic anisotropy of $DyFe_2Zn_{20}$	Kazuaki Iwasa	Tohoku University
70	スピン格子結合系 $CuFeO_2$ のスピン波分散関係の一軸応力変化	満田 節生	東京理科大学	理学部　物理	Spin wave dispersion relation in a spin-lattice coupled system $CuFeO_2$ ander uniaxial stress	Setsuo Mitsuda	Tokyo University of Science
71	強磁性量子臨界点近傍の遍歴電子フラストレート磁性体 Fe_3Mo_3N およびその Co 置換系の動的スピン相関	田畑 吉計	京都大学	大学院工学研究科	Dynamic spin correlations in novel itinerant-electron frustrated magnets Fe_3Mo_3N and its Co-substituted systems	Yoshikazu Tabata	Kyoto University
72	希釈反強磁性体 $Ho_xY_{1-x}Ru_2Si_2$ における動的長距離磁気相関状態とパーコレーション転移	田畑 吉計	京都大学	大学院工学研究科	Dynamically-fluctuating long-range correlated state and percolation transition in the diluted antiferromagnet $Ho_xY_{1-x}Ru_2Si_2$	Yoshikazu Tabata	Kyoto University
73	正方格子磁性体における新規磁気相の探索	益田 隆嗣	東京大学	物性研究所	Novel magnetic state in a series of new square-lattice magnets	Takatsugu Masuda	The University of Tokyo
74	酸素吸着 Cu ジカルボン酸の低エネルギー励起	益田 隆嗣	東京大学	物性研究所	Low energy excitation in O_2 adsorbed Cu-dicarboxylic acid	Takatsugu Masuda	The University of Tokyo
75	空間反転対称性と磁性	繁岡 透	山口大学	大学院理工学研究科	Magnetism in non-centrosymmetoric and centrosymmetric systems	Toru Shigeoka	Yamaguchi University
76	新規 T’ 構造ホールドープ銅酸化物 $Pr_{2-x}Ca_xCuO_4$ における磁気相関の研究	藤田 全基	東北大学	金属材料研究所	Study of spin correlations in novel T’ -structured cuprate oxide $Pr_{2-x}Ca_xCuO_4$	Masaki Fujita	Tohoku university
77	高精度測定による Fe-LSCO の異方的磁気秩序ピークの起源の研究	藤田 全基	東北大学	金属材料研究所	Origin of anisotropic magnetic peak in Fe-LSCO studied by high resolution neutron-scattering measurement	Masaki Fujita	Tohoku university
78	量子スピン液体の研究	門脇 広明	首都大学東京	理工学研究科物理学専攻		Hiroaki Kadowaki	Tokyo Metropolitan University
79	量子臨界点近傍にある $YbCo_2Zn_{20}$ の磁気励起	阿曽 尚文	琉球大学	理学部物質地球科学科	Magnetic excitations in $YbCo_2Zn_{20}$ in vicinity of a quantum critical point	Naofumi Aso	University of the Ryukyus
80	空間反転対称性をもたない超伝導体 $CeRhSi_3$ の磁気励起	阿曽 尚文	琉球大学	理学部物質地球科学科	Magnetic fluctuations in a non-centrosymmetric superconductor $CeRhSi_3$	Naofumi Aso	University of the Ryukyus

No.	課題名	氏名	所属		Title	Name	Organization
81	ホールドープ型鉄系超伝導体のスピン揺動	李 哲虎	産業技術総合研究所	エネルギー技術研究部門	Spin fluctuations of hole-doped Fe-based superconductors	Chul-Ho Lee	National Institute of Advanced Industrial Science and Technology
82	ダイマーモット絶縁体 κ-(BEDT-TTF)$_2$Cu$_2$(CN)$_3$ におけるスピン液体状態の研究	松浦 直人	総合科学研究機構	東海事業センター利用研究促進部		Masato Matsuura	CROSS-Tokai
・申請装置 C1-2: SANS-U							
83	SANS-U（二次元位置測定小角散乱装置）IRT 課題	柴山　充弘	東京大学	物性研究所	IRT: SANS-U (Small Angle Neutron Scattering Instrument, The University of Tokyo)	Mitsuhiro Shibayama	The University of Tokyo
84	ナノディスクの構造と集積化挙動の評価	中野 実	富山大学	大学院医学薬学研究部	Structure and stacking behavior of nanodiscs	Minoru Nakano	University of Toyama
85	膜貫通ペプチドのフリップフロップ誘起能の評価	中野 実	富山大学	大学院医学薬学研究部	Induction of flip-flop by transmembrane peptides	Minoru Nakano	University of Toyama
86	膜脂質のダイナミクスに及ぼす膜の曲率の評価	中野 実	富山大学	大学院医学薬学研究部	Effects of curvature on dynamics of membrane lipids	Minoru Nakano	University of Toyama
87	中性子小角散乱法による多孔性放射線合成ゲルのナノ構造解析	佐藤 信浩	京都大学	原子炉実験所	SANS analysis on the nano structure of radiation-synthesized porous polymer gels	Nobuhiro Sato	Kyoto University
88	中性子小角散乱実験による Sr_2RuO_4 の異常金属状態の研究	古川 はづき	お茶の水女子大学	大学院人間文化創成科学研究科	Anomalous vortex state in Sr_2RuO_4 studied by SANS experiments	Hazuki Furukawa	Ochanomizu University
89	空間反転対称性の破れた超伝導体のヘリカル磁束格子の観測	古川 はづき	お茶の水女子大学	大学院人間文化創成科学研究科	Herical vortex phase on non-centrosymmetric superconductors	Hazuki Furukawa	Ochanomizu University
90	Fe 系超伝導体の磁束研究	古川 はづき	お茶の水女子大学	大学院人間文化創成科学研究科	Vortex study on Fe-based superconductors	Hazuki Furukawa	Ochanomizu University
91	希釈冷凍機温度領域における $CeCoIn_5$ の磁束構造の磁場方向依存性	古川 はづき	お茶の水女子大学	大学院人間文化創成科学研究科	Field direction dependence of vortex lattice structure on $CeCoIN_5$ in Dilution temperature.	Hazuki Furukawa	Ochanomizu University
92	強磁性超伝導体における自発的磁束格子構造の研究	古川 はづき	お茶の水女子大学	大学院人間文化創成科学研究科	Spontaneous vortex phase in ferromagnetic superconductors	Hazuki Furukawa	Ochanomizu University
93	イオン液体と界面活性剤の混合物の相分離現象	吉田 亨次	福岡大学	理学部	Phase separation of ionic liquids and surfactant mixtures	Koji Yoshida	Fukuoka University
94	金属磁性体 MnP における長周期ドメイン磁気構造の観測	山崎 照夫	東京理科大学	理工学部	Observation of the long period magnetic domain structure in metallic helimagnet MnP	Teruo Yamazaki	Tokyo University of Science
95	ナノスケールにおける Arfaptin タンパク質によるリン脂質ベシクルの変形	山田 悟史	高エネルギー加速器研究機構	物質構造科学研究所		Norifumi L. Yamada	KEK
96	クラフト転移で自発形成するベシクルの臨界ベシクル濃度近傍でのダイナミクス	川端 庸平	首都大学東京	理工学研究科		Youhei Kawabata	Tokyo Metropolitan University

No.	課題名	氏名	所属		Title	Name	Organization
97	crowding 環境下における生体脂質リポソームとタンパク質の相互作用	平井 光博	群馬大学	理工学研究院（荒牧）	Interaction between protein and lipid liposome under crowding environment	Mituhiro HIRAI	Gunma University
98	GM1 含有 Bicelle に結合したタンパク質の構造変化	杉山 正明	京都大学	原子炉実験所		Masaaki Sugiyama	Kyoto University
99	温度および塩濃度応答性界面不活性／界面活性転移高分子のミセル形成とナノ構造転移	松岡 秀樹	京都大学	工学研究科高分子化学専攻	Micelle formation and nanostructure transition of temperature and salt concentration responsive non-surface active/surface active transition	Hideki Matsuoka	Kyoto University
100	二軸延伸フィルムの広い空間スケールでの解析	松葉 豪	山形大学	大学院理工学研究科	Structural analysis of biaxially oriented films in the wide spatial scale	Go Matsuba	Yamagata University
101	毛髪の内部構造解析	柴山 充弘	東京大学	物性研究所中	Structural analysis of hair	Mitsuhiro Shibayama	The University of Tokyo
102	均一な両親媒性共連続相構造を有する高分子ゲルの構造解析	柴山 充弘	東京大学	物性研究所	Structure study on amphiphilic ideal co-network gel	Mitsuhiro Shibayama	The University of Tokyo
103	ビタミンＥ内包マイクロエマルションの構造に関する研究	柴山 充弘	東京大学	物性研究所	Study on structure of vitamin E microemulsion	Mitsuhiro Shibayama	The University of Tokyo
104	親油性高分子電解質ゲルの各種誘電率を持つ溶媒下での網目構造解析	柴山 充弘	東京大学	物性研究所	Structural analysis of lipophilic polyelectrolyte gels in non-polar solvents	Mitsuhiro Shibayama	The University of Tokyo
105	スピン誘導型強誘電体における誘電（磁気）ドメイン駆動	満田 節生	東京理科大学	理学部　物理		Setsuo Mitsuda	Tokyo University of Science
106	Phosphonate 型イオン液体を溶解剤とするセルロースの溶存構造	藤井 健太	東京大学	物性研究所	Solution structure of phosphonate-based ionic liquid containing cellulose	Kenta Fujii	The University of Tokyo
107	時分割 SANS 測定によるイオン液体中で特有な多分岐高分子のゲル化反応機構	藤井 健太	東京大学	物性研究所	Gelation mechanism of Tetra-PEG ion gel studied by time-resolved small angle neutron scattering	Kenta Fujii	The University of Tokyo
108	二本鎖アニオン型イオン液体／水二成分混合系で形成する ナノスケール会合体の構造解析	藤井 健太	東京大学	物性研究所		Kenta Fujii	The University of Tokyo
109	界面不活性の働きをする界面活性剤	貞包 浩一朗	立命館大学	理工学部物理科学科	Surfactant molecules behaving as a surface-inactive agent	Koichiro Sadakane	Ritsumeikan University
110	高圧条件下における２成分混合溶液の新奇な臨界挙動	貞包 浩一朗	立命館大学	理工学部物理科学科	Novel critical behavior in a mixture of water / organic solvent under high-pressure condition	Koichiro Sadakane	Ritsumeikan University
111	エポキシ樹脂の重合誘起相分離と架橋構造	金谷 利治	京都大学	化学研究所	Polymerization induced phase separation of epoxy resin and network structure	Toshiji Kanaya	Kyoto University
112	シシケバブ生成における分子量の効果	金谷 利治	京都大学	化学研究所	Effects of molecular weights on shish-kebab formation	Toshiji Kanaya	Kyoto University
113	イミダゾリウム系イオン液体添加によるリゾチウムの３次構造の安定化	高椋 利幸	佐賀大学	大学院工学系研究科循環物質化学専攻	Stabilization of tertiary structure of lysozyme in aqueous solutions on adding imidazolium-based ionic liquids	Toshiyuki Takamuku	Saga University

No.	課題名	氏名	所属		Title	Name	Organization
114	含水飽和圧縮モンモリロナイトの原子炉型中性子小角散乱法によるキャラクタリゼーション	高橋 宏明	東北大学	工学研究科	Characterization of water-saturated compaced montmorillonites by reactor type small-angle nutron scattering	Hiroaki Takahashi	Tohoku University
115	結び目を有する環状高分子の溶液中のコンフォメーション	高野 敦志	名古屋大学	工学研究科　化学・生物工学専攻	Chain conformation of knotted ring polymers in solutions.	Atsushi Takano	Nagoya University
116	超巨大磁気抵抗を示すペロブスカイト型マンガン酸化物における自己相似プロファイルの研究	松浦 直人	総合科学研究機構	東海事業センター利用研究促進部	Investigation of power law profile of the ferromagnetic cluster in perovskite Manganite	Masato Matsuura	CROSS-Tokai
117	リラクサー強誘電体における自己相似プロファイルの研究	松浦 直人	総合科学研究機構	東海事業センター利用研究促進部	Investigation of self-similar correlations in relaxor ferroelectrics	Masato Matsuura	CROSS-Tokai
118	塑性変形による鋼板中 Cu 粒子の変形挙動の解析	大場 洋次郎	京都大学	原子炉実験所	Investigation of plastic-working-induced deformation of Cu particle in steel	OBA, Yojiro	Kyoto University
119	イオン液体中における刺激応答性高分子の温度応答性相転移	柴山 充弘	東京大学	物性研究所	Thermo-responsive phase behavior of polymer in ionic liquid	Mitsuhiro Shibayama	The University of Tokyo
・申請装置 C1-3: ULS							
120	ULS（極小角散乱装置）IRT 課題	大竹　淑恵	理化学研究所	仁科加速器センター	IRT: ULS (Ultra Small Angle Scattering Instrument)	Yoshie Otake	RIKEN
121	結晶内電場を用いた中性子電気双極子能率探索のための結晶評価	北口 雅暁	名古屋大学	現象解析研究センター	Study of crystal-diffraction for search of neutron EDM	Masaaki Kitaguchi	Nagoya University
・申請装置 C1-3: mf-SANS							
122	C_1-3 小型集束型小角散乱装置 IRT 課題	古坂　道弘	北海道大学	大学院工学研究科	IRT: mf-SANS (mini-focusing Small Angle Neutron Scattering Instrument)	Michihiro Furusaka	Hokkaido University
・申請装置 C2-3-1: iNSE							
123	iNSE（中性子スピンエコー分光器）IRT 課題	柴山　充弘	東京大学	物性研究所	IRT: iNSE (New issp Neutron Spin Echo Spectrometer)	Mitsuhiro Shibayama	The University of Tokyo
124	イオン液体と界面活性剤の混合物の相分離現象	吉田 亨次	福岡大学	理学部	Phase separation of ionic liquids and surfactant mixtures	Koji Yoshida	Fukuoka University
125	リチウムイオン電解液の構造緩和	吉田 亨次	福岡大学	理学部		Koji Yoshida	Fukuoka University
126	界面活性剤 2 分子膜のゲル状態での膜面内ダイナミクス	川端 庸平	首都大学東京	理工学研究科	Dynamics in a gel-like surfactant membrane	Youhei Kawabata	Tokyo Metropolitan University
127	クラフト転移で自発形成するベシクルの臨界ベシクル濃度近傍でのダイナミクス	川端 庸平	首都大学東京	理工学研究科		Youhei Kawabata	Tokyo Metropolitan University

No.	課題名	氏名	所属		Title	Name	Organization
128	crowding 環境下における生体脂質リポソームとタンパク質の相互作用	平井 光博	群馬大学	理工学研究院（荒牧）	Interaction between protein and lipid liposome under crowding environment	Mituhiro Hirai	Gunma University
129	界面不活性の働きをする界面活性剤	貞包 浩一朗	立命館大学	理工学部物理科学科	Surfactant molecules behaving as a surface-inactive agent	Koichiro Sadakane	Ritsumeikan University
・申請装置 C3-1-1: AGNES							
130	AGNES（高分解能パルス冷中性子分光器）IRT 課題	山室　修	東京大学	物性研究所	IRT: AGNES (Angle Focusing Cold Neutron Spectrometer)	Osamu Yamamuro	The University of Tokyo
131	メタノール水溶液における疎水性水和による水分子の拡散遅延効果	丸山 健二	新潟大学	理学部化学科	The retardation effect of hydrophobic hydrationon diffusion dynamics of water molecules in methanol aqueous solution	kenji maruyama	Niigata University
132	H_2-SF_6 ハイドレート中の水素の拡散ダイナミクス	古府 麻衣子	東京大学	物性研究所	Diffusion dynamics of hydrogen molecules in H_2-SF_6 hydrate	Maiko Kofu	The University of Tokyo
133	Zn-Ln-Zn 単分子磁石のスピンダイナミクス	古府 麻衣子	東京大学	物性研究所	Spin dynamics of Zn-Ln-Zn single-molecule magnets	Maiko Kofu	The University of Tokyo
134	メソポーラス物質に閉じ込めたジオキサン−水二成分溶液中の水分子のダイナミクス	山口 敏男	福岡大学	理学部	Dynamics of water molecule in dioxane-water binary solutions confined in mesoporous materials	Toshio Yamaguchi	Fukuoka University
135		山室 修	東京大学	物性研究所	New process of hydrogen diffusion in palladium hydrides	Osamu Yamamuro	The University of Tokyo
136		山室 修	東京大学	物性研究所	Dynamics of an ionic liquid C_{16}mimPF_6 in SmA liquid crystal and liquid phases	Osamu Yamamuro	The University of Tokyo
137	部分重水素化試料を用いたシンジオタクチックポリスチレンの 分子ふるい構造の動的性質に関する研究	金子 文俊	大阪大学	理学研究科高分子科学専攻	Study on dynamical properties of molecular sieve structure of syndiotactic polystyrene using partially deuterated samples	Fumitoshi Kaneko	Osaka University
138		山室 修	東京大学	物性研究所	Collective dynamics of alkyl-methyl imidaozlium based ionic liquids with liquid crystallline phase	Osamu Yamamuro	The University of Tokyo
・申請装置 C3-1-2: MINE1							
139	MINE1（京大炉：多層膜中性子干渉計・反射率計）IRT 課題	日野　正裕	京都大学	原子炉実験所	IRT: MINE (Multilayer Interferometer and Refrectmeter for Neutron) 1	Masahiro Hino	Kyoto University
140	2 次元中性子集光デバイスの開発	日野 正裕	京都大学	原子炉実験所	Development of 2-dimensional focusing device	Masahiro Hino	Kyoto University
・申請装置 C3-1-2: MINE2							
141	MINE2（京大炉：多層膜中性子干渉計・反射率計）IRT 課題	日野　正裕	京都大学	原子炉実験所	IRT: MINE (Multilayer Interferometer and Refrectmeter for Neutron) 2	Masahiro Hino	Kyoto University

No.	課題名	氏名	所属		Title	Name	Organization
142	界面相互作用が高分子薄膜内部におけるガラス転移温度の分布に及ぼす影響	井上 倫太郎	京都大学	化学研究所		Rintaro Inoue	Kyoto University
143	超冷中性子光学のためのデバイス開発	北口 雅暁	名古屋大学	現象解析研究センター	Development of optical devices for ultra cold neutrons	Masaaki Kitaguchi	Nagoya University
144	中性子反射率法による潤滑下摩擦低減のための金属基板上ポリマーブラシ層の膜厚・密度測定	平山 朋子	同志社大学	理工学部	Thickness and density of polymer brush layer on metal surface under lubrication measured by neutron reflectometry	Tomoko Hirayama	Doshisha University
145	2 次元中性子集光デバイスの開発	日野 正裕	京都大学	原子炉実験所	Development of 2-dimensional focusing device	Masahiro Hino	Kyoto University
146	高分子 / 水界面領域におけるタンパク質吸着状態に関する研究	松野 寿生	九州大学	大学院工学研究院応用化学部門	Study of adsorbed proteins at the polymer/water interfaces	Hisao Matsuno	Kyushu University
147	混合液体と接した高分子界面の凝集状態	田中 敬二	九州大学	大学院工学研究院　応用化学部門	Aggregation state of interface between polymers and mixed non-solvents	Keiji Tanaka	Kyushu University
148	多層膜冷中性子干渉計による重力起因位相の精密測定	関 義親	理化学研究所	光量子工学研究領域		Yoshichika Seki	RIKEN
・申請装置 T1-1: HQR							
149	HQR（高分解能中性子散乱装置）IRT 課題	吉沢　英樹	東京大学	物性研究所	IRT: HQR (High Q Resolution Triple Axis Spectrometer)	Hideki Yoshizawa	The University of Tokyo
150	鉄系超伝導体母物質 FeTe のスピン・格子結合に対する一軸圧力効果	中島 多朗	東京理科大学	理学部物理学科	Uniaxial pressure effect on a parent compound of Fe-based superconductor FeTe	Taro Nakajima	Tokyo University of Science
151	$MnSb_2O_6$ の磁場中磁気構造	佐藤 卓	東北大学	多元物質科学研究所	Magnetic structure of $MnSb_2O_6$ under external field	Taku J Sato	Tohoku University
152	$CeTe_3$ および $TbTe_3$ における量子臨界現象および磁性と超伝導の相関の研究	佐藤 憲昭	名古屋大学	理学研究科物質理学専攻（物理）	Study on the quantum criticality and correlation of magnetism and superconductivity in $CeTe_3$ and $TbTe_3$	Noriaki Sato	Nagoya University
153	時間分割中性子散乱測定による磁気構造変化過程の実時間追跡	元屋 清一郎	東京理科大学	理工学部　物理学科	Real-time observation of magnetic structural change by means of time-resolved neutron scattering experiments	Kiyoichiro Motoya	Tokyo University of Science
154	スピン格子結合系における磁気相転移と電気分極の一軸応力制御	満田 節生	東京理科大学	理学部　物理	Uniaxial-stress control of magnetic phase transition and electric polarization in a spin-lattice coupled system	Setsuo Mitsuda	Tokyo University of Science
155	空間反転対称性を欠く二次元的系 $CeNiC_2$ の磁気構造	片野 進	埼玉大学	理工学研究科		Susumu Katano	Saitama University
156	秩序型ペロブスカイト $CaCu_3Ti_4O_{12}$ のフォノン	留野 泉	秋田大学		Phonons in ordered perovskite $CaCu_3Ti_4O_{12}$	Izumi Tomeno	Akita University
157	混晶系 $Ba_{1-x}Ca_xTiO_3$ のフォノン	留野 泉	秋田大学		Phonons in $Ba_{1-x}Ca_xTiO_3$	Izumi Tomeno	Akita University

No.	課題名	氏名	所属		Title	Name	Organization
158	$NdCoO_3$ の格子ダイナミックス	留野 泉	秋田大学		Lattice dynamics in $NdCoO_3$	Izumi Tomeno	Akita University
159	空間反転対称性と磁性	繁岡 透	山口大学	大学院理工学研究科	Magnetism in non-centrosymmetoric and centrosymmetric systems	Toru Shigeoka	Yamaguchi University
160	$EuRu_2P_2$ の磁気構造解析	藤原 哲也	山口大学	大学院理工学研究科	Magnetic structure analysis of $EuRu_2P_2$	Tetsuya Fujiwara	Yamaguchi University
161	$EuCo_2P_2$ の磁気構造解析	藤原 哲也	山口大学	大学院理工学研究科	Magnetic structure analysis of $EuCo_2P_2$	Tetsuya Fujiwara	Yamaguchi University
162	新規スピンラダー系 $BiCu_2PO_6$ の磁気相関の研究	藤田 全基	東北大学	金属材料研究所	Study of magnetic correlations in novel spin-ladder system $BiCu_2PO_6$	Masaki Fujita	Tohoku university
163	強誘電体の相転移機構（変位型及び秩序–無秩序型）に関する統一的理解の確立	重松 宏武	山口大学	教育学部	Establishment of the unified explanation about the phase transition mechanism (displacive and order-disorder type) in Ferroelectrics	Hirotake Shigematsu	Yamaguchi University
164	スピンフラストレート系 1147 フェライトの磁気励起 - 中性子散乱による -	蒲沢 和也	総合科学研究機構	利用研究促進部		Kazuya Kamazawa	CROSS-Tokai
・申請装置 T1-2: AKANE							
165	AKANE（東北大金研：三軸型中性子分光器 ）IRT 課題	平賀　晴弘	東北大学	金属材料研究所	IRT: AKANE (Advanced Kinken Neutron Spectrometer)	Haruhiro Hiraka	KEK
166	遍歴電子反強磁性体 Mn_3Si における動的スピン階層構造の研究	平賀 晴弘	高エネルギー加速器研究機構	物質構造科学研究所		Haruhiro Hiraka	KEK
167	マルチフェロイック物質 $SmMn_2O_5$ の磁気秩序と強誘電性	木村 宏之	東北大学	多元物質科学研究所	Antiferromagnetism and ferroelectricity in multiferroic compounds of $SmMn_2O_5$	Hiroyuki Kimura	Tohoku University
168	マルチフェロイック物質 YMn_2O_5 における磁性と強誘電性の磁性イオン置換効果	木村 宏之	東北大学	多元物質科学研究所	Substitution effect of magnetic ions on magnetism and ferroelectricity in multiferroic YMn_2O_5	Hiroyuki Kimura	Tohoku University
169	新規 T’ 構造ホールドープ銅酸化物 $Pr_{2-x}Ca_xCuO_4$ における磁気相関の研究	藤田 全基	東北大学	金属材料研究所	Study of spin correlations in novel T’ -structured cuprate oxide $Pr_{2-x}Ca_xCuO_4$	Masaki Fujita	Tohoku university
170	高精度測定による Fe-LSCO の異方的磁気秩序ピークの起源の研究	藤田 全基	東北大学	金属材料研究所	Origin of anisotropic magnetic peak in Fe-LSCO studied by high resolution neutron-scattering measurement	Masaki Fujita	Tohoku university
171	MPO_4 (M: 遷移金属) のカイラル磁気構造の検証	高阪 勇輔	青山学院大学	理工学部	Chiral magnetism in MPO_4 (M: Transition Metal)	Yusuke Kousaka	Aoyama-Gakuin University
172	新規スピンラダー系 $BiCu_2PO_6$ の磁気相関の研究	藤田 全基	東北大学	金属材料研究所	Study of magnetic correlations in novel spin-ladder system $BiCu_2PO_6$	Masaki Fujita	Tohoku university
173	CrX (Cr=Si, Ge) のカイラル磁気構造の検証	高阪 勇輔	青山学院大学	理工学部	Chiral magnetic structure in CrX (X=Si, Ge)	Yusuke Kousaka	Aoyama-Gakuin University

No.	課題名	氏名	所属		Title	Name	Organization
174	幾何学的フラストレート系 (Mn,Mg)Cr_2O_4 におけるらせん磁気構造のクロスオーバー	高阪 勇輔	青山学院大学	理工学部	Crossover between conical and screw magnetic phase in (Mn,Mg)Cr_2O_4	Yusuke Kousaka	Aoyama-Gakuin University
175	ホールドープ型鉄系超伝導体のスピン揺動	李 哲虎	産業技術総合研究所	エネルギー技術研究部門	Spin fluctuations of hole-doped Fe-based superconductors	Chul-Ho Lee	National Institute of Advanced Industrial Science and Technology
・申請装置 T1-3 HERMES							
176	HERMES（東北大金研：中性子粉末回折装置）IRT 課題	大山　研司	東北大学	金属材料研究所	IRT: HERMES(Kinken Powder Diffractometer for High Efficiency and High Resolution MEasurementS)	Kenji Ohoyama	Tohoku University
177	層状ペロブスカイト型酸化物の結晶構造とイオン拡散経路	八島 正知	東京工業大学	大学院理工学研究科・物質科学専攻	Crystal structure and ion-diffusion path of layered perovskite-type oxides	Masatomo Yashima	Tokyo Institute of Technology
178	可視光応答型酸窒化物光触媒の構造物性	八島 正知	東京工業大学	大学院理工学研究科・物質科学専攻	Structure-property correlation of visible-light responsive metal-oxynitride photocatalysts	Masatomo Yashima	Tokyo Institute of Technology
179	二層三角格子反強磁性体 $Fe_2Ga_2S_5$ の結晶構造と磁気構造	南部 雄亮	東北大学	多元物質科学研究所	Crystal and magnetic structures of the bilayer triangular antiferromagnet $Fe_2Ga_2S_5$	Yusuke Nambu	Tohoku University
180	希土類ー遷移金属複合酸化物の磁気構造	土井 貴弘	北海道大学	大学院理学研究院化学部門		Yoshihiro Doi	Hokkaido University
181	粉末中性子回折を用いたホイスラー化合物 Fe_2VAl における 特異な低温物性の起源の解明	宮崎　秀俊	名古屋工業大学	若手研究イノベータ養成センター	Clarify of the origin the anomalous low-temperature physical transport behavior in Heusler-type Fe_2VAl alloys by neutron powder diffraction method	Hidetoshi Miyazaki	Nagoya Institute of Technology
182	$Sr_{0.78}Y_{0.22-x}La_xCoO_y$ の中性子回折	寺崎 一郎	名古屋大学		Neutron diffraction study on $Sr_{0.78}Y_{0.22-x}La_xCoO_y$	Ichiro Terasaki	Nagoya University
183	Isotope effect on low-temperature structure of palladium hydrides	山室 修	東京大学	物性研究所		Osamu Yamamuro	The University of Tokyo
184	異常高原子価鉄を持つ (Ba,Sr)FeO_3 の磁気構造と相境界の解明	山本 隆文	京都大学	工学研究科	Investigation for magnetic structure and phase boundary of (Ba,Sr)FeO_3 with an unusually high valence strate of iron	Takafumi Yamamoto	Kyoto University
185	クロム複合硫化物の結晶構造と磁気転移	手塚 慶太郎	宇都宮大学	工学研究科機能創成研究部門	Crystal structures and magnetic transitions of chromium complex sulfides	Keitaro Tezuka	Utsunomiya University
186	電子ドープ型マンガン酸化物の磁化の反転と磁気構造	松川 倫明	岩手大学	工学部	Magnetization reversal and magnetic structure in electron doped manganites	Michiaki Matsukawa	Iwate University
187	新しいタイプの遍歴電子フラストレート磁性体 Fe_6W_6C, Co_6W_6C における磁気相関	田畑 吉計	京都大学	大学院工学研究科	Spin correlatons in novel itinerant-electron frustrated magnets Fe_6W_6C and Co_6W_6C	Yoshikazu Tabata	Kyoto University
188	シャンダイト型遷移金属化合物 $Co_3(Sn_{1-x}In_x)_2S_2$ の磁気構造解析	田畑 吉計	京都大学	大学院工学研究科	Magnetic structure of shandite-type transition-metal compound $Co_3(Sn_{1-x}In_x)_2S_2$	Yoshikazu Tabata	Kyoto University
189	機械的特性に優れた新規磁性化合物 M_2AX の磁気構造解析	田畑 吉計	京都大学	大学院工学研究科	Magnetic structure of novel magnetic compounds with outstanding mechanical properties M_2AX	Yoshikazu Tabata	Kyoto University

No.	課題名	氏名	所属		Title	Name	Organization
190	一次元フラストレート鎖 AM(VO_4)(OD) (A=Ca,Sr;M=Co,Ni) の磁気構造	萩原 雅人	東京理科大学	理工学部物理学科	Magnetic structure of frustrated chain magnetism AM(VO_4) (OD) (A=Ca,Sr;M=Co,Ni)	Masato Hagihala	Tokyo University of Science
191	新規ペロブスカイト関連 AA' BO_4 型構造をもつ混合イオン伝導体の結晶構造とイオン伝導経路の解明	藤井 孝太郎	東京工業大学	理工学研究科物質科学専攻		Kotaro Fujii	Tokyo Institute of Technology
192	T' 構造銅酸化物の超伝導発現と結晶構造の関係	藤田 全基	東北大学	金属材料研究所	Relation between superconducting mechanism and crystal structure in T' cuprate oxide	Masaki Fujita	Tohoku university
193	固溶系 $Nd_{1-x}Sr_xCoO_2$ における正方晶−斜方晶転移の観察	陰山 洋	京都大学	工学研究科物質エネルギー化学専攻	Investigation of the tetragonal and orthorhombic phase transition of the $Nd_{1-x}Sr_xCoO_2$ solid solution	Hiroshi Kageyama	Kyoto University
194	新規バナジウム化合物の構造、アニオン拡散、磁性の解明	陰山 洋	京都大学	工学研究科物質エネルギー化学専攻	Investigation of structure, ion diffusion and magnetism in a newly realized vanadate system	Hiroshi Kageyama	Kyoto University
195	酸化物格子内での H-/H+ 共存	陰山 洋	京都大学	工学研究科物質エネルギー化学専攻	Coexistence of hydride and protons in an oxide lattice	Hiroshi Kageyama	Kyoto University
196	ペロブスカイト型酸窒化物に対する水素化物イオン挿入	陰山 洋	京都大学	工学研究科物質エネルギー化学専攻	Hydride insertion into perovskite oxynitrides	Hiroshi Kageyama	Kyoto University
197	新規カイラル磁性体 MPO_4 (M: 遷移金属) の磁気構造解析	高阪 勇輔	青山学院大学	理工学部	Magnetic structure analysis in new chiral magnetic compounds MPO_4 (M: transition metal)	Yusuke Kousaka	Aoyama-Gakuin University
198	新規カイラル磁性体 CrX(X: Si, Ge) の磁気構造解析	高阪 勇輔	青山学院大学	理工学部	Magnetic structure analysis in new chiral magnetic compounds CrX (X: Si, Ge)	Yusuke Kousaka	Aoyama-Gakuin University
199	鉄系超伝導体の結晶構造と超伝導の相関	李 哲虎	産業技術総合研究所	エネルギー技術研究部門	Relationship between crystal structure and superconductivity in Fe-based superconductors	Chul-Ho Lee	National Institute of Advanced Industrial Science and Technology
200	白金含有ペロブスカイト型酸化物の中性子回折測定	野村 勝裕	産業技術総合研究所	ユビキタスエネルギー研究部門	Neutron diffraction study of platinum containing perovskite oxides	Katsuhiro Nomura	National Institute of Advanced Industrial Science and Technology
201	中性子散乱による $Sr_{1-x}La_xRuO_3$ のクラスターグラス相の研究	川崎 郁斗	理化学研究所	仁科加速器研究センター	Neutron study of cluster-glass phase in $Sr_{1-x}La_xRuO_3$	Ikuto Kawasaki	RIKEN
202	新規鉄ペロブスカイト酸化物の結晶構造・磁気構造の決定	山田 幾也	大阪府立大学	21 世紀科学研究機構ナノ科学・材料研究センター	Crystal and magnetic structures determination of novel iron-based perovskite oxides containing unusual high valence ions	Ikuya Yamada	Osaka Prefecture University
203	正方格子系反強磁性体 $A_2FeGe_2O_7$ の磁気構造	益田 隆嗣	東京大学	物性研究所	Magnetic structure of square lattice antiferromagnets $A_2FeGe_2O_7$	Takatsugu Masuda	The University of Tokyo
204	S=2 籠目格子反強磁性体の磁気構造	田中 秀数	東京工業大学	大学院理工学研究科	Magnetic structure of the S=2 kagome antiferromagnet	Hidekazu Tanaka	Tokyo Institute of Technology
・申請装置 T2-2: FONDER							
205	FONDER（中性子 4 軸回折装置）IRT 課題	木村 宏之	東北大学	多元物質科学研究所	IRT: FONDER (Four-circle-Off-center-type Neutron Diffractometer)	Hiroyuki Kimura	Tohoku University

No.	課題名	氏名	所属		Title	Name	Organization
206	塑性歪みを加えた Pt_3Fe 反強磁性体における強磁性の発現機構	小林 悟	岩手大学	工学部マテリアル工学科	Mechanism of ferromagnetism in plastically deformed Pt_3Fe antiferromagnet	Satoru Kobayashi	Iwate University
207	スピン三重項超伝導体 Sr_2RuO_4 の一軸圧力下中性子散乱実験	山崎 照夫	東京理科大学	理工学部	Neutron scattering of the triplet superconductor Sr_2RuO_4 under uniaxial pressures	Teruo Yamazaki	Tokyo University of Science
208	$DyFe_2Zn_{20}$ における異方性変化を伴う逐次磁気相転移	岩佐 和晃	東北大学	大学院理学研究科	Successive magnetic phase transition accompanying switch in magnetic anisotropy of $DyFe_2Zn_{20}$	Kazuaki Iwasa	Tohoku University
209	マルチフェロイック物質 $SmMn_2O_5$ の磁気秩序と強誘電性	木村 宏之	東北大学	多元物質科学研究所	Antiferromagnetism and ferroelectricity in multiferroic compounds of $SmMn_2O_5$	Hiroyuki Kimura	Tohoku University
210	マルチフェロイック物質 YMn_2O_5 における磁性と強誘電性の磁性イオン置換効果	木村 宏之	東北大学	多元物質科学研究所	Substitution effect of magnetic ions on magnetism and ferroelectricity in multiferroic YMn_2O_5	Hiroyuki Kimura	Tohoku University
211	I 型熱電クラスレートにおける非中心型非調和振動	金子 耕士	日本原子力研究開発機構	量子ビーム応用研究センター	Off-center rattling in thermoelectric clathrates	Koji Kaneko	Japan Atomic Energy Agency
212	β- パイロクロア超伝導体における非調和振動	金子 耕士	日本原子力研究開発機構	量子ビーム応用研究センター	Anharmonic oscillation in β-pyrochlore superconductors	Koji Kaneko	Japan Atomic Energy Agency
・申請装置 Accsessory							
213	アクセサリー IRT 課題	上床　美也	東京大学	物性研究所	IRT: Accsessory	Yoshiya Uwatoko	The University of Tokyo

平成 26 年度 軌道放射物性研究施設 共同利用課題一覧 / Joint Research List of Syncrotron Radiation Researcher 2014

No.	課題名	氏名	所属		Title	Name	Organization
1	偏光を利用した高輝度軟 X 線実験技術開発の促進	松田　巌	東京大学	物性研究所	Promoting technical development for high brilliant soft X-ray experiments using light polarization	Iwao Matsuda	The University of Tokyo
2	省エネ・創エネ・蓄電デバイスのオペランドナノ分光	尾嶋　正治	東京大学	放射光連携研究機構	Operando nano-spectroscopy for energy efficient, power generation and energy storage devices	Masaharu Oshima	The University of Tokyo
3	大気圧下の角度分解型超高分解能軟X線発光分光システムの開発	原田　慈久	東京大学	物性研究所	Development of angle resolved ultrahigh resolution soft X-ray emission spectroscopy in atmospheric pressure	Yoshihisa Harada	The University of Tokyo
4	モットハバード型強磁性 V 酸化物の時間分解磁気カー効果観測	和達　大樹	東京大学	物性研究所	Observation of time-resolved magneto-optical Kerr effect in Mott-Hubbard-type ferromagnetic V oxides	Hiroki Wadachi	The University of Tokyo
5	可変偏光顕微高分解能二次元光電子分光による電子レベルの構造物性開拓	大門　寛	奈良先端科学技術大学院大学	凝縮系物性学研究室	Electronic-level structural materials science by arbitrally-polarized-light high-energy-resolution two-dimensional microscopic photoelectron spectroscopy	Hiroshi Daimon	Nara Institute of Science and Technology
6	チタニア光触媒における励起キャリアダイナミクスの時間分解光電子分光法を用いた研究	小澤　健一	東京工業大学	大学院理工学研究科　物質科学専攻	Photoinduced carrier dynamics on titania photocatalyst studied by time-resolved photoelectron spectroscopy	Kenichi Ozawa	Tokyo Institute of Technology
7	リチウムイオン電池用高電圧正極材料・および低電圧負極材料のオペランド軟 X 線吸収 / 発光分光	朝倉　大輔	産業技術総合研究所	エネルギー技術研究部門	Operando soft x-ray absorption/emission spectroscopy studies of high-voltage cathode materials and low-voltage anode materials for Li-ion batteries	Daisuke Asakura	National Institute of Advanced Industrial Science and Technology
8	量子臨界物質 Yb（Al,Fe)B_4 の価数揺動状態の軟 X 線時間分解光電子分光	大川　万里生	東京理科大学	理学部第一部	Valence fluctuating state in quantum critical Yb(Al,Fe) B_4 studied using soft x-ray time-resolved photoemission spectroscopy	Mario Okawa	Tokyo University of Science
9	$SrRuO_3/SrTiO_3$ 界面における表面光起電力効果の緩和過程の研究	松田　巌	東京大学	物性研究所	Study of temporal relaxation of the photovoltage effect at the $SrRuO_3/SrTiO_3$ interface	Iwao Matsuda	The University of Tokyo
10	時間分解軟 X 線光電子分光法を用いた酸化物・金属界面におけるサイト選択的キャリアダイナミクスの解明	山本　達	東京大学	物性研究所	Site-specific carrier dynamics at the oxide/metal interface studied by time-resolved soft x-ray photoelectron spectroscopy	Susumu Yamamoto	The University of Tokyo
11					Lighting up the role of the redox-inactive metal M in $[Mn_3M(\mu_4\text{-}O)(\mu_2\text{-}O)]$ mimics of Nature's Mn_4O_5Ca oxygen-evolving complex	Van Schooneveld Matti	Max Planck Institute for C-hemical Energy Conversion
12					Probing by RIXS the nature of low-energy excitations in cuprates across the insulator-to-superconductor phase boundary	Grioni Marco	Ecole Polytechnique Federale de Lausanne
13					In-situ resonant inelastic x-ray scattering study on the (auto) reducibility of novel carbon nanotube supported core-shell cobalt-iron fischer-tropsch catalysts	Liu Boyang	Utrecht University
14	有機薄膜太陽電池界面のエネルギー損失に関する研究	櫻井　岳暁	筑波大学	数理物質系	Study of energy loss processes at donor/acceptor interfaces in organic solar cells	Takeaki Sakurai	University of Tsukuba
15	オペランド 3D nano-ESCA を用いた二次元原子薄膜ヘテロ接合系の観察とデバイス応用 (I) モデル試料：グラフェンを用いたオペランド顕微分光法の基盤の確立	吹留　博一	東北大学	大学院工学研究科	Operando analysis and device applications of hetero-junctioned 2D atomic layers (I) Establishment of operando spectromicroscopy using graphene as a model system	Hirokazu Fukidome	Tohoku University
16	時間分解共鳴磁気光学カー効果による鉄ナノ薄膜内スピン緩和過程の研究	松田　巌	東京大学	物性研究所	Study of spin relaxation process in iron nanofilms by time-resolved resonant magneto-optical Kerr effect	Iwao Matsuda	The University of Tokyo

No.	課題名	氏名	所属		Title	Name	Organization
17	巨大磁歪物質 $Tb_{0.3}Dy_{0.7}Fe_2$ の磁場中 RIXS 測定	宮脇　淳	東京大学	物性研究所	RIXS of giant magnetostrictive material, $Tb_{0.3}Dy_{0.7}Fe_2$ in magnetic field	Miyawaki Jun	The University of Tokyo
18	リチウムイオン電池用高電圧正極材料・および低電圧負極材料のオペランド軟 X 線吸収 / 発光分光　その２	朝倉　大輔	産業技術総合研究所	エネルギー界面技術グループ	Operando soft x-ray absorption/emission spectroscopy studies of high-voltage cathode materials and low-voltage anode materials for Li-ion batteries II	Asakura Daisuke	National Institute of Advanced Industrial Science and Technology
19	顕微高分解能二次元光電子分光による遷移金属化合物の構造物性解析	大門　寛	奈良先端科学技術大学院大学	凝縮系物性学研究室	Analysis of structures and electronic states of transition metal compounds by microscopic high-resolution two-dimensional photoelectron spectroscopy	Daimon Hiroshi	Nara Institute of Science and Technology
20	光誘起キャリアによる Si(111)-In 吸着表面の金属 - 絶縁体相転移ダイナミクス	虻川　匡司	東北大学	多元物質科学研究所	Dynamics of metal-to-insulator phase-transition of Si(111)-in surface by photo induced carrier	Abukawa Tadashi	Tohoku University
21	強磁性 Cr, Fe 酸化物の磁場中軟 X 線共鳴非弾性 X 線散乱	藤原　秀紀	大阪大学	理学系研究科	Magnetic field dependence of SX-RIXS for Cr and Fe based Ferromagnetic transition metal oxides	Fujiwara Hideki	Osaka Universtiy
22	雰囲気 X 線光電子分光による Cu ステップ表面における CO_2 の活性化と水素化の研究	吉信　淳	東京大学	物性研究所	Activation and hydrogenation of CO_2 on Cu stepped surfaces studied by ambient pressure X-ray photoelectron spectroscopy	Jun Yoshinobu	The University of Tokyo
23					Study of temporal relaxation of the photo-Dember effect on a InN surface	Tang Shu Jung	National Tsing Hua University (NTHU)
24					Charge injection in prototype solar cells sampled by fast XPS	Flavell Wendy	The University of Manchester

平成 26 年度　スーパーコンピュータ 共同利用課題一覧 / Joint Research List of Supercomputer system 2014

No.	課題名	氏名	所属	Title	Name	Organization
1. 第一原理計算 / First-Principles Calculation of Materials Properties						
1	ハード及びソフトナノ物質の原子構造と電子物性	押山　淳	東京大学工学系研究科	Atomic structures and electronic properties of hard- and soft-nanomaterials	Atsushi Oshiyama	The University of Tokyo
2	SiC ベースの次世代パワーデバイスの設計指針の第一原理量子論による獲得	白石　賢二	名古屋大学　大学院　工学研究科	First principles design of future SiC-based power devices	Kenji Shiraishi	Nagoya University
3	ナイロン分解酵素 NylC の加水分解反応に関する理論的研究	重田　育照	筑波大学大学院数理物質科学研究科	Theoretical analyses on hydrolysis mechanism of Nyl C	Yasuteru Shigeta	The University of Tokyo
4	物質構造・電子状態の新しい第一原理シミュレーション手法の開発と応用	常行　真司	東京大学大学院理学系研究科物理学専攻	Development and application of new methods for first-principles simulation of material structure and electronic properties	Shinji Tsuneyuki	The University of Tokyo
5	有機・金属界面で誘起される磁気分極に関する理論的研究	柳澤　将	琉球大学理学部物質地球科学科物理系	Theoretical investigation of spin polarization induced at the organic-metal interfaces	Susumu Yanagisawa	University of the Ryukyus
6	界面における構造、電子状態、および、反応過程の第一原理シミュレーション	森川　良忠	大阪大学 大学院工学研究科 精密科学・応用物理学専攻	First-principles simulations of atomic geometries, electronic properties, and chemical reactions at interfaces	Yoshitada Morikawa	Osaka University
7	極限的パルス光と物質の相互作用に対する実時間第一原理計算	矢花　一浩	筑波大学計算科学研究センター	First-principles calculation of interactions between extreme pulse light and matter	Kazuhiro Yabana	University of Tsukuba
8	第一原理計算と革新的数理手法に基づく並列化超大規模電子構造理論	星　健夫	鳥取大学大学院工学研究科機械宇宙工学専攻	Parallelized ultra-large-scale electronic-structure theory based on first principle calculation and novel numerical method	Takeo Hoshi	Tottori University
9	ハード及びソフトナノ物質の原子構造と電子物性	押山　淳	東京大学工学系研究科	Atomic structures and electronic properties of hard- and soft-nanomaterials	Atsushi Oshiyama	The University of Tokyo
10	電極電位一定の方法を用いた電気化学反応シミュレーション	大谷　実	産業技術総合研究所	Simulation of electrochemical reaction using constant electrode potential method	Minoru Otani	National Institute of Advanced Industrial Science and Technology
11	有機分子半導体における金属原子の吸着・クラスター化の研究	中山　隆史	千葉大学理学部物理学科	Adsorption and clustering of metal atoms on organic molecular semiconductors	Takashi Nakayama	Chiba University
12	不純物ドープ型カーボン系物質の原子構造、安定性と電子構造	藤本　義隆	東京工業大学大学院理工学研究科物性物理学専攻	Atomic structures, structural stabilities, and electronic properties of impurity-doped carbon-based materials	Yoshitaka Fujimoto	Tokyo Institute of Technology
13	界面における構造、電子状態、および、反応過程の第一原理シミュレーション	森川　良忠	大阪大学 大学院工学研究科 精密科学・応用物理学専攻	First-principles emulations of atomic geometries, electronic properties, and chemical reactions at interfaces	Yoshitada Morikawa	Osaka University
14	ナノスケール炭素物質の物質設計	岡田　晋	筑波大学大学院数理物質科学研究科	Design of nanoscale carbon materials	Susumu Okada	University of Tsukuba
15	水素結合型分子性機能物質における重水素効果の理論的解析	立川　仁典	横浜市立大学	Theoretical analysis of deuterated effect on hydrogen-bonded molecular materials	Masanori Tachikawa	Yokohama Citu University

No.	課題名	氏名	所属	Title	Name	Organization
16	第一原理メタダイナミックス計算による CARE 加工プロセスの解明 -GaN,SiC および SiO_2 のエッチング反応障壁の解析 -	稲垣　耕司	大阪大学大学院工学研究科	First-principles meta-dynamics analysis in Catalytic Referred Etching method (reaction barrier in etching of GaN, SiC and SiO_2)	Kouji Inagaki	Osaka University
17	DFT 自由エネルギー計算手法を用いた電池・触媒界面の酸化還元反応機構解析	館山　佳尚	物質・材料研究機構　国際ナノアーキテクトニクス研究拠点	DFT free energy analysis of redox reaction mechanism at interfaces in batteries and catalysts	Yoshitaka Tateyama	National Institute for Materials Science
18	DFT 自由エネルギー計算手法を用いた電池・触媒界面の酸化還元反応機構解析	館山　佳尚	物質・材料研究機構　国際ナノアーキテクトニクス研究拠点	DFT free energy analysis of redox reaction mechanism at interfaces in batteries and catalysts	Yoshitaka Tateyama	National Institute for Materials Science
19	ナイロン分解酵素 NylC の熱耐性の理論解析	重田　育照	筑波大学大学院数理物質科学研究科	Theoretical studies on heat resistance of Nyl-C	Yasuteru Shigeta	University of Tsukuba
20	第一原理メタダイナミックス計算による CARE 加工プロセスの解明 -GaN,SiC および SiO_2 のエッチング反応障壁の解析 -	稲垣　耕司	大阪大学大学院工学研究科	First-principles meta-dynamics analysis of Catalytic Referred Etching method (Reaction barrier in etching of GaN, SiC and SiO_2)	Kouji Inagaki	Osaka University
21	遷移金属薄膜・有機金属錯体の電子構造と磁性に関する第一原理計算	中村　浩次	三重大学大学院工学研究科物理工学専攻	First principles calculations on electronic structures and magnetism in transition-metal films and organic metal complexes	Kohji Nakamura	Mie University
22	有機半導体薄膜の成長に関する第一原理計算による研究	西館　数芽	岩手大学工学部	Ab-initio study of organic semiconductor thin film growth	Kazume Nishidate	IWATE University
23	外場に応答するナノ構造の励起電子状態と非断熱過程の第一原理計算	渡辺　一之	東京理科大学理学部	Ab initio study of excited electronic states and nonadiabatic processes of nanostructures under external fields	Kazuyuki Watanabe	Tokyo University of Science
24	鉄化合物の磁性と電子状態計算	小畑　修二	東京電機大学理工学部	Magnetization and electronic structure calculations of Fe compounds	Shuji Obata	Tokyo Denki University
25	二次元半導体の欠陥・表面・界面の物性と構造の解明	影島　博之	島根大学大学院総合理工学研究科	Study on physical and structural properties of defects, surfaces, and interfaces for 2D semiconductors	Hiroyuki Kageshima	Shimane University
26	酸化物接合によるスピントロニクス磁気異方性電界効果材料の探索	小田　竜樹	金沢大学理工研究域数物科学系	Exploratory study on electric field effect of the magnetic anisotropy in the spintronics material with the oxide layer	Tatsuki Oda	Kanazawa University
27	遷移金属酸化物における磁性・誘電性・トポロジカル性質の電子状態計算	山内　邦彦	大阪大学産業科学研究所	Ab-initio study of magnetism, ferroelectricity, and topological properties in transition-metal oxides	Kunihiko Yamauchi	Osaka University
28	遷移金属化合物の第一原理計算	小口　多美夫	大阪大学産業科学研究所	First-principles calculation of transition-metal compounds	Tamio Oguchi	Osaka University
29	シリコン表面における金属ナノクラスターの安定性とダイナミクスの密度汎関数理論による研究	濱田　幾太郎	物質・材料研究機構	Density functional theory study of stability and dynamics of metal nanoclusters on a silicon surface	Ikutaro Hamada	National Institute for Materials Science
30	第一原理計算による二次電池正極材料の充放電機構解析	籾田　浩義	大阪大学産業科学研究所	First-principles study on charge-discharge reaction mechanism in cathode materials of secondary batteries	Hiroyoshi Momida	Osaka University
31	実空間差分法に基づく大規模第一原理電子状態・輸送特性計算手法の開発とシミュレーション	小野　倫也	筑波大学計算科学研究センター	Development of first-principles electronic-structure and transport calculation method based on real-space finite-difference approach	Tomoya Ono	University of Tsukuba
32	高圧力下における共有結合性液体の構造と電子状態の第一原理計算	下條　冬樹	熊本大学大学院自然科学研究科	First-principles molecular-dynamics study of structural and electronic properties of covalent liquids under pressure	Fuyuki Shimojo	Kumamoto University

No.	課題名	氏名	所属	Title	Name	Organization
33	外場に応答するナノ構造の励起電子状態と非断熱過程の第一原理計算	渡辺　一之	東京理科大学理学部	Ab initio study of excited electronic states and nonadiabatic processes of nanostructures under external fields	Kazuyuki Watanabe	Tokyo University of Science
34	水・界面活性剤界面の第一原理 MD シミュレーション	大戸　達彦	大阪大学大学院基礎工学研究科	First-principles molecular dynamics simulation of the water/surfactant interfaces	Tatsuhiko Ohto	Osaka University
35	スピントロニクス材料の原子構造、磁気状態、および電子状態の解析	小田　竜樹	金沢大学理工研究域数物科学系	Analyses on atomic structure, magnetism, and electronic structure in spintronics materials	Tatsuki Oda	Kanazawa University
36	固体表面・界面ナノ領域における水素及び酸素の反応解析	笠井　秀明	大阪大学大学院工学研究科	Analysis of hydrogen and oxygen reactions on solid surface/interface	Hideaki Kasai	Osaka University
37	NdFeB 主相ー副相界面の磁気異方性	合田　義弘	東京工業大学大学院総合理工学研究科材料物理科学専攻	Interface magnetic anisotropy of NdFeB magnets	Yoshihiro Gohda	Tokyo Institute of Technology
38	不純物ドープ型カーボン系物質の原子構造、安定性と電子構造	藤本　義隆	東京工業大学大学院理工学研究科物性物理学専攻	Atomic structures, structural stabilities, and electronic properties of impurity-doped carbon-based materials	Yoshitaka Fujimoto	Tokyo Institute of Technology
39	ナノ構造の量子伝導の第一原理計算	小林　伸彦	筑波大学 数理物質科学研究科 電子・物理工学専攻	First-principles study of quantum transport in nanostructures	Nobuhiko Kobayashi	University of Tsukuba
40	実空間差分法に基づく大規模第一原理電子状態・輸送特性計算手法の開発とシミュレーション	小野　倫也	筑波大学計算科学研究センター	Development of first-principles electronic-structure and transport calculation method based on real-space finite-difference approach	Tomoya Ono	University of Tsukuba
41	高圧力下における共有結合性液体の構造と電子状態の第一原理計算	下條　冬樹	熊本大学大学院自然科学研究科	First-principles molecular-dynamics study of structural and electronic properties of covalent liquids under pressure	Fuyuki Shimojo	Kumamoto University
42	ナノ構造の電子およびイオン輸送特性の理論解析	渡邉　聡	東京大学大学院工学系研究科マテリアル工学専攻	Theoretical analyses on electronic and ionic transport properties of nanostructures	Satoshi Watanabe	The University of Tokyo
43	スピントロニクス材料および分子性磁性体の原子構造、磁気状態、電子状態の解析	小田　竜樹	金沢大学理工研究域数物科学系	Analyses on atomic structure, magnetism, and electronic structure in spintronics materials and molecular magnets	Tatsuki Oda	Kanazawa University
44	ナノ構造の量子伝導の第一原理計算	小林　伸彦	筑波大学 数理物質科学研究科 電子・物理工学専攻	First-principles study of quantum transport in nanostructures	Nobuhiko Kobayashi	University of Tsukuba
45	エネルギー変換過程における基礎過程の研究と高変換効率化に向けた大規模第一原理計算	山下　晃一	東京大学大学院工学系研究科	Large scale ab initio calculations on the fundamental processes of energy convergence devices and on their optimization for high conversion efficiency	Koichi Yamashita	The University of Tokyo
46	第一原理及び古典分子動力学計算による固液界面の構造及び電子状態評価	福井　賢一	大阪大学大学院基礎工学研究科	Structural and electronic properties of solid / liquid interfaces using first-principles and classical molecular dynamics	Ken-Ichi Fukui	Osaka University
47	固体表面・界面ナノ領域における水素及び酸素の反応解析	笠井　秀明	大阪大学大学院工学研究科	Analysis of hydrogen and oxygen reactions on solid surface/interface	Hideaki Kasai	Osaka University
48	ハイブリッド ab initio QM/MM 計算による生体高分子の生物機能の解析	舘野　賢	兵庫県立大学大学院　生命理学研究科	Hybrid ab initio QM/MM calculations of biological macromolecules	Masaru Tateno	University of Hyogo
49	$SrVO_3$ および $SrRuO_3$ の第一原理 GW スペクトル関数	中村　和磨	九州工業大学	Ab initio GW calculations for $SrVO_3$ and $SrRuO_3$	Kazuma Nakamura	Kyushu Institute of Technology

No.	課題名	氏名	所属	Title	Name	Organization
50	次世代メモリ素子に関する第一原理モデリング	洗平　昌晃	名古屋大学大学院工学研究科	First-principles modeling on emerging memory devices	Masaaki Araidai	Graduate School of Engineering, Nagoya University
51	全固体電池材料の固体 / 固体界面構造における電子構造解析	大野　隆央	物質・材料研究機構	Ab initio analysis on solid/solid interfaces for all-solid-state batteries	Takahisa Ohno	National Institute for Materials Science
52	全電子第一原理 GW+Bethe-Salpeter 法の開発と応用計算	野口　良史	東京大学物性研究所	All-electron first-principles GW+Bethe-Salpeter method: development and application	Yoshifumi Noguchi	The University of Tokyo
53	電圧印加密度汎関数計算によるナノキャパシタンス解析	安藤　康伸	東京大学 工学系研究科	Nano-capacitance analysis based on density functional theory with applied bias	Yasunobu Ando	The University of Tokyo
54	マルチスケール電気伝導・熱伝導計算	広瀬　賢二	物質材料研究機構	Multi-scale electric and thermal transport calculations	Kenji Hirose	National Institute for Materials Science
55	ナノ構造の電子およびイオン輸送特性の理論解析	渡邉　聡	東京大学大学院工学系研究科マテリアル工学専攻	Theoretical analyses on electronic and ionic transport properties of nanostructures	Satoshi Watanabe	The University of Tokyo
56	遷移金属酸化物界面の第一原理計算	石井　史之	金沢大学理工研究域数物科学系	First-principles calculation of transition metal oxides interfaces	Fumiyuki Ishii	Kanazawa University
57	酸化物界面原子構造及び電子特性	幾原　雄一	東京大学大学院工学系研究科総合研究機構	Atomic Structure and Electronic Property of Oxide Interfaces	Yuichi Ikuhara	The University of Tokyo
58	αアルミナ粒界における点欠陥構造の第一原理計算	桑原　彰秀	ファインセラミックスセンター	First principles calculations of point defects nearby grain boundaries of alpha Al_2O_3	Akihide Kuwabara	Japan Fine Ceramics Center
59	酸化物電極触媒	杉野　修	東京大学物性研究所	Oxide electrocatalysts	Osamu Sugino	The University of Tokyo
60	遷移金属酸化物ヘテロ構造・超格子構造超伝導体の軌道純化理論に立脚した物質設計	榊原　寛史	理化学研究所	Theoretical material design of transition metal oxide hetero structure based on the orbital distillation effect	Hirofumi Sakakibara	RIKEN
61	スピントロニクス向け材料の電子物性シミュレーション	斎藤　峯雄	金沢大学理学部計算科学科	Simulation of electronic properties in materials for spintronics	Mineo Saito	Kanazawa University
62	第一原理及び古典分子動力学計算による電解質溶液 / 電極界面の微視的研究	福井　賢一	大阪大学大学院基礎工学研究科	First-principles and classical molecular dynamics investigations of electrolyte solution / electrode interfaces	Ken-Ichi Fukui	Osaka University
63	半導体格子欠陥の第一原理計算	山内　淳	慶應義塾大学理工学部	First-principles study on the defects in semiconductors	Jun Yamauchi	Keio University
64	動的電子輸送解析に向けた第一原理計算手法の開発と応用	江上　喜幸	北海道大学大学院工学研究院	Development and application of first-principles simulator for dynamics of electron transport	Yoshiyuki Egami	Hokkaido University
65	有機分子会合体や結晶の電子的性質に関する理論的研究	柳澤　将	琉球大学理学部物質地球科学科物理系	Theoretical investigation on electronic structures of organic molecular aggregates and solids	Susumu Yanagisawa	University of the Ryukyus
66	第一原理分子動力学法による X-FEL 照射に伴う分子解離ダイナミクス	大村　訓史	広島工業大学　工学部	Ab initio molecular dynamics study of molecular dissociation by irradiation of X-FEL	Satoshi Ohmura	Hiroshima Institute of Technology

No.	課題名	氏名	所属	Title	Name	Organization
67	第一原理計算による遷移金属酸化物の原子配列構造の解明と磁性の研究	豊田　雅之	大阪大学産業科学研究所	First-principles study on magnetism and atomic structures of transition-metal oxides	Masayuki Toyoda	Osaka University
68	電子デバイスのための自己組織化ナノインターフェイスの理論	レービガー ハンネス	横浜国立大学　大学院工学研究院　物理工学コース	Theory of self-organized nano-interfaces for electronic devices	Hannes Raebiger	Yokohama National University
69	トレオニン合成酵素の全反応機構の解明	庄司　光男	筑波大学数理物質科学研究科	Theoretical elucidation on the full reaction mechanism of threonine synthase	Mitsuo Shoji	University of Tsukuba
70	多元系カルコパイライト型半導体の格子熱伝導率低下メカニズム解明	泰岡　顕治	慶應義塾大学理工学部機械工学科	First principles study on lattice thermal conductivity reduction in multinary chalcopyrite semiconductors	Kenji Yasuoka	Keio University
71	第一原理計算を援用した固体表面・界面領域における電子状態と反応解析	國貞　雄治	北海道大学大学院工学研究院　附属エネルギー・マテリアル融合領域研究センター	First principles based analysis of electronic structures and reactions on surfaces/interfaces	Yuji Kunisada	Hokkaido University
72	有機・金属界面で誘起される磁気分極に関する理論的研究	柳澤　将	琉球大学理学部物質地球科学科物理系	Theoretical investigation of spin polarization induced at the organic-metal interfaces	Susumu Yanagisawa	University of the Ryukyus
73	グラフェンに担持した Pt クラスターに対する van der Waals 相互作用の第一原理計算	濱本　雄治	大阪大学 大学院工学研究科 精密科学・応用物理学専攻	First principles calculation of van der Waals interaction in Pt clusters on graphene	Yuji Hamamoto	Osaka University
74	磁性電極を架橋する分子の熱電特性の第一原理計算	大戸　達彦	大阪大学大学院基礎工学研究科	Ab initio study of thermoelectric properties of molecules between magnetic electrodes	Tatsuhiko Ohto	Osaka University
75	グラフェンに担持した Pt クラスターに対する van der Waals 相互作用の第一原理計算	濱本　雄治	大阪大学 大学院工学研究科 精密科学・応用物理学専攻	First principles calculation of van der Waals interaction in Pt clusters on graphene	Yuji Hamamoto	Osaka University
76	有機分子会合体や結晶の電子的性質に関する理論的研究	柳澤　将	琉球大学理学部物質地球科学科物理系	Theoretical investigation on electronic structures of organic molecular aggregates and solids	Susumu Yanagisawa	University of the Ryukyus
77	動的電子輸送解析に向けた第一原理計算手法の開発と応用	江上　喜幸	北海道大学大学院工学研究院	Development and application of first-principles simulator for dynamics of electron transport	Yoshiyuki Egami	Hokkaido University
78	酸化物トポロジカル絶縁体の第一原理計算	石井　史之	金沢大学理工研究域数物科学系	First-principles calculation of oxide topological insulators	Fumiyuki Ishii	Kanazawa University
79	スタンナイト Cu_2FeSnS_4 の相安定性及び欠陥の性質	泰岡　顕治	慶應義塾大学理工学部機械工学科	Phase stability and defect properties of stannite Cu_2FeSnS_4	Kenji Yasuoka	Keio University
80	磁気物性値とスピン軌道相互作用系の第一原理計算	三宅　隆	産総研ナノシステム研究部門	First-principles approach to magnetic properties and spin-orbit interaction	Takashi Miyake	AIST
81	ハイブリッド ab initio QM/MM 計算による生体高分子の生物機能の解析	舘野　賢	兵庫県立大学大学院　生命理学研究科	Hybrid ab initio QM/MM calculations of biological macromolecules	Masaru Tateno	University of Hyogo
82	担持金属ナノクラスターの構造と触媒機能	豊浦　和明	名古屋大学工学研究科マテリアル理工学専攻	Structures and catalytic properties of supported metal nanoclusters	Kazuaki Toyoura	Nagoya University
83	新たなナノスケール界面の電子物性の探索	小林　功佳	お茶の水女子大学理学部物理学科	Search for electronic properties of new nanoscale interfaces	Katsuyoshi Kobayashi	Ochanomizu University

No.	課題名	氏名	所属	Title	Name	Organization
84	Si 表面上の原子吸着系のモデル計算	服部　賢	奈良先端科学技術大学院大学物質創成科学研究科	Model calculations in Si surfaces with adsorbates	Ken Hattori	Nara Institute of Science and Technology
85	第一原理計算を援用した固体表面・界面領域における電子状態と反応解析	國貞　雄治	北海道大学大学院工学研究院　附属エネルギー・マテリアル融合領域研究センター	First principles based analysis of electronic structures and reactions on surfaces/interfaces	Yuji Kunisada	Hokkaido University
86	金属表面の欠陥と有機分子の結合状態	首藤　健一	横浜国立大学・工学部	Bonding states of organic molecules adsorbed at defects on metal surface	Ken-Ichi Shudo	Yokohama Nat' l University
87	全固体電池におけるイオン伝導特性の計算科学的解析	大野　隆央	物質・材料研究機構	Computational analysis on ionic conduction properties of all solid-state lithium secondary battery materials	Takahisa Ohno	National Institute for Materials Science
88	無機複合型プロトン電解質の結晶界面におけるイオン伝導度の評価	大友　順一郎	東京大学大学院新領域創成科学研究科環境システム学専攻	Evaluation of ion conductivity at interfaces in proton conducting composite electrolyte	Junichiro Otomo	The University of Tokyo
89	第一原理分子動力学による Pt(322) ステップ表面における水バイレイヤー中の水の解離	木崎　栄年	大阪大学大学院工学研究科	First-principles molecular dynamics simulations on a water dissociation in water-bi-layer on stepped Pt(322)	Hidetoshi Kizaki	Osaka University
90	照射損傷と格子間原子との相互作用の研究	大澤　一人	九州大学応用力学研究所	Study of interaction between radiation damage and interstitial atom	Kazuhito Ohsawa	Kyushu University
91	第一原理 GW 計算による遷移金属酸化物のプラズマロン状態の解析	中村　和磨	九州工業大学	Ab initio GW analysis for low-energy plasmaron states of transition-metal oxides	Kazuma Nakamura	Kyushu Institute of Technology
92	スピントロニクス向け材料の電子物性シミュレーション	斎藤　峯雄	金沢大学理学部計算科学科	Simulation of electronic properties in materials for spintronics	Mineo Saito	Kanazawa University
93	希土類磁石材料の電子状態	赤井　久純	東京大学物性研究所	Electronic structure of rare earth magnets	Hisazumi Akai	The University of Tokyo
94	磁性電極を架橋する分子の熱電特性の第一原理計算	大戸　達彦	大阪大学大学院基礎工学研究科	Ab initio study of thermoelectric properties of molecules between magnetic electrodes	Tatsuhiko Ohto	Osaka University
95	第一原理 GW 計算によるプラズマロン状態の解析	中村　和磨	九州工業大学	Ab initio GW analysis for low-energy plasmaron states	Kazuma Nakamura	Kyushu Institute of Technology
96	固体電解質におけるイオン伝導現象の第一原理計算	桑原　彰秀	ファインセラミックスセンター	First principles calculations of ionic conductivity in solid electrolytes	Akihide Kuwabara	Japan Fine Ceramics Center
97	無機複合型プロトン電解質の結晶界面におけるイオン伝導度の評価	大友　順一郎	東京大学大学院新領域創成科学研究科環境システム学専攻	Evaluation of ion conductivity of interfaces in composite-type proton conducting electrolyte	Junichiro Otomo	The University of Tokyo
98	下部マントル鉱物の格子熱伝導率に対する鉄固溶効果の第一原理計算	出倉　春彦	愛媛大学地球深部ダイナミクス研究センター	First-principles calculations of iron solid solution effects on the lattice thermal conductivity of lower mantle minerals	Haruhiko Dekura	Ehime University
99	固体表面における有機分子の磁性	高木　紀明	東京大学新領域創成科学研究科物質系専攻	Magnetism of organic molecules on solid surfaces	Noriaki Takagi	The University of Tokyo
100	セラミックスの粒界における原子配列および電子状態の第一原理計算	佐藤　幸生	九州大学大学院工学研究院材料工学部門	First-principles calculation of atomic arrangement and electronic structure in ceramic grain boundaries	Yukio Sato	Kyushu University

No.	課題名	氏名	所属	Title	Name	Organization
101	磁性薄膜におけるノンコリニア磁気構造の第一原理計算	三浦　良雄	京都工芸繊維大学　工芸科学研究科	A first-principles study on noncollinear magnetic structures in magnetic films	Yoshio Miura	Kyoto Institute of Technology
102	金属酸化物の酸化還元反応における担体効果シミュレーション	大友　順一郎	東京大学大学院新領域創成科学研究科環境システム学専攻	Numerical simulation of metal oxides redox reaction on various supports	Junichiro Otomo	The University of Tokyo
103	高イオン伝導物質の理論的設計	大野　隆央	物質・材料研究機構	Theoretical design of the high ionic conductor	Takahisa Ohno	National Institute for Materials Science
104	低次元ハニカムシートの物性探索	高木　紀明	東京大学新領域創成科学研究科物質系専攻	Exploring low-dimensional honeycomb sheets	Noriaki Takagi	The University of Tokyo
105	超精密ダイヤモンド工具の損耗機構	宇田　豊	大阪電気通信大学工学部機械工学科	Wear mechanism of diamond tool	Yutaka Uda	Osaka Electro-Communication University
106	磁性薄膜における交換スティフネスの第一原理計算	三浦　良雄	京都工芸繊維大学　工芸科学研究科	A first-principles study on exhange stiffness constants in magnetic films	Yoshio Miura	Kyoto Institute of Technology
107	14 族原子によるハニカムシートの構造と電子状態	高木　紀明	東京大学新領域創成科学研究科物質系専攻	Geometric and electronic structures of honeycomb sheet consisting of atoms in 14th group	Noriaki Takagi	The University of Tokyo
108	金属電極にコンタクトした分子の幾何構造と磁性	高木　紀明	東京大学新領域創成科学研究科物質系専攻	Geometric structure and magnetism of molecules connecting with metal electrode	Noriaki Takagi	The University of Tokyo
109	液体金属による Al 合金の粒界脆化抑制メカニズムの第一原理解析	谷垣　健一	大阪大学大学院基礎工学研究科	First principles analysis for suppression of grain boundary embrittlement of aluminum alloys by liquid metals	Kenichi Tanigaki	Osaka University
110	照射損傷と格子間原子との相互作用の研究	大澤　一人	九州大学応用力学研究所	Study of interaction between radiation damage and interstitial atom	Kazuhito Ohsawa	Kyushu University
111	Cu_3Au 型結晶構造を持つ Mn 規則合金の磁気構造と電子状態の理論	内田　尚志	北海道科学大学	Theory of magnetic and electronic structure for Mn-based ordered alloys with Cu_3Au-type crystal structure	Takashi Uchida	Hokkaido University of Science
112	液体酸素・液体窒素の超高圧構造の解明	大村　訓史	広島工業大学　工学部	Ultrahigh-pressure structures of liquid oxygen and nitrogen	Satoshi Ohmura	Hiroshima Institute of Technology
113	層状人工格子界面の電子状態と近接効果	平井　國友	奈良県立医科大学医学部物理学	Electronic state and proximity effects around interface in layered superlattices	Kunitomo Hirai	Nara Medical University
114	超精密ダイヤモンド工具の損耗機構	宇田　豊	大阪電気通信大学工学部機械工学科	Wear mechanism of diamond tool	Yutaka Uda	Osaka Electro-Communication University
115	Cu_3Au 型結晶構造を持つ Mn 規則合金の磁気構造と電子状態の温度依存性	内田　尚志	北海道科学大学	Temperature dependence of magnetic and electronic structure for Mn-based ordered alloys with Cu_3Au-type crystal structure	Takashi Uchida	Hokkaido University of Science
116	第一原理計算を用いた希薄窒化物半導体 InSbN のバンド構造に関する研究	藤代　博記	東京理科大学	Study of band structure for InSbN based dilute nitride semiconductor by using first-principle simulation	Hiroki Fujishiro	Tokyo University of Science
117	第一原理計算を用いた遷移金属化合物の物性研究	榊原　寛史	理化学研究所	Physical analysis of transition metal compounds performing the first-principles calculation	Hirofumi Sakakibara	RIKEN

No.	課題名	氏名	所属	Title	Name	Organization
118	第一原理計算による水分解用光触媒材料の解析	山田　太郎	東京大学大学院工学系研究科化学システム工学専攻	Ab-initio DFT calculations of photocatalyst material for water splitting	Taro Yamada	The University of Tokyo
119	状態選択的化学反応の理解と制御	寺本　央	北海道大学電子科学研究所	Understandings and control of state-selective chemical reactions in terms of dynamical systems theory	Teramoto Hiroshi	Hokkaido University of Science
2. 強相関 / Strongly Correlated Quantum Systems						
120	スピン軌道相互作用と電子相関の協奏による新奇量子相の数値的研究	今田　正俊	東京大学工学系研究科物理工学専攻	Numerical studies on novel quantum phases induced by cooperative spin-orbit couplings and electron correlations	Masatoshi Imada	The University of Tokyo
121	強相関電子系の新奇電子状態に関する理論的研究	松浦　弘泰	東京大学理学研究科物理学専攻	Theoretical study of novel electronic states in strongly correlated electron systems	Hiroyasu Matsuura	The University of Tokyo
122	鉄系および銅酸化物高温超伝導体における圧力効果の研究	黒木　和彦	大阪大学	Study on the pressure effect of iron-based and cuprate superconductors	Kazuhiko Kuroki	Osaka University
123	パイロクロア格子系における磁気・軌道自由度による多極子秩序の研究	宇田川　将文	東京大学大学院工学系研究科物理工学専攻	Study of multipolar ordering composed of magnetic and orbital degrees of freedom in pyrochlore lattice systems	Masafumi Udagawa	The University of Tokyo
124	数値繰り込み群法による電子・フォノン系の近藤効果の研究	堀田　貴嗣	首都大学東京理工学研究科物理学専攻	Study of Kondo effect in electron-phonon systems by numerical renormalization group method	Takashi Hotta	Tokyo Metropolitan University
125	ドープされたバンド絶縁体における非従来型超伝導メカニズムに関する研究	黒木　和彦	大阪大学	Study of superconducting mechanisms in carrier doped band insulators	Kazuhiko Kuroki	Osaka University
126	非対称的な斥力相互作用における三成分フェルミ粒子系の超流動安定性	古賀　昌久	東京工業大学	Stability of the superfluid state in three-component Fermions with asymmetric repulsive interaction	Akihisa Koga	Tokyo Institute of Technology
127	スピン軌道相互作用の強い多体電子系における電子の局在と分化の数値的研究	山地　洋平	東京大学大学院工学系研究科物理工学専攻	Numerical studies on localization and fractionalization of many-body electrons with strong spin-orbit couplings	Youhei Yamaji	The University of Tokyo
128	連続時間量子モンテカルロ法による多軌道強相関電子系の研究	有田　亮太郎	理化学研究所創発物性科学研究センター	Study of strongly-correlated multiorbital systems with continuous-time quantum Monte Carlo method	Ryotaro Arita	RIKEN Center for Emergent Materials Science
129	CaV_4O_9 型格子上ハバード模型におけるモット転移	柳　有起	東京理科大学理工学部物理学科	Mott transition in the Hubbard model on the CaV_4O_9 lattice	Yuki Yanagi	Tokyo University of Science
130	2 次元ペンローズ格子におけるサイト間相関効果	古賀　昌久	東京工業大学	Inter site electron correlations in two-dimensional Hubbard Penrose lattice	Akihisa Koga	Tokyo Institute of Technology
131	強相関フラーレン系の超伝導の非経験的研究	有田　亮太郎	理化学研究所創発物性科学研究センター	Nonempirical study of superconductivity in correlated fullerenes	Ryotaro Arita	RIKEN Center for Emergent Materials Science
132	内部自由度のある系における超流動安定性	古賀　昌久	東京工業大学	Stability of the superfluid state with internal degree of freedom	Akihisa Koga	Tokyo Institute of Technology
133	鉄系超伝導体の類似物質 LaMnAsO, LaMnPO の第一原理電子状態計算	三澤　貴宏	東京大学大学院工学研究科物理工学専攻	Ab initio calculations for Mn analog of iron-based superconductors LaMnAsO and LaMnPO	Takahiro Misawa	The University of Tokyo

No.	課題名	氏名	所属	Title	Name	Organization
134	熱的量子純粋状態の方法を用いた Fermion 系の数値解析	清水　明	東京大学総合文化研究科広域科学専攻相関基礎科学系	Thermal pure quantum state calculus of Fermion systems	Akira Shimizu	The University of Tokyo
135	非一様系の量子相形成における相関効果の理論的研究	川上　則雄	京都大学大学院理学研究科物理学宇宙物理学専攻	Theoretical studies of correlation effects on quantum phase formation in inhomogeneous systems	Norio Kawakami	Kyoto University
136	超伝導体および電子・格子系における非平衡相転移	青木　秀夫	東京大学大学院理学系研究科	Non-equilibrium phase transitions in superconductors and electron-phonon systems	Hideo Aoki	The University of Tokyo
137	強相関電子系のヘテロ接合・超格子構造における量子物性の理論的解析	川上　則雄	京都大学大学院理学研究科物理学宇宙物理学専攻	Theoretical analysis of quantum properties at heterostructures and superlattices of strongly correlated systems	Norio Kawakami	Kyoto University
138	正方格子ハバード模型における反強磁性転移近傍の電気伝導の研究	佐藤　年裕	独立行政法人理化学研究所	Electric transport near the antiferromagnetic transition in a square-lattice Hubbard model	Toshihiro Sato	RIKEN
139	モンテカルロ法を用いたカイラルらせん磁性体の研究	星野　晋太郎	東京大学総合文化研究科	Monte Carlo approach to Chiral helimagnets	Shintaro Hoshino	The University of Tokyo
140	1/5 周期欠損正方格子ハバード模型における反強磁性	柳　有起	東京理科大学理工学部物理学科	Antiferromagnetism in 1/5-depleted square lattice Hubbard model	Yuki Yanagi	Tokyo University of Science
141	多変数変分モンテカルロ法を用いたホルシュタイン・ハバードモデルの研究	大越　孝洋	東京大学大学院工学系研究科物理工学専攻	Multi-variable variational Monte Carlo study of the Holstein-Hubbard model	Takahiro Ohgoe	The University of Tokyo
142	ALPS/MPS の開発とその２次元格子量子模型への応用	五十嵐　亮	東京大学物性研究所	Development of ALPS/MPS and its application to 2-dimensional quantum lattice system	Ryo Igarashi	The University of Tokyo
143	鉄系超伝導体における動的スピンゆらぎ増強機構	伏屋　雄紀	電気通信大学	Enhancement mechanism of dynamical spin-fluctuation in iron-based superconductors	Yuki Fuseya	University of Electro-Communications
144	量子モンテカルロ法と第一原理計算による強相関系の研究	柳沢　孝	産業技術総合研究所	Quantum Monte Carlo simulations and electronic state calculations in correlated electron systems	Takashi Yanagisawa	National Institute of Advanced Industrial Science and Technology
145	量子モンテカルロ法と第一原理計算による強相関系の研究	柳沢　孝	産業技術総合研究所	Quantum Monte Carlo simulations and first principles calculations in correlated electron systems	Takashi Yanagisawa	National Institute of Advanced Industrial Science and Technology
146	1 次元量子系における磁束クエンチの数値的研究	押川　正毅	東京大学物性研究所	Numerical study of flux quench in one-dimensional quantum systems	Masaki Oshikawa	The University of Tokyo
147	多自由度電子系における非平衡ダイナミクスの研究	石原　純夫	東北大学大学院理学研究科	Study of non-equilibrium states in correlated electron systems with multi-degrees of freedom	Sumio Ishihara	Department of Physics, Tohoku University
148	動的平均場理論の拡張理論による非従来型超伝導の研究	大槻　純也	東北大学大学院理学研究科	Investigation of unconventional superconductivities by extension of the dynamical mean-field theory	Junya Otsuki	Tohoku University
149	電子相関系における誘電応答・光応答とそのダイナミクス	石原　純夫	東北大学大学院理学研究科	Dielectric and optical responses and dynamics in correlated electron systems	Sumio Ishihara	Tohoku University
150	多軌道強相関電子系の輸送現象の微視的理論	荒川　直也	理化学研究所創発物性科学研究センター	Microscopic theory for transport phenomena of multi-orbital strongly correlated electron systems	Naoya Arakawa	RIKEN

No.	課題名	氏名	所属	Title	Name	Organization
151	基板吸着 ^{4}He の数値解析	本山　裕一	東京大学物性研究所	Numerical simulation of ^{4}He adsorbed on substrates	Yuichi Motoyama	The University of Tokyo
152	スピン軌道相互作用が強い多軌道電子系における絶縁相の性質	佐藤　年裕	独立行政法人理化学研究所	Insulating state of multi-orbital electronic system with strong spin-orbit coupling	Toshihiro Sato	RIKEN
153	バンド間相互作用がもたらすエキシトン凝縮・CDW・超伝導に関する理論的研究	渡部　洋	理化学研究所　創発物性科学研究センター	Theoretical study for exciton condensation, CDW, and superconductivity induced by interband interaction	Hiroshi Watanabe	RIKEN Center for Emergent Matter Science
154	強相関電子系の研究	山田　篤志	千葉大学理学研究科	Studies on strongly correlated electron systems	Atsushi Yamada	Chiba University
3. 巨視系の協同現象 / Cooperative Phenomena in Complex, Macroscopic Systems						
155	フラストレート磁性体におけるトポロジカル相転移の研究	大久保　毅	東京大学物性研究所	Topological phase transition in the frustrated magnets	Tsuyoshi Okubo	The University of Tokyo
156	テンソルネットワーク法の並列化	川島　直輝	東京大学物性研究所	Parallelization of tensor network methods	Naoki Kawashima	The University of Tokyo
157	バルクエッジ対応の数値的研究	初貝　安弘	筑波大学大学院数理物質科学研究科物理学専攻	Numerical studies of bulk-edge correspondence	Yasuhiro Hatsugai	University of Tsukuba
158	高分子溶融体の要素変形を考慮したマルチスケールシミュレーション	村島　隆浩	東北大学大学院理学研究科	Multiscale simulation of polymer melts with element deformation	Takahiro Murashima	Tohoku University
159	フラストレート磁性体における新奇秩序	川村　光	大阪大学理学研究科	Novel order in frustrated magnets	Hikaru Kawamura	Osaka University
160	フラストレート磁性体における新奇秩序	川村　光	大阪大学理学研究科	Novel order in frustrated magnets	Hikaru Kawamura	Osaka University
161	量子スピン系におけるリング交換がもたらす新しい量子相	坂井　徹	日本原子力研究開発機構量子ビーム応用研究部門	Ring exchange induced new quantum phases in quantum spin systems	Toru Sakai	Japan Atomic Energy Agency
162	テンソルネットワーク法の並列化	川島　直輝	東京大学物性研究所	Parallelization of tensor network methods	Naoki Kawashima	The University of Tokyo
163	拡張アンサンブル法による複雑系の研究	岡本　祐幸	名古屋大学大学院理学研究科	Study on complex systems by generalized-ensemble algorithms	Yuko Okamoto	Nagoya University
164	スピンナノチューブの新しい量子相についての数値的研究	坂井　徹	日本原子力研究開発機構量子ビーム応用研究部門	Numerical study on novel phases of the spin nanotubes	Toru Sakai	Japan Atomic Energy Agency
165	空間構造をもつ一次元量子スピン系の数値的研究	利根川　孝	神戸大学大学院理学研究科	Numerical study of the one-dimensional quantum spin systems with spatial structures	Takashi Tonegawa	Kobe University
166	界面活性剤系のマルチラメラ高次構造形成ダイナミクス	芝　隼人	東京大学物性研究所	Dynamics of higher-order structure formation in surfactant membranes	Hayato Shiba	The University of Tokyo

No.	課題名	氏名	所属	Title	Name	Organization
167	空間構造をもつ一次元量子スピン系の数値的研究	利根川　孝	神戸大学大学院理学研究科	Numerical study of the one-dimensional quantum spin systems with spatial structures	Takashi Tonegawa	Kobe University
168	ソフトマター系における流体効果の協同運動に及ぼす効果	古川　亮	東京大学生産技術研究所	Hydrodynamic effects on the collective dynamics of soft matter systems	Akira Furukawa	The University of Tokyo
169	相転移現象の新奇機構の開拓	宮下　精二	東京大学理学系研究科物理学専攻	Explore in new aspects of phase transitions	Seiji Miyashita	The University of Tokyo
170	非平衡準安定状態での遅い緩和過程	渕崎　員弘	愛媛大学理工学研究科	Slow dynamical processes in nonequilibrium metastable states	Kazuhiro Fuchizaki	Ehime University
171	強相関超伝導体における非平衡現象	岡　隆史	東京大学工学系研究科物理工学専攻	Theoretical study of non-equilibrium phase transitions in strongly correlated superconductors	Takashi Oka	The University of Tokyo
172	有限次元模型のレプリカ対称性の破れの可能性	福島　孝治	東京大学大学院総合文化研究科	A possible replica symmetry breaking in finite-dimensional statistical-mechanics models	Koji Hukushima	The University of Tokyo
173	希土類金属化合物における磁気秩序と逐次相転移現象	鈴木　隆史	兵庫県立大学　大学院工学研究科	Succsessive phase transition and magnetic orders in rare-earth metals	Takafumi Suzuki	University of Hyogo
174	蜂の巣格子磁性体 Na_2IrO_3 の動的性質	鈴木　隆史	兵庫県立大学　大学院工学研究科	Dynamical properties of honeybomb lattice magnets	Takafumi Suzuki	University of Hyogo
175	有限次元模型のレプリカ対称性の破れの可能性	福島　孝治	東京大学大学院総合文化研究科	A possible replica symmetry breaking in finite dimensional statistical-mechanics models	Koji Hukushima	The University of Tokyo
176	フラストレート磁性体における新奇秩序の探索	大久保　毅	東京大学物性研究所	Novel phases in frustrated magnets	Tsuyoshi Okubo	The University of Tokyo
177	蛋白質物性に強く関与するソフトモードの効率的サンプリングシミュレーション	北尾　彰朗	東京大学分子細胞生物学研究所	Efficient sampling simulation of the soft modes significantly contribute to protein properties	Akio Kitao	The University of Tokyo
178	乱れたトポロジカル絶縁体の相図と臨界現象	大槻　東巳	上智大学理工学部	Phase diagram and critical properties of disordered topological insulators	Tomi Ohtsuki	Sophia University
179	フラストレート磁性体における新奇秩序の探索	大久保　毅	東京大学物性研究所	Novel phases in the frustrated magnets	Tsuyoshi Okubo	The University of Tokyo
180	摩擦の物理	松川　宏	青山学院大学理工学部	Physics of friction	Hiroshi Matsukawa	Aoyama Gakuin University
181	非平衡準安定状態での遅い緩和過程	渕崎　員弘	愛媛大学理工学研究科	Slow dynamical processes in nonequilibrium metastable states	Kazuhiro Fuchizaki	Ehime University
182	量子スピン系の低エネルギー状態に関する数値的研究	中野　博生	兵庫県立大学大学院物質理学研究科	Numerical study on low-energy states of quantum spin systems	Hiroki Nakano	University of Hyogo
183	生体膜上での膜タンパク質の自己集合	野口　博司	東京大学物性研究所	Protein self-assembly on biomembranes	Hiroshi Noguchi	The University of Tokyo

No.	課題名	氏名	所属	Title	Name	Organization
184	量子スピン系の非磁性相に関する数値的研究	原田　健自	京都大学大学院情報学研究科	Numerical study of non-magnetic phase in quantum spin systems	Kenji Harada	Kyoto University
185	並列化マルチワームアルゴリズムを用いたカゴメ格子上ハードコアボゾンのエッジ状態	正木　晶子	理化学研究所	Quantum Monte Carlo study of the edge state of hardcore bosons on a Kagome lattice	Akiko Masaki-Kato	RIKEN
186	密度行列繰り込み群法によるフラストレートスピン梯子系の研究	遠山　貴己	東京理科大学理学部応用物理学科	DMRG study of a frustrated two-leg spin ladder	Takami Tohyama	Tokyo University of Science
187	量子スピン系における量子相関とトポロジカルな秩序に関する研究	藤堂　眞治	東京大学大学院理学系研究科物理学専攻	Study of quantum correlations and topological order in quantum spin systems	Synge Todo	The University of Tokyo
188	構造ガラスの超大規模シミュレーションによる静的動的不均一性の探索	芝　隼人	東京大学物性研究所	Quest for static and dynamical heterogeneities in structural glass by huge-scale molecular simulation	Hayato Shiba	The University of Tokyo
189	気泡の Ostwald 的成長過程におけるスケーリング解析	渡辺　宙志	東京大学物性研究所	Scaling analysis for Ostwald-like ripening of bubbles	Hiroshi Watanabe	The University of Tokyo
190	3 次元量子スピン液体の有限温度相転移とその特徴付け	求　幸年	東京大学大学院工学系研究科	Finite-temperature phase transitions and their characterization in 3D quantum spin liquids	Yukitoshi Motome	The University of Tokyo
191	スピン秩序構造の異方性と磁気熱量効果の関係の探索	田村　亮	国立研究開発法人 物質・材料研究機構	Study on relation between anisotropic magnetic structure and magnetocaloric effect	Ryo Tamura	National Institute for Materials Science
192	微細横溝加工を施した鉛直平板を流れる凝縮液膜流の熱輸送特性	足立　高弘	秋田大学工学資源学部機械工学科	Heat transfer characteristics of condensate film flow along vertical plates with microscopic grooves	Takahiro Adachi	Akita University
193	統計物理学を基盤とした量子情報科学の展開	田中　宗	早稲田大学 高等研究所	Study on quantum information science based on statistical physics	Shu Tanaka	Waseda University
194	フラストレーションのある統計力学模型における相転移の探求	田中　宗	早稲田大学 高等研究所	Study on phase transition in frustrated spin systems	Shu Tanaka	Waseda University
195	膜タンパクの結合、化学反応による脂質２重膜の形状変化	野口　博司	東京大学物性研究所	Shape transformation of lipid membranes induced by protein adsorption and chemical reaction	Hiroshi Noguchi	The University of Tokyo
196	磁場印加下でのフラストレート磁性体が示す新規機能物性の探索	田村　亮	国立研究開発法人 物質・材料研究機構	Quest for exotic functional properties under magnetic field in frustrated systems	Ryo Tamura	National Institute for Materials Science
197	微細横溝加工を施した鉛直平板を流れる凝縮液膜流の熱輸送特性	足立　高弘	秋田大学工学資源学部機械工学科	Heat transfer characteristics of condensate film flow along vertical plates with microscopic grooves	Takahiro Adachi	Akita University
198	複雑流体の熱流動に対するマルチスケールシミュレーション	安田　修悟	兵庫県立大学大学院シミュレーション学研究科	Multiscale simulation for non-isothermal flows of complex fluids	Shugo Yasuda	Graduate School of Simulation Studies
199	ジャンクションレストランジスタにおける不純物散乱	植田　暁子	筑波大学数理物質系	Impurity scattering in Junctionless transistor	Akiko Ueda	The University of Tokyo
200	カーネル法による動的スケーリングの改良と非平衡緩和解析への応用	尾関　之康	電気通信大学情報理工学研究科	Improvement of dynamical scaling by the use of kernel method and its applications to nonequilibrium relaxation analyses	Yukiyasu Ozeki	The University of Electro-Communications

No.	課題名	氏名	所属	Title	Name	Organization
201	シュウ酸カルシウム一水和物による氷核生成促進機構の分子動力学シミュレーション研究	灘　浩樹	産業技術総合研究所	Molecular dynamics simulation study of mechanism of ice nucleation promotion by calcium oxalate monohydrate	Hiroki Nada	National Institute of Advanced Industrial Science and Technology
202	不均一ソフトマター系のレオロジー	古川　亮	東京大学生産技術研究所	Rheology of heterogeneous soft matter systems	Akira Furukawa	The University of Tokyo
203	疎 Pfaffian の高速計算アルゴリズムの開発とイジング系への応用	溜渕　継博	静岡大学理学部	Development of fast algorythms for sparse Pfaffians and their applications to Ising systems	Tsuguhiro Tamaribuchi	Shizuoka University
204	ナノ構造界面での熱輸送特性の評価	塩見　淳一郎	東京大学工学系研究科	Characterization of thermal transport at nanostructure interface	Junichiro Shiomi	The University of Tokyo
205	量子スピン系の非磁性相に関する数値的研究	原田　健自	京都大学大学院情報学研究科	Numerical study of non-magnetic phase in quantum spin systems	Kenji Harada	Kyoto University
206	地震の統計モデルの数値シミュレーション	川村　光	大阪大学理学研究科	Numerical simulations on statistical models of earthquakes	Hikaru Kawamura	Osaka University
207	非従来型超伝導体の束縛状態	永井　佑紀	日本原子力研究開発機構	Bound states in unconventional superconductors	Yuki Nagai	Japan Atomic Energy Agency
208	地震の統計モデルの数値シミュレーション	川村　光	大阪大学理学研究科	Numerical simulations on statistical models of earthquakes	Hikaru Kawamura	Osaka University
209	固体表面に創成された低次元電子系の物性とその制御	稲岡　毅	琉球大学理学部	Physical properties of low-dimensional electron systems created at solid surfaces and their control	Takeshi Inaoka	University of the Ryukyus
210	ハニカム格子磁性体を用いた非自明な磁気現象に関する数値的研究	下川　統久朗	大阪大学大学院 理学研究科 宇宙地球科学専攻	Numerical study of the novel magnetic phenomenon on the honeycomb magnetism	Tokuro Shimokawa	Osaka University
211	カーネル法による動的スケーリングの改良と非平衡緩和法への応用	尾関　之康	電気通信大学情報理工学研究科	Improvement of dynamical scaling by the use of kernel method and its applications to nonequilibrium relaxation analyses	Yukiyasu Ozeki	The University of Electro-Communications
212	ネマチック液晶中の高分子鎖の挙動 II	荒木　武昭	京都大学大学院理学研究科物理学・宇宙物理学専攻	Conformations of polymer chains in nematic liquid crystals II	Takeaki Araki	Kyoto University
213	ボルツマン液体の基底状態と固化	簑口　友紀	東京大学大学院総合文化研究科	The ground state properties of Boltzmann liquid and its crystallization	Tomoki Minoguchi	The University of Tokyo
214	X 線 n 波回折とタンパク質結晶構造解析における位相問題の研究	沖津　康平	東京大学 大学院工学系研究科	Study on X-ray n-beam diffraction and phase problem in protein crystal structure analysis	Kouhei Okitsu	The University of Tokyo
215	ハニカム格子磁性体を用いた非自明な磁気現象に関する数値的研究	下川　統久朗	大阪大学大学院 理学研究科 宇宙地球科学専攻	Numerical study of the novel magnetic phenomenon on the honeycomb magnetism	Tokuro Shimokawa	Osaka University
216	クーロングラス系の動的性質	寺尾　貴道	岐阜大学工学部	Dynamical properties of Coulomb glass	Takamichi Terao	Gifu University
217	クーロングラス系の動的性質	寺尾　貴道	岐阜大学工学部	Dynamical properties of Coulomb glass	Takamichi Terao	Gifu University

No.	課題名	氏名	所属	Title	Name	Organization
218	グラフェン量子素子デバイスの理論的創成	草部　浩一	大阪大学大学院基礎工学研究科	Theoretical design of graphene quantum devices	Koichi Kusakabe	Osaka University
219	フラストレート量子スピン鎖の励起ダイナミクス	大西　弘明	日本原子力研究開発機構 先端基礎研究センター	Excitation dynamics of frustrated quantum spin chain	Hiroaki Onishi	Japan Atomic Energy Agency
220	エネルギー地形計算によるタンパク質内相互作用フラストレーションの検出	松下　勝義	大阪大学 CMC	Detection of frustration of intra-protein interaction based on energy landscape calculation	Katsuyoshi Matsushita	Osaka University
221	低レイノルズ非ブラウン粒子懸濁液の吸収状態転移と粘弾性	芝　隼人	東京大学物性研究所	Absorbing states and viscoelasticity in low-Re non-Browninan particle dispersions	Hayato Shiba	The University of Tokyo
222	熱電物質におけるスピン軌道相互作用の効果	伏屋　雄紀	電気通信大学	Effect of spin-orbit interactions in thermoelectric materials	Yuki Fuseya	University of Electro-Communications
223	X線 n 波動力学および運動学理論とその解法の研究	沖津　康平	東京大学 大学院工学系研究科	Study on X-ray n-beam dynamical and kinematical diffraction theories and numerical methods to solve them	Kouhei Okitsu	The University of Tokyo
224	量子スピン系におけるフォノンの効果とフラストレーションの関連性	安田　千寿	琉球大学理学部	Phonon effects and frustration in quantum spin systems	Chitoshi Yasuda	University of Ryukyus
225	モンテカルロ法による効率的スペクトル解析法の開発と量子スピン系への応用	諏訪　秀麿	東京大学大学院理学系研究科物理学専攻	Efficient Monte Carlo spectral analysis and application to quantum spin systems	Hidemaro Suwa	The University of Tokyo
226	1次元フラストレート量子スピン系の数値的研究	飛田　和男	埼玉大学大学院理工学研究科物質科学部門	Numerical study of one dimensional frustrated quantum spin systems	Kazuo Hida	Saitama University
227	Feigenbaum 定数の高精度計算 2	城　真範	産業技術総合研究所	High precision computation of Feigenbaum constant, 2nd.	Masanori Shiro	National Institute of Advanced Industrial Science and Technology
228	変分モンテカルロ法におけるトポロジカルな量子数射影の開発	森田　悟史	東京大学物性研究所	Topological quantum-number projection in variational Monte Carlo method	Satoshi Morita	The University of Tokyo
229	内部自由度を持つ冷却原子気体における熱平衡状態の普遍性クラス	小林　未知数	京都大学大学院理学研究科	Universality class of thermally equilibrium states for cold atoms with internal degrees of freedom	Michikazu Kobayashi	Kyoto University
230	非局所動的ＣＰＡ理論に基づく長距離磁気相関の数値的研究	梯　祥郎	琉球大学理学部物理系	Numerical study of long-range magnetic correlations based on the nonlocal dynamical CPA	Yoshiro Kakehashi	University of Ryukyus
231	シェル・モデルを用いた誘電体の分子動力学シミュレーション	橋本　保	産業技術総合研究所	Molecular dynamics simulation of ferroelectrics using shell models	Tamotsu Hashimoto	National Institute of Advanced Industrial Science and Technology
232	タンパク質折りたたみエネルギー地形のマルチカノニカルサンプリング手法による構成	松下　勝義	大阪大学 CMC	Reconstruction of protein folding energy landscape based on a Multicanonical sampling method	Katsuyoshi Matsushita	Osaka University
233	スピン系の厳密対角化パッケージの並列化と高精度化	坂下　達哉	東京大学物性研究所	Parallelization and high precision computation of exact diagonalization package for spin systems	Tatsuya Sakashita	The University of Tokyo
234	高密剛体球系の非平衡相転移と大規模分子動力学シミュレーション	礒部　雅晴	名古屋工業大学	Nonequilibirum phase transition in the large scale dense hard sphere molecular dynamics simulation	Masaharu Isobe	Nagoya Institute of Technology

No.	課題名	氏名	所属	Title	Name	Organization
235	量子 Hall 系のスケーリング理論に対する運動量依存摂動の効果の研究	宮田　直幸	富山県工業技術センター	Study on effects of momentum-dependent perturbation on the scaling theory of the quantum Hall systems	Naoyuki Miyata	Toyama Industrial Technology Center
236	多成分剛体球の稠密充填状態の並列 Wang-Lanadu 法による探索	能川　知昭	東邦大学医学部	Search of close packing states of multicomponent hard-sphere systems by the parallelized Wang-Landau sampling	Tomoaki Nogawa	Faculty of Medicine, Toho University
237	両親媒性溶液中におけるミセル形状変化の分子シミュレーション研究	藤原　進	京都工芸繊維大学大学院工芸科学研究科	Molecular simulation study of Micellar shape change in amphiphilic solution	Susumu Fujiwara	Kyoto Instituteof Technology
238	多成分剛体球の稠密充填状態の並列 Wang-Lanadu 法による探索	能川　知昭	東邦大学医学部	Search of close packing states of multicomponent hard-sphere systems by the parallelized Wang-Landau sampling	Tomoaki Nogawa	Faculty of Medicine, Toho University
239	カイロペンタゴン格子上量子スピンの磁場中相転移	礒田　誠	香川大学教育学部	The phase transition under magnetic field of the quantum spin on the Cairo pentagon lattice	Makoto Isoda	Faculty of Education, Kagawa University
240	スカーミオン構造を持つ磁性体におけるジョセフソン効果	横山　毅人	東京工業大学大学院理工学研究科	Josephson effect through magnetic skyrmion	Takehito Yokoyama	Tokyo Institute of Technology
241	シリコンナノワイヤにおけるプラズモンの電子輸送への影響	植田　暁子	筑波大学数理物質系	Effect of plasmon on electron transport in Si nanowires	Akiko Ueda	University of Tsukuba
242	Pruisken スケーリング理論に対する周期磁場の効果の研究	宮田　直幸	富山県工業技術センター	On effects of periodic magnetic field on the scaling theory of Pruisken	Naoyuki Miyata	Toyama Industrial Technology Center
243	決定論的モンテカルロ計算アルゴリズムの解析	鈴木　秀幸	東京大学大学院情報理工学系研究科	Analysis of deterministic Monte Carlo algorithms	Hideyuki Suzuki	The University of Tokyo

平成 26 年度　スーパーコンピュータ CMSI 戦略課題一覧 / CMSI Project List of Supercomputer system 2014

No.	課題名	氏名	所属		Title	Name	Organization
1	分子における電子の動的過程と多体量子動力学	高塚 和夫	東京大学	大学院総合文化研究科	Nonadiabatic electron dynamics and many-body nuclear dynamics in molecules	Kazuo Takatsuka	The University of Tokyo
2	スピン軌道相互作用と電子相関の協奏が生む新量子相	今田 正俊	東京大学	大学院工学系研究科	Novel quantum phase induced by synergetic effects of spin-orbit interaction and electron correlation	Masatoshi Imada	The University of Tokyo
3	強相関電子系の励起ダイナミクスの研究	遠山 貴己	東京理科大学	理学部	Study of excitation dynamics in strongly correlated electron systems	Takami Tohyama	Tokyo University of Science
4	量子モンテカルロ法による新しい量子相・量子臨界現象に関する研究	川島 直輝	東京大学	物性研究所	Monte Carlo study of novel quantum phases and critical phenemena	Naoki Kawashima	The University of Tokyo
5	ナノ構造の電子状態から機械的性質までのマルチスケールシミュレーション	尾形 修司	名古屋工業大学	工学部	Multi-scale simulation of nano-structured devices from electronic structures to mechanical properties	Shuji Ogata	Nagoya Institute of Technology
6	密度汎関数法によるナノ構造の電子機能予測に関する研究	押山 淳	東京大学	大学院工学系研究科	Density functional study on prediction of electronic properties of nanostructures	Atsushi Oshiyama	The University of Tokyo
7	新材料探索のための第一原理計算手法開発	常行 真司	東京大学	大学院理学系研究科	Development of first-principles simulation software for exploration of new materials	Shinji Tsuneyuki	The University of Tokyo
8	スピントロニクス / マルチフェロイックスの応用へ指向した材料探索	斎藤 峯雄	金沢大学	理工研究域	Materials design for spintronics/multiferroics applications	Mineo Saito	Kanazawa University
9	ナノ構造体における光誘起電子ダイナミクスと光・電子機能性量子デバイスの開発	信定 克幸	分子科学研究所	理論・計算分子科学研究領域	Photo-induced electron dynamics in nanostructures and development of quantum devices with optical and electronic functionality	Katsuyuki Nobusada	Institute for Molecular Science
10	全原子シミュレーションによるウィルスの分子科学の展開	岡崎 進	名古屋大学	大学院工学研究科	Molecular science of virus by all-atom simulation	Susumu Okazaki	Nagoya University
11	太陽電池における光電変換の基礎過程の研究と変換効率最適化にむけた大規模数値計算	山下 晃一	東京大学	大学院工学系研究科	Large scale calculations on the fundamental processes of solar cells and their optimization in conversion efficiency and long lifetime	Koichi Yamashita	The University of Tokyo
12	エネルギー変換の界面科学	杉野 修	東京大学	物性研究所	Interface science on energy conversion	Osamu Sugino	The University of Tokyo
13	バイオマス利用のための酵素反応解析	吉田　紀生	九州大学	大学院理学研究院	Analysis of enzymatic reaction for biomass energy creation	Norio Yoshida	Kyushu University
14	剪断流下の脂質膜系の欠陥ダイナミクスの研究	芝 隼人	東京大学	物性研究所	Study of defect dynamics of surfactant membranes under shear flow	Hayato Shiba	The University of Tokyo
15	フラストレート磁性体の計算科学的研究	中野 博生	兵庫県立大学	大学院物質理学研究科	Computational-science study of frustrated magnets	Hiroki Nakano	University of Hyogo
16	Screened KKR 法による永久磁石材料の第一原理電子状態計算	土居 抄太郎	東京大学	物性研究所	First-principles electronic structure calculation of permanent magnets using the screened KKR Green's function method	Shotaro Doi	The University of Tokyo

No.	課題名	氏名	所属		Title	Name	Organization
17	フラストレート磁性体におけるトポロジカル励起の秩序化	大久保 毅	東京大学	物性研究所	Ordering of topological excitations of the frustrated magnets	Tsuyoshi Okubo	The University of Tokyo
18	物質デザインのための確率論的手法に基づく多成分系量子化学の高度化	立川 仁典	横浜市立大学	大学院生命ナノシステム科学研究科	Development of multicomponent quantum chemistry based on stochastic method for material design	Masanori Tachikawa	Yokohama City University

Publications

Division of New Materials Science

Takigawa group

We have been performing nuclear magnetic resonance experiments on various quantum spin systems and strongly correlated electron systems to explore novel quantum phases with exotic ordering and fluctuation phenomena. The major achievements in the year 2014 include: (1) Investigation by 11B-NMR of the real space imaging of a spin polaron generated by non-magnetic defects in the Shastry-Sutherland spin system $SrCu_2(BO_3)_2$, (2) Microscopic examination by angle resolved 27Al-NMR of the quarupole order and mutipolar fluctuations in $PrTi_2Al_{20}$, (3) Continued investigation on single crystals of volborthite, a frustrated quantum spin system with distorted Kagome lattice aimed at the full understanding of the phase diagram and magnetic structure in magnetic field.

1. †*Field-induced incommensurate phase in the strong-rung spin ladder with ferromagnetic legs: H. Yamaguchi, H. Miyagai, M. Yoshida, M. Takigawa, K. Iwase, T. Ono, N. Kase, K. Araki, S. Kittaka, T. Sakakibara, T. Shimokawa, T. Okubo, K. Okunishi, A. Matsuo and Y. Hosokoshi, Phys. Rev. B **89** (2014) 220402(R)(1-7).

2. †Search for a spin-nematic phase in the quasi-one-dimensional frustrated magnet $LiCuVO_4$: N. Büttgen, K. Nawa, T. Fujita, M. Hagiwara, P. Kuhns, A. Prokofiev, A. P. Reyes, L. E. Svistov, K. Yoshimura and M. Takigawa, Phys. Rev. B **90** (2014) 134401(1-7).

3. *Novel Phase Transitions in the Breathing Pyrochlore Lattice:^{7}Li-NMR on $LiInCr_4O_8$ and $LiGaCr_4O_8$: Y. Tanaka, M. Yoshida, M. Takigawa, Y. Okamoto and Z. Hiroi, Phys. Rev. Lett. **113** (2014) 227204(1-5).

4. †Real Space Imaging of Spin Polarons in Zn-Doped $SrCu_2(BO_3)_2$: M. Yoshida, H. Kobayashi, I. Yamauchi, M. Takigawa, S. Capponi, D. Poilblanc, F. Mila, K. Kudo, Y. Koike and N. Kobayashi, Phys. Rev. Lett. **114** (2015) 056402(1-5).

Sakakibara group

We study magnetism and superconductivity of materials having low characteristic temperatures. These include heavy-electron systems, quantum spin systems and frustrated spin systems. The followings are some selected achievements in the fiscal year 2014. (1) Field and temperature variations of the specific heat $C(H,T)$ of the heavy fermion superconductor UBe_{13} (T_c=0.9 K) were examined at temperatures down to 80 mK. Quite unexpectedly, the magnetic-field dependence of $C(H)$ is linear in H with no angular dependence at low fields in the superconducting state, implying that the gap is fully open over the Fermi surfaces, in stark contrast to the previous expectation. (2) Magnetization and magnetic torque of a high-quality single crystal of Sr_2RuO_4 have been measured down to 100 mK under a precise control of the magnetic-filed orientation. When the magnetic field is applied exactly parallel to the ab plane, a sharp magnetization jump at the upper critical field is observed at low temperatures, evidencing the first-order superconducting-normal transition. A strong magnetic torque appearing when H is slightly tilted away from the ab plane confirms the intrinsic anisotropy $\Gamma = \xi_a / \xi_c$ of as large as 60 even at 100 mK. The present results raises fundamental issues in both the existing spin-triplet and spin-singlet scenarios.

1. †Fine-Tuning of Magnetic Interactions in Organic Spin Ladders: H. Yama80guchi, H. Miyagai, T. Shimokawa, K. Iwase, T. Ono, Y. Kono, N. Kase, K. Araki, S. Kittaka, T. Sakakibara, T. Kawakami, K. Okunishi and Y. Hosokoshi, J. Phys. Soc. Jpn. **83** (2014) 033707(1-4).

1. Novel Electronic States of Heavy Fermion Compound $YbCo_2Zn_{20}$: F. Honda, Y. Taga, Y. Hirose, S. Yoshiuchi, Y. Tomooka, M. Ohya, J. Sakaguchi, T. Takeuchi, R. Settai, Y. Shimura, T. Sakakibara, I. Sheikin, T. Tanaka, Y. Kubo and Y. Onuki, J. Phys. Soc. Jpn. **83** (2014) 044703(1-9).

2. †Possible Evolution of Antiferromagnetism in Zn-Doped Heavy-Fermion Superconductor $CeCoIn_5$: M. Yokoyama, K. Fujimura, S. Ishikawa, M. Kimura, T. Hasegawa, I. Kawasaki, K. Tenya, Y. Kono and T. Sakakibara, J. Phys. Soc. Jpn. **83** (2014) 033706(1-5).

3. Thermodynamic Study of Nodal Structure and Multiband Superconductivity of KFe_2As_2: S. Kittaka, Y. Aoki, N. Kase, T. Sakakibara, T. Saito, H. Fukazawa, Y. Kohori, K. Kihou, C. Ho Lee, A. Iyo, H. Eisaki, K. Deguchi, N. K. Sato, Y.

* Joint research among groups within ISSP.

Tsutsumi and K. Machida, J. Phys. Soc. Jpn. **83** (2014) 013704(1-4).

4. †*Field-induced incommensurate phase in the strong-rung spin ladder with ferromagnetic legs: H. Yamaguchi, H. Miyagai, M. Yoshida, M. Takigawa, K. Iwase, T. Ono, N. Kase, K. Araki, S. Kittaka, T. Sakakibara, T. Shimokawa, T. Okubo, K. Okunishi, A. Matsuo and Y. Hosokoshi, Phys. Rev. B **89** (2014) 220402(R)(1-7).

5. Sharp magnetization jump at the first-order superconducting transition in Sr_2RuO_4: S. Kittaka, A. Kasahara, T. Sakakibara, D. Shibata, S. Yonezawa, Y. Maeno, K. Tenya and K. Machida, Phys. Rev. B **90** (2014) 220502(R) (1-5).

6. Measurement of the spin-orbit coupling in superconducting Sr_2RuO_4 using polarized light and spin-resolved photoemission spectroscopy: Evidence for a breakdown in the singlets and triplets pairing mechanisms: C. N. Veenstra, Z. -H. Zhu, M. Raichle, B. M. Ludbrook, A. Nicolaou, B. Slomski, G. Landolt, S. Kittaka, Y. Maeno, J. H. Dil, I. S. Elfimov, M. W. Haverkort and A. Damascelli, Phys. Rev. Lett. **112** (2014) 127002(1-4).

7. Multiband superconductivity with unexpected deficiency of nodal quasiparticles in $CeCu_2Si_2$: S. Kittaka, Y. Aoki, Y. Shimura, T. Sakakibara, S. Seiro, C. Geibel, F. Steglich, H. Ikeda and K. Machida, Phys. Rev. Lett. **112** (2014) 067002(1-5).

8. Spin-Chirality-Driven Ferroelectricity on a Perfect Triangular Lattice Antiferromagnet: H. Mitamura, R. Watanuki, K. Kaneko, N. Onozaki, Y. Amou, S. Kittaka, R. Kobayashi, Y. Shimura, I. Yamamoto, K. Suzuki, S. Chi and T. Sakakibara, Phys. Rev. Lett. **113** (2014) 147202 (1-5).

9. Anisotropic Superconductivity of the Caged Compound $Y_5Rh_6Sn_{18}$ with Unusual Normal-State Electrical Resistivity: N. Kase, S. Kittaka, T. Sakakibara and J. Akimitsu, JPS Conf. Proc. **3** (2014) 015042 (1-5).

10. †*Low Temperature Magnetic Properties of Frustrated Quantum Spin Chain System $Rb_2Cu_2Mo_3O_{12}$: Y. Yasui, R. Okazaki, I. Terasaki, M. Hase, M. Hagihala, T. Masuda and T. Sakakibara, JPS Conf. Proc. **3** (2014) 014014 (1-6).

11. Low Temperature Magnetization of Yb_2Pt_2Pb Along the Hard Magnetization Axis: Y. Shimura, T. Sakakibara, K. Iwakawa, K. Sugiyama and Y. Onuki, JPS Conf. Proc. **3** (2014) 014029 (1-6).

12. *Magnetization and Specific Heat of the Caged Compound PrV_2Al_{20}: K. Araki, Y. Shimura, N. Kase, T. Sakakibara, A. Sakai and S. Nakatsuji, JPS Conf. Proc. **3** (2014) 011093(1-5).

13. Magnetization Study of the Quantum Critical Behavior of the One Dimensional Spin-1/2 Heisenberg Antiferromagnet CuPzN: Y. Kono, T. Sakakibara, C. Aoyama, M. M. Turnbull, C. Landee and Y. Takano, JPS Conf. Proc. **3** (2014) 012015 (1-5).

14. †Metal-Insulator Transition in Pyrochlore Oxide $(Nd_{1-x}Pr_x)_2Ir_2O_7$ ($0.7 \leq x \leq 1$): K. Matsuhira, K. Kuroda, T. Sakakibara, M. Wakeshima and Y. Hinatsu, JPS Conf. Proc. **3** (2014) 013017 (1-6).

15. †Quantum phase near the saturation field in the S=1/2 frustrated spin ladder: H. Yamaguchi, H. Miyagai, Y. Kono, S. Kittaka, T. Sakakibara, K. Iwase, T. Ono, T. Shimokawa and Y. Hosokoshi, Phys. Rev. B **91** (2015) 125104 (1-5).

16. †S=1/2 ferromagnetic-antiferromagnetic alternating Heisenberg chain in a zinc-verdazyl complex: H. Yamaguchi, Y. Shinpuku, T. Shimokawa, K. Iwase, T. Ono, Y. Kono, S. Kittaka, T. Sakakibara and Y. Hosokoshi, Phys. Rev. B **91** (2015) 085117 (1-6).

17. Field-Induced Quantum Criticality and Universal Temperature Dependence of the Magnetization of a Spin-1/2 Heisenberg Chain: Y. Kono, T. Sakakibara, C. P. Aoyama, C. Hotta, M. M. Turnbull, C. P. Landee and Y. Takano, Phys. Rev. Lett. **114** (2015) 037202 (1-5).

18. Field-Orientation Dependence of Low-Energy Quasiparticle Excitations in the Heavy-Electron Superconductor UBe_{13}: Y. Shimizu, S. Kittaka, T. Sakakibara, Y. Haga, E. Yamamoto, H. Amitsuka, Y. Tsutsumi and K. Machida, Phys. Rev. Lett. **114** (2015) 147002 (1-5).

19. *Antiferromagnetic transition of the caged compound $TmTi_2Al_{20}$: N. Kase, Y. Shimura, S. Kittaka, T. Sakakibara, S. Nakatsuji, T. Nakano, N. Takeda and J. Akimitsu, J. Phys.: Conf. Ser. **592** (2015) 012052.

Mori group

We have successfully developed and characterized the functional molecular materials. The major achievements in 2014 are (1) to discover the conductivity and magnetism switching caused by coupled deuterium and electron transfer in the organic single-component crystal κ-D_3(Cat-EDT-TTF)$_2$, (2) to find the solid-solid interconversion with dynamic change of donor arrangement and electrical properties related to bending of hydrogen-bonded unit for the organic crystal β'-H_3(Cat-EDO-TTF)$_2BF_4$, and (3)to observe the anisotropic transport behavior under uniaxial strain in the pressure indeuced superconductor

† Joint research with outside partners.

β-(*meso*-DMBEDT-TTF)$_2$PF$_6$. The introduction of a large variety of molecule degree of freedom to solid promises the development of new trends in functional molecular materials.

1. Gapless Quantum Spin Liquid in an Organic Spin-1/2 Triangular-Lattice κ-H$_3$(Cat-EDT-TTF)$_2$: T. Isono, H. Kamo, A. Ueda, K. Takahashi, M. Kimata, H. Tajima, S. Tsuchiya, T. Terashima, S. Uji and H. Mori, Phys. Rev. Lett. **112** (2014) 177201.

2. A biferrocenium salt containing paramagnetic tetracyanoquinodimethane hexamers: charge disproportionation via donor–acceptor interactions: T. Mochida, Y. Funasako, K. Takahashi, M. Inokuchi, T. Sakurai, S. Ikeda, H. Ohta, H. Mori and M. Uruichi, Chem. Commun. **50** (2014) 13370.

3. Solid-solid phase interconversion in an organic conductor crystal: hydrogen-bond-mediated dynamic changes in π-stacked molecular arrangement and physical properties: J. Yoshida, A. Ueda, A. Nakao, R. Kumai, H. Nakao, Y. Murakami and H. Mori, Chem. Commun. **50** (2014) 15557.

4. Hydrogen-Bond-Dynamics-Based Switching of Conductivity and Magnetism: A Phase Transition Caused by Deuterium and Electron Transfer in a Hydrogen-Bonded Purely Organic Conductor Crystal: A. Ueda, S. Yamada, T. Isono, H. Kamo, A. Nakao, R. Kumai, H. Nakao, Y. Murakami, K. Yamamoto, Y. Nishio and H. Mori, J. Am. Chem. Soc. **136** (2014) 12184.

5. Protonation of Pyridyl-Substituted TTF Derivatives: Substituent Effects in Solution and in the Proton-Electron Correlated Charge-Transfer Complexes: S. C. Lee, A. Ueda, A. Nakao, R. Kumai, H. Nakao, Y. Murakami and H. Mori, Chem. Eur. J. **20** (2014) 1909.

6. Synergistic Spin Transition between Spin Crossover and Spin-Peierls-like Singlet Formation in the Halogen-Bonded Molecular Hybrid System: [Fe(Iqsal)$_2$][Ni(dmit)$_2$]·CH$_3$CN·H$_2$O: K. Fukuroi, K. Takahashi, T. Mochida, T. Sakurai, H. Ohta, T. Yamamoto, Y. Einaga and H. Mori, Angew. Chem. Int. Ed. **53** (2014) 1983.

7. Uniaxial Strain Effect of the Moderately Dimerized Molecular Conductor β-(*meso*-DMBEDT-TTF)$_2$PF$_6$: Y. Nishida, T. Isono, A. Ueda and H. Mori, Eur. J. Inorg. Chem. **2014** (2014) 3845.

8. Dynamics of Charge Ordering in the Nonlinear Regime of θ-(BEDT-TTF)$_2$CsZn(SCN)$_4$: M. Abdel-Jawad, I. Terasaki, T. Mori and H. Mori, J. Phys. Soc. Jpn. **84** (2015) 033707.

9. Phase-change memory function of correlated electrons in organic conductors: H. Oike, F. Kagawa, N. Ogawa, A. Ueda, H. Mori, M. Kawasaki and Y. Tokura, Phys. Rev. B **91** (2015) 041101.

10. 電子とプロトンが協奏する新しい分子機能性結晶の展開 : 森 初果 , 上田 顕 , 磯野 貴之 , 固体物理 **49** (2014) 149-160.

11. 化学の力を生かした新しい分子性機能材料の開発 : 森 初果 , 化学 **69**、**No1** (2014) 20-21.

12. 金属状態を示す純有機単成分導体 : 森 初果 , 工業材料 **62**　**No1** (2014) 26-27.

13. Women in Physics に参加して : 森 初果 , 東京大学理学部ニュース　理学エッセイ **No13** (2014) https://www.s.u-tokyo.ac.jp/ja/s.

Nakatsuji group

Our group explores novel quantum phases and phase transitions in rare-earth and transition metal based compounds. The followings are some relevant results obtained in 2014. (1) We have succeeded in growing high quality single crystals of PrV$_2$Al$_{20}$ and discovered heavy fermion superconductivity due to orbital fluctuations in the antiferro-quadrupolar state. Our results suggest a proximity to the quadrupolar quantum criticality due to the competition between quadrupolar Kondo effect and multipolar ordering. Indeed, we found that the application of the magnetic field suppresses the quadrupolar transition and induces a novel type of quantum criticality. Our results indicate that PrTr$_2$Al$_{20}$ provides a model system to investigate the quantum criticality purely associated with the multipolar (orbital) degrees of freedom. (2) Our high resolution thermodynamic measurements at very low temperatures on β-YbAlB$_4$ has revealed that two components associated with quantum criticality and heavy fermion behaviour exist in this intermediate valence material. The similar type of heavy fermion component dominates in the properties of α-analog. Future comparative studies will clarify the origin of the spontaneous quantum criticality of the β-phase. (3) Finally, the magnetic domain control of antiferromagnetism is an interesting subject for both basic science and their technological application. We found that the magnetic domains in the well-known antiferromagnetic Mott insulator NiS$_2$ may be controlled by the cooling procedure under magnetic fields. Further investigation such as the magnetoresistance and Hall resistivity would be important to find out useful functions in these non-collinear antiferromagnets.

1. Electronic Structure of Quantum Spin-liquid Coupound Ba$_3$CuSb$_2$O$_9$: T. Sugimoto, T. Mizokawa, H. Wadati, K. Takubo, A. Damascelli, T. Z. Regier, G. A. Sawatzky, N. Katayama, H. Sawa, K. Kimura and S. Nakatsuji, J. Phys. Soc. Jpn. **3** (2014) 014007 (1-4).

---

* Joint research among groups within ISSP.

2. †*Heavy fermion superconductivity under pressure in the quadrupole system $PrTi_2Al_{20}$: K. Matsubayashi, T. Tanaka, J. Suzuki, A. Sakai, S. Nakatsuji, K. Kitagawa, Y. Kubo and Y. Uwatoko, J. Phys. Soc. Jpn. **3** (2014) 011077 (1-5).

3. Sample Dependence of the Quadrupolar Transition in the Nonmagnetic cubic Γ_3 Compound PrV_2Al_{20}: M. Tsujimoto, A. Sakai and S. Nakatsuji, J. Phys. Soc. Jpn. **3** (2014) 011066(1-6).

4. Structural and Magnetic Properties of α-$Yb(Al_{1-x}Fe_x)B_4$ under Hydtostatic Pressure: Y. Sakaguchi, S. Ikeda, K. Kuga, S. Nakatsuji, N. Hirao, Y. Ohishi and H. Kobayashi, J. Phys. Soc. Jpn. **3** (2014) 011059 (1-6).

5. Superconducting properties of the ferroquadrupolar cubic Γ_3 compound $PrTi_2Al_{20}$: A. Sakai, K. Kuga and S. Nakatsuji, J. Phys. Soc. Jpn. **3** (2014) 011066 (1-6).

6. Suppression of the Heavy Fermion State in Magnetic Fields in the Mixed Valent α-$YbAlB_4$: Y. Matsumoto, K. Kentaro and S. Nakatsuji, J. Phys. Soc. Jpn. **3** (2014) 011076(1-5).

7. Two magnetic phases in α-YbAl1-xFexB_4: K. Kuga, S. Suzuki and S. Nakatsuji, J. Phys. Soc. Jpn. **3** (2014) 012013(1-4).

8. $CeCu_2Ge_2$: Challenging our understanding of quantum criticality: B. Zeng, Q. R. Zhang, D. Rhodes, Y. Shimura, D. Watanabe, R. E. Baumbach, P. Schlottmann, T. Ebihara and L. Balicas, Phys. Rev. B **90** (2014) 155101.

9. Experimental realization of a quantum breathing pyrochlore antiferromagnet: K. Kimura, S. Nakatsuji and T. Kimura, Phys. Rev. B **90** (2014) 060414.

10. Heavy-Fermion Superconductivity in the Quadrupole Ordered State of PrV_2Al_{20}: M. Tsujimoto, Y. Matsumoto, T. Tomita, A. Sakai and S. Nakatsuji, Phys. Rev. Lett. **113** (2014) 267001 (1-5).

11. 銅酸化物磁性体におけるスピン・軌道の特異な量子状態：澤 博 , 中辻 知 , 固体物理 **49** (2014) 533-543.

12. Quantum criticality in a metallic spin liquid: Y. Tokiwa, J. J. Ishikawa, S. Nakatsuji and P. Gegenwart, Nature Mater. **13** (2014) 356-359.

13. X-ray Photoemission and X-ray Absorption Spectroscopy of Hexagonal $Ba_3CuSb_2O_9$: T. Sugimoto, T. Mizokawa, H. Wadati, K. Takubo, A. Damascelli, T. Z. Regier, G. A. Sawatzky, N. Katayama, H. Sawa, K. Kimura and S. Nakatsuji, J. Phys. Soc. Jpn **63** (2014) 549-550.

14. Magnetic and Thermal Properties of the Single Crystalline $Pr_2Zr_2O_7$ in a [111] field: K. Kimura and S. Nakatsuji, JPS Conf. Proc. **3** (2014) 014027[5 pages].

15. *Magnetization and Specific Heat of the Caged Compound PrV_2Al_{20}: K. Araki, Y. Shimura, N. Kase, T. Sakakibara, A. Sakai and S. Nakatsuji, JPS Conf. Proc. **3** (2014) 011093(1-5).

16. *Magnetization of Yb-based mixed-valent compounds at megagauss fields: T. Terashima, Y. H. Matsuda, K. Kuga, Y. Matsumoto and S. Nakatsuji, J. Phys. Conf. Proc. **3** (2014) 011027(1-5).

17. Conduction electron spin resonance in the α-$Yb_{1-x}Fe_xAlB_4$ ($0 \le x \le 0.50$) and α-$LuAlB_4$ compounds: L. Holanda, G. Lesseux, E. Magnavita, R. Ribeiro, S. Nakatsuji, K. Kuga, Z. Fisk, S. Oseroff, R. Urbano, C. Rettori and P. Pagliuso, J. Phys.: Condens. Matter **27** (2015) 255601/1-5.

18. Field Evolution of Quantum Critical and Heavy Fermi-Liquid Components in the Magnetization of the Mixed Valence Compound β-$YbAlB_4$: Y. Matsumoto, K. Kuga, Y. Karaki, Y. Shimura, T. Sakakibara, M. Tokunaga, K. Kindo and S. Nakatsuji, J. Phys. Soc. Jpn. **84** (2015) 024710(1-7).

19. Magnetization Anomaly due to the Non-Coplanar Spin Structure in NiS_2: T. Higo and S. Nakatsuji, J. Phys. Soc. Jpn. **84** (2015) 053702(1-5).

20. Field-induced quadrupolar quantum criticality in PrV_2Al_{20}: Y. Shimura, M. Tsujimoto, B. Zeng, L. Balicas, A. Sakai and S. Nakatsuji, Phys. Rev. B **91** (2015) 241102/1-5.

21. 電子軌道の量子ゆらぎによる新しい超伝導：松本 洋介 , パリティ **30-7** (2015) (2-6).

22. Anisotropic transverse magnetoresistivity in α-$YbAlB_4$: Y. Matsumoto, J. Hong, K. Kuga and S. Nakatsuji, J. Phys.: Conf. Ser. **592** (2015) 012086.

23. Anomalous Enhancement of Seebeck Coefficient in Pr-Based 1-2-20 System with Non-Kramers Doublet Ground States: Y. Machida, T. Yoshida, T. Ikeura, K. Izawa, A. Nakama, R. Higashinaka, Y. Aoki, H. Sato, A. Sakai, S. Nakatsuji, N. Nagasawa, K. Matsumoto, T. Onimaru and T. Takabatake, J. Phys.: Conf. Ser. **592** (2015) 012025.

† Joint research with outside partners.

24. Anomalous specific heat behaviour in the quadrupolar Kondo system PrV_2Al_{20}: M. Tsujimoto, Y. Matsumoto and S. Nakatsuji, J. Phys.: Conf. Ser. **592** (2015) 012023.

25. *Antiferromagnetic transition of the caged compound $TmTi_2Al_{20}$: N. Kase, Y. Shimura, S. Kittaka, T. Sakakibara, S. Nakatsuji, T. Nakano, N. Takeda and J. Akimitsu, J. Phys.: Conf. Ser. **592** (2015) 012052.

26. *High Pressure Measurements of the Resistivity of β-$YbAlB_4$: T. Tomita, K. Kuga, Y. Uwatoko and S. Nakatsuji, J. Phys.: Conf. Ser. **592** (2015) 012019.

27. Shubnikov-de Haas Oscillation in the cubic Γ_3-based heavy fermion superconductor PrV_2Al_{20}: Y. Shimura, M. Tsujimoto, A. Sakai, B. Zeng, L. Balicas and S. Nakatsuji, J. Phys.: Conf. Ser. **592** (2015) 012026.

28. †*Synchrotron X-ray spectroscopy study on the valence state and magnetization in α-$YbAl_{1-x}Fe_xB_4$ (x = 0.115) at low temperatures and high magnetic fields: T. Terashima, Y. H. Matsuda, K. Kuga, S. Suzuki, Y. Matsumoto, S. Nakatsuji, A. Kondo, K. Kindo, N. Kawamura, M. Mizumaki and T. Inami, J. Phys.: Conf. Ser. **592** (2015) 012020 (6 pages).

29. High-Field Multi-Frequency ESR in the Rare-Earth Spinel Compound CdYb2S4: D. Yoshizawa, T. Kida, S. Nakatsuji, K. Iritani, M. Halim, T. Takeuchi and M. Hagiwara, Appl. Magn. Reson. **NIL** (2015) 0937-9347.

30. Absence of Jahn-Teller transition in the hexagonal $Ba_3CuSb_2O_9$ single crystal: N. Katayama, K. Kimura, Y. Han, J. Nasu, N. Drichko, Y. Nakanishi, M. Halim, Y. Ishiguro, R. Satake, E. Nishibori, M. Yoshizawa, T. Nakano, Y. Nozue, Y. Wakabayashi, S. Ishihara, M. Hagiwara, H. Sawa and S. Nakatsuji, Proceedings of the National Academy of Sciences (2015), in print.

Division of Condensed Matter Theory

K. Ueda group

Metal-insulator (MI) transition is one of the most intriguing phenomena of the strongly correlated electron systems. Nature of the MI transitions depends on lattice structure even if the orbital degeneracy is not taken into account. We investigate the MI transitions of the Hubbard model on the one-fifth-depleted square lattice by using the cellular dynamical mean field theory, assuming paramagnetic phases. It is shown that the MI transition is of the first order on the plaquette side of the parameter space, while it is continuous on the dimer side. The continuous MI transition is a Lifshitz transition driven by the electron-electron interaction.

1. Continuous Mott transition in a two-dimensional Hubbard model: Y. Yanagi and K. Ueda, Phys. Rev. B **90** (2014) 085113.

2. Magnetic Phases and Edge States of the 1/5-Depleted Square-Lattice Hubbard Model at 1/4 Filling: Y. Yamashita, M. Tomura, Y. Yanagi and K. Ueda, JPS Conf. Proc **3** (2014) 016012.

3. Quantum Phase Transition in the 1/5 Depleted Square Lattice Hubbard Model: Y. Yanagi and K. Ueda, JPS Conf. Proc **3** (2014) 013005.

Takada group

Employing several techniques including the Green's-function approach, quantum Monte Carlo simulations, and several types of variational approaches, we are studying various aspects of quantum many-body problems in condensed matter physics, based mainly on the first-principles Hamiltonian. This year we have obtained a couple of outstanding results: (1) We have revealed that the system of a proton embedded in the electron gas with the density parameter r_s in the region between 2 and 12.5 yields a Kondo spin-singlet resonance state with the Kondo temperature T_K well beyond 1,000K as its ground state, indicating that if a macroscopic number of protons are embedded in a regular array into a metal in this density region to form a periodic Kondo lattice, superconductivity is expected to occur at a temperature as high as $T_K/10$ by referring to heavy-fermion physics. (2) In the electron gas with the density as low as r_s~20, a new phase transition is found to occur as signaled by the anomalous behavior in the momentum distribution function, along with the unusual property of vanishing effective mass at the Fermi level m*~0, leading to a new filed of "light-fermion physics".

1. Structural evolution of the one-dimensional spectral function from the low- to the high-energy limit: H. Maebashi and Y. Takada, Phys. Rev. B **89** (2014) 201109(R) (1-5).

2. Generic Features of an Electron Injected into the Luttinger Liquid: H. Maebashi and Y. Takada, J Supercond Nov Magn

* Joint research among groups within ISSP.

28 (2015) 1331-1335.

3. 第1原理からの超伝導理論：高田 康民，物性研究 電子版 **Vol.3, No.1** (2014) 031203(1-29).

4. Theory for Reliable First-Principles Prediction of the Superconducting Transition Temperature: Y. Takada, in: *Carbon-based New Superconductors: Toward high-Tc superconductivity (ISBN 978-981-4303-30-9 (Hardcover), 978-981-4303-31-6 (eBook))*, Ch 8, edited by J. Haruyama, (Pan Stanford Publishing Pte. Ltd., 2015), pp. 193-230.

5. Theory of Superconductivity in Graphite Intercalation Compounds: Y. Takada, in: *Materials Science and Materials Engineering*, edited by S. Mahfoudh and M. Nicholls, (Elsevier, 2015), in print.

Oshikawa group

We studied a wide range of fundamental problems in condensed matter theory and statistical mechanics. In particular, we studied the total orbital angular momentum of chiral superfluids. Superfluids/superconductors with vanishing viscosity or resistivity often arise as a result of condensation of pairs of the constituent fermions. Usually, each pair does not involve a circular motion and has zero angular momentum. However, in the superfluid-A phase of liquid Helium-3, for example, each pair is rotating in a particular orientation around its center. We may then expect that the superfluid carries a total angular momentum, i.e. is rotating as a whole. There have been, however, conflicting arguments, and the problem has remained unresolved for more than 30 years. We studied this long-standing question carefully, to find a rather surprising answer: the superfluid indeed has a large total angular momentum, only if each pair has the minimal angular momentum 1. When each pair carries a higher angular momentum (2, 3, 4, ...), the total angular momentum almost vanishes. This counter-intuitive phenomenon is a consequence of subtle quantum mechanical nature of the superfluids.

1. †Quantum criticality in an asymmetric three-leg spin tube: A strong rung-coupling perspective: Y. Fuji, S. Nishimoto, H. Nakada and M. Oshikawa, Phys. Rev. B **89** (2014) 054425 (1-13).

2. †Valence bond distribution and correlation in bipartite Heisenberg antiferromagnets: D. Schwandt, F. Alet and M. Oshikawa, Phys. Rev. B **89** (2014) 104416 (1-14).

3. Beats and expansion of two-component Bose–Einstein condensates in the Thomas–Fermi limit: J. Q. Quach, J. Phys. B: At. Mol. Opt. Phys. **47** (2014) 215007.

4. †Selection of factorizable ground state in a frustrated spin tube: Order by disorder and hidden ferromagnetism: X. Plat, Y. Fuji, S. Capponi and P. Pujol, Phys. Rev. B **91** (2015) 064411 (1-21).

5. Distinct Trivial Phases Protected by a Point-Group Symmetry in Quantum Spin Chains: Y. Fuji, F. Pollmann and M. Oshikawa, Phys. Rev. Lett. **114** (2015) 177204.

6. Gravitational Casimir Effect: J. Q. Quach, Phys. Rev. Lett. **114** (2015) 081104 (1-5).

7. †Orbital Angular Momentum and Spectral Flow in Two-Dimensional Chiral Superfluids: Y. Tada, W. Nie and M. Oshikawa, Phys. Rev. Lett. **114** (2015) 195301.

8. 「物性物理学」～物質に潜む普遍的概念～：押川 正毅，数理科学 **620** (2015) 40-45.

9. †Absence of Quantum Time Crystals: H. Watanabe and M. Oshikawa, Phys. Rev. Lett. (2015), accepted for publication.

10. † ウラン系強磁性超伝導における強磁性ゆらぎが誘起するスピン三重項超伝導：石田 憲二，服部 泰佑，佐藤 憲昭，出口 和彦，多田 靖啓，藤本 聡，固体物理 **50** (2015) 123-132.

Tsunetsugu group

We have studied an unidentified phase transition observed in the heavy fermion compound $PrIr_2Zn_{20}$. Each Pr ion has two f-orbital electrons, and its local ground state is a non-Kramers doublet. We investigated how this degeneracy is lifted due to interactions between neighbor sites. We have performed a detailed analysis of mean-field approximation and phenomenological approach and determined the phase diagram upon controlling temperature and magnetic field. At low temperature, electric quadrupoles show a few types of antiferro orders, and the phase diagram is particularly rich when magnetic field is applied along (1,0,0) direction. An important finding is that the antiferro quadrupole order at zero magnetic field is accompanied by a weak ferro order, which is the secondary order parameter induced due to quadrupole anisotropy. Our calculation demonstrates that the induced ferro component also exhibits singular behaviors below the transition temperature, and this would explain the anomaly observed in ultrasound experiments. We have also investigated dynamics near the Mott metal-insulator transition. Using the cluster dynamical mean-field theory, we calculated dynamical correlations between doublon and holon, and demonstrated different behaviors between the metallic and insulating phases.

† Joint research with outside partners.

1. Antiferro Quadrupole Orders in Non-Kramers Doublet Systems: K. Hattori and H. Tsunetsugu, J. Phys. Soc. Jpn. **83** (2014) 034709 (19 pages).

2. Doublon dynamics of the Hubbard model on a triangular lattice: T. Sato and H. Tsunetsugu, Phys. Rev. B **90** (2014) 115114.

3. Quantum impurity in a Tomonaga-Luttinger liquid: Continuous-time quantum Monte Carlo approach: K. Hattori and A. Rosch, Phys. Rev. B **90** (2014) 115103.

Kohmoto group

Energy versus magnetic field (Hofstadter butterfly diagram) in twisted bilayer graphene is studied theoretically. If we take the usual Landau gauge, we cannot take a finite periodicity even when the magnetic flux through a supercell is a rational number. We show that the periodic Landau gauge, which has the periodicity in one direction, makes it possible to obtain the Hofstadter butterfly diagram. Since a supercell can be large, magnetic flux through a supercell normalized by the flux quantum can be a fractional number with a small denominator, even when a magnetic field is not extremely strong. As a result, quantized Hall conductance can be a solution of the Diophantine equation which cannot be obtained by the approximation of the linearized energy dispersion near the Dirac points.

Sugino group

In this fiscal year, we have studied the electrode-solution interface using the density functional theory (DFT) and the excited states of molecules using the time-dependent DFT and the two-particle Green's function method. In the former research, we focused on Pt(111)/solution interface and studies hydrogen distribution, the solvent fluctuation effect, and the oxygen reduction reaction. In the latter research, we studied the non-adiabatic effect, and in addition, started study on the firefly luciferin in collaboration with Akiyama group. The tensor-decomposition approach to very accurate first-principles calculation was also intensively studied.

1. †Effect of thermal motion on catalytic activity of nanoparticles in polar solvent: N. Bonnet, O. Sugino and M. Otani, J. Chem. Phys. **140** (2014) 044703.

2. †*First-Principles Investigation on Rydberg excitations of Firefly Luciferin Anion in Vacuum: Y. Noguchi, M. Hiyama, H. Akiyama and N. Koga, J. Chem. Phys. **141** (2014) 044309.

3. †Performance of Tamm-Dancoff approximation on nonadiabatic couplings by time-dependent density functional theory: C. Hu, O. Sugino and K. Watanabe, J. Chem. Phys. **140** (2014) 054106.

4. †Exceptionally long-ranged lattice relaxation in oxygen-deficient Ta2O5: Y. Yang, O. Sugino and Y. Kawazoe, Solid State Communications **195** (2014) 16.

5. First-principles thermodynamic description of hydrogen electroadsorption on the Pt(111) surface: T. T. T. Hanh, Y. Takimoto and O. Sugino, Surf. Sci. **625** (2014) 104.

6. †Self-Poisoning Dynamical Effects in the Oxygen Reduction Reaction on Pt(111) from a Top-Down Kinetic Analysis: N. Bonnet, M. Otani and O. Sugino, J. Phys. Chem. C **118** (2014) 13638.

7. All-electron GW+Bethe-Salpeter calculations on small molecules: D. Hirose, Y. Noguchi and O. Sugino, Phys. Rev. B **91** (2015) 205111.

8. Symmetry breaking and excitonic effects on optical properties of defective nanographenes: Y. Noguchi and O. Sugino, J. Chem. Phys. **142** (2015) 064313.

9. †TOMBO: All-electron mixed-basis approach to condensed matter physics: S. Ono, Y. Noguchi, R. Sahara, Y. Kawazoe and K. Ohno, Computer Physics Communications **189** (2015) 20.

10. *First-Principles Investigation of Strong Excitonic Effects in Oxygen 1s X-ray Absorption Spectra: Y. Noguchi, M. Hiyama, H. Akiyama, Y. Harada and N. Koga, J. Chem. Theory Comput. **11** (2015) 1668-1673.

11. *Vibronic Structures in Absorption and Fluorescence Spectra of Firefly Oxyluciferin in Aqueous Solutions: M. Hiyama, Y. Noguchi, H. Akiyama, K. Yamada and N. Koga, Photochem Photobiol (2015) published online, in print.

12. Configuration interaction with antisymmetrized geminal powers: W. Uemura, S. Kasamatsu and O. Sugino, Phys. Rev. A (2015), accepted for publication.

---

* Joint research among groups within ISSP.

Kato group

The main research subject of our laboratory is theory of nonequilibrium properties in nanoscale devices. We have performed (1) research on exact solutions for a multiorbital Anderson impurity at high bias voltages and (2) calculation of photon-assisted current noises under strong AC fields in quantum dot systems. We have also evaluated rare transition rates in evolutionary game theory in semiclassical analysis based on the path-integral formalism.

1. Dephasing in single-electron generation due to environmental noise probed by Hong-Ou-Mandel interferometry: E. Iyoda, T. Kato, K. Koshino and T. Martin, Phys. Rev. B **89** (2014) 205318(1-8).
2. Spatial effect on stochastic dynamics of bistable evolutionary games: K. H. Z. So, H. Otsuki and T. Kato, J. Stat. Mech. **-** (2014) P10020(1-34).
3. 双安定進化ゲームの確率的ダイナミクスに対する空間自由度の影響 : 曽弘 博 , 物性研究・電子版 **3** (2014) 032601(1-80).
4. メゾスコピック系の物理―基礎から最近の話題まで―（第 58 回物性若手夏の学校 : 講義）: 加藤 岳生 , 物性研究・電子版 **3** (2014) 031201(1-26).
5. Effects of Coulomb interaction on photon-assisted current noise through a quantum dot: T. J. Suzuki and T. Kato, Phys. Rev. B **91** (2015) 165302(1-12).
6. Exact Green's function for a multiorbital Anderson impurity at high bias voltages: A. Oguri and R. Sakano, Phys. Rev. B **91** (2015) 115429(1-14).

Division of Nanoscale Science

Iye group

Highly anisotropic magneto-transport is observed in single-layer graphene grown on a vicinal SiC(0001) substrate, which has a step-and-terrace morphology providing a uni-directional modulation. The anisotropy is attributed to the presence of parallel conduction due to remnant carriers in the SiC substrate which primarily conduct in the direction parallel to the steps. Well-developed quantum Hall state with zero resistance manifests itself for the current along the steps, whereas the QHE is obscured by pronounced positive magnetoresistance with quadratic magnetic-field dependence for the current across the steps. In the low field range conspicuous negative magnetoresiatance due to localization effect and oscillatory behavior attributed to geometrical resonance and observed.

1. [†*]Highly Anisotropic Parallel Conduction in the Stepped Substrate of Epitaxial Graphene Grown on Vicinal SiC: A. Endo, F. Komori, K. Morita, T. Kajiwara and S. Tanaka, J Low Temp Phys **179** (2015) 237-250.

Katsumoto group

By using spin-polarization at quantum point contacts (QPCs) spin interference effect in ring shaped interferometer circuit has been examined. Conductance oscillation pattern characteristic in the spin-interference effect appeared only when spin-polarized electrons were emitted into the circuit. This is probably due to the fixing of dynamical nuclear polarization. Spin injections from ferromagnets to two-dimensional electrons in quantum wells and also to two-dimensional system of graphene have been studied. In the former high spin injection efficiency of 34% has been attained. In the latter, appearance of spin-orbit interaction due to slight hydrogenaration has been detected through the inverse spin Hall effect.

1. High-efficiency graphene nanomesh magnets realized by controlling mono-hydrogenation of pore edges: T. Kato, T. Nakamura, J. Kamijyo, T. Kobayashi, Y. Yagi and J. Haruyama, Appl. Phys. Lett. **104** (2014) 252410.
2. 半導体量子輸送物性 : 勝本 信吾 , (培風館 , 東京 , 2014).
3. 量子の匠 : 勝本 信吾 , (丸善 , 東京 , 2014).

Otani group

Our research topics this year include diffusive spin transport, spin Hall effects, magnonic crystals and vortex dynamics. Concerning the diffusive spin transport, we have succeeded in fully describing spin current properties including the anisotropic spin absorption in lateral spin valves, which enable one to elucidate intrinsic spin transport and relaxation mechanisms in nonmagnets including graphene. As to spin Hall effects, we comprehensively discussed extrinsic spin Hall effects based on our

† Joint research with outside partners.

experimental results on SHE in Cu based dilute alloys. We also developed a new scheme for determining the eigenfrequency of magnetic vortex dynamics, which has been hardly detected electrically because of its nanoscale diameter on the order of the exchange length, without exploiting large magnetoresistive materials or distorted core trajectories for homodyne spin torque diode detection.

1. Propagation of nonlinearly generated harmonic spin waves in microscopic stripes: O. Rousseau, M. Yamada, K. Miura, S. Ogawa and Y. Otani, J. Appl. Phys. **115** (2014) 053914.

2. Width dependent transition of quantized spin-wave modes in Ni80Fe20 square nanorings: C. Banerjee, S. Saha, S. Barman, O. Rousseau, Y. Otani and A. Barman, J. Appl. Phys. **116** (2014) 163912.

3. Effect of anisotropic spin absorption on the Hanle effect in lateral spin valves: H. Idzuchi, Y. Fukuma, S. Takahashi, S. Maekawa and Y. Otani, Phys. Rev. B **89** (2014) 081308.

4. Extrinsic spin Hall effects measured with lateral spin valve structures: Y. Niimi, H. Suzuki, Y. Kawanishi, Y. Omori, T. Valet, A. Fert and Y. Otani, Phys. Rev. B **89** (2014) 054401.

5. Spin Injection into a Superconductor with Strong Spin-Orbit Coupling: T. Wakamura, N. Hasegawa, K. Ohnishi, Y. Niimi and Y. Otani, Phys. Rev. Lett. **112** (2014) 036602.

6. Inverse spin Hall effect in a closed loop circuit: Y. Omori, F. Auvray, T. Wakamura, Y. Niimi, A. Fert and Y. Otani, Appl. Phys. Lett. **104** (2014) 242415.

7. Modulation of effective damping constant using spin Hall effect: S. Kasai, K. Kondou, H. Sukegawa, S. Mitani, K. Tsukagoshi and Y. Otani, Appl. Phys. Lett. **104** (2014) 092408.

8. Thickness dependence of spin torque ferromagnetic resonance in Co75Fe25/Pt bilayer films: A. Ganguly, K. Kondou, H. Sukegawa, S. Mitani, S. Kasai, Y. Niimi, Y. Otani and A. Barman, Appl. Phys. Lett. **104** (2014) 072405.

9. Tunable spin wave dynamics in two-dimensional Ni80Fe20 nanodot lattices by varying dot shape: B. K. Mahato, B. Rana, D. Kumar, S. Barman, S. Sugimoto, Y. Otani and A. Barman, Appl. Phys. Lett. **105** (2014) 012406.

10. Critical exponents and domain structures of magnetic semiconductor EuS and Gd-doped EuS films near Curie temperature: H. Idzuchi, Y. Fukuma, H. S. Park, T. Matsuda, T. Tanigaki, S. Aizawa, M. Shirai, D. Shindo and Y. Otani, Appl. Phys. Express **7** (2014) 113002.

11. Detection of a symmetric circular gyration of the vortex core via the second-order harmonic magnetoresistance oscillation: S. Sugimoto, N. Hasegawa, Y. Niimi, Y. Fukuma, S. Kasai and Y. Otani, Appl. Phys. Express **7** (2014) 023006.

12. The 2014 Magnetism Roadmap: R. L. Stamps, S. Breitkreutz, J. Åkerman, A. V. Chumak, Y. Otani, G. E. W. Bauer, J.-U. Thiele, M. Bowen, S. A. Majetich, M. Kläui, I. L. Prejbeanu, B. Dieny, N. M. Dempsey and B. Hillebrands, J. Phys. D: Appl. Phys. **47** (2014) 333001.

13. Spin transport in non-magnetic nano-structures induced by non-local spin injection: H. Idzuchi, Y. Fukuma and Y. Otani, Physica E: Low-dimensional Systems and Nanostructures **68** (2015) 239.

Komori group

Electronic structures of the Au-adsorbed Ge(001) surface with a one-dimensional atomic structure were studied by high-resolution ARPES and STS. Two-dimensional Fermi surface of the surface state and decreasing density of states (DOS) toward Fermi energy are confirmed by ARPES. The latter is also confirmed by STS and attributed to the disorder of the surface lattice. The unoccupied band structure of a topological insulator BiSb alloy was studied using quasiparticle interference measured by STM. Absence of the surface band crossing is clarified, indicating this system is a dual topological insulator with the mirror Chern number −1.

1. †Systematic study of surface magnetism in Si(111)-Fe system grown by solid phase epitaxy: In situ schematic magnetic phase diagram of Si(111)-Fe: A. N. Hattori, K. Hattori, K. Kataoka, E. Takematsu, A. Ishii, F. Komori and H. Daimon, J. Magn. Magn. Mater. **363** (2014) 158-165.

2. †Absence of Luttinger liquid behavior in Au-Ge wires: A high-resolution scanning tunneling microscopy and spectroscopy study: J. Park, K. Nakatsuji, T.-H. Kim, S. K. Song, F. Komori and H. W. Yeom, Phys. Rev. B **90** (2014) 165410 (5).

3. *Robust Protection from Backscattering in the Topological Insulator $Bi_{1.5}Sb_{0.5}Te_{1.7}Se_{1.3}$: S. Kim, S. Yoshizawa, Y. Ishida, K. Eto, K. Segawa, Y. Ando, S. Shin and F. Komori, Phys. Rev. Lett. **112** (2014) 136802(1-5).

4. †*Observing hot carrier distribution in an n-type epitaxial graphene on a SiC substrate: T. Someya, H. Fukidome,

* Joint research among groups within ISSP.

Y. Ishida, R. Yoshida, T. Iimori, R. Yukawa, K. Akikubo, Sh. Yamamoto, S. Yamamoto, T. Yamamoto, T. Kanai, K. Funakubo, M. Suemitsu, J. Itatani, F. Komori, S. Shin and I. Matsuda, Appl. Phys. Lett. **104** (2014) 161103(1-4).

5. †*Scanning tunneling microscopic and spectroscopic studies on a crystalline silica monolayer epitaxially formed on hexagonal SiC(000-1) surfaces: H. Tochihara, T. Shirasawa, T. Suzuki, T. Miyamachi, T. Kajiwara, K. Yagyu, S. Yoshizawa, T. Takahashi, S. Tanaka and F. Komori, Appl. Phys. Lett. **104** (2014) 051601(1-4).

6. †*Electronic Structure and Photoelectrochemical Properties of an Ir-Doped $SrTiO_3$ Photocatalyst: S. Kawasaki, R. Takahashi, K. Akagi, J. Yoshinobu, F. Komori, K. Horiba, H. Kumigashira, K. Iwashina, A. Kudo and M. Lippmaa, J. Phys. Chem. C **118** (2014) 20222-20228.

7. †Formation of linearly linked Fe clusters on Si(111)-7x7-C_2H_5OH surface: W. Ding, D. Ju, Y. Guo, K.-I. Tanaka and F. Komori, Nanoscale Res Lett **9** (2014) 377 (6).

8. †Nonlinear terahertz field-induced carrier dynamics in photoexcited epitaxial monolayer graphene: H. A. Hafez, I. Al-Naib, M. M. Dignam, Y. Sekine, K. Oguri, F. Blanchard, D. G. Cooke, S. Tanaka, F. Komori, H. Hibino and T. Ozaki, Phys. Rev. B **91** (2015) 035422 (9).

9. *Scanning tunneling spectroscopy study of quasiparticle interference on dual topological insulator $Bi_{1-x}Sb_x$: S. Yoshizawa, F. Nakamura, A. A. Taskin, T. Iimori, K. Nakatsuji, I. Matsuda, Y. Ando and F. Komori, Phys. Rev. B **91** (2015) 045423-1,-6.

10. †*Highly Anisotropic Parallel Conduction in the Stepped Substrate of Epitaxial Graphene Grown on Vicinal SiC: A. Endo, F. Komori, K. Morita, T. Kajiwara and S. Tanaka, J Low Temp Phys **179** (2015) 237-250.

11. フェルミガス的に振る舞う表面 1 次元金属電子：矢治 浩一郎，小森 文夫，表面科学 **35** (2014) 426-431.

Yoshinobu group

We conducted several research projects in the fiscal year 2014. (1) The activation and hydrogenation of CO_2 on Cu(997) studied by SR-PES and IRAS. (2) The adsorption and decomposition of formic acid on Zn-Cu(111) studied by SR-PES and IRAS. (3) Spectroscopic characterization of chemically modified graphene (4)Construction of ambient-pressure XPS system at SPring-8. (5) The formation and characterization of oxynitride of $SrTiO_3$.

1. Quantitative analysis of chemical interaction and doping of the Si(111) native oxide surface with tetrafluorotetracyanoquinodimethane: S. Yoshimoto, M. Furuhashi, T. Koitaya, Y. Shiozawa, K. Fujimaki, Y. Harada, K. Mukai and J. Yoshinobu, J. Appl. Phys. **115** (2014) 143709 (6 pages).

2. †Configurational change of NO on Cu(110) as a function of temperature: A. Shiotari, T. Mitsui, H. Okuyama, S. Hatta, T. Aruga, T. Koitaya and J. Yoshinobu, J. Chem. Phys. **140** (2014) 214706 (6 pages).

3. Core level excitations of a fingerprint of structural and electronic properties of epitaxial silicene: R. Friedlein, A. Fleurence, K. Aoyagi, M. P. de Jong, H. Van Bui, F. B. Wiggers, S. Yoshimoto, T. Koitaya, S. Shimizu, H. Noritake, K. Mukai, J. Yoshinobu and Y. Yamada- Takamura, J. Chem. Phys. **140** (2014) 184704 (6 pages).

4. †Electronic structure of α-sexithiophene ultrathin films grown on passivated Si(001) surfaces: K. Hiraga, H. Toyoshima, H. Tanaka, K. Inoue, S. Ohno, K. Mukai, J. Yoshinobu and M. Tanaka, Appl. Surf. Sci. **307** (2014) 520-524.

5. Aqueous-Phase Oxidation of Epitaxial Graphene on the Silicon Face of SiC(0001): Md. Zakir Hossain, M. B. A. Razak, S. Yoshimoto, K. Mukai, T. Koitaya, J. Yoshinobu, H. Sone, S. Hosaka and M. C. Hersam, J. Phys. Chem. C **118** (2014) 1014-1020.

6. †*Electronic Structure and Photoelectrochemical Properties of an Ir-Doped $SrTiO_3$ Photocatalyst: S. Kawasaki, R. Takahashi, K. Akagi, J. Yoshinobu, F. Komori, K. Horiba, H. Kumigashira, K. Iwashina, A. Kudo and M. Lippmaa, J. Phys. Chem. C **118** (2014) 20222-20228.

7. †Monolayer selective methylation of epitaxial graphene on SiC(0001) through two-step chlorination-alkylation reactions: Md. Zakir Hossain, M. B. A. Razak, H. Noritake, Y. Shiozawa, S. Yoshimoto, K. Mukai, T. Koitaya, J. Yoshinobu and S. Hosaka, J. Phys. Chem. C **118** (2014) 22096-22101.

8. Structure and Photo-Induced Charge Transfer of Pyridine Molecules Adsorbed on TiO_2(110): A NEXAFS and Core-Hole-Clock Study: H. Kondoh, Y. Higashi, M. Yoshida, Y. Monya, R. Toyoshima, K. Mase, K. Amemiya, F. Tsukioka, M. Nagasaka, Y. Iwasawa, H. Orita, K. Mukai and J. Yoshinobu, Electrochemistry **82** (2014) 341-345.

9. Interface state and energy level alignment of F_4-TCNQ sandwiched between a pentacene film and the ethylene-terminated Si(100) surface: S. Yoshimoto, K. Kameshima, T. Koitaya, Y. Harada, K. Mukai and J. Yoshinobu, Organic

† Joint research with outside partners.

Electronics **15** (2014) 356-364.

10. 淡青評論「東京大学憲章を読んでみませんか」：吉信 淳 , 学内広報 **1450** (2014) 12.

11. The Quantum Nature of CH···metal Interaction: Vibrational Spectra and Kinetic and Geometric Isotope Effects of Adsorbed Cyclohexane: T. Koitaya and J. Yoshinobu, The Chemical Record **14** (2014) 848-856.

12. 「水素の事典」のうち 5 章 1-a（p.86-p.89）を分担執筆．：水素エ ネルギー協会編 , (朝倉書店 , 東京 , 2014).

Hasegawa group

Using a low temperature scanning tunneling microscopy (LT-STM), we investigated electrical conductance at atomic point contact and found that the conductance depends on the atomic site on the substrate where the point contact is formed. For instance, the point contact conductance measured on a 3-fold hollow site of the Pb(111) substrate is larger than that measured at on-top site. We also found that the conductances measured at the two sites were reversed when the tip and substrate was separated by 20 pm from the contact. These contact-atomic-site and gap-distance dependences can be explained with the number of the substrate atoms chemically interacted with the tip-apex atom. We also studied vortices on superconducting surface structure of the Si(111)-($\sqrt{7} \times \sqrt{3}$)-In using a LT-STM. At step edges of the two-dimensional superconductor we observed vortices whose shape was elongated along the step edges and whose core still exhibited a weak superconducting gap. These anomalous features can be explained by the Josephson vortices localized at the step edges, and this also evidences the Josephson coupling at the step edges. We also studied the relation of magnetic anisotropy and stacking fault in hcp Co island structures formed on the Ag(111) substrate using a spin-polarized STM. From a magnetization curve we measured on individual islands, we found that the hcp-stacked Co islands exhibit perpendicular magnetic anisotropy whereas the ones with stacking fault have in-plane magnetization. First principle calculations clearly demonstrate the weakened magnetocrystalline anisotropy and dominance of the shape anisotropy by the stacking fault insertion into the hcp island structures.

1. †Imaging Josephson Vortices on the Surface Superconductor Si(111)-($\sqrt{7} \times \sqrt{3}$)-In using a Scanning Tunneling Microscope: S. Yoshizawa, H. Kim, T. Kawakami, Y. Nagai, T. Nakayama, X. Hu, Y. Hasegawa and T. Uchihashi, Phys. Rev. Lett. **113** (2014) 247004(1-5).

2. †Microscopic origin of the π states in epitaxial silicene: A. Fleurence, Y. Yoshida, C. -C. Lee, T. Ozaki, Y. Yamada-Takamura and Y. Hasegawa, Appl. Phys. Lett. **104** (2014) 021605 (4 pages).

3. †Scanning tunneling microscopy/spectroscopy of picene thin films formed on Ag(111): Y. Yoshida, H.-H. Yang, H.-S. Huang, S.-Y. Guan, S. Yanagisawa, T. Yokosuka, M.-T. Lin, W.-B. Su, C.-S. Chang, G. Hoffmann and Y. Hasegawa, J. Chem. Phys. **141** (2014) 114701(1-8).

4. †Excitation spectrum of Josephson vortices on surface superconductor: T. Kawakami, Y. Nagai, S. Yoshizawa, H. Kim, Y. Hasegawa, T. Nakayama, T. Uchihashi and X. Hu, J. Phys.: Conf. Ser. **568** (2014) 022022(1-5).

5. Site-Dependent Evolution of Electrical Conductance from Tunneling to Atomic Point Contact: H. Kim and Y. Hasegawa, Phys. Rev. Lett. **114** (2015) 206801(1-5).

6. †Impact of Surface Conditions on the Superconductivity of Si(111)-($\sqrt{7} \times \sqrt{3}$)-In: S. Yoshizawa, H. Kim, T. Kawakami, Y. Nagai, T. Nakayama, X. Hu, Y. Hasegawa and T. Uchihashi, e-J. Surf. Sci. Nanotech. **13** (2015) 151-154.

Lippmaa group

Our main projects are related to the development of photocatalytic oxides and nanoscale multiferroic materials. In catalyst development, we look the effects of noble metal doping in $SrTiO_3$. Recent work shows that Ir and Pt dopants tend to segregate into metallic clusters at specific oxygen activities during crystal growth. The segregated metals form nanoscale pillar structures that are embedded in the perovskite lattice and can function as embedded charge collections electrodes that help to extract photogenerated charge from the bulk of the photocatalyst. Our recent work on multiferroic materials has proven that a polar state appears in magnetite immediately at the charge ordering temperature of 120 K. A new double perovskite oxide phase, La_2NiMnO_6 was found to become multiferroic under epitaxial strain. The cause of the polar state was found to be an offset of La ions at the perovskite *A* site.

1. Growth temperature effect on the structural and magnetic properties of Fe_3O_4 films grown by the self-template method: R. Takahashi, H. Misumi and M. Lippmaa, J. Appl. Phys. **116** (2014) 033918(1-7).

2. Pulsed laser deposition of epitaxial BeO thin films on sapphire and $SrTiO_3$: T. Peltier, R. Takahashi and M. Lippmaa, Appl. Phys. Lett. **104** (2014) 231608(1-4).

3. †*Electronic Structure and Photoelectrochemical Properties of an Ir-Doped $SrTiO_3$ Photocatalyst: S. Kawasaki, R. Takahashi, K. Akagi, J. Yoshinobu, F. Komori, K. Horiba, H. Kumigashira, K. Iwashina, A. Kudo and M. Lippmaa, J.

* Joint research among groups within ISSP.

Phys. Chem. C **118** (2014) 20222-20228.

4. Spontaneous Growth of Strain-Free Magnetite Nanocrystals via Temperature-Driven Dewetting: R. Takahashi, H. Misumi, T. Yamamoto and M. Lippmaa, Crystal Growth & Design **14** (2014) 1264-1271.

5. Interfacial capacitance between a ferroelectric Fe_3O_4 thin film and a semiconducting Nb:$SrTiO_3$ substrate: R. Takahashi, Y. Cho and M. Lippmaa, J. Appl. Phys. **117** (2015) 014104(1-10).

6. A-site-driven ferroelectricity in strained ferromagnetic La_2NiMnO_6 thin films: R. Takahashi, I. Ohkubo, K. Yamauchi, M. Kitamura, Y. Sakurai, M. Oshima, T. Oguchi, Y. Cho and M. Lippmaa, Phys. Rev. B **91** (2015) 134107 (1-9).

7. †Determination of band diagram for a p-n junction between Mott insulator $LaMnO_3$ and band insulator Nb:$SrTiO_3$: M. Kitamura, M. Kobayashi, E. Sakai, R. Takahashi, M. Lippmaa, K. Horiba, H. Fujioka and H. Kumigashira, Appl. Phys. Lett. **106** (2015) 061605 (1-5).

8. †Photo-electrochemical epitaxy of silver-oxide clathrate Ag_7O_8M (M=NO_3, HSO_4) on rutile-type Nb-doped TiO_2 single crystals: R. Tanaka, R. Takahashi, S. Takata, M. Lippmaa and Y. Matsumoto, CrystEngComm **17** (2015) 3701-3707.

Division of Physics in Extreme Conditions

Uwatoko group

The electrical resistivity of the nonmagnetic quadrupolar system $PrTi_2Al_{20}$ under pressure has been measured. The experimental results suggest that critical fluctuations associated with the ferroquadrupole order may mediate superconductivity. The resistivity and ac susceptibility measurements of the topological insulator Bi_2Te_3 single crystals have been reported up to 11 GPa. Under highly hydrostatic pressure conditions generated in a multi-anvil high-pressure apparatus, a pressure- induced superconductivity only appears above a critical pressure PC ~ 7 GPa, coinciding with a structural transition from a rhombohedral to a monoclinic structure. By using an integrated-fin gasket technique made from the semi-sintered MgO ceramics and the tungsten-carbide anvils of 2.5 mm square top, we successfully generate pressures over 16 GPa at both room and cryogenic temperatures down to 0.5 K. We report on the discovery of superconductivity on the verge of antiferromagnetic order in CrAs via the application of external pressure. Bulk superconductivity with Tc≈2 K emerges at the critical pressure Pc≈8 kbar, where the first-order antiferromagnetic transition at TN≈265 K under ambient pressure is completely suppressed.

1. †*Heavy fermion superconductivity under pressure in the quadrupole system $PrTi_2Al_{20}$: K. Matsubayashi, T. Tanaka, J. Suzuki, A. Sakai, S. Nakatsuji, K. Kitagawa, Y. Kubo and Y. Uwatoko, J. Phys. Soc. Jpn. **3** (2014) 011077 (1-5).

2. †Magnetic and Fermi Surface Properties of Antiferromagnet $EuCd_{11}$: A. Nakamura, Y. Hiranaka, T. Uejo, T. Takeuchi, F. Honda, H. Harima, K. Matsubayashi, Y. Uwatoko, M. Hedo, T. Nakama and Y. Onuki, J. Phys. Soc. Jpn. **83** (2014) 074714.

3. †Superconductivity on a Crossover Phenomenon of Spin–Ladder System $SrCa_{13}Cu_{24}O_{41}$ Single Crystals: A. Hisada, K. Matsubayashi, Y. Uwatoko, N. Fujiwara, G. Deng, E. Pomjakushina, K. Conder, D. M. Radheep, R. Thiyagarajan, S. Esakkimuthu and S. Arumugam, J. Phys. Soc. Jpn. **83** (2014) 073703.

4. †Anomalous pressure dependence of the superconductivity in noncentrosymmetric LaNiC2: Evidence of strong electronic correlations: S. Katano, H. Nakagawa, K. Matsubayashi, Y. Uwatoko, H. Soeda, T. Tomita and H. Takahashi, Phys. Rev. B **90** (2014) 220508 (1-4).

5. *Doping- and pressure-induced change of electrical and magnetic properties in the Fe-based spin-ladder compound $BaFe_2Se_3$: F. Du, Y. Hirata, K. Matsubayashi, Y. Uwatoko, Y. Ueda and K. Ohgushi, Phys. Rev. B **90** (2014) 085143.

6. *High-pressure effects in anti-post-perovskite superconductors V_3PnN_x (Pn = P, As): B. S. Wang, J. -G. Cheng, K. Matsubayashi, Y. Uwatoko and K. Ohgushi, Phys. Rev. B **89** (2014) 144510 (1-4).

7. Long-range antiferromagnetic order in the frustrated XY pyrochlore antiferromagnet $Er_2Ge_2O_7$: X. Li, W. M. Li, K. Matsubayashi, Y. Sato, C. Q. Jin, Y. Uwatoko, T. Kawae, A. M. Hallas, C. R. Wiebe, A. M. Arevalo-Lopez, J. P. Attfield, J. S. Gardner, R. S. Freitas, H. D. Zhou and J. -G. Cheng, Phys. Rev. B **89** (2014) 064409 (1-7).

8. Superconductivity in the topological insulator Bi_2Te_3 under hydrostatic pressure: K. Matsubayashi, T. Terai, J. S. Zhou and Y. Uwatoko, Phys. Rev. B **90** (2014) 125126.

9. Integrated-fin gasket for palm cubic-anvil high pressure apparatus: J. -G. Cheng, K. Matsubayashi, S. Nagasaki, A. Hisada, T. Hirayama, M. Hedo, H. Kagi and Y. Uwatoko, Rev. Sci. Instrum. **85** (2014) 093907(1-6).

† Joint research with outside partners.

10. Abnormal Elastic and Vibrational Behaviors of Magnetite at High Pressures: J.-F. Lin, J. Wu, J. Zhu, Z. Mao, A. H. Said, B. M. Leu, J. Cheng, Y. Uwatoko, C. Jin and J. Zhou, Sci. Rep. **4** (2014) 6282(1-11).

11. †Magnetic Field Effect on Magnetic and Electrical Properties of$Mn_{2-x}Cu_xSb$: Y. Matsumoto, H. Orihashi, K. Matsubayashi, Y. Uwatoko, M. Hiroi and K. Koyama, IEEE Transactions on Magnetics **50** (2014) 1000704(1-4).

12. High Pressure Effect on Superconductivity of Hole-Doped Pr0.75Sr0.25FeAsO Iron Pnictides: N. R. Tamilselvan, M. Kanagaraj, K. Murata, H. Yoshino, S. Arumugam, A. Yamada, Y. Uwatoko and S. Kumararaman, J Supercond Nov Magn **27** (2014) 1381-1385.

13. Superconductivity in the vicinity of antiferromagnetic order in CrAs: W. Wu, J. Cheng, K. Matsubayashi, P. Kong, F. Lin, C. Jin, N. Wang, Y. Uwatoko and J. Luo, Nat Comms **5** (2014) 5508.

14. Correlation between T_c and Crystal Structure in S-Doped FeSe Superconductors under Pressure: Studied by X-ray Diffraction of $FeSe_{0.8}S_{0.2}$ at Low Temperatures: T. Tomita, H. Takahashi, H. Takahashi, H. Okada, Y. Mizuguchi, Y. Takano, S. Nakano, K. Matsubayashi and Y. Uwatoko, J. Phys. Soc. Jpn. **84** (2015) 024713(1-8).

15. *Temperature and composition phase diagram in the iron-based ladder compounds $Ba_{1-x}Cs_xFe_2Se_3$: T. Hawai, Y. Nambu, K. Ohgushi, F. Du, Y. Hirata, M. Avdeev, Y. Uwatoko, Y. Sekine, H. Fukazawa, J. Ma, S. Chi, Y. Ueda, H. Yoshizawa and T. J. Sato, Phys. Rev. B **91** (2015) 184416.

16. Pressure Induced Superconductivity on the border of Magnetic Order in MnP: J. -G. Cheng, K. Matsubayashi, W. Wu, J. P. Sun, F. K. Lin, J. L. Luo and Y. Uwatoko, Phys. Rev. Lett. **114** (2015) 117001(1-18).

17. Pressure-Induced Valence Crossover and Novel Metamagnetic Behavior near the Antiferromagnetic Quantum Phase Transition of $YbNi_3Ga_9$: K. Matsubayashi, T. Hirayama, T. Yamashita, S. Ohara, N. Kawamura, M. Mizumaki, N. Ishimatsu, S. Watanabe, K. Kitagawa and Y. Uwatoko, Phys. Rev. Lett. **114** (2015) 086401(1-5).

18. *High Pressure Measurements of the Resistivity of β -$YbAlB_4$: T. Tomita, K. Kuga, Y. Uwatoko and S. Nakatsuji, J. Phys.: Conf. Ser. **592** (2015) 012019.

19. Electron transport in TTF-CA under High pressures: R. Takehara, K. Miyagawa, K. Kanoda, T. Miyamoto, H. Matsuzaki, H. Okamoto, H. Taniguchi, K. Matsubayashi and Y. Uwatoko, Physica B: Condensed Matter **460** (2015) 83-87.

20. Charge disproportionation and the pressure-induced insulator–metal transition in cubic perovskite $PbCrO_3$: J. Cheng, K. E. Kweon, S. A. Larregola, Y. Ding, Y. Shirako, L. G. Marshall, Z. -Y. Li, X. Li, A. M. D. Santos, M. R. Suchomel, K. Matsubayashi, Y. Uwatoko, G. S. Hwang, J. B. Goodenough and J. -S. Zhou, Proc Natl Acad Sci USA **112** (2015) 1670-1674.

Osada group

Using a simple Slater-Koster-Harrison LCAO model, we have qualitatively studied the edge state of bilayer phosphorene, which is a unit structure of the layered crystal of black phosphorus. This model successfully reproduces the isolated edge state in the bulk gap in monolayer phosphorene. In bilayer phosphorene, however, it shows that edge states are almost buried in the valence band and there is no isolated midgap edge state at the zigzag edge. Since the buried edge state works as acceptor, holes are doped from the edge state into the bulk. This gives a possible explanation for p-type conduction in undoped black phosphorus. Under the vertical electric field, the intrinsic hole doping is reduced because a part of edge states move into the gap. These features of bilayer phosphorene might be better suited for device application.

1. 有機ディラック電子系における量子ホール状態：田嶋 尚也，佐藤 光幸，鴻池 貴子，長田 俊人，固体物理 **49** (2014) 229-240.

2. Edge State and Intrinsic Hole Doping in Bilayer Phosphorene: T. Osada, J. Phys. Soc. Jpn. **84** (2015) 013703/1-4.

3. Surface Transport in the n=0 Quantum Hall Ferromagnetic State in the Organic Dirac Fermion System: T. Osada, J. Phys. Soc. Jpn. **84** (2015) 053704/1-4.

Yamashita group

From longitudinal and transverse thermal transport measurements of kagome material Volborthite, we've found a magnon thermal conduction below the Neel temperature. We also found that there is a finite thermal Hall effect in the kagome insulator above the Neel temperature, which indicate a formation of a non-trivial spin texture as entering the QSL phase. We also have made thermal transport measurements of an organic QSL candidate, kappa-H3(CAT-EDT-TTF)2, down to 100 mK. We find that the phonons are strongly scattered in this compound down to very low temperature, although the material is very clean. By comparing the thermal conductivity of the pristine and the deuterated samples, we find the proton fluctuations in the pristine

* Joint research among groups within ISSP.

compound persist down to 300 mK. This proton fluctuation can be the origin to stabilize the QSL state of the material. As a joint research with Prof. Sasaki from IMR, Tohoku University, we've performed magnetic torque measurements at ultra-low temperatures. By using the nuclear demagnetization cryostat inherited from Ishimoto group, we've cooled organic superconductors down to 2 mK and measured the dHvA oscillations. To our best knowledge, this is the very first trial to measure a quantum oscillation below the dilution temperature. Moreover, from the temperature dependence of the torque-field curve, we succeeded to extend the vortex phase diagram of the 2D superconductor down to the ultra-low temperatures. As a joint project with Dr. Yoshida from Takigawa group in ISSP, we've also performed NMR measurements of kagome volborthite by using the ultra-low cryostat. We've found that the NMR spectrum at low fields shows a drastic change at the ultra-low temperatures, which is expected to clarify the unconventional magnetic order of the kagomé compound.

Materials Design and Characterization Laboratory

Hiroi group

A new type of magnetically frustrated lattice was found in the layered fluoride $NaBa_2Mn_3F_{11}$. A kagome-type array of regular triangles composed of Mn2+ ions (spin 5/2) deforms so as to generate the next-nearest-neighbor interaction J2 between three out of six spins in the hexagon of a normal kagome lattice, in addition to the nearest-neighbor interaction J1. As a function of |J2/J1|, this lattice can interconnect the kagome (J2 = 0) and the triangular (J2 = J1) lattices and thus is called the kagome–triangular (KT) lattice. Magnetic susceptibility and heat capacity measurements performed on a polycrystalline sample of $NaBa_2Mn_3F_{11}$ show an intensive short-range antiferromagnetic correlation below 14 K probably due to the specific magnetic frustration of the KT lattice. In addition, a long-range order at 2.0 K is observed, which is significantly low compared with the antiferromagnetic Weiss temperature of 32.3 K. Theoretical considerations of Heisenberg spins in the KT lattice reveal unique non-coplanar magnetic orders in the case of ferromagnetic J1 and antiferromagnetic J2. $NaBa_2Mn_3F_{11}$ may actually exist in this regime according to the results of our analysis based on classical Monte-Carlo simulation. In a frustrated J1–J2 chain with the nearest-neighbor ferromagnetic interaction J1 and the next-nearest-neighbor antiferromagnetic interaction J2, novel magnetic states such as a spin-nematic state are theoretically expected. However, they have been rarely examined in experiments because of the difficulty in obtaining suitable model compounds. We show here that the quasi-one-dimensional antiferromagnet $NaCuMoO_4(OH)$, which comprises edge-sharing CuO2 chains, is a good candidate J1–J2 chain antiferromagnet. The exchange interactions are estimated as J1 = −51 K and J2 = 36 K by comparing the magnetic susceptibility, heat capacity, and magnetization data with the data obtained using calculations by the exact diagonalization method. High-field magnetization measurements at 1.3 K show a saturation above 26 T with little evidence of a spin nematic state expected just below the saturation field, which is probably due to smearing effects caused by thermal fluctuations and the polycrystalline nature of the sample.

1. Novel rattling of K atoms in aluminium-doped defect pyrochlore tungstate: E. Shoko, G. J. Kearley, V. K. Peterson, H. Mutka, M. M. Koza, J.-I. Yamaura, Z. Hiroi and G. J. Thorogood, J. Phys.: Condens. Matter **26** (2014) 305401.

2. *Absence of Metallic Conductivity in Tetragonal and Cubic $PbVO_3$ at High Pressure: A. A. Belik, T. Yamauchi, H. Ueda, Y. Ueda, H. Yusa, N. Hirao and M. Azuma, J. Phys. Soc. Jpn. **83** (2014) 074711.

3. †*Electronic State of $CeFe_4As_{12}$ Investigated by Using Single Crystals Grown under High Pressure of 4 GPa: Y. Ogawa, H. Sato, M. Watanabe, T. Namiki, S. Tatsuoka, R. Higashinaka, Y. Aoki, K. Kuwahara, J.-I. Yamaura and Z. Hiroi, J. Phys. Soc. Jpn. **83** (2014) 034710.

4. *Kagome–Triangular Lattice Antiferromagnet $NaBa_2Mn_3F_{11}$: H. Ishikawa, T. Okubo, Y. Okamoto and Z. Hiroi, J. Phys. Soc. Jpn. **83** (2014) 043703(1-5).

5. †*$NaCuMoO_4(OH)$ as a Candidate Frustrated J_1–J_2 Chain Quantum Magnet: K. Nawa, Y. Okamoto, A. Matsuo, K. Kindo, Y. Kitahara, S. Yoshida, S. Ikeda, S. Hara, T. Sakurai, S. Okubo, H. Ohta and Z. Hiroi, J. Phys. Soc. Jpn. **83** (2014) 103702.

6. *Superconductivity in the Hypervalent Compound $Ba_2Bi(Sb_{1-x}Bi_x)_2$ with a Square-Honeycomb Lattice: T. Yajima, F. Takeiri, Y. Nozaki, Z. Li, T. Tohyama, M. A. Green, Y. Kobayashi and H. Kageyama, J. Phys. Soc. Jpn. **83** (2014) 073705.

7. Helical order and multiferroicity in the S=12 quasi-kagome system KCu3As2O7(OD)3: G. J. Nilsen, Y. Okamoto, H. Ishikawa, V. Simonet, C. V. Colin, A. Cano, L. C. Chapon, T. Hansen, H. Mutka and Z. Hiroi, Phys. Rev. B **89** (2014) 140412.

8. *Novel Phase Transitions in the Breathing Pyrochlore Lattice: ^{7}Li-NMR on $LiInCr_4O_8$ and $LiGaCr_4O_8$: Y. Tanaka, M. Yoshida, M. Takigawa, Y. Okamoto and Z. Hiroi, Phys. Rev. Lett. **113** (2014) 227204(1-5).

9. †*Phase transitions and hydrogen bonding in deuterated calcium hydroxide: High-pressure and high-temperature neutron

† Joint research with outside partners.

diffraction measurements: R. Iizuka, K. Komatsu, H. Kagi, T. Nagai, A. Sano-Furukawa, T. Hattori, H. Gotou and T. Yagi, J. Solid State Chem. **218** (2014) 95.

10. †*Pressure-induced oligomerization of benzene at room temperature as a precursory reaction of amorphization: A. Shinozaki, K. Mimura, H. Kagi, K. Komatu, N. Noguchi and H. Gotou, J. Chem. Phys. **141** (2014) 084306.

11. †*Spin Polarization Measurements of Heusler Alloy $Ru_{0.2}Fe_{1.8}CrSi$ by Andreev Reflection Technique: I. Shigeta, Y. Maeda, K. Harumori, Y. Nishisako, M. Ito, T. Yamauchi and M. Hiroi, IEEE Trans. Magn. **50** (2014) 1.

12. Spin dynamics of Mn pyrochlore lattice in $YMn_2Zn_{20-x}In_x$: M. Miyazaki, R. Kadono, M. Hiraishi, I. Yamauchi, A. Koda, K. M. Kojima, I. Kawasaki, I. Watanabe, Y. Okamoto and Z. Hiroi, J. Phys.: Conf. Ser. **551** (2014) 012019.

13. Thermoelectric properties of Sr and Mg double-substituted LaCoO3 at room temperature: A. Jiamprasertboon, Y. Okamoto, Z. Hiroi and T. Siritanon, Ceramics International **40** (2014) 12729.

14. *Charge Order Induced by Cation Order in δ-$Ag_{2/3}V_2O_5$: T. Baba, T. Yamauchi, S. Yamazaki, H. Ueda, M. Isobe, Y. Matsushita and Y. Ueda, J. Phys. Soc. Jpn. **84** (2015) 024718.

15. *Superconductivity in 122-type antimonide $BaPt_2Sb_2$: M. Imai, S. Ibuka, N. Kikugawa, T. Terashima, S. Uji, T. Yajima, H. Kageyama and I. Hase, Phys. Rev. B **91** (2015) 014513.

16. Structural instability of the rutile compounds and its relevance to the metal–insulator transition of VO2: Z. Hiroi, Progress in Solid State Chemistry **43** (2015) 47.

17. *Substrate-induced anion rearrangement in epitaxial thin films of $LaSrCoO_{4-x}H_x$: G. Bouilly, T. Yajima, T. Terashima, Y. Kususe, K. Fujita, C. Tassel, T. Yamamoto, K. Tanaka, Y. Kobayashi and H. Kageyama, CrystEngComm **16** (2015) 9669-9674.

18. *Superconducting properties of $BaTi_2Pn_2O$ (Pn = Sb, Bi): T. Yajima, K. Nakano, Y. Nozaki and H. Kageyama, Physica C: Superconductivity **504** (2015) 36-38.

19. Superconductivity in LaPd2As2 with a collapsed 122 structure: S. Ganesanpotti, T. Yajima, K. Nakano, Y. Nozaki, T. Yamamoto, C. Tassel, Y. Kobayashi and H. Kageyama, Journal of Alloys and Compounds **613** (2015) 370-374.

20. Lifshitz metal–insulator transition induced by the all-in/all-out magnetic order in the pyrochlore oxide Cd2Os2O7: Z. Hiroi, J. Yamaura, T. Hirose, I. Nagashima and Y. Okamoto, APL Mater. **3** (2015) 041501.

Kawashima group

We have been investigating quantum spin/boson systems and frustrated systems by means of large-scale numerical simulation. We also develop new numerical techniques. Our group's achievements of 2014 include: (1) accumulating evidences for the deconfined critical phenomena in the SU(N) J-Q Heisenberg model, (2) proposal of new update scheme for quantum Monte Carlo method, which is based on the worm algorithm, but, unlike the conventional one, can be run by space-decomposition parallelization, and (3) large-scale non-equilibrium molecular dynamics simulation of bubble growth in under-pressured near-transition liquid.

1. *Kagome–Triangular Lattice Antiferromagnet $NaBa_2Mn_3F_{11}$: H. Ishikawa, T. Okubo, Y. Okamoto and Z. Hiroi, J. Phys. Soc. Jpn. **83** (2014) 043703(1-5).

2. Parallelized Quantum Monte Carlo Algorithm with Nonlocal Worm Updates: A. Masaki-Kato, T. Suzuki, K. Harada, S. Todo and N. Kawashima, Phys. Rev. Lett. **112** (2014) 140603(1-5).

3. Phase Transitions with Discrete Symmetry Breaking in Antiferromagnetic Heisenberg Models on a Triangular Lattice: R. Tamura, S. Tanaka and N. Kawashima, JPS Conf. Proc. --- Proceedings of the 12th Asia Pacific Physics Conference (APPC12) **1** (2014) 012125(1-5).

4. 大規模並列化量子モンテカルロ法の開発と冷却ボーズ原子系のシミュレーション： 正木　晶子，スーパーコンピューティングニュース **16-6** (2014) 15-24.

5. Thermal phase transition of generalized Heisenberg models for SU(N) spins on square and honeycomb lattices: T. Suzuki, K. Harada, H. Matsuo, S. Todo and N. Kawashima, Phys. Rev. B **91** (2015) 094414.

6. Thermal phase transitions to valence-bond-solid phase in the two dimensional; generalized SU(N) Heisenberg models: T. Suzuki, K. Harada, H. Matsuo, S. Todo and N. Kawashima, J. Phys.:Conf. Ser. **592** (2015) 012114.

7. Scaling relation for dangerously irrelevant symmetry-breaking fields: T. Okubo, K. Oshikawa, H. Watanabe and N. Kawashima, Phys. Rev. B (2015), accepted for publication.

* Joint research among groups within ISSP.

Noguchi group

We have studied morphologies of a double-bilayer vesicle theoretically and experimentally in collaboration with Prof. M. Imai. We found that the confinement of the outer vesicle induces several shapes of the inner vesicles that had not been observed in unilamellar vesicles: double and quadruple stomatocytes, slit vesicle, and vesicles of two or three compartments with various shapes. Our simulations reproduced the experimental results very well. We also studied the assembly of banana-shaped proteins on biomembrane and dynamics of deformable microsimmers.

1. Deformable microswimmer in a swirl: Capturing and scattering dynamics: M. Tarama, A. M. Menzel and H. Löwen, Phys. Rev. E **90** (2014) 032907.
2. Morphological variation of a lipid vesicle confined in a spherical vesicle: A. Sakashita, M. Imai and H. Noguchi, Phys. Rev. E **89** (2014) 040701.
3. Tunable dynamic response of magnetic gels: Impact of structural properties and magnetic fields: M. Tarama, P. Cremer, D. Y. Borin, S. Odenbach, H. Löwen and A. M. Menzel, Phys. Rev. E **90** (2014) 042311/1-9.
4. Individual and collective dynamics of self-propelled soft particles: M. Tarama, Y. Itino, A. M. Menzel and T. Ohta, Eur. Phys. J. Spec. Top. **223** (2014) 121.
5. Multiscale modeling of blood flow: from single cells to blood rheology: D. A. Fedosov, H. Noguchi and G. Gompper, Biomech. Model. Mechanobiol. **13** (2014) 239-258.
6. Two- or three-step assembly of banana-shaped proteins coupled with shape transformation of lipid membranes: H. Noguchi, EPL **108** (2014) 48001.
7. 界面活性剤系の構造形成の粗視化分子シミュレーション : 芝隼 人 , 野口 博司 , 分子シミュレーション研究会会誌 “アンサンブル” **16** (2014) 59-65.
8. 粒子描像の流体力学計算手法 III: 野口 博司 , 分子シミュレーション研究会会誌 “アンサンブル” **16(3)** (2014) 211-214.
9. 粒子描像の流体力学計算手法 II: 野口 博司 , 分子シミュレーション研究会会誌 “アンサンブル” **16(2)** (2014) 118-121.
10. 粒子描像の流体力学計算手法 IV: 野口 博司 , 分子シミュレーション研究会会誌 “アンサンブル” **16(4)** (2014) 252-254.
11. Morphological changes of amphiphilic molecular assemblies induced by chemical reactions: K. M. Nakagawa and H. Noguchi, Soft Matter **11** (2015) 1403-1411.
12. Shape transformations of toroidal vesicles: H. Noguchi, A. Sakashita and M. Imai, Soft Matter **11** (2015) 193.

Materials Synthesis and Characterization group

1. †*Electronic State of $CeFe_4As_{12}$ Investigated by Using Single Crystals Grown under High Pressure of 4 GPa: Y. Ogawa, H. Sato, M. Watanabe, T. Namiki, S. Tatsuoka, R. Higashinaka, Y. Aoki, K. Kuwahara, J.-I. Yamaura and Z. Hiroi, J. Phys. Soc. Jpn. **83** (2014) 034710.
2. *Superconductivity in the Hypervalent Compound $Ba_2Bi(Sb_{1-x}Bi_x)_2$ with a Square-Honeycomb Lattice: T. Yajima, F. Takeiri, Y. Nozaki, Z. Li, T. Tohyama, M. A. Green, Y. Kobayashi and H. Kageyama, J. Phys. Soc. Jpn. **83** (2014) 073705.
3. †Magnetic properties of Mn–Bi melt-spun ribbons: T. Saito, R. Nishimura and D. Nishio-Hamane, J. Magn. Magn. Mater. **349** (2014) 9.
4. †Successive phase transitions driven by orbital ordering and electron transfer in quasi-two-dimensional $CrSe_2$ with a triangular lattice: S. Kobayashi, H. Ueda, D. Nishio-Hamane, C. Michioka and K. Yoshimura, Phys. Rev. B **89** (2014) 054413.
5. †*Phase transitions and hydrogen bonding in deuterated calcium hydroxide: High-pressure and high-temperature neutron diffraction measurements: R. Iizuka, K. Komatsu, H. Kagi, T. Nagai, A. Sano-Furukawa, T. Hattori, H. Gotou and T. Yagi, J. Solid State Chem. **218** (2014) 95.
6. †*Pressure-induced oligomerization of benzene at room temperature as a precursory reaction of amorphization: A. Shinozaki, K. Mimura, H. Kagi, K. Komatu, N. Noguchi and H. Gotou, J. Chem. Phys. **141** (2014) 084306.
7. †*Spin Polarization Measurements of Heusler Alloy $Ru_{0.2}Fe_{1.8}CrSi$ by Andreev Reflection Technique: I. Shigeta, Y. Maeda, K. Harumori, Y. Nishisako, M. Ito, T. Yamauchi and M. Hiroi, IEEE Trans. Magn. **50** (2014) 1.

† Joint research with outside partners.

8. †Magnetic properties of $SmCo_{5-x}Fe_x$ (x=0–4) melt-spun ribbon: T. Saito and D. Nishio-Hamane, J. Alloys Compd. **585** (2014) 423.

9. †Electrochemical properties of $LiMn_xFe_{1-x}PO_4$ (x = 0, 0.2, 0.4, 0.6, 0.8 and 1.0)/vapor grown carbon fiber core–sheath composite nanowire synthesized by electrospinning method: K. Kagesawa, E. Hosono, M. Okubo, D. Nishio-Hamane, T. Kudo and H. Zhou, J. Power Sources **248** (2014) 615.

10. †Electrically Conductive and Mechanically Elastic Titanium Nitride Ceramic Microsprings: S. Yang, X. Chen, K. Yamamoto, M. Iitake, D. Nishio-Hamane, H. Sakai and M. Abe, J. Nanosci. Nanotech. **14** (2014) 4292.

11. Structural discrimination of double-walled carbon nanotubes by chiral diporphyrin nanocalipers: G. Liu, Y. Saito, D. Nishio-Hamane, A. K. Bauri, E. Flahaut, T. Kimura and N. Komatsu, J. Mater. Chem. A **2** (2014) 19067.

12. Adachiite, a Si–poor member of the tourmaline supergroup from the Kiura mine, Oita Prefecture, Japan: D. Nishio–Hamane, T. Minakawa, J. Yamaura, T. Oyama, M. Ohnishi and N. Shimobayashi, J. Miner. Petrol. Sci. **109** (2014) 74.

13. Iwateite, $Na_2BaMn(PO_4)_2$, a new mineral from the Tanohata mine, Iwate Prefecture, Japan: D. Nishio-Hamane, T. Minakawa and H. Okada, J. Miner. Petrol. Sci. **109** (2014) 34.

14. Spin transition, substitution, and partitioning of iron in lower mantle minerals: K. Fujino, D. Nishio-Hamane, T. Nagai, Y. Seto, Y. Kuwayama, M. Whitaker, H. Ohfuji, T. Shinmei and T. Irifune, Phys. Earth Planet. In. **228** (2014) 186.

15. Ultrafast hydrothermal synthesis of Pr-doped $Ca_{0.6}Sr_{0.4}TiO_3$ red phosphor nanoparticles using corrosion resistant micro-fluidic devices with Ti-lined structure under high-temperature and high-pressure condition: K. Sue, T. Ono, Y. Hakuta, H. Takashima, D. Nishio-Hamane, T. Sato, M. Ohara, M. Aoki, Y. Takebayashi, S. Yoda, T. Hiaki and T. Furuya, Chem. Eng. J. **239** (2014) 360.

16. Magnetic properties of Sm-Fe-N bulk magnets prepared from $Sm_2Fe_{17}N_3$ melt-spun ribbons: T. Saito and D. Nishio-Hamane, J. Appl. Phys. **117** (2015) 17D130.

17. *Superconductivity in 122-type antimonide $BaPt_2Sb_2$: M. Imai, S. Ibuka, N. Kikugawa, T. Terashima, S. Uji, T. Yajima, H. Kageyama and I. Hase, Phys. Rev. B **91** (2015) 014513.

18. Effect of surfactant/water ratio and reagents' concentration on size distribution of manganese carbonate nanoparticles synthesized by microemulsion mediated route: G. Granata, F. Pagnanelli, D. Nishio-Hamane and T. Sasaki, Appl. Surf. Sci. **331** (2015) 463.

19. New hard magnetic phase in Mn–Ga–Al system alloys: T. Saito and D. Nishio-Hamane, J. Alloys Compd. **632** (2015) 486.

20. *Substrate-induced anion rearrangement in epitaxial thin films of $LaSrCoO_{4-x}H_x$: G. Bouilly, T. Yajima, T. Terashima, Y. Kususe, K. Fujita, C. Tassel, T. Yamamoto, K. Tanaka, Y. Kobayashi and H. Kageyama, CrystEngComm **16** (2015) 9669-9674.

21. *Superconducting properties of $BaTi_2Pn_2O$ (Pn = Sb, Bi): T. Yajima, K. Nakano, Y. Nozaki and H. Kageyama, Physica C: Superconductivity **504** (2015) 36-38.

22. Synthesis of oxamate and urea by oxidative single and double carbonylation of amines using immobilized palladium metal-containing ionic liquid@SBA-15: S. T. Gadge, E. N. Kusumawati, K. Harada, T. Sasaki, D. Nishio-Hamane and B. M. Bhanage, J. Mol. Catal. A: Chem. **400** (2015) 170.

23. Synthesis of Polyester Amide by Carbonylation–Polycondensation Reaction Using Immobilized Palladium Metal Containing Ionic Liquid on SBA-15 as a Phosphine-Free Catalytic System: A. Satapathy, S. T. Gadge, E. N. Kusumawati, K. Harada, T. Sasaki, D. Nishio-Hamane and B. M. Bhanage, Catal. Lett. **145** (2015) 824.

Neutron Science Laboratory

Shibayama group

Shibayama group has been exploring the structure and dynamics of soft matter, especially polymer gels, micelles, and phenolic resin, utilizing a combination of small-angle neutron scattering (SANS), neutron spin echo (NSE), and dynamic light scattering (DLS). The objectives are to elucidate the mysterious relationship between the structure and variety of novel properties/functions of polymer gels/resins. The highlights of 2013 include structural investigations of (1) Poly(ethylene glycol) in ionic liquids, (2) UCST-type phase separation of poly(N-isopropylacrylamide) in ionic liquids, (3) catalyst ink of fuel cell, (4) defect-

* Joint research among groups within ISSP.

controlled polymer networks, and so on. We also developed a dynamic light scattering microscope capable of accessing opaque samples with high spatial resolution, which sheds a light for investigations of particle dynamics and characterization in dense systems.

1. Gelation and cross-link inhomogeneity of phenolic resins studied by small- and wide-angle X-ray scattering and 1H-pulse NMR spectroscopy: A. Izumi, T. Nakao and M. Shibayama, Polymer **59** (2014) 226-233.

2. Water-in-Ionic Liquid Microemulsion Formation in Solvent Mixture of Aprotic and Protic Imidazolium-Based Ionic Liquids: T. Kusano, K. Fujii, K. Hashimoto and M. Shibayama, Langmuir **30** (2014) 11890-11896.

3. Kinetic Aspect on Gelation Mechanism of Tetra-PEG Hydrogel: K. Nishi, K. Fujii, Y. Katsumoto, T. Sakai and M. Shibayama, Macromolecules **47** (2014) 3274-3281.

4. Multiscale Dynamics of Inhomogeneity-Free Polymer Gels: T. Hiroi, M. Ohl, T. Sakai and M. Shibayama, Macromolecules **47** (2014) 763.

5. Small-Angle Neutron Scattering Study on Defect-Controlled Polymer Networks: K. Nishi, H. Asai, K. Fujii, Y.-S. Han, T.-H. Kim, T. Sakai and M. Shibayama, Macromolecules **47** (2014) 1801.

6. SANS および SAXS によるフェノール樹脂硬化物の構造解析：和泉 篤士，中尾 俊夫，岩瀬 裕希，柴山 充弘，波紋 **24** (2014) 11-14.

7. CO2 Separation Using High-toughness Ion Gel with Tetraarmed olymer Network: K. Fujii, T. Makino, K. Hashimoto, T. Sakai, M. Kanakubo and M. Shibayama, Chem. Lett. **44** (2014) 17-19.

8. Self-Oscillating Vesicles: Spontaneous Cyclic Structural Changes of Synthetic Diblock Copolymers: R. Tamate, T. Ueki, M. Shibayama and R. Yoshida, Angew. Chem. Int. Ed. **53** (2014) 11248-11252.

9. 中性子散乱を用いた構造解析手法　概説とエラストマー・高分子ゲル解析への応用：柴山 充弘，ゴム協会編 (2014) 1-10.

10. SANS studies on catalyst ink of fuel cell: M. Shibayama, T. Matsunaga, T. Kusano, K. Amemiya, N. Kobayashi and T. Yoshida, J. Appl. Polym. Sci. **131** (2014) 1-7.

11. Gelation Mechanism of Tetra-Armed Poly(ethylene glycol) in Aprotic Ionic Liquid Containing Non-volatile Proton Source, Protic Ionic Liquid: K. Hashimoto, K. Fujii, K. Nishi, T. Sakai, N. Yoshimoto, M. Morita and M. Shibayama, J. Phys. Chem. B **119** (2015) 4795-4801.

12. Dynamic light scattering study on curing mechanisms of novolac-type phenolic resins: Y. Shudo, A. Izumi, T. Takeuchi, T. Nakao and M. Shibayama, Polym. J. (2015), in print.

13. 中性子小角散乱を用いた分子集合体の解析：草野 巧巳，柴山 充弘，Colloid & Interface Communication **39** (2014) 16-18.

14. Computer simulation of network formation in natural rubber (NR): T. Nakao and S. Kohjiya, in: *Chemistry, Manufacture and Applications of Natural Rubber, Kohjiya S. and Ikeda, Y. Eds.*, edited by S. Kohjiya and Y. Ikeda, (Woodhead, Cambridge, UK, 2014), 216-246.

Yoshizawa group

A systematic study on spin dynamics in a two-dimensional transition-metal Ni oxide has been carried out with use of the high resolution chopper spectrometer installed at BL12 in the Material and Life Science Facility, J-PARC. The checkerboard-type spin-charge ordering in the highly hole-doped region of the layered nickelate was studied in detail. The nature of the excitation spectra and the thermodynamic properties in the checkerboard phase was found to show qualitative differences from those in the stripe phase. Magnetic structures and spin fluctuations in a few quantum spin systems as well as Ce-based heavy Fermion systems were also studied.

1. Magnetic structure of the conductive triangular-lattice antiferromagnet $PdCrO_2$: H. Takatsu, G. Nénert, H. Kadowaki, H. Yoshizawa, M. Enderle, S. Yonezawa, Y. Maeno, J. Kim, N. Tsuji, M. Takata, Y. Zhao, M. Green and C. Broholm, Phys. Rev. B **89** (2014) 104408.

2. Dynamical Properties of Spins and Holes in Carrier Doped Quantum Haldane Chain: T. Yokoo, S. Itoh, D. Kawana, H. Yoshizawa and J. Akimitsu, J. Phys.: Conf. Ser. **502** (2014) 012045.

3. Spin and Hole Dynamics in Carrier-Doped Quantum Haldane Chain: T. Yokoo, S. Itoh, S. Ibuka, H. Yoshizawa and J. Akimitsu, J. Phys.: Conf. Ser. **568** (2014) 042035.

4. Neutron Diffraction Study of Parasitic Nd-Moment Order in the Checkerboard-Type Phase $Nd_{1.3}Sr_{0.7}NiO_4$: R.

† Joint research with outside partners.

Kobayashi, H. Yoshizawa, M. Matsuda, R. Kajimoto, K. Ishizaka and Y. Tokura, J. Phys. Soc. Jpn. **84** (2015) 064711.

5. Resistance Anomalies Accompanying Crossover from Heavy-Fermion Regime to Intermediate-Valence Regime: A Study of Cu–Ni Substitution and Pressure Effects on $CeCu_2Si_2$: Y. Ikeda, Y. Ito, S. Araki, T. C. Kobayashi and H. Yoshizawa, J. Phys. Soc. Jpn. **84** (2015) 024702.

6. Transport and Thermodynamic Studies of Stripe and Checkerboard Ordering in Layered Nickel Oxides $R_{2-x}Sr_xNiO_4$ (R = La and Nd): Y. Ikeda, S. Suzuki, T. Nakabayashi, H. Yoshizawa, T. Yokoo and S. Itoh, J. Phys. Soc. Jpn. **84** (2015) 023706.

7. *Temperature and composition phase diagram in the iron-based ladder compounds $Ba_{1-x}Cs_xFe_2Se_3$: T. Hawai, Y. Nambu, K. Ohgushi, F. Du, Y. Hirata, M. Avdeev, Y. Uwatoko, Y. Sekine, H. Fukazawa, J. Ma, S. Chi, Y. Ueda, H. Yoshizawa and T. J. Sato, Phys. Rev. B **91** (2015) 184416.

8. Characterization of Ferromagnetic Order in $CePd_2P_2$: Y. Ikeda, H. Yoshizawa, S. Konishi, S. Araki, T. C. Kobayashi, T. Yokoo and S. Itoh, J. Phys.: Conf. Ser. **592** (2015) 012013.

Yamamuro group

Our laboratory is studying chemical physics of complex condensed matters by using neutron scattering, X-ray diffraction, calorimetric, dielectric, and viscoelastic techniques. Our target materials are glasses, liquids, and various disordered systems. This year, there were two important outcomes in the study of nano-particles of palladium hydrides. The neutron powder diffraction experiment of nano-PdD has demonstrated that D atoms are located not only at the octahedral sites of the fcc lattice of Pd but also at the tetrahedral sites probably due to the surface and/or distortion effects of nano-particles. The quasielastic neutron scattering experiment of nano-PdH has revealed a new relaxation, which has much smaller activation energy than that in bulk PdH. This relaxation could be due to the jump of H atoms among the tetrahedral sites. One more important topic is that our low-temperature (3 K) vapor-deposition method has produced glassy carbon dioxide that is the simplest molecular glass in the history of the glass study. Other than above topics, we have made some progresses in the studies on liquid-crystalline ionic liquids and rare-earth metal-based single molecule magnets.

1. †Relationship between the local dynamics and gas permeability of polyacetylenes containing polymethylated indan/tetrahydronaphtalene moieties: R. Inoue, T. Kanaya, Y. Hu, T. Masuda, K. Nishida and O. Yamamuro, Polymer **55** (2014) 182-186.

2. イミダゾリウム系イオン液体の不均一ダイナミクス：古府 麻衣子，山室 修，波紋 **24** (2014) 126-131.

3. Proton Dynamics of Two Dimensional Oxalate-Bridged Coordination Polymers: S. Miyatsu, M. Kofu, A. Nagoe, T. Yamada, M. Sadakiyo, T. Yamada, H. Kitagawa, M. Tyagi, V. Garcia Sakai and O. Yamamuro, Phys. Chem. Chem. Phys. **16** (2014) 17295-17304.

4. Thermal and Structural Studies of Imidazolium-Based Ionic Liquids with and without Liquid-Crystalline Phases: The Origin of Nanostructure: F. Nemoto, M. Kofu and O. Yamamuro, J. Phys. Chem. B **119** (2015) 5028-5034.

5. Inelastic neutron scattering study on boson peaks of imidazolium-based ionic liquids: M. Kofu, Y. Inamura, Y. Moriya, A. Podlesnyak, G. Ehlers and O. Yamamuro, J. Mol. Liq. (2015), accepted for publication.

6. 連載講座「中性子散乱による原子・分子のダイナミクスの観測」III-2　中性子非弾性散乱法による固体表面での分子分光：山室 修，古府 麻衣子，RADIOISOTOPES **63** (2014) 453-459.

7. 中性子散乱で観たイオン液体の階層的構造とダイナミクス：山室 修，根本 文也，古府 麻衣子，高圧力学会誌 **25** (2015), in print.

Masuda group

The goal of our research is to discover a new quantum phenomenon and to reveal the mechanism of it. In this fiscal year we studied the following topics; multiferroic property in integer spin systems with large single-ion anisotropy, low temperature magnetic properties of frustrated quantum spin system $Rb_2Cu_2Mo_3O_{12}$, spin gap in antiferromagnetic alternating spin 3/2 chain substances $RCrGeO_5$ (R=Y or 154Sm), and Inhomogeneous ordering in weakly coupled Heisenberg S=1/2 chains with random bonds.

1. †*Experimental confirmation of spin gap in antiferromagnetic alternating spin-3/2 chain substances $RCrGeO_5$(R=Y or Sm-154) by inelastic neutron scattering experiments: M. Hase, M. Soda, T. Masuda, D. Kawana, T. Yokoo, S. Itoh, A. Matsuo, K. Kindo and M. Kohno, Phys. Rev. B **90** (2014) 024416.

2. Inhomogeneous ordering in weakly coupled Heisenberg S=1/2 chains with random bonds: M. Thede, T. Haku, T.

* Joint research among groups within ISSP.

Masuda, C. Baines, E. Pomjakushina, G. Dhalenne, A. Revcolevschi, E. Morenzoni and A. Zheludev, Phys. Rev. B **90** (2014) 144407.

3. Spin-Nematic Interaction in the Multiferroic Compound $Ba_2CoGe_2O_7$: M. Soda, M. Matsumoto, M. Mansson, S. Ohira-Kawamura, K. Nakajima, R. Shiina and T. Masuda, Phys. Rev. Lett. **112** (2014) 127205.

4. †*Low Temperature Magnetic Properties of Frustrated Quantum Spin Chain System $Rb_2Cu_2Mo_3O_{12}$: Y. Yasui, R. Okazaki, I. Terasaki, M. Hase, M. Hagihala, T. Masuda and T. Sakakibara, JPS Conf. Proc. **3** (2014) 014014 (1-6).

5. Theoretical Study on Multiferroic Properties in Integer Spin Systems with Large Single-Ion Anisotropy: M. Matsumoto, M. Soda and T. Masuda, JPS Conf. Proc. **3** (2014) 014033.

6. Complex magnetostructural order in the frustrated spinel LiInCr4O8: G. J. Nilsen, Y. Okamoto, T. Masuda, J. Rodriguez-Carvajal, H. Mutka, T. Hansen and Z. Hiroi, Phys. Rev. B **91** (2015) 174435.

7. マルチフェロイック物質 Ba2CoGe2O7 におけるスピン・ネマティック相互作用の観測： 益田 隆嗣，左右田 稔，固体物理 **50** (2015) 111.

8. A magnetic anti-cancer compound for magnet-guided delivery and magnetic resonance imaging: H. Eguchi, M. Umemura, R. Kurotani, H. Fukumura, I. Sato, J.-H. Kim, Y. Hoshino, J. Lee, N. Amemiya, M. Sato, K. Hirata, D. J. Singh, T. Masuda, M. Yamamoto, T. Urano, K. Yoshida, K. Tanigaki, M. Yamamoto, M. Sato, S. Inoue, I. Aoki and Y. Ishikawa, Sci. Rep. **5** (2015) 9194.

International MegaGauss Science Laboratory

Takeyama group

Recently, the technique for the electro-magnetic flux compression at the International Megagauss Science Laboratory is well established and a peak magnetic field more than 700 T is reproducibly generated with the peak field almost approaching to 800 T. We have developed a calculation code, which is used for dynamical simulation of the magnetic-flux compression. This simulation assists comprehension of the time and 3 dimensional special distribution of magnetic field inside the imploding liner, and very useful for further development for achieving 1000 T. The exciton-magnon optical absorption spectra in $HgCr_2O_4$ was investigated in various magnetic phases up to the full saturation, and compared with other preceding results of the lattice and the electron-spin-resonance measurements. The existence of the novel phase, most possibly the spin nematic phase, prior to the full saturation is suggested. This phase is very similar to that discovered in other chromium spinel oxide, $CdCr_2O_4$, and $ZnCr_2O_4$. We have found that relative ordering between optical bright and dark band-edge excitons is chirality dependent in semiconductor single wall carbon nanotubes, and a bright exciton can stay at the lowest energy for a certain chirality carbon nanotube.

1. Canted 2:1:1 Magnetic Supersolid Phase in a Frustrated Magnet $MgCr_2O_4$ as a Small Limit of the Biquadratic Spin Interaction: A. Miyata, H. Ueda and S. Takeyama, J. Phys. Soc. Jpn. **83** (2014) 063702(1-4).

2. Optical Detection of Magnetic Orders in $HgCr_2O_4$ Frustrated Spin Magnet under Pulsed High Magnetic Fields: D. Nakamura, A. Miyata, Y. Aida, H. Ueda and S. Takeyama, J. Phys. Soc. Jpn. **83** (2014) 113703(1-3).

3. *Entropy of the quantum soliton lattice and multiple magnetization steps in $BiCu_2PO_6$: Y. Kohama, K. Mochidzuki, T. Terashima, A. Miyata, A. DeMuer, T. Klein, C. Marcenat, Z. L. Dun, H. Zhou, G. Li, L. Balicas, N. Abe, Y. H. Matsuda, S. Takeyama, A. Matsuo and K. Kindo, Phys. Rev. B **90** (2014) 060408(1-4).

4. Negative initial phase shift of Kerr rotation generated from the building-up process of resident electron spin polarization in a CdTe single quantum well: L. -P. Yan, M. Kurosawa, R. Kaji, G. Karczewski, S. Takeyama and S. Adachi, Phys. Rev. B **90** (2014) 205307(1-6).

5. Note: Experimental evidence of three-dimensional dynamics of an electromagnetically imploded liner: D. Nakamura, H. Sawabe and S. Takeyama, Rev. Sci. Instrum. **85** (2014) 036102.

6. †*Novel Phase of Solid Oxygen Induced by Ultrahigh Magnetic Fields: T. Nomura, Y. H. Matsuda, S. Takeyama, A. Matsuo, K. Kindo, J. L. Her and T. C. Kobayashi, Phys. Rev. Lett. **112** (2014) 247201 (5 pages).

7. †* 固体酸素の超強磁場誘起新規相：野村 肇宏，松田 康弘，嶽山 正二郎，小林 達生，固体物理 **Vol. 49, No. 12** (2014) 687-694.

8. †*Optical anisotropy and diamagnetic energy shifts in InP–GaP lateral quantum wells: Y. H. Shin, Y. Kim, J. D. Song, Y. T. Lee, H. Saito, D. Nakamura, Y. H. Matsuda and S. Takeyama, Journal of Luminescence **151** (2014) 244-246.

† Joint research with outside partners.

9. *Development of Techniques for Radio Frequency Conductivity Experiments in Ultra High Magnetic Fields: S. Lee, Y. H. Matsuda, D. Nakamura, S. Takeyama, T.-H. Arima and S. Yamada, JPS Conf. Proc. **3** (2014) 013009 (6 pages).

10. Relative Ordering between Bright and Dark Excitons in Single-walled Carbon Nanotubes: W. Zhou, D. Nakamura, H. Liu, H. Kataura and S. Takeyama, Scientific Reports **4** (2014) 6999.

11. †*Orbital Zeeman Effect of Liquid Oxygen in High Magnetic Fields: T. Nomura, Y. H. Matsuda, S. Takeyama, A. Matsuo, K. Kindo and T. C. Kobayashi, J. Phys. Soc. Jpn. Conf. Proc. **3** (2014) 017004(1-6).

12. *Magnetic-Field-Induced Insulator–Metal Transition in $(Pr_{1-y}Y_y)_{0.7}Ca_{0.3}CoO_3$ at Ultrahigh Magnetic Fields: S. Lee, Y. H. Matsuda, T. Naito, D. Nakamura and S. Takeyama, J. Phys. Soc. Jpn. **84** (2015) 044703 (5pages).

13. Exciton splitting in semiconducting carbon nanotubes in ultrahigh magnetic fields above 300 T: D. Nakamura, T. Sasaki, W. Zhou, H. Liu, H. Kataura and S. Takeyama, Phys. Rev. B **91** (2015) 235427.

14. *Effect of very high magnetic field on the optical properties of firefly light emitter oxyluciferin: W. Zhou, D. Nakamura, Y. Wang, T. Mochizuki, H. Akiyama and S. Takeyama, Journal of Luminescence **165** (2015) 15.

Kindo group

The heat capacity measurement by using long pulsed field with duration of about 1 sec has been opened for outer user. Newly manufactured Cu-Ag wire shows reliability and long life which enables to carry out 75 T measurement with short pulse duration.

1. †Almost Perfect Frustration in the Dimer Magnet $Ba_2CoSi_2O_6Cl_2$: H. Tanaka, N. Kurita, M. Okada, E. Kunihiro, Y. Shirata, K. Fujii, H. Uekusa, A. Matsuo, K. Kindo and H. Nojiri, J. Phys. Soc. Jpn. **83** (2014) 103701.

2. †Collapse of Anisotropic Hybridization Gap below 20 K in Kondo Semiconductor $CeFe_2Al_{10}$ by Pressure and Magnetic Field: H. Tanida, M. Nakamura, M. Sera, A. Kondo, K. Kindo, T. Nishioka and M. Matsumura, J. Phys. Soc. Jpn. **83** (2014) 084708.

3. Exchange Interactions of the Chromium Spinel Oxide $HgCr_2O_4$ in High Magnetic Fields Examined by the Magnetoelastic Theory: S. Kimura, M. Hagiwara, T. Takeuchi, H. Yamaguchi, H. Ueda and K. Kindo, J. Phys. Soc. Jpn. **83** (2014) 113709.

4. †Field-Induced Spin-State Transition in $LaCo_{1-x}M_xO_3$ (M = Al, Ga, Rh, and Ir): K. Sato, A. Matsuo, K. Kindo, Y. Hara, K. Nakaoka, Y. Kobayashi and K. Asai, J. Phys. Soc. Jpn. **83** (2014) 114712.

5. †*$NaCuMoO_4(OH)$ as a Candidate Frustrated J_1–J_2 Chain Quantum Magnet: K. Nawa, Y. Okamoto, A. Matsuo, K. Kindo, Y. Kitahara, S. Yoshida, S. Ikeda, S. Hara, T. Sakurai, S. Okubo, H. Ohta and Z. Hiroi, J. Phys. Soc. Jpn. **83** (2014) 103702.

6. †Spin Frustration and Field-Induced Transitions of Modified Pyrochlore Fluorides ACr_2F_6 (A = Rb and Cs): H. Ueda, A. Matsuo, K. Kindo and K. Yoshimura, J. Phys. Soc. Jpn. **83** (2014) 014701(1-6).

7. †Spin-Singlet Ground State of Two-Dimensional Quantum Spin Antiferromagnet $(CuCl)Ca_2Nb_3O_{10}$: Y. Tsujimoto, A. Kitada, M. Nishi, Y. Narumi, K. Kindo, T. Goko, Y. J. Uemura, A. A. Aczel, T. J. Williams, G. M. Luke, Y. Ajiro and H. Kageyama, J. Phys. Soc. Jpn. **83** (2014) 074712.

8. †*Successive Magnetic Transitions of $Ca_2CoSi_2O_7$ in High Magnetic Fields: M. Akaki, H. Kuwahara, A. Matsuo, K. Kindo and M. Tokunaga, J. Phys. Soc. Jpn. **83** (2014) 093704(1-4).

9. †Anomalous itinerant-electron metamagnetic transition in the layered $Sr_{1-x}Ca_xCo_2P_2$ system: M. Imai, C. Michioka, H. Ohta, A. Matsuo, K. Kindo, H. Ueda and K. Yoshimura, Phys. Rev. B **90** (2014) 014407.

10. *Entropy of the quantum soliton lattice and multiple magnetization steps in $BiCu_2PO_6$: Y. Kohama, K. Mochidzuki, T. Terashima, A. Miyata, A. DeMuer, T. Klein, C. Marcenat, Z. L. Dun, H. Zhou, G. Li, L. Balicas, N. Abe, Y. H. Matsuda, S. Takeyama, A. Matsuo and K. Kindo, Phys. Rev. B **90** (2014) 060408(1-4).

11. †*Experimental confirmation of spin gap in antiferromagnetic alternating spin-3/2 chain substances $RCrGeO_5$(R=Y or Sm-154) by inelastic neutron scattering experiments: M. Hase, M. Soda, T. Masuda, D. Kawana, T. Yokoo, S. Itoh, A. Matsuo, K. Kindo and M. Kohno, Phys. Rev. B **90** (2014) 024416.

12. †Observation of two ferromagnetic phases in Fe_3Mo_3N: T. Waki, S. Terazawa, Y. Tabata, K. Sato, A. Kondo, K. Kindo and H. Nakamura, Phys. Rev. B **90** (2014) 014416.

13. †Unconventional spin freezing in the highly two-dimensional spin-l/2 kagome antiferromagnet

* Joint research among groups within ISSP.

$Cd_2Cu_3(OH)_6(SO_4)24H_2O$: Evidence of partial order and coexisting spin singlet state on a distorted kagome lattice: M. Fujihala, X.-G. Zheng, H. Morodomi, T. Kawae, A. Matsuo, K. Kindo and I. Watanabe, Phys. Rev. B **89** (2014) 100401(1-5).

14. †*Novel Phase of Solid Oxygen Induced by Ultrahigh Magnetic Fields: T. Nomura, Y. H. Matsuda, S. Takeyama, A. Matsuo, K. Kindo, J. L. Her and T. C. Kobayashi, Phys. Rev. Lett. **112** (2014) 247201 (5 pages).

15. †High-magnetic-field phase transitions and H–T phase diagram of the Kagome-staircase compound $Ni_3V_2O_8$: Z. Q. Lin, M. Yang, H. W. Wang, Q. Guo, Y. J. Liu, X. T. Han, Y. B. Han, J. F. Wang, Z. Z. He and K. Kindo, J. Magn. Magn. Mater. **382** (2015) 7.

16. †Successive magnetic phase transitions in α-$RuCl_3$: XY-like frustrated magnet on the honeycomb lattice: Y. Kubota, H. Tanaka, T. Ono, Y. Narumi and K. Kindo, Phys. Rev. B **91** (2015) 094422.

17. †Valence-specific magnetization of the charge-ordered multiferroelectric $LuFe_2O_4$ using soft x-ray magnetic circular dichroism under 30 T pulsed high magnetic fields: Y. Narumi, T. Nakamura, K. Saito, T. Morioka, Y. Fukada, T. Kambe, N. Ikeda, Y. Kotani, T. Kinoshita, K. Kindo and H. Nojiri, Phys. Rev. B **91** (2015) 014410.

18. †*Anisotropy in the upper critical field of FeSe and $FeSe_{0.33}Te_{0.67}$ single crystals: J. L. Her, Y. Kohama, Y. H. Matsuda, K. Kindo, W.-H. Yang, D. A. Chareev, E. S. Mitrofanova, O. S. Volkova, A. N. Vasiliev and J.-Y. Lin, Supercond. Sci. Technol. **28** (2015) 045013 (6 pages).

19. †*Synchrotron X-ray spectroscopy study on the valence state and magnetization in α-$YbAl_{1-x}Fe_xB_4$ (x = 0.115) at low temperatures and high magnetic fields: T. Terashima, Y. H. Matsuda, K. Kuga, S. Suzuki, Y. Matsumoto, S. Nakatsuji, A. Kondo, K. Kindo, N. Kawamura, M. Mizumaki and T. Inami, J. Phys.: Conf. Ser. **592** (2015) 012020 (6 pages).

Tokunaga group

With using the measurement technique developed in the previous year, we studied the inverse magneto-caloric effects (IMCEs) in metamagnetic shape-memory alloys NiCoMnIn. We quantitatively estimated the contribution of magnetic, lattice, and charge degrees of freedom to the IMCEs, and revealed that the lattice sector played the dominant role in these phenomena.

1. †*Successive Magnetic Transitions of $Ca_2CoSi_2O_7$ in High Magnetic Fields: M. Akaki, H. Kuwahara, A. Matsuo, K. Kindo and M. Tokunaga, J. Phys. Soc. Jpn. **83** (2014) 093704/1-4.

2. Anisotropic Upper Critical Field of BiS_2-Based Superconductor $LaO_{0.5}F_{0.5}BiS_2$: Y. Mizuguchi, A. Miyake, K. Akiba, M. Tokunaga, J. Kajitani and O. Miura, Phys. Rev. B **89** (2014) 174515(1-7).

3. Direct measurements of inverse magnetocaloric effects in metamagnetic shape-memory alloy NiCoMnIn: T. Kihara, X. Xu, W. Ito, R. Kainuma and M. Tokunaga, Phys. Rev. B **90** (2014) 214409(1-6).

4. Novel multiferroic phase of CsCuCl3 in High Magnetic Fields: J. Shibuya, M. Akaki, Y. Kohama, A. Miyake, M. Tokunaga and H. Tanaka, J. Phys.: Conf. Ser. **568** (2014) 042030(1-5).

5. Magnetic Field-Induced Reverse Martensitic Transformation and Thermal Transformation Arrest Phenomenon of $Ni_{41}Co_9Mn_{39}Sb_{11}$ Alloy: R. Umetsu, X. Xu, W. Ito, T. Kihara, K. Takahashi, M. Tokunaga and R. Kainuma, Metals **4** (2014) 609-622.

6. Possible Excitonic Phase of Graphite in the Quantum Limit State: K. Akiba, A. Miyake, H. Yaguchi, A. Matsuo, K. Kindo and M. Tokunaga, J. Phys. Soc. Jpn. **84** (2015) 054709(1-6).

7. Magnetic control of transverse electric polarization in $BiFeO_3$: M. Tokunaga, M. Akaki, T. Ito, S. Miyahara, A. Miyake, H. Kuwahara and N. Furukawa, Nat. Commun. **6** (2015) 5878(1-5).

8. High field studies on BiFeO3 single crystals grown by the laser-diode heating floating zone method: M. Tokunaga, M. Akaki, A. Miyake, T. Ito and H. Kuwahara, Journal of Magnetism and Magnetic Materials **383** (2015) 259-261.

Y. Matsuda group

A novel phase of solid oxygen was discovered in ultrahigh magnetic fields of up to 193 T. The phase transition is expected to be driven by rearrangement of oxygen molecules. The nearest neighbor molecules are coupled with the parallel H-geometry at low magnetic fields and the exchange interaction is antiferromagnetic. The H-geometry becomes unstable at high magnetic fields owing to its antiferromagnetic exchange interaction and a new geometry is likely to realize so that the exchange coupling becomes ferromagnetic. The cubic crystal symmetry is most plausible for the novel phase that we term θ phase. Other than solid oxygen, heavy fermion compounds such as $YbAlB_4$ and $CeRh_2Si_2$ were investigated in pulsed high magnetic fields. A

† Joint research with outside partners.

small metamagnetic transition was observed in $YbAlB_4$ and the origin of the transition can be the valence change of Yb. As for $CeRh_2Si_2$, a field-induced valence change of Ce at around 25 T was directly observed by X-ray absorption spectroscopy done at SPring-8. In order to realize the electrical transport measurement in destructive magnetic fields over 100 T, a contactless radio frequency technique was developed. Magnetic-field-induced insulator-metal transition of $Pr_{0.6}Ca_{0.4}MnO_3$ was successfully observed in pulsed fields up to 80 T produced by the single-turn coil method.

1. *Entropy of the quantum soliton lattice and multiple magnetization steps in $BiCu_2PO_6$: Y. Kohama, K. Mochidzuki, T. Terashima, A. Miyata, A. DeMuer, T. Klein, C. Marcenat, Z. L. Dun, H. Zhou, G. Li, L. Balicas, N. Abe, Y. H. Matsuda, S. Takeyama, A. Matsuo and K. Kindo, Phys. Rev. B **90** (2014) 060408(1-4).

2. †*Novel Phase of Solid Oxygen Induced by Ultrahigh Magnetic Fields: T. Nomura, Y. H. Matsuda, S. Takeyama, A. Matsuo, K. Kindo, J. L. Her and T. C. Kobayashi, Phys. Rev. Lett. **112** (2014) 247201 (5 pages).

3. †* 固体酸素の超強磁場誘起新規相：野村 肇宏，松田 康弘，嶽山 正二郎，小林 達生，固体物理 **Vol. 49, No. 12** (2014) 687-694.

4. †*Optical anisotropy and diamagnetic energy shifts in InP–GaP lateral quantum wells: Y. H. Shin, Y. Kim, J. D. Song, Y. T. Lee, H. Saito, D. Nakamura, Y. H. Matsuda and S. Takeyama, Journal of Luminescence **151** (2014) 244-246.

5. *Development of Techniques for Radio Frequency Conductivity Experiments in Ultra High Magnetic Fields: S. Lee, Y. H. Matsuda, D. Nakamura, S. Takeyama, T.-H. Arima and S. Yamada, JPS Conf. Proc. **3** (2014) 013009 (6 pages).

6. Valence State in Ce-based Heavy Fermion Compounds at High Magnetic Fields: Y. H. Matsuda, J.-L. Her, S. Michimura, T. Inami, T. Ebihara and H. Amitsuka, JPS Conf. Proc. **3** (2014) 011044 (6 pages).

7. †*Orbital Zeeman Effect of Liquid Oxygen in High Magnetic Fields: T. Nomura, Y. H. Matsuda, S. Takeyama, A. Matsuo, K. Kindo and T. C. Kobayashi, J. Phys. Soc. Jpn. Conf. Proc. **3** (2014) 017004(1-6).

8. *Magnetization of Yb-based mixed-valent compounds at megagauss fields: T. Terashima, Y. H. Matsuda, K. Kuga, Y. Matsumoto and S. Nakatsuji, J. Phys. Conf. Proc. **3** (2014) 011027(1-5).

9. *Magnetic-Field-Induced Insulator–Metal Transition in $(Pr_{1-y}Y_y)_{0.7}Ca_{0.3}CoO_3$ at Ultrahigh Magnetic Fields: S. Lee, Y. H. Matsuda, T. Naito, D. Nakamura and S. Takeyama, J. Phys. Soc. Jpn. **84** (2015) 044703 (5pages).

10. †*Anisotropy in the upper critical field of FeSe and $FeSe_{0.33}Te_{0.67}$ single crystals: J. L. Her, Y. Kohama, Y. H. Matsuda, K. Kindo, W.-H. Yang, D. A. Chareev, E. S. Mitrofanova, O. S. Volkova, A. N. Vasiliev and J.-Y. Lin, Supercond. Sci. Technol. **28** (2015) 045013 (6 pages).

11. † 超強磁場で誘起される固体酸素の新しい相：松田 康弘，パリティ **30** (2015) 48-51.

12. †*Synchrotron X-ray spectroscopy study on the valence state and magnetization in α-$YbAl_{1-x}Fe_xB_4$ (x = 0.115) at low temperatures and high magnetic fields: T. Terashima, Y. H. Matsuda, K. Kuga, S. Suzuki, Y. Matsumoto, S. Nakatsuji, A. Kondo, K. Kindo, N. Kawamura, M. Mizumaki and T. Inami, J. Phys.: Conf. Ser. **592** (2015) 012020 (6 pages).

Center of Computational Materials Science

Akai group

(1) In order to seek better permanent magnet materials, the mechanisms that govern the magnetic anisotropy, magnetisation, and the Curie temperature were investigated. For typical permanent magnet materials $Nd_2Fe_{17}B$ and $Sm_2Fe_{17}N_3$, the local magnetic moments, hyperfine fields, the magnetic exchange couplings, the magnetic anisotropy energy are calculated within the density functional theory using all-eletron KKR Green's function method. The importance of hybridisation between the 4f states of rare earth elements and N and B are pointed out. (2)New scheme of calculating Keldysh Green's function in the framework of KKR Green's function was proposed and successfully applied to some test cases. The method open up a possibility to deal with non-equlibrium process in the framework of KKR all -electron scheme. (3)Extension of the optimised effective potential method (OEP) so as to include the correlation of RPA level was developed together with some reformulation of OEP that as it stood had shown ill behaviour for spin polarised cases.

1. Ab initio study of ^{59}Co NMR spectra in $Co_2FeAl_{1-x}Si_x$ Heusler alloys: H. Nishihara, K. Sato, H. Akai, C. Takiguchi, M. Geshi, T. Kanomata, T. Sakon and T. Wada, Physica B **485** (2015) 66-70.

2. Optimized effective potential method and application to a static RPA correlation: T. Fukazawa and H. Akai, J. Phys.: Condens. Matter **27** (2015) 115502(1-10).

* Joint research among groups within ISSP.

3. Formulation of the augmented plane-wave and muffin-tin orbital method: T. Kotani, H. Kino and H. Akai, J. Phys. Soc. Jpn. **84** (2015) 034701(1-9(.

4. The metamagnetic behavior and giant inverse magnetocaloric effect in Ni–Co–Mn– (Ga, In, Sn) Heusler alloys: P. Entel, V. V. Sokolovskiy, V. D. Buchelnikov, M. Ogura, M. E. Gruner, A. Gruenebohm, D. Comtesse and H. Akai, J. Magn. Magn. Mater. **385** (2015) 193-197.

5. Role of N in permeant magnet materials $Sm_2Fe_{17}N_x$: M. Ogura, A. Mashiyama and H. Akai, J. Phys. Soc. Jpn. (2015), in print.

6. Basic and applications of Moessbauer spectrometry and the electronics structure of matters: H. Akai, ISOTOPES **63** (2014) 163-174.

7. 鉄の事典 : 赤井 久純 , (朝倉書店 , 東京 , 2014).

Ozaki group

Although it is believed that two-dimensional honeycomb structures consisting of silicon atoms do not exist experimentally due to relative instability of its hybridized sp_2 orbitals, a recent experiment clearly demonstrates that silicene, honeycomb structure of silicon atoms, can be fabricated on ZrB_2 (0001) thin films. We have performed detailed studies on geometrical and electronic structures of silicene on ZrB_2 and a related two-dimensional structure by means of electronic structure calculations based on density functional theories (DFT), guided by a close collaboration with experimental groups. Theoretical chemical shift of Si-2p states and band structure calculations strongly support the formation of silicene having a planar-like structure. The stability of the planar-like structure over the regularly buckled structure can be understood by interaction between states of the silicene and surface states consisting of the d-orbital of the top Zr atoms. We have also proposed a possible mechanism for the formation of the domain structure of silicene on ZrB_2. It is inferred that the domain structure is induced by an instability of a phonon having a nearly zero frequency, and is formed in such a way that the k-points having the zero frequency can be removed from the first Brillouin zone. The mechanism is verified by performing large-scale total energy calculations. We have further explored a possible structure of multi-layer silicene, and find that the MoS_2 structure consisting of silicon atoms is stabilized with atoms in the inner layer having a sixfold coordination, which results in cigar-shaped nematic orbitals originating from the Si-sp_2 orbitals.

1. Systematic study of electronic and magnetic properties for $Cu_{12-x}TM_xSb_4S_{13}$ (TM= Mn, Fe, Co, Ni, and Zn) tetrahedrite: K. Suekuni, Y. Tomizawa, T. Ozaki and M. Koyano, J. Appl. Phys. **115** (2014) 143702.

2. Avoiding critical-point phonon instabilities in two-dimensional materials: The origin of the stripe formation in epitaxial silicene: C. -C. Lee, A. Fleurence, R. Friedlein, Y. Yamada-Takamura and T. Ozaki, Phys. Rev. B **90** (2014) 241402(R).

3. Band structure of silicene on zirconium diboride (0001) thin-film surface: Convergence of experiment and calculations in the one-Si-atom Brillouin zone: C. -C. Lee, A. Fleurence, Y. Yamada-Takamura, T. Ozaki and R. Friedlein, Phys. Rev. B **90** (2014) 075422.

4. Competing magnetism in π-electrons in graphene with a single carbon vacancy: C. -C. Lee, Y. Yamada-Takamura and T. Ozaki, Phys. Rev. B **90** (2014) 014401.

5. Diverse forms of bonding in two-dimensional Si allotropes: Nematic orbitals in the MoS_2 structure: F. Gimbert, C. -C. Lee, R. Friedlein, A. Fleurence, Y. Yamada-Takamura and T. Ozaki, Phys. Rev. B **90** (2014) 165423.

6. Microscopic origin of the π states in epitaxial silicene: A. Fleurence, Y. Yoshida, C. -C. Lee, T. Ozaki, Y. Yamada-Takamura and Y. Hasegawa, Appl. Phys. Lett. **104** (2014) 021605.

7. Strain effects on the magnetic anisotropy of $Y_2Fe_{14}B$ examined by first-principles calculations: Z. Torbatian, T. Ozaki, S. Tsuneyuki and Y. Gohda, Appl. Phys. Lett. **104** (2014) 242403.

8. A method of orbital analysis for large-scale first-principles simulations: T. Ohwaki, M. Otani and T. Ozaki, J. Chem. Phys. **140** (2014) 244105.

9. First-principles electronic transport calculations of graphene nanoribbons on SiO_2/Si: H. Jippo, T. Ozaki and M. Ohfuchi, Appl. Phys. Express **7** (2014) 025101.

10. A decomposition method with minimum communication amount for parallelization of multi-dimensional FFTs: T. V. T. Duy and T. Ozaki, Comput. Phys. Commun. **185** (2014) 153.

11. A three-dimensional domain decomposition method for large-scale DFT electronic structure calculations: T. V. T. Duy and T. Ozaki, Comput. Phys. Commun. **185** (2014) 777.

† Joint research with outside partners.

Laser and Synchrotron Research Center

Suemoto group

(1) Coherent control and observation of spin dynamics by using terahertz (THz) wave: The spin orientation during the spin reorientation transition was precisely determined in an orthoferrite $Dy_{0.7}Er_{0.3}FeO_3$ by THz TDS (time domain spectroscopy) and the advantage of this method over a standard SQUID measurement was demonstrated. By using a high intensity THz source, instantaneous non-linear response was found in $ErFeO_3$. (2) THz spectroscopy for d-electron dynamics: Behavior of photo-generated d-electrons in MnO was investigated by optical-pump-THz-probe spectroscopy and the relaxation path to magnetic self-trapped exciton was suggested, comparing with luminescence measurement. (3) Ultrafast time-resolved luminescence spectroscopy: Luminescence dynamics was studied in graphenes and the importance of Fermi energy to the hot electron relaxation was shown. Femtosecond infrared luminescence was firstly observed in semimetals (Bi, Sb) and in a topological insulator ($TlBiSe_2$). (4) Single-shot soft x-ray imaging: A single-shot soft-x-ray microscope with a Fresnel's zone plate was constructed and a good performance with a spatial resolution of 200 nm was demonstrated.

1. †Enhanced spin-precession dynamics in a spin-metamaterial coupled resonator observed in terahertz time-domain measurements: T. Kurihara, K. Nakamura, K. Yamaguchi, Y. Sekine, Y. Saito, M. Nakajima, K. Oto, H. Watanabe and T. Suemoto, Phys. Rev. B **90** (2014) 144408(1-5).

2. †Nonlinear photoluminescence properties of trions in hole-doped single-walled carbon nanotubes: N. Akizuki, M. Iwamura, S. Mouri, Y. Miyauchi, T. Kawasaki, H. Watanabe, T. Suemoto, K. Watanabe, K. Asano and K. Matsuda, Phys. Rev. B **89** (2014) 195432.

3. †Ultrafast dynamics of photoinduced semiconductor-to-metal transition in optical switching nano-oxide Ti_3O_5: A. Asahara, H. Watanabe, H. Tokoro, S. Ohkoshi and T. Suemoto, Phys. Rev. B **90** (2014) 014303(1-7).

4. *Gain-switching dynamics in optically pumped single-mode InGaN vertical-cavity surface-emitting lasers: S. Chen, A. Asahara, T. Ito, J. Zhang, B. Zhang, T. Suemoto, M. Yoshita and H. Akiyama, Optics Express **22** (2014) 4196-4201.

5. †Domain growth and aggregation dynamics in photo-induced phase transition phenomena: H. Watanabe, S. Ishige, A. Asahara, H. Tokoro, S. Ohkoshi and T. Suemoto, J. Lumin **152** (2014) 108-111.

6. *Direct generation of 2-ps blue pulses from gain-switched InGaN VCSEL assessed by up-conversion technique: A. Asahara, S. Chen, T. Ito, M. Yoshita, W. Liu, B. Zhang, T. Suemoto and H. Akiyama, Sci. Rep. **4** (2014) 6401.

7. *Spectral dynamics of picosecond gain-switched pulses from nitride-based vertical-cavity surface-emitting lasers: S. Chen, T. Ito, A. Asahara, M. Yoshita, W. Liu, J. Zhang, B. Zhang, T. Suemoto and H. Akiyama, Sci. Rep. **4** (2014) 4325.

8. †Submicron scale image observation with a grazing incidence reflection-type single-shot soft X-ray microscope: M. Baba, M. Nishikino, N. Hasegawa, T. Tomita, Y. Minami, R. Takei, M. Yamagiwa, T. Kawachi and T. Suemoto, Jpn J. App. Phys. **53** (2014) 080302.

9. †Time-Resolved Soft X-Ray Imaging of Femtosecond Laser Ablation Processes on MetalsTomita: M. Nishikino, N. Hasegawa, Y. Minami, R. Takei, M. Baba, T. Eyama, S. Takayoshi, T. Kaihori, T. Morita, Y. Hirano, T. Kawachi, M. Yamagiwa and T. Suemoto, J. Laser Micro Nanoengineering **9** (2014) 137-142.

10. †High-frequency millimeter wave absorption of indium-substituted epsilon-Fe_2O_3 spherical nanoparticles: M. Yoshikiyo, A. Namai, M. Nakajima, K. Yamaguchi, T. Suemoto and S. Ohkoshi, J. App. Phys. **15** (2014) 172613.

11. †Ultraviolet stimulated emission from high-temperature-annealed MgO microcrystals at room temperature: H. Soma, Y. Uenaka, A. Asahara, T. Suemoto and T. Uchino, Appl. Phys. Lett. **106** (2015) 041116(1-5).

Shin group

We studied high Tc Fe-pnictide superconductors using 7-eV laser. High resolution photoemission study with polarization dependence is very powerful for the study of the superconducting mechanism. Orbital fluctuation mechanism is also important in addition to the spin fluctuation mechanism.

1. Electronic structure of CeCuAs2: A. Chainani, M. Matsunami, M. Taguchi, R. Eguchi, Y. Takata, M. Oura, S. Shin, K. Sengupta, E. V. Sampathkumaran, Th. Doert, Y. Senba, H. Ohashi, K. Tamasaku, Y. Kohmura, M. Yabashi and T. Ishikawa, Phys. Rev. B **89** (2014) 235117.

2. *Evidence for excluding the possibility of d-wave superconducting-gap symmetry in Ba-doped KFe_2As_2: Y. Ota, K. Okazaki, Y. Kotani, T. Shimojima, W. Malaeb, S. Watanabe, C. -T. Chen, K. Kihou, C. H. Lee, A. Iyo, H. Eisaki, T. Saito, H. Fukazawa, Y. Kohori and S. Shin, Phys. Rev. B **89** (2014) 081103(1-5).

---

* Joint research among groups within ISSP.

3. †*Evidence of a universal relation between electron-mode coupling and T_c in $Ba_{1-x}K_xFe_2As_2$ superconductor from laser angle-resolved photoemission spectroscopy: W. Malaeb, T. Shimojima, Y. Ishida, T. Kondo, K. Okazaki, Y. Ota, K. Ohgushi, K. Kihou, C. H. Lee, A. Iyo, H. Eisaki, S. Ishida, M. Nakajima, S. Uchida, H. Fukazawa, T. Saito, Y. Kohori and S. Shin, Phys. Rev. B **90** (2014) 195124(1-6).

4. †*Observation of a giant Kerr rotation in a ferromagnetic transition metal by M-edge resonant magneto-optic Kerr effect: Sh. Yamamoto, M. Taguchi, M. Fujisawa, R. Hobara, S. Yamamoto, K. Yaji, T. Nakamura, K. Fujikawa, R. Yukawa, T. Togashi, M. Yabashi, M. Tsunoda, S. Shin and I. Matsuda, Phys. Rev. B **89** (2014) 064423(1-6).

5. *Pseudogap formation above the superconducting dome in iron pnictides: T. Shimojima, T. Sonobe, W. Malaeb, K. Shinada, A. Chainani, S. Shin, T. Yoshida, S. Ideta, A. Fujimori, H. Kumigashira, K. Ono, Y. Nakashima, H. Anzai, M. Arita, A. Ino, H. Namatame, M. Taniguchi, M. Nakajima, S. Uchida, Y. Tomioka, T. Ito, K. Kihou, C. H. Lee, A. Iyo, H. Eisaki, K. Ohgushi, S. Kasahara, T. Terashima, H. Ikeda, T. Shibauchi, Y. Matsuda and K. Ishizaka, Phys. Rev. B **89** (2014) 045101(1-10).

6. †*Ultrafast photoinduced transition of an insulating VO_2 thin film into a nonrutile metallic state: R. Yoshida, T. Yamamoto, Y. Ishida, H. Nagao, T. Otsuka, K. Saeki, Y. Muraoka, R. Eguchi, K. Ishizaka, T. Kiss, S. Watanabe, T. Kanai, J. Itatani and S. Shin, Phys. Rev. B **89** (2014) 205114(1-7).

7. *Time-resolved photoemission apparatus achieving sub-20-meV energy resolution and high stability: Y. Ishida, T. Togashi, K. Yamamoto, M. Tanaka, T. Kiss, T. Otsu, Y. Kobayashi and S. Shin, Rev. Sci. Instrum. **85** (2014) 123904(1-9).

8. *Robust Protection from Backscattering in the Topological Insulator $Bi_{1.5}Sb_{0.5}Te_{1.7}Se_{1.3}$: S. Kim, S. Yoshizawa, Y. Ishida, K. Eto, K. Segawa, Y. Ando, S. Shin and F. Komori, Phys. Rev. Lett. **112** (2014) 136802(1-5).

9. Selective Probing of the OH or OD Stretch Vibration in Liquid Water Using Resonant Inelastic Soft-X-Ray Scattering: Y. Harada, T. Tokushima, Y. Horikawa, O. Takahashi, H. Niwa, M. Kobayashi, M. Oshima, Y. Senba, H. Ohashi, KT. Wikfeldt, A. Nilsson, LGM. Pettersson and S. Shin, Phys. Rev. Lett. **111** (2014) 193001(1-5).

10. レーザー光電子分光による分子性導体の電子構造の観測：石坂 香子，小泉 健二，木須 孝幸，辛 埴，固体物理 **49** (2014) 153-162.

11. †*Observing hot carrier distribution in an n-type epitaxial graphene on a SiC substrate: T. Someya, H. Fukidome, Y. Ishida, R. Yoshida, T. Iimori, R. Yukawa, K. Akikubo, Sh. Yamamoto, S. Yamamoto, T. Yamamoto, T. Kanai, K. Funakubo, M. Suemitsu, J. Itatani, F. Komori, S. Shin and I. Matsuda, Appl. Phys. Lett. **104** (2014) 161103(1-4).

12. †*Solvation dependence of valence electronic states of water diluted in organic solvents probed by soft X-ray spectroscopy: T. Tokushima, Y. Horikawa, O. Takahashi, H. Arai, K. Sadakane, Y. Harada, Y. Takata and S. Shin, Phys. Chem. Chem. Phys. **16** (2014) 10753-10761.

13. *Superconductivity in an electron band just above the Fermi level: possible route to BCS-BEC superconductivity: K. Okazaki1, Y. Ito, Y. Ota, Y. Kotani, T. Shimojima, T. Kiss, S. Watanabe, C. -T. Chen, S. Niitaka, T. Hanaguri, H. Takagi, A. Chainani and S. Shin, Sci. Rep. **4** (2014) 4109(1-6).

14. Development of a single-shot CCD-based data acquisition system for time-resolved X-ray photoelectron spectroscopy at an X-ray free-electron laser facility: M. Oura, T. Wagai, A. Chainani, J. Miyawaki, H. Sato, M. Matsunami, R. Eguchi, T. Kiss, T. Yamaguchi, Y. Nakatani, T. Togashi, T. Katayama, K. Ogawa, M. Yabashi, I. Y. Tanaka, Y. Kohmura, K. Tamasaku, S. Shin and T. Ishikawa, J.Syn.Rad. **21** (2014) 183-192.

15. The electronic structure of carbonate ion in aqueous solution studied by soft X-ray emission spectroscopy: Y. Horikawa A. Yoshida, O. Takahashi, H. Araia, T. Tokushima, T. Gejo and S. Shin, J.Mol.Liq **189** (2014) 9-12.

16. †*New soft X-ray beamline BL07LSU at SPring-8: S. Yamamoto, Y. Senba, T. Tanaka, H. Ohashi, T. Hirono, H. Kimura, M. Fujisawa, J. Miyawaki, A. Harasawa, T. Seike, S. Takahashi, N. Nariyama, T. Matsushita, M. Takeuchi, T. Ohata, Y. Furukawa, K. Takeshita, S. Goto, Y. Harada, S. Shin, H. Kitamura, A. Kakizaki, M. Oshima and I. Matsuda, J Synchrotron Rad **21** (2014) 352-365.

17. Observation of quadrupole helix chirality and its domain structure in DyFe3(BO3)4: T. Usui, Y. Tanaka, H. Nakajima, M. Taguchi, A. Chainani, M. Oura, S. Shin, N. Katayama, H. Sawa, Y. Wakabayashi and T. Kimura, Nature materials **13** (2014) 611-618.

18. Ultrahigh-spatial-resolution chemical and magnetic imaging by laser-based photoemission electron microscopy: T. taniuchi, Y. Kotani and S. Shin, Rev. Sci. Instrum. **86** (2015) 023701.

19. *Emergent photovoltage on SmB_6 surface upon bulk-gap evolution revealed by pump-and-probe photoemission spectroscopy: Y. Ishida, T. Otsu, T. Shimada, M. Okawa, Y. Kobayashi, F. Iga, Y. Takabatake and S. Shin, Sci. Rep. **5**

† Joint research with outside partners.

(2015) 8160(1-6).

20. * 鉄タンパク質の電子状態と機能：原田 慈久 , 辛 埴 , (朝倉書店「鉄の事典」, 3.11.d 節 , 2014).

Takahashi group

We have been studying the structure and phase transition of surfaces and interfaces with diffraction techniques. Atomic structure and electronic transport properties of Cu-doped topological insulator Bi_2Se_3 thin-films were investigated by surface X-ray diffraction and magnetotransport measurements. It is reported that Cu-doped Bi_2Se_3 bulk crystals show superconductivity at low temperature below 4 K. But the thin-film samples never showed superconductivity. This suggests that such bulk crystals contain impurity sub-phases responsible to superconductivity. On the other hand, we investigated the surface structure of Si(111)-5x2-Au, a typical prototype of one dimensional structure, that has not been solved for a long time since its first observation by LEED in 1969. We have experimentally determined the atomic structure without ambiguity with an aid of a holographic method in surface X-ray diffraction.

1. †Structure and transport properties of Cu doped Bi_2Se_3 films: T. Shirasawa, M. Sugiki, T. Hirahara, M. Aitani, T. Shirai, S. Hasegawa and T. Takahashi, Phys. Rev. B **89** (2014) 195311(1-6).

2. †Structure determination of multilayer silicene grown on Ag(111) films by electron diffraction: Evidence for Ag segregation at the surface: T. Shirai, T. Shirasawa, T. Hirahara, N. Fukui, T. Takahashi and S. Hasegawa, Phys. Rev. B **89** (2014) 241403(R)(1-5).

3. Identification of the Structure Model of the Si(111)-(5×2)-Au Surface: T. Shirasawa, W. Voegeli, T. Nojima, Y. Iwasawa, Y. Yamaguchi and T. Takahashi, Phys. Rev. Lett. **113** (2014) 165501(1-4).

4. †*Scanning tunneling microscopic and spectroscopic studies on a crystalline silica monolayer epitaxially formed on hexagonal SiC(000-1) surfaces: H. Tochihara, T. Shirasawa, T. Suzuki, T. Miyamachi, T. Kajiwara, K. Yagyu, S. Yoshizawa, T. Takahashi, S. Tanaka and F. Komori, Appl. Phys. Lett. **104** (2014) 051601(1-4).

5. †Determination of atomic positions in silicene on Ag(111) by low-energy electron diffraction: K. Kawahara, T. Shirasawa, R. Arafune, C. -L. Lin, T. Takahashi, M. Kawai and N. Takagi, Surf. Sci. **623** (2014) 25-28.

Akiyama group

In 2014, we developed experimental study on subcells diagnosis in a multi-junction solar cell via absolute electroluminescence-efficiency measurements, on the basis of a detailed-balance or reciprocity relation. Collaborations on GaAs quantum wells pumped by an intense single-cycle terahertz pulse were also developed. We studied spectral dynamics in pico-second short-pulse generation via gain switching in InGaN VCSELs and double-core-slab-waveguide semiconductor lasers for end optical pumping. We studied temperature dependence of quantitative green and orange/red emission intensities in firefly bioluminescence, and made intensive studies on theoretical quantum-chemistry calculations on luciferins and oxyluciferins.

1. Mode imaging and loss evaluation of semiconductor waveguides: T. Mochizuki, C. Kim, M. Yoshita, T. Nakamura, H. Akiyama, L. N. Pfeiffer and K. W. West, Rev. Sci. Instrum. **85** (2014) 053109.

2. Impact of Sub-cell Internal Luminescence Yields on Energy Conversion Efficiencies of Tandem Solar Cells: A design principle: L. Zhu, C. Kim, M. Yoshita, S. Chen, S. Sato, T. Mochizuki, H. Akiyama and Y. Kanemitsu, Appl. Phys. Lett. **104** (2014) 031118.

3. Robust red-emission spectra and yields in firefly bioluminescence against temperature changes: T. Mochizuki, Y. Wang, M. Hiyama and H. Akiyama, Appl. Phys. Lett. **104** (2014) 213704.

4. Spectroscopic Study of Firefly Oxyluciferin in an Enzymatic Environment on the Basis of Stability Monitoring: Y. Wang, Y. Hayamizu and H. Akiyama, J. Phys. Chem. B **118** (2014) 2070–2076.

5. †*First-Principles Investigation on Rydberg excitations of Firefly Luciferin Anion in Vacuum: Y. Noguchi, M. Hiyama, H. Akiyama and N. Koga, J. Chem. Phys. **141** (2014) 044309.

6. ホタル生物発光と物理：秋山 英文 , 望月 敏光 , 樋山 みやび , 日本物理学会誌 **69** (2014) 218.

7. *Gain-switching dynamics in optically pumped single-mode InGaN vertical-cavity surface-emitting lasers: S. Chen, A. Asahara, T. Ito, J. Zhang, B. Zhang, T. Suemoto, M. Yoshita and H. Akiyama, Optics Express **22** (2014) 4196-4201.

8. Analysis of Photoexcitation Energy Dependence in the Photoluminescence of Firefly Luciferin: M. Hiyama, H. Akiyama, T. Mochizuki, K. Yamada and N. Koga, Photochem. Photobiol. **90** (2014) 820-828.

* Joint research among groups within ISSP.

9. Atomically Engineered Metal-Insulator Transition at the $TiO_2/LaAlO_3$ Heterointerface: M. Minohara, T. Tachikawa, Y. Nakanishi, Y. Hikita, L. F. Kourkoutis, J.-S. Lee, C.-C. Kao, M. Yoshita, H. Akiyama, C. Bell and H. Y. Hwang, Nano Lett. **14 (11)** (2014) 6743-6746.

10. Gain switching of a double-core-waveguide semiconductor laser via traveling-wave optical pumping: H. Nakamae, T. Nakamura, T. Ito, T. Mochizuki, C. Kim, S. Chen, M. Yoshita and H. Akiyama, Appl. Phys. Express **7** (2014) 062701.

11. *Direct generation of 2-ps blue pulses from gain-switched InGaN VCSEL assessed by up-conversion technique: A. Asahara, S. Chen, T. Ito, M. Yoshita, W. Liu, B. Zhang, T. Suemoto and H. Akiyama, Sci. Rep. **4** (2014) 6401.

12. *Spectral dynamics of picosecond gain-switched pulses from nitride-based vertical-cavity surface-emitting lasers: S. Chen, T. Ito, A. Asahara, M. Yoshita, W. Liu, J. Zhang, B. Zhang, T. Suemoto and H. Akiyama, Sci. Rep. **4** (2014) 4325.

13. Balance sheets of energy and carriers and subcell characteristics in a InGaP/GaAs/Ge tandem solar cell: S. Chen, L. Zhu, M. Yoshita, T. Mochizuki, C. Kim, H. Akiyama, M. Imaizumi and Y. Kanemitsu, Photovoltaic Specialists Conference Proceedings **IEEE 40th** (2014) 1780-1783.

14. Conversion efficiency limits and optimized designs for tandem solar cells with realistic sub-cell material quality: L. Zhu, T. Mochizuki, M. Yoshita, S. Chen, S. Sato, C. Kim, H. Akiyama and Y. Kanemitsu, Photovoltaic Specialists Conference Proceedings **IEEE 40th** (2014) 3404-3408.

15. Time-resolved photoluminescence measurements for determining voltage-dependent charge-separation efficiencies of subcells in triple-junction solar cells: D. M. Tex, T. Ihara, H. Akiyama, M. Imaizumi and Y. Kanemitsu, Appl. Phys. Lett. **106** (2015) 013905.

16. 多接合太陽電池の診断・設計と発光絶対値・発光量子効率の評価：秋山 英文 , 応用物理 **84** (2015) 319-325.

17. Multi-junction-solar-cell designs and characterizations based on detailed-balance principle and luminescence yields: H. Akiyama, L. Zhu, M. Yoshita, C. Kim, S. Chen, T. Mochizuki and Y. Kanemitsu, Proc. SPIE **9358** (2015) 93580B1-8.

18. Time-resolved observation of excitonic dynamics under coherent terahertz excitation in GaAs quantum wells: K. Uchida, H. Hirori, T. Aoki, C. Wolpert, K. Tanaka, T. Mochizuki, C. Kim, M. Yoshita, H. Akiyama, L. N. Pfeiffer and K. W. West, Proc. SPIE **9361** (2015) 93611L1-6.

19. Analysis of Oxyluciferin Photoluminescence Pathways in Aqueous Solutions: M. Hiyama, T. Mochizuki, H. Akiyama and N. Koga, Photochem. Photobiol. **91** (2015) 74.

20. *Effect of very high magnetic field on the optical properties of firefly light emitter oxyluciferin: W. Zhou, D. Nakamura, Y. Wang, T. Mochizuki, H. Akiyama and S. Takeyama, Journal of Luminescence **165** (2015) 15.

21. On the importance of cavity-length and heat dissipation in GaN-based vertical-cavity surface-emitting lasers: W. J. Liu, X. L. Hu, L. Y. Ying, S. Q. Chen, J. Y. Zhang, H. Akiyama, Z. P. Cai and B. P. Zhang, Sci. Rep. **5** (2015) 9600.

22. Thorough subcells diagnosis in a multi-junction solar cell via absolute electroluminescence-efficiency measurements: S. Chen, L. Zhu, M. Yoshita, T. Mochizuki, C. Kim, H. Akiyama, M. Imaizumi and Y. Kanemitsu, Sci. Rep. **5** (2015) 7836.

23. *First-Principles Investigation of Strong Excitonic Effects in Oxygen 1s X-ray Absorption Spectra: Y. Noguchi, M. Hiyama, H. Akiyama, Y. Harada and N. Koga, J. Chem. Theory Comput. **11** (2015) 1668-1673.

24. Strong localization effect and carrier relaxation dynamics in self-assembled InGaN quantum dots emitting in the green: G.-E. Weng, W.-R. Zhao, S.-Q. Chen, H. Akiyama, Z.-C. Li, J.-P. Liu and B.-P. Zhang, Nanoscale Res. Lett. **10** (2015) 31.

25. *Vibronic Structures in Absorption and Fluorescence Spectra of Firefly Oxyluciferin in Aqueous Solutions: M. Hiyama, Y. Noguchi, H. Akiyama, K. Yamada and N. Koga, Photochem Photobiol (2015) published online, in print.

I. Matsuda group

Developments and experiments of the advanced spectroscopies have been carried out by using vacuum ultraviolet (VUV) and soft X-rays (SX). At SPring-8 BL07LSU, we have adjusted phase shifters with electromagnetic coils of the segmented cross-type undulator in the electron storage ring to realize fast switching of the light polarizations. At the end-station, we routinely supported picosecond-time-resolved SX photoemission spectroscopy experiments of joint-researches. Studies of photovoltaics and photocatalysis have been carried out mainly. As a new experimental tool for investigating spin dynamics, we have continued development of the rotating analyzer ellipsometry method for measuring the resonant magneto-optical Ker effect (RMOKE) using VUV and SX rays. Using a seeded free-electron laser at FERMI@ELETTRA in Italy, we have succeeded in tracing the photo-induced femtoseconds-spin-flipping in the ferrimagnetic material by RMOKE.

† Joint research with outside partners.

1. Anisotropic electronic conduction in metal nanofilms grown on a one-dimensional surface superstructure: N. Nagamura, R. Hobara, T. Uetake, T. Hirahara, K. Kobayashi, I. Matsuda and S. Hasegawa, Phys. Rev. B **89** (2014) 125415-1,-5.

2. †*Observation of a giant Kerr rotation in a ferromagnetic transition metal by M-edge resonant magneto-optic Kerr effect: Sh. Yamamoto, M. Taguchi, M. Fujisawa, R. Hobara, S. Yamamoto, K. Yaji, T. Nakamura, K. Fujikawa, R. Yukawa, T. Togashi, M. Yabashi, M. Tsunoda, S. Shin and I. Matsuda, Phys. Rev. B **89** (2014) 064423(1-6).

3. Electron-hole recombination on ZnO(0001) single-crystal surface studied by time-resolved soft X-ray photoelectron spectroscopy: R. Yukawa, S. Yamamoto, K. Ozawa, M. Emori, M. Ogawa, Sh. Yamamoto, K. Fujikawa, R. Hobara, S. Kitagawa, H. Daimon, H. Sakama and I. Matsuda, Appl. Phys. Lett. **105** (2014) 151602-1,-4.

4. †*Observing hot carrier distribution in an n-type epitaxial graphene on a SiC substrate: T. Someya, H. Fukidome, Y. Ishida, R. Yoshida, T. Iimori, R. Yukawa, K. Akikubo, Sh. Yamamoto, S. Yamamoto, T. Yamamoto, T. Kanai, K. Funakubo, M. Suemitsu, J. Itatani, F. Komori, S. Shin and I. Matsuda, Appl. Phys. Lett. **104** (2014) 161103(1-4).

5. Non-linear kinetic model for oscillatory relaxation of the photovoltage effect on a Si(111)7x7 surface: M. Ogawa, R. -Y. Liu, C. -H. Lin, S. Yamamoto, R. Yukawa, R. Hobara, S. -J. Tang and I. Matsuda, Surf. Sci. **624** (2014) 70-75.

6. 反射高速陽電子回折（RHEPD）による Ag(111) 表面上のシリセンの構造決定：深谷 有喜，望月 出海，前川 雅樹，和田 健，兵頭 俊夫，松田 巌，河裾 厚男，PF News **32** (2014) 10-14.

7. 表面電子化合物：松田 巌，深谷 有喜，PF News **31** (2014) 33-37.

8. †Electron–Hole Recombination Time at TiO_2 Single-Crystal Surfaces: Influence of Surface Band Bending: K. Ozawa, M. Emori, S. Yamamoto, R. Yukawa, S. Yamamoto, R. Hobara, K. Fujikawa, H. Sakama and I. Matsuda, J. Phys. Chem. Lett. **5** (2014) 1953-1957.

9. Rashba effects within the space charge layer of a semiconductor: C.-H. Lin, T.-R. Chang, Ro. -Ya. Liu, C.-M. Cheng, K.-D. Tsuei, H. -T. Jeng, C.-Y. Mou, I. Matsuda and S. -J. Tang, New. J. Phys. **16** (2014) 045003-1,-12.

10. †*New soft X-ray beamline BL07LSU at SPring-8: S. Yamamoto, Y. Senba, T. Tanaka, H. Ohashi, T. Hirono, H. Kimura, M. Fujisawa, J. Miyawaki, A. Harasawa, T. Seike, S. Takahashi, N. Nariyama, T. Matsushita, M. Takeuchi, T. Ohata, Y. Furukawa, K. Takeshita, S. Goto, Y. Harada, S. Shin, H. Kitamura, A. Kakizaki, M. Oshima and I. Matsuda, J Synchrotron Rad **21** (2014) 352-365.

11. †*Development of an electromagnetic phase shifter using a pair of cut-core coils for a cross undulator: I. Matsuda, A. Kuroda, J. Miyawaki, Y. Kosegawa, S. Yamamoto, T. Seike, T. Bizen, Y. Harada, T. Tanaka and H. Kitamura, Nucl. Instrum. Methods Phys. Res. A **767** (2014) 296-299.

12. †Titanium-induced charge of Si(001) surface dependent on local configuration: K. Shudo, T. Aoki, S. Ohno, K. Yamazaki, F. Nakayama, M. Tanaka, T. Okuda, A. Harasawa, I. Matsuda, T. Kakizaki and M. Uchiyama, J. Elec. Spec. Rel, Phen. **192** (2014) 35.

13. 時間分解軟X線光電子分光法による表面キャリアダイナミクス研究の進展：山本 達，松田 巌，日本放射光学会誌 **27** (2014) 241.

14. *Scanning tunneling spectroscopy study of quasiparticle interference on dual topological insulator $Bi_{1-x}Sb_x$: S. Yoshizawa, F. Nakamura, A. A. Taskin, T. Iimori, K. Nakatsuji, I. Matsuda, Y. Ando and F. Komori, Phys. Rev. B **91** (2015) 045423-1,-6.

15. †Experimental evidence for two-dimensional states localized in subsurface region in Ge(111): K. Yaji, Y. Ohtsubo, S. Hatta, H. Okuyama, R. Yukawa, I. Matsuda, P. Le Fevre, F. Bertran, A. Taleb-Ibrahimi, A. Kakizaki and T. Aruga, J. Elec. Spec. Rel. Phenom. (2014), in print.

Kobayashi group

We have demonstrated high-power high-harmonic generation from 30-m cavity. The obtained VUV coherent light had a comparable brightness to a synchrotron radiation. We are developing very-high repetition-rate mode-locked laser for astronomical applications. Long-term stable optical frequency comb is also developing. We have stated to develop a mid-infrared optical frequency comb for medical applications.

1. *Time-resolved photoemission apparatus achieving sub-20-meV energy resolution and high stability: Y. Ishida, T. Togashi, K. Yamamoto, M. Tanaka, T. Kiss, T. Otsu, Y. Kobayashi and S. Shin, Rev. Sci. Instrum. **85** (2014) 123904(1-9).

2. *Wavefront analysis of high-efficiency, large-scale, thin transmission gratings: C. Zhou, T. Seki, T. Kitamura, Y.

* Joint research among groups within ISSP.

Kuramoto, T. Sukegawa, N. Ishii, T. Kanai, J. Itatani, Y. Kobayashi and S. Watanabe, Opt. Express **22** (2014) 5995-6008.

3. デュアルコム分光 FT-IR にかわる高速広帯域精密分光 : 久世 直也 , 小澤 陽 , 小林 洋平 , 日本物理学会 **69** (2014) 29.

4. エンハンスメントキャビティー、フォトンリングを用いた高強度レーザー実現の試み : 小林 洋平 , プラズマ・核融合学会誌 第 90 巻 8 号 (2014) 462-467.

5. 300-mW narrow-linewidth deep-ultraviolet light generation at 193 nm by frequency mixing between Yb-hybrid and Er-fiber lasers: H. Xuan, Z. Zhao, H. Igarashi, S. Ito, K. Kakizaki and Y. Kobayashi, Opt. Express **23** (2015) 10564-10572.

6. Direct 15-GHz mode-spacing optical frequency comb with a Kerr-lens mode-locked Yb:Y_2O_3 ceramic laser: M. Endo, I. Ito and Y. Kobayashi, Opt. Express **23** (2015) 1276-1282.

7. *Emergent photovoltage on SmB_6 surface upon bulk-gap evolution revealed by pump-and-probe photoemission spectroscopy: Y. Ishida, T. Otsu, T. Shimada, M. Okawa, Y. Kobayashi, F. Iga, Y. Takabatake and S. Shin, Sci. Rep. **5** (2015) 8160(1-6).

8. Development of compact and ultra-high-resolution spectrograph with multi-GHz optical frequency comb: M. Endo, T. Sukegawa, A. Silva and Y. Kobayashi, in: *Ground-based and Airborne Instrumentation for Astronomy V* (Proc. SPIE 9147, 2014), 91477Y.

9. Development of narrow-linewidth Yb- and Er- fiber lasers and frequency mixing for ArF excimer laser seeding: H. Xuan, Z. Zhao, H. Igarashi, S. Ito, K. Kakizaki and Y. Kobayashi, in: *Fiber Lasers XI: Technology, Systems, and Applications* (Proc. SPIE 8961, 2014), 89612M.

Itatani group

We have continued to develop an infrared (IR) optical parametric chirped pulse amplifier (OPCPA) to produce coherent soft X ray via high harmonic generation. Comparison between the observed carrier-envelope phase dependence of high harmonic spectra and a quantum simulation suggested the generation of isolated attosecond pulses that covered the carbon K edge(~284 eV). This is an important milestone for realizing ultrafast soft-X-ray spectroscopy using laser-based light sources. The long-term stability of the carrier-envelope phase of the IR OPCPA was examined by monitoring the high-energy photoelectron spectra in above-threshold ionization, revealing the excellent long-term passive stabilization up to 47 hours. The molecular control experiments using intense THz pulses was extended to a novel double-pulse scheme. We successfully controlled the two-level coherence that were probed by the velocity map technique. We also kept collaboration with Shin, Komori, and Matsuda groups at LASOR-ISSP on time-resolved ARPES using a femtosecond EUV source. Several experiments on the ultrafast relaxation of photo-induced states in VO_2 and graphene were successfully performed.

1. †*Ultrafast photoinduced transition of an insulating VO_2 thin film into a nonrutile metallic state: R. Yoshida, T. Yamamoto, Y. Ishida, H. Nagao, T. Otsuka, K. Saeki, Y. Muraoka, R. Eguchi, K. Ishizaka, T. Kiss, S. Watanabe, T. Kanai, J. Itatani and S. Shin, Phys. Rev. B **89** (2014) 205114(1-7).

2. †*Observing hot carrier distribution in an n-type epitaxial graphene on a SiC substrate: T. Someya, H. Fukidome, Y. Ishida, R. Yoshida, T. Iimori, R. Yukawa, K. Akikubo, Sh. Yamamoto, S. Yamamoto, T. Yamamoto, T. Kanai, K. Funakubo, M. Suemitsu, J. Itatani, F. Komori, S. Shin and I. Matsuda, Appl. Phys. Lett. **104** (2014) 161103(1-4).

3. 高次高調波によるコヒーレント軟 X 線の発生とその応用 : 板谷 治郎 , 光学 **43** (2014) 419-425.

4. Selecting rotational two-level coherence in polar molecules by double terahertz pulses: K. Kitano, N. Ishii, T. Kanai and J. Itatani, Phys. Rev. A **90** (2014) 041402(R)-1-5.

5. Long-term passive stabilization of the carrier-envelope phase of an intense infrared few-cycle pulse source: H. Geiseler, N. Ishii, K. Kaneshima, T. Kanai and J. Itatani, Appl. Phys. B **117** (2014) 941-946.

6. High-energy half-cycle cutoffs in high harmonic and rescattered electron spectra using waveform-controlled few-cycle infrared pulses: H. Geiseler, N. Ishii, K. Kaneshima, K. Kitano, T. Kanai and J. Itatani, J. Phys. B: At. Mol. Opt. Phys. **47** (2014) 204011-1-8.

7. *Wavefront analysis of high-efficiency, large-scale, thin transmission gratings: C. Zhou, T. Seki, T. Kitamura, Y. Kuramoto, T. Sukegawa, N. Ishii, T. Kanai, J. Itatani, Y. Kobayashi and S. Watanabe, Opt. Express **22** (2014) 5995-6008.

8. Carrier-envelope phase-dependent high harmonic generation in the water window using few-cycle infrared pulses: N. Ishii, K. Kaneshima, K. Kitano, T. Kanai, S. Watanabe and J. Itatani, Nat. Commun. **5** (2014) 3331.

9. Ultrabroadband infrared chirped mirrors characterized by a white-light Michelson interferometer: K. Kaneshima, M.

† Joint research with outside partners.

Sugiura, K. Tamura, N. Ishii and J. Itatani, Appl. Phys. B **119** (2015) 347-353.

Harada group

Soft X-ray absorption/emission spectroscopy in a real ambient condition is an urgent requisite since the ultrahigh vacuum needed to transmit soft X-rays hampers the use of this unique method among various spectroscopies for a long time. Therefore, this is one of the major goals of our project. From 2013, we have developed a system for ambient pressure soft X-ray emission spectroscopy using originally-developed differential pumping system. In 2014, we have introduced a co-axial sample monitor and a beam profile monitor, which has facilitated the alignment of the apertures and a nozzle for differential pumping to efficiently transmit incident soft X-rays to the sample. Finally we have enabled 10 orders of magnitude different pressure (from 10^{-5} Pa to 10^{5} Pa) at only around 400 mm distance. As a demonstration we performed O 1s RIXS of H_2O ice under the pressure around 10^{-1}Pa. We also have introduced a system to apply a magnetic field on the sample up to 0.3 T. We have accepted 7 collaborative works at BL07LSU HORNET endstation, which are i) Observation of 100 meV-order multiphonon excitations in Ti 2p RIXS of anatase TiO_2, which reveals real bulk sensitive isotropic phonon modes for the first time; ii) Development of damage-free RIXS technique for highly valent manganese complex as a model manganese cluster for oxygen evolving complex in photosystem II; iii) Study on the structure making/breaking characteristics of hydrated water around a series of hydrophobic phase-transfer catalysts: TBA, TPA, TEA and TMA, which followed a general trend even in the electronic structure level from structure-breaking to structure-making as the size of the catalyst decreases; iv) MCD-RIXS experiments applying the 0.3 T magnetic field, one is terfenol-D, the most famous magnetostrictive material and the other is half metal CrO_2 which demonstrated a beautiful selection rule of dd excitations depending on the polarization of the incident photon due to fully spin-polarized HOMO state under the magnetic field; v) Operando Fe 2p RIXS spectroscopy of the cathode electrode $LiFePO_4$ for lithium ion batteries by characterizing electrochemical property.

1. †Unveiling the impurity band induced ferromagnetism in the magnetic semiconductor (Ga,Mn)As: M. Kobayashi, I. Muneta, Y. Takeda, Y. Harada, A. Fujimori, J. Krempaský, T. Schmitt, S. Ohya, M. Tanaka, M. Oshima and V. N. Strocov, Phys. Rev. B **89** (2014) 205204(1-8).

2. †Electronic Excitations of a Magnetic Impurity State in the Diluted Magnetic Semiconductor (Ga,Mn)As: M. Kobayashi, H. Niwa, Y. Takeda, A. Fujimori, Y. Senba, H. Ohashi, A. Tanaka, S. Ohya, P. N. Hai, M. Tanaka, Y. Harada and M. Oshima, Phys. Rev. Lett. **112** (2014) 107203(1-7).

3. Reabsorption of Soft X-Ray Emission at High X-Ray Free-Electron Laser Fluences: S. Schreck, M. Beye, J. A. Sellberg, T. McQueen, H. Laksmono, B. Kennedy, S. Eckert, D. Schlesinger, D. Nordlund, H. Ogasawara, R. G. Sierra, V. H. Segtnan, K. Kubicek, W. F. Schlotter, G. L. Dakovski, S. P. Moeller, U. Bergmann, S. Techert, L. G. M. Pettersson, P. Wernet, M. J. Bogan, Y. Harada, A. Nilsson and A. Föhlisch, Phys. Rev. Lett. **113** (2014) 153002(1-6).

4. Spin and orbital magnetic moments of Fe in the n-type ferromagnetic semiconductor (In,Fe)As: M. Kobayashi, L. D. Anh, P. N. Hai, Y. Takeda, S. Sakamoto, T. Kadono, T. Okane, Y. Saitoh, H. Yamagami, Y. Harada, M. Oshima, M. Tanaka and A. Fujimori, Appl. Phys. Lett. **105** (2014) 032403(1-4).

5. †*Solvation dependence of valence electronic states of water diluted in organic solvents probed by soft X-ray spectroscopy: T. Tokushima, Y. Horikawa, O. Takahashi, H. Arai, K. Sadakane, Y. Harada, Y. Takata and S. Shin, Phys. Chem. Chem. Phys. **16** (2014) 10753-10761.

6. †Distinguishing between High- and Low-Spin States for Divalent Mn in Mn-Based Prussian Blue Analogue by High-Resolution Soft X-ray Emission Spectroscopy: D. Asakura, Y. Nanba, M. Okubo, Y. Mizuno, H. Niwa, M. Oshima, H. Zhou, K. Okada and Y. Harada, J. Phys. Chem. Lett. **5** (2014) 4008-4013.

7. †*New soft X-ray beamline BL07LSU at SPring-8: S. Yamamoto, Y. Senba, T. Tanaka, H. Ohashi, T. Hirono, H. Kimura, M. Fujisawa, J. Miyawaki, A. Harasawa, T. Seike, S. Takahashi, N. Nariyama, T. Matsushita, M. Takeuchi, T. Ohata, Y. Furukawa, K. Takeshita, S. Goto, Y. Harada, S. Shin, H. Kitamura, A. Kakizaki, M. Oshima and I. Matsuda, J Synchrotron Rad **21** (2014) 352-365.

8. Iron-Nitrogen Coordination in Modified Graphene Catalyzes a Four-Electron-Transfer Oxygen Reduction Reaction: K. Kamiya, H. Koshikawa, H. Kiuchi, Y. Harada, M. Oshima, K. Hashimoto and S. Nakanishi, ChemElectroChem **1** (2014) 877-884.

9. †*Development of an electromagnetic phase shifter using a pair of cut-core coils for a cross undulator: I. Matsuda, A. Kuroda, J. Miyawaki, Y. Kosegawa, S. Yamamoto, T. Seike, T. Bizen, Y. Harada, T. Tanaka and H. Kitamura, Nucl. Instrum. Methods Phys. Res. A **767** (2014) 296-299.

10. †Multi-Phonon Excitations in Fe 2*p* RIXS on Mg_2FeH_6: K. Kurita, D. Sekiba, I. Harayama, K. Chito, Y. Harada, H. Kiuchi, M. Oshima, S. Takagi, M. Matsuo, R. Sato, K. Aoki and S.-I. Orimo, J. Phys. Soc. Jpn. **84** (2015) 043201 1-3.

11. X-ray Emission Spectroscopy of Bulk Liquid Water in "No-man's Land": J. Sellberg, T. McQueen, H. Laksmono, S.

* Joint research among groups within ISSP.

Schreck, M. Beye, D. DePonte, B. O'Kennedy, D. Nordlund, R. Sierra, D. Schlesinger, T. Tokushima, S. Eckert, V. Segtnan, H. Ogasawara, K. Kubicek, S. Techert, U. Bergmann, G. Dakovski, W. Schlotter, Y. Harada, I. Zhovtobriukh, M. Bogan, P. Wernet, A. Föhlisch, L. Pettersson and A. Nilsson, J. Chem. Phys. **142** (2015) 044505 1-9.

12. †Enhancement in Kinetics of the Oxygen Reduction Reaction on a Nitrogen-Doped Carbon Catalyst by Introduction of Iron via Electrochemical Methods: J. Wu, D. Zhang, H. Niwa, Y. Harada, M. Oshima, H. Ofuchi, Y. Nabae, T. Okajima and T. Ohsaka, Langmuir **31** (2015) 5529-5536.

13. Active site formation mechanism of carbon-based oxygen reduction catalysts derived from a hyperbranched iron phthalocyanine polymer: Y. Hiraike, M. Saito, H. Niwa, M. Kobayashi, Y. Harada, M. Oshima, J. Kim, Y. Nabae and M.-A. Kakimoto, Nanoscale Res Lett **10** (2015) 179 1-11.

14. †Operando soft x-ray emission spectroscopy of $LiMn_2O_4$ thin film involving Li-ion extraction/insertion reaction: D. Asakura, E. Hosono, H. Niwa, H. Kiuchi, J. Miyawaki, Y. Nanba, M. Okubo, H. Matsuda, H. S. Zhou, M. Oshima and Y. Harada, Electrochem. Commun. **50** (2015) 93-96.

15. *First-Principles Investigation of Strong Excitonic Effects in Oxygen 1s X-ray Absorption Spectra: Y. Noguchi, M. Hiyama, H. Akiyama, Y. Harada and N. Koga, J. Chem. Theory Comput. **11** (2015) 1668-1673.

16. カーボンアロイ触媒の開発、そしてその可能性：難波江 裕太 , 原田 慈久 , 尾嶋 正治 , (シーエムシー出版 , SPring-8 の高輝度放射光を利用したグリーンエネルギー分野における電池材料開発、第５章電池における触媒開発 , 2014).

17. * 鉄タンパク質の電子状態と機能：原田 慈久 , 辛 埴 , (朝倉書店「鉄の事典」, 3.11.d 節 , 2014).

Wadati group

Our main experimental techniques are synchrotron-based x-ray spectroscopy and scattering. We studied the orbital and magnetic phase transitions in $Pr_{0.5}Ca_{0.5}MnO_3/La_{Sr}Ca_{0.5}MnO_3$ superlattices by resonant soft x-ray scattering and observed dimensional crossover as a function of temperature. We also performed time-resolved x-ray diffraction study of $Pr_{0.5}Ca_{0.5}MnO_3$ thin films by using x-ray free electron laser in LCLS (USA), and observed a time-dependent order parameter by creating coherent phonons.

1. Antiferromagnetic Order of the Co^{2+} High-Spin State with a Large Orbital Angular Momentum in $La_{1.5}Ca_{0.5}CoO_4$: J. Okamoto, H. Nakao, Y. Yamasaki, H. Wadati, A. Tanaka, M. Kubota, K. Horigane, Y. Murakami and K. Yamada, J. Phys. Soc. Jpn. **83** (2014) 044705(1-6).

2. Insulator-to-Superconductor Transition upon Electron Doping in a BiS_2-Based Superconductor $Sr_{1-x}La_xFBiS_2$: H. Sakai, D. Kotajima, K. Saito, H. Wadati, Y. Wakisaka, M. Mizumaki, K. Nitta, Y. Tokura and S. Ishiwata, J. Phys. Soc. Jpn. **83** (2014) 014709(1-7).

3. Bond order and the role of ligand states in stripe-modulated $IrTe_2$: K. Takubo, R. Comin, D. Ootsuki, T. Mizokawa, H. Wadati, Y. Takahashi, G. Shibata, A. Fujimori, R. Sutarto, F. He, S. Pyon, K. Kudo, M. Nohara, G. Levy, I. Elfimov, G. A. Sawatzky and A. Damascelli, Phys. Rev. B **90** (2014) 081104(R)(1-5).

4. Photoemission and DMFT study of electronic correlations in $SrMoO_3$: Effects of Hund's rule coupling and possible plasmonic sideband: H. Wadati, J. Mravlje, K. Yoshimatsu, H. Kumigashira, M. Oshima, T. Sugiyama, E. Ikenaga, A. Fujimori, A. Georges, A. Radetinac, K. S. Takahashi, M. Kawasaki and Y. Tokura, Phys. Rev. B **90** (2014) 205131(1-8).

5. Orbital correlations and dimensional crossover in epitaxial $Pr_{0.5}Ca_{0.5}MnO_3/La_{0.5}Sr_{0.5}MnO_3$ superlattices: H. Wadati, J. Okamoto, M. Garganourakis, V. Scagnoli, U. Staub, E. Sakai, H. Kumigashira, T. Sugiyama, E. Ikenaga, M. Nakamura, M. Kawasaki and Y. Tokura, New J. Phys. **16** (2014) 073044(1-10).

6. Revealing orbital and magnetic phase transitions in $Pr_{0.5}Ca_{0.5}MnO_3$ epitaxial thin films by resonant soft x-ray scattering: H. Wadati, J. Geck, E. Schierle, R. Sutarto, F. He, D. G. Hawthorn, M. Nakamura, M. Kawasaki, Y. Tokura and G. A. Sawatzky, New J. Phys. **16** (2014) 033006(1-12).

7. A time-dependent order parameter for non-equilibrium phase transitions: P. Beaud, A. Caviezel, S. O. Mariager, L. Rettig, G. Ingold, C. Dornes, S.-W. Huang, J. A. Johnson, M. Radovic, T. Huber, T. Kubacka, A. Ferrer, H. T. Lemke, M. Chollet, D. Zhu, J. M. Glownia, M. Sikorski, A. Robert, H. Wadati, M. Nakamura, M. Kawasaki, Y. Tokura, S. L. Johnson and U. Staub, Nat. Mater. **13** (2014) 923-927.

8. X-ray spectroscopic study of $BaFeO_3$ thin films; an Fe^{4+} ferromagnetic insulator: T. Tsuyama, T. Matsuda, S. Chakraverty, J. Okamoto, E. Ikenaga, A. Tanaka, T. Mizokawa, H. Y. Hwang, Y. Tokura and H. Wadati, Phys. Rev. B **91** (2015) 115101(1-7).

9. Engineering a spin-orbital magnetic insulator by tailoring superlattices: J. Matsuno, K. Ihara, S. Yamamura, H. Wadati, K. Ishii, V. V. Shankar, H.-Y. Kee and H. Takagi, Phys. Rev. Lett. **114** (2015) 247209(1-5).

† Joint research with outside partners.

10. Observation of a Devil's Staircase in the Novel Spin-Valve System $SrCo_6O_{11}$: T. Matsuda, S. Partzsch, T. Tsuyama, E. Schierle, E. Weschke, J. Geck, T. Saito, S. Ishiwata, Y. Tokura and H. Wadati, Phys. Rev. Lett. **114** (2015) 236403(1-5).

Kondo group

A central issue in the search for the mechanism of high temperature conductivity is to determine the bosons which mediate electron pairing. Electron coupling with a bosonic mode changes the slope of the band dispersion within its excitation energy. Such a band renormalization or ''kink''is usually observed in superconducting materials. By using laser-based angle-resolved photoemission spectroscopy, capable of ultrahigh energy resolution, we found a universal relation between electron-mode coupling and Tc in the pnictide high-Tc superconductor.

1. †*Evidence of a universal relation between electron-mode coupling and T_c in $Ba_{1-x}K_xFe_2As_2$ superconductor from laser angle-resolved photoemission spectroscopy: W. Malaeb, T. Shimojima, Y. Ishida, T. Kondo, K. Okazaki, Y. Ota, K. Ohgushi, K. Kihou, C. H. Lee, A. Iyo, H. Eisaki, S. Ishida, M. Nakajima, S. Uchida, H. Fukazawa, T. Saito, Y. Kohori and S. Shin, Phys. Rev. B **90** (2014) 195124(1-6).

2. Fermi Surface and Pseudogap Evolution in a Cuprate Superconductor.: Y. He, Y. Yin, M. Zech, A. Soumyanarayanan, M. M. Yee, T. Williams, M. C. Boyer, K. Chatterjee, W. D. Wise, I. Zeljkovic, T. Kondo, T. Takeuchi, H. Ikuta, P. Mistark, R. S. Markiewicz, A. Bansil, S. Sachdev, E. W. Hudson and J. E. Hoffman, Science **344** (2014) 608-611.

3. Pairing, pseudogap and Fermi arcs in cuprates.: A. Kaminski, T. Kondo, T. Takeuchi and G. Gu, Philosophical Magazine **95** (2015) 453-466.

Okazaki group

We have developed and improved a time- and angle-resolved photoemission (TARPES) apparatus using an EUV and SX laser by high harmonics generation (HHG). In 2014, we have installed a new chamber for HHG with a gas cell, a spectrometer for checking spectra of high harmonics, and a chamber for multi-layer mirrors to select a single order of the harmonics. Now, we can use 28, 40, and 70 eV for a probe light. We have also installed an optical parametric amplifier (OPA) system for a pump light, and succeeded in obtaining TRPES spectra of graphite using this system. We have studied nonequilibrium electronic states of graphenes, iron-based superconductors, strongly correlated electron systems, and valence fluctuating heavy fermion systems. In addition, we have also investigated superconducting-gap structures of iron-based superconductors and BiS2-based superconductors by a low-temperature and high-resolution laser ARPES apparatus.

1. *Evidence for excluding the possibility of d-wave superconducting-gap symmetry in Ba-doped KFe_2As_2: Y. Ota, K. Okazaki, Y. Kotani, T. Shimojima, W. Malaeb, S. Watanabe, C. -T. Chen, K. Kihou, C. H. Lee, A. Iyo, H. Eisaki, T. Saito, H. Fukazawa, Y. Kohori and S. Shin, Phys. Rev. B **89** (2014) 081103(1-5).

2. †*Evidence of a universal relation between electron-mode coupling and T_c in $Ba_{1-x}K_xFe_2As_2$ superconductor from laser angle-resolved photoemission spectroscopy: W. Malaeb, T. Shimojima, Y. Ishida, T. Kondo, K. Okazaki, Y. Ota, K. Ohgushi, K. Kihou, C. H. Lee, A. Iyo, H. Eisaki, S. Ishida, M. Nakajima, S. Uchida, H. Fukazawa, T. Saito, Y. Kohori and S. Shin, Phys. Rev. B **90** (2014) 195124(1-6).

3. *Superconductivity in an electron band just above the Fermi level: possible route to BCS-BEC superconductivity: K. Okazaki1, Y. Ito, Y. Ota, Y. Kotani, T. Shimojima, T. Kiss, S. Watanabe, C. -T. Chen, S. Niitaka, T. Hanaguri, H. Takagi, A. Chainani and S. Shin, Sci. Rep. **4** (2014) 4109(1-6).

* Joint research among groups within ISSP.